

THE UNIVERSITY OF MICHIGAN  
INDUSTRY PROGRAM OF THE COLLEGE OF ENGINEERING

DETERMINATION OF NITRIDE SOLUBILITY PRODUCTS  
IN THE SOLVENT LIQUID IRON

*evans*  
Donald B. Evans

A dissertation submitted in partial fulfillment  
of the requirements for the degree of  
Doctor of Philosophy in the  
University of Michigan  
Department of Chemical and Metallurgical Engineering  
1963

February, 1963

IP-606

Engn

UMR

1396

## ACKNOWLEDGMENTS

The author takes this opportunity to express his appreciation of the assistance rendered him from numerous sources during the preparation of this dissertation.

The greatest debt is owed to Professor Robert D. Pehlke who chaired the doctoral committee. Professor Pehlke, whose own doctoral thesis formed the point of departure for this research, was always available for consultation and made many important and valuable suggestions in shaping the course of the investigation.

The guidance of the remainder of the doctoral committee, Professor Richard E. Balzhiser, Professor Lee O. Case, Professor Clarence A. Siebert, and Professor Lawrence H. Van Vlack is also appreciated. Professor Siebert was particularly helpful in the experimental phase of the investigation.

Mr. Robert N. Katz who is presently associated with the Watertown Arsenal, Watertown, Massachusetts made the x-ray analyses of the extracted nitrides.

Dr. David L. Sponseller who is presently Assistant Professor of Metallurgy at the University of Notre Dame, South Bend, Indiana developed the method of fabrication of the TiN crucibles used in the quenching method of this study. Both his equipment and his knowledge of fabrication techniques were generously made available to the author.

Professor J. H. Burkhalter of the College of Pharmacy, University of Michigan provided assistance in the development of the Kjeldahl analytical procedure used in analyzing the quenched ingots. He also made laboratory facilities available for the initial stages of this work.

The Carborundum Company donated the AlN crucibles which were used in the quenching experiments.

Financial assistance to the author during the course of the investigation was provided by a research contract sponsored by the Atomic Energy Commission.

The reproduction of the dissertation was performed by the Industry Program of the College of Engineering, of the University of Michigan. Mr. David F. Evans aided in the preparation of the manuscript.

## TABLE OF CONTENTS

	<u>Page</u>
ACKNOWLEDGMENTS.....	ii
LIST OF TABLES.....	vii
LIST OF FIGURES.....	x
ABSTRACT.....	xiii
I. INTRODUCTION.....	1
II. SURVEY OF PREVIOUS WORK.....	2
A. Solubility of Nitrogen in Pure Liquid Iron and Ad- herence of Dilute Alloys to Sieverts' Law.....	2
B. Nitride Solubility Products in Liquid and Solid Iron.....	4
C. Nitride Phase Compositions.....	7
III. OUTLINE OF THE PROBLEM.....	10
A. General.....	10
B. Systems Chosen for Experimentation.....	10
C. Experimental Methods.....	11
D. Possible Methods of Correlating the Experimental Results.....	11
IV. EXPERIMENTAL METHODS AND PROCEDURES.....	22
A. Comparison of Sieverts Method and Quenching Method..	22
B. Experimental Procedure for the Sieverts Method.....	26
C. Experimental Procedure for the Quenching Method.....	34
D. Determination of the Nitride Phase Composition.....	38
V. RESULTS AND DISCUSSION.....	40
A. Calculation of Results From the Sieverts Measure- ments.....	40
B. Summary of the Nitrogen Absorption Curves De- termined by the Sieverts Method.....	41

TABLE OF CONTENTS CONT'D

	<u>Page</u>
C. Calculation and Summary of the Interaction Parameters $e_N^j$ and $e_j^N$ .....	43
D. Calculation and Summary of the Interaction Parameters $e_j^j$ .....	59
E. Calculation of the Nitride Solubility Product by the Method of Interaction Parameters.....	62
F. Calculation of the Nitride Solubility Product Using the Nitrogen Activity Determined by the Gas Phase..	62
G. Calculation of the Nitride Solubility Product Using the $j$ Activity Estimated From Fe-j Binary Data.	68
H. Calculation and Summary of Enthalpy and Entropy of Decomposition of Nitrides in Liquid Iron.....	71
I. Discussion of Results of the Various Methods Used to Calculate the Nitride Solubility Products.....	80
J. Summary of the Nitride Solubility Products Measured by the Quenching Method.....	87
K. Summary of Methods Used to Determine the Nitride Phase Compositions.....	96
VI. DISCUSSION OF ERRORS.....	103
A. Sieverts Method.....	103
B. Quenching Method.....	107
VII. CONCLUSIONS.....	109
VIII. APPENDICES.....	111
A. Charge Material Analyses.....	111
B. Temperature Calibration.....	115
C. Flowmeter Calibration.....	117
D. Methods of Chemical Analysis.....	120
E. Methods of Fabrication of Nitride Crucibles.....	122
F. Nitrogen Absorption Curves.....	125

TABLE OF CONTENTS CONT'D

	<u>Page</u>
G. Calculation of Nitride Compositions by Phase Rule Analysis.....	156
H. X-ray Data.....	161
I. Calculation of Activity Coefficients in Liquid Iron.....	167
J. Free Energy of Formation of AlN from the Pure Components.....	170
IX. BIBLIOGRAPHY.....	172

LIST OF TABLES

<u>Table</u>	<u>Page</u>
I. Summary of Denitrifying Constants Estimated by Chipman <sup>(7)</sup> .....	4
II. Advantages and Disadvantages of the Sieverts Method....	23
III. Summary of Measured Values of the Interaction Parameters $e_N^j$ and $e_j^N$ .....	58
IV. Summary of Values of the Interaction Parameter $e_j^j$ ....	61
V. Summary of the Solubility Products $K'$ and $K$ Calculated by the Interaction Parameter Method.....	63
VI. Summary of the Solubility Products $K'$ and $K$ Calculated Using the Nitrogen Activity Determined from the Gas Phase for the Systems Boron, Vanadium, Columbium, and Tantalum.....	66
VII. Comparison of $K$ Values for the Vanadium System Calculated for Different Values of the Interaction Parameter $e_V^V$ .....	67
VIII. Activity of Silicon in Fe-Si Solutions at 1420°C. From the Data of Chipman <u>et al</u> <sup>(34)</sup> .....	70
IX. Calculated Activity of Silicon in Fe-Si Solutions of 34.0% and 36.7% Silicon at Temperatures from 1420°C to 1700°C.....	72
X. Summary of $K$ Values for the Silicon System Calculated Using the Activity of Silicon Estimated from Fe-Si Binary Data.....	73
XI. Summary of Values of Enthalpy and Entropy of Decomposition of Nitrides in Liquid Iron.....	81
XII. Summary of Results Obtained by the Quenching Method....	90
XIII. Results of Wet Chemical Analysis of Extracted AlN Residue.....	99



LIST OF TABLES CONT'D

Appendices

<u>Table</u>	<u>Page</u>
A-I. Supplier's Analysis of Iron Melting Stock.....	111
A-II. Supplier's Analysis of Aluminum Melting Stock.....	112
A-III. Supplier's Analysis of Boron Melting Stock.....	112
A-IV. Supplier's Analysis of Columbium Melting Stock.....	112
A-V. Supplier's Analysis of Silicon Melting Stock.....	113
A-VI. Supplier's Analysis of Tantalum Melting Stock.....	113
A-VII. Supplier's Analysis of Titanium Melting Stock.....	113
A-VIII. Supplier's Analysis of Vanadium Melting Stock.....	114
A-IX. Supplier's Analysis of Zirconium Melting Stock.....	114
B-I. Comparison Between True and Observed Temperature Scales for the Sieverts Apparatus.....	116
B-II. Comparison Between True and Observed Temperature Scales for the Quenching Apparatus.....	116
C-I. Flowmeter Calibration Data for the Quenching Apparatus.....	118
C-II. Calculated Nitrogen Pressure for Various Combinations of Flowmeter Settings.....	119
G-I. Nitride Compositions Calculated from the Phase Rule Analysis.....	156
H-I. X-ray Data for Titanium Nitride Samples from the Sieverts Apparatus.....	161
H-II. X-ray Data for Aluminum Nitride Samples from the Sieverts Apparatus.....	162
H-III. X-ray Data for Boron Nitride Samples from the Sieverts Apparatus .....	163
H-IV. X-ray Data for Columbium Nitride Samples from the Sieverts Apparatus.....	163

LIST OF TABLES CONT'D

Appendices

<u>Table</u>		<u>Page</u>
H-V.	X-ray Data for Vanadium Nitride Samples from the Sieverts Apparatus.....	164
H-VI.	X-ray Data on Raw Materials Used to Fabricate Nitride Crucibles for the Quenching Method.....	165
I-I.	Calculated Values of $\gamma_j$ for the Titanium, Zirconium, Aluminum, and Boron Systems.....	169
J-I.	Free Energy of Formation of AlN from the Pure Components.....	171

LIST OF FIGURES

<u>Figure</u>		<u>Page</u>
1	Absorption of Nitrogen by an Fe-j Melt.....	14
2	Schematic Diagram of the Sieverts Apparatus.....	27
3	Sieverts Apparatus Reaction Chamber.....	28
4	Relation Between Apparent Hot Volume of Reaction Bulb and Pressure at 1600°C.....	32
5	Schematic Diagram of the Quenching Apparatus.....	36
6	Effect of Titanium on the Solubility of Nitrogen.....	45
7	Effect of Zirconium on the Solubility of Nitrogen.....	46
8	Effect of Aluminum on the Solubility of Nitrogen.....	47
9	Effect of Boron on the Solubility of Nitrogen.....	48
10	Effect of Vanadium on the Solubility of Nitrogen.....	49
11	Effect of Columbium on the Solubility of Nitrogen.....	50
12	Effect of Tantalum on the Solubility of Nitrogen.....	51
13	Effect of Silicon on the Solubility of Nitrogen.....	52
14	Variation of $e_N^{Ti}$ and $e_N^{Zr}$ with Reciprocal Temper- ature.....	54
15	Variation of $e_N^{Al}$ , $e_N^{Cb}$ , $e_N^V$ , and $e_N^{Ta}$ with Recip- rocal Temperature.....	55
16	Variation of $e_N^B$ with Reciprocal Temperature.....	56
17	Variation of $e_N^{Si}$ with Reciprocal Temperature.....	57
18	Activity of Silicon in Binary Fe-Si Solutions at 1420°C.....	69
19	Variation of Equilibrium Constant With Temperature for the Reaction $TiN(s) = \underline{Ti} + \underline{N}$ .....	74
20	Variation of Equilibrium Constant With Temperature for the Reaction $ZrN(s) = \underline{Zr} + \underline{N}$ .....	74
21	Variation of Equilibrium Constant With Temperature for the Reaction $AlN(s) = \underline{Al} + \underline{N}$ .....	75

LIST OF FIGURES CONT'D

<u>Figure</u>		<u>Page</u>
22	Variation of Equilibrium Constant With Temperature for the Reaction $\text{BN}_{(s)} = \underline{\text{B}} + \underline{\text{N}}$ .....	76
23	Variation of Equilibrium Constant With Temperature for the Reaction $\text{VN}_{(s)} = \underline{\text{V}} + \underline{\text{N}}$ .....	77
24	Variation of Equilibrium Constant With Temperature for the Reaction $\text{CbN}_{(s)} = \underline{\text{Cb}} + \underline{\text{N}}$ .....	78
25	Variation of Equilibrium Constant With Temperature for the Reaction $\text{Si}_{3/4}\text{N}_{(s)} = 3/4\underline{\text{Si}} + \underline{\text{N}}$ .....	79
26	Extrapolation of log K' to Zero Percent j in the Aluminum and Boron Systems.....	88
27	Extrapolation of log K' to Zero Percent j in the Vanadium and Columbium Systems.....	89
28	Solubility of Nitrogen in Pure Liquid Iron at 1600°C...	92
29	Variation of Equilibrium Constant With Temperature for the Reactions $\text{TiN}_{(s)} = \underline{\text{Ti}} + \underline{\text{N}}$ , $\text{Ti}_{1.7}\text{N}_{(s)} = 1.7\underline{\text{Ti}} + \underline{\text{N}}$ , and $\text{Ti}_{2.4}\text{N}_{(s)} = 2.4\underline{\text{Ti}} + \underline{\text{N}}$ .....	98
30	Variation of Equilibrium Constant With Temperature for the Reaction $\text{V}_{2.5}\text{N}_{(s)} = 2.5\underline{\text{V}} + \underline{\text{N}}$ .....	100
31	Variation of Equilibrium Constant With Temperature for the Reaction $\text{Cb}_2\text{N}_{(s)} = 2\underline{\text{Cb}} + \underline{\text{N}}$ .....	100

LIST OF FIGURES CONT'D

Appendices

<u>Figure</u>		<u>Page</u>
F-1 - F-6	Nitrogen Absorption Curves for the Titanium System.....	126 - 128
F-7 - F-15	Nitrogen Absorption Curves for the Zirconium System.....	129 - 134
F-16 - F-24	Nitrogen Absorption Curves for the Aluminum System.....	134 - 140
F-25 - F-30	Nitrogen Absorption Curves for the Boron System.....	141 - 146
F-31 - F-35	Nitrogen Absorption Curves for the Vanadium System..	147 - 151
F-36 - F-39	Nitrogen Absorption Curves for the Columbium System.	151 - 153
F-40	Nitrogen Absorption Curve for the Tantalum System...	154
F-41 - F-42	Nitrogen Absorption Curves for the Silicon System...	155
G-1	Phase Rule Analysis of the 0.228% Titanium Nitrogen Absorption Curve.....	157
G-2	Phase Rule Analysis of the 0.318% Titanium Nitrogen Absorption Curve.....	158
G-3	Phase Rule Analysis of the 1.34% Aluminum Nitrogen Absorption Curve.....	159
G-4	Phase Rule Analysis of the 1.57% Aluminum Nitrogen Absorption Curve.....	160

## ABSTRACT

The object of this investigation was to determine the solubility products of several alloy nitrides in the solvent liquid iron at temperatures in the vicinity of 1600°C, the temperature range of steel-making processes. The alloying elements chosen for study were titanium, zirconium, aluminum, boron, vanadium, columbium, tantalum, and silicon. The variables studied were the concentrations of alloying element and nitrogen in the solution from which the nitride was precipitated and the temperature of the solution.

Two experimental approaches were employed, a Sieverts method and a quenching method. In the Sieverts method a liquid iron melt containing a known concentration of alloying element at a known temperature was equilibrated with nitrogen gas at various pressures between zero and one atmosphere. The nitrogen solubility at which a departure from Sieverts' Law appeared was measured. From this nitrogen concentration and the known alloy concentration, the alloy nitride solubility product was calculated. In the quenching method a melt of pure iron was equilibrated at a known temperature under a known partial pressure of nitrogen gas with a crucible made of the alloy nitride whose solubility product was to be measured. The melt was then quenched and analyzed by wet chemical methods for dissolved nitrogen and the alloying element. From these analyses the alloy nitride solubility product was calculated. The composition of the alloy nitride phase was determined primarily by

x-ray analysis. Good agreement of results between the two experimental methods was achieved.

The stability of the nitrides studied in contact with liquid iron at 1600°C was found to decrease in the order TiN, ZrN, AlN, BN, VN, CbN, TaN, and Si<sub>3</sub>N<sub>4</sub>. Only TiN, ZrN, and AlN were found sufficiently stable to contain a liquid iron melt without seriously contaminating it under conditions approaching thermodynamic equilibrium. The solubilities of all nitrides were found to increase with increasing temperature. A thorough investigation of the variables composition and temperature permitted the calculation of the free energy, enthalpy, and entropy of precipitation of the nitrides from liquid iron solution.

The interaction parameter approach proposed by Wagner was found to give a reasonably accurate representation of the activities of the alloying element and nitrogen in liquid iron solution at concentrations up to the nitride solubility limits for all of the alloying elements except silicon.

## I. INTRODUCTION

The solubility of nitrogen in liquid iron alloys and the interaction of nitrogen with dissolved alloying elements in liquid iron has been the subject of a number of research investigations. Most of this work however has been reported for concentrations well below those necessary for the formation of the alloy nitride phase. Data in the concentration region near the solubility limit of the alloy nitride, particularly for systems exhibiting stable nitrides, are important for at least two purposes not served by data taken in the dilute concentration region. First they are necessary in evaluating the denitrifying power of various alloying elements in a metal bath. Second they are necessary in determining the stability of a given nitride if it is used as a refractory to contain liquid iron alloys. This latter application of nitrides in particular has recently been receiving considerable attention.



## II. SURVEY OF PREVIOUS WORK

### A. Solubility of Nitrogen in Pure Liquid Iron and Adherence of Dilute Alloys to Sieverts' Law

The published work of the past twenty-five years on the solubility of nitrogen in pure liquid iron at one atmosphere nitrogen pressure and 1600°C has been well summarized by Pehlke and Elliott.<sup>(1)</sup> They present solubility values in weight per cent nitrogen dissolved from nineteen different researches. The solubility values range from 0.030% up to 0.055% with the majority lying between 0.040% and 0.050%. Values have been measured by both the Sieverts method and the sampling method and no trend depending on the experimental method is apparent. The same researches show the temperature coefficient of nitrogen solubility to be small and positive ranging generally between zero and  $3 \times 10^{-5}$  weight per cent nitrogen per degree centigrade.

A number of investigations have also been carried out to determine the effect of nitrogen pressure on solubility both in pure liquid iron and in various liquid alloys. It is universally agreed that for pure iron and sufficiently dilute alloys this can be expressed by the well known Sieverts' Law relation:

$$\text{wt. \%N} = C \sqrt{P_{N_2}} \quad (1)$$

Pehlke and Elliott<sup>(1)</sup> have tested this relationship at nitrogen pressures from 0.5 to 1.0 atmospheres for pure liquid iron at 1600°C and for alloys of about 10% chromium, tantalum, tungsten and cobalt and find that it holds quite accurately. Humbert and Elliott<sup>(2)</sup> have found

that it holds over the same pressure range in Fe-Cr alloys up to 57% Cr. However they find deviations for alloys of 61% Cr and above in which wt. %N ceases to be proportional to  $\sqrt{P_{N_2}}$ . Kashyap and Parlee<sup>(3)</sup> made repeated measurements on pure iron at 1600°C between nitrogen pressures of 50 and 750 mm and found adherence to Sieverts' Law with reasonably good reproducibility in the value of the constant C. Their results substantiate the work of Kootz<sup>(4)</sup> who also verified Sieverts' Law in pure iron at 1600°C at nitrogen pressures between 0.2 and 1.0 atmospheres. Brick and Creevy<sup>(5)</sup> made measurements on liquid Fe-Cr alloys and on pure liquid chromium at 1 atmosphere and 2 atmospheres nitrogen pressure. They state that both these alloys follow Sieverts' Law with values for C of 0.85 for an Fe-34% Cr alloy and 0.9 for pure chromium where the units of C are weight per cent  $\frac{N}{(atm.)^{1/2}}$ . However the fact that nitrogen solubilities were determined for only two nitrogen pressures and the fact that the equilibration temperatures were not well known makes these conclusions questionable, particularly in view of the fact that they conflict with the apparently more accurate measurements of Humbert and Elliott.<sup>(2)</sup>

Finally Schenk, Froberg, and Graf<sup>(6)</sup> have verified Sieverts' Law in pure iron at 1600°C between nitrogen pressures of 0.3 and 1.0 atmospheres. They have also determined the effect of additions of carbon, molybdenum, sulfur, and silicon on the value of C. They show a nearly linear decrease in C up to 3% S, 5% C, and 12% Si, and a nearly linear increase in C up to 13% Mo. This indicates that no nitrides were formed at these compositions since formation of a nitride presumably would have caused a discontinuous change in the value of C at the composition at which the nitride formed.

B. Nitride Solubility Products  
in Liquid and Solid Iron

Although several authors have calculated solubility products of nitrides in iron using thermodynamic data derived from various sources, the number of reported experimental attempts to measure them is small. Chipman<sup>(7)</sup> presents calculated values of the denitrifying constant  $K' = \%j \times \%N$  for six nitrides which are reproduced in the following table.

TABLE I

SUMMARY OF DENITRIFYING CONSTANTS  
ESTIMATED BY CHIPMAN<sup>(7)</sup>

Element j	Compound	Constant K'	Value at 1600°C
Al	AlN	$\%Al \times \%N$	0.55
Si	Si <sub>3</sub> N <sub>4</sub>	$(\%Si)^{3/4} \times \%N$	14.
Ti	TiN	$\%Ti \times \%N$	0.00014
V	VN	$\%V \times \%N$	1.5
B	BN	$\%B \times \%N$	like Al
Zr	ZrN	$\%Zr \times \%N$	like Ti

Chipman admits these are "rough estimates" made from data on the free energies of formation of the compounds from the pure elements and the free energies of solution of the pure components in liquid iron.

Pearson and Ende<sup>(8)</sup> present calculated plots of standard free energies of formation of various nitrides from their pure components at temperatures of 1800°C and below derived from thermodynamic data calculated by Kelley<sup>(9)</sup> and others. Pearson and Ende's results are significant in

that the nitrides follow about the same order of increasing stability and their assumed compositions are the same as in Table I.

Several experimentors who have investigated the effect of various alloying elements on the solubility of nitrogen in liquid iron have reported the appearance of solid phases, possibly nitrides, at sufficiently high alloy concentrations. Maekawa, Nakagawa, and Yanagawa<sup>(10)</sup> who have made solubility measurements of nitrogen in Fe-Al and Fe-Ti alloys report the appearance of a solid phase on top of the melt at alloy contents of 0.3% Ti and 8.0% Al at 1700°C under one atmosphere of nitrogen. They state that at 1600°C sufficient solid phase formed to make solubility measurements in the liquid Fe-Ti and Fe-Al alloys impossible. They suggest that these phases were presumably TiN and AlN but made no attempt to measure their solubility products. Their statements are contrasted with the statements of Pehlke and Elliott<sup>(1)</sup> who at 1600°C noted a solid phase appearing on top of Fe-Al melts containing greater than 0.5% Al under one atmosphere nitrogen pressure and who were unable to measure any solubility of nitrogen in Fe-Ti melts at one atmosphere nitrogen pressure because of the formation of a solid phase at very low Ti contents.

Pehlke<sup>(11)</sup> reports values for solubility products of titanium and zirconium nitrides at 1600°C as follows:

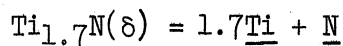
$$\text{for TiN } K' = \%Ti \times \%N = 0.000112$$

$$\text{for ZrN } K' = \%Zr \times \%N = 0.00726$$

These values were calculated from chemical analyses made on ingots which had been equilibrated with one atmosphere of nitrogen gas in a Sieverts' Apparatus. The original aim of these equilibrations was to determine

the interaction parameters of titanium and zirconium with nitrogen in liquid iron but a solid phase appeared on the melt and interfered.

The most comprehensive experimental determination of nitride solubility products in liquid iron has been reported by Rao and Parlee.<sup>(12)</sup> They used a Sieverts' method to measure the weight per cent nitrogen absorbed by melts of Fe-V and Fe-Ti as the nitrogen pressure varied between zero and one atmosphere. They report adherence to Sieverts' Law in alloys of 10% and 20% vanadium up to one atmosphere nitrogen pressure at 1760°C but state that this high equilibration temperature was necessary because the melt tended to solidify at lower temperatures. The "solidification" they observed may well have been the formation of vanadium nitride. With Fe-Ti alloys of 0.5% to 0.8% Ti they determined the solubility product of titanium nitride by measuring the nitrogen concentration at which the nitrogen absorption curve departs from Sieverts' Law. They attempted to calculate the composition of the nitride formed by fitting a Sieverts' Law line for pure iron to the high pressure end of their absorption curves and extrapolating the pure iron line down to zero pressure to determine the weight of nitrogen in the precipitated nitride. They report the following results at 1600°C:



$$K' = (f_{\text{Ti}} \cdot \% \text{Ti})^{1.7} \times (f_{\text{N}} \cdot \% \text{N}) = 0.0020$$

The method appears very ingenious and useful but the quantity and accuracy of their data leave something to be desired. Specifically there

are not sufficient data points to determine precisely enough the shape of the nitrogen absorption curves.

Fountain and Chipman<sup>(13)</sup> have used the same method to determine the solubility product of vanadium nitride in solid iron. They indicate that different points of deviation from Sieverts' Law can be determined depending on whether the nitrogen pressure is being increased or reduced. They offer several possible explanations for this, among them the existence of vanadium nitride of more than one composition and the possibility of non-equilibrium existing above the solubility limit.

### C. Nitride Phase Compositions

A number of nitrides are known or suspected to exist over a range of compositions. For several evidence of a systematic variation of composition with lattice parameter is known.

Ehrlich<sup>(14)</sup> has studied the variation of lattice parameter with composition in titanium nitride produced by heating pure titanium powder in a nitrogen gas atmosphere. He finds that  $TiN$ , which has the NaCl structure, can exist over the range  $TiN_{0.42}$  to  $TiN_{1.1}$ . It exhibits a maximum lattice parameter of  $4.23\overset{\circ}{A}$  corresponding to a composition of  $TiN$ . As the Ti/N ratio varies from 1.0 in either direction the lattice parameter decreases. He also states that titanium nitride has a defect structure with about 4% of the lattice points unoccupied for the composition  $TiN$ .

Chiotti<sup>(15)</sup> reports results of x-ray measurements and chemical analyses on nitrides of titanium, tantalum, and zirconium. He gives a lattice constant of  $4.23\overset{\circ}{A}$  for a nitride which analyzed chemically 77.4% Ti

and 20.1% N . This corresponds to  $TiN_{0.89}$  . He reports that tantalum nitride is hexagonal with  $a = 3.04\overset{\circ}{\text{Å}}$  and  $c/a = 1.62$  and suggests that its composition may vary between  $TaN$  and  $Ta_2N$  . He reports a zirconium nitride phase of 10.45% nitrogen calculated from a weight gain of zirconium metal heated to 1500°C in a nitrogen atmosphere which has a lattice parameter of  $4.57\overset{\circ}{\text{Å}}$ . This corresponds to a composition of  $Zr_{1.3}N$  . He suggests that this nitride phase is composed of the nitride  $ZrN$  with the NaCl structure and a hexagonal metal phase of zirconium containing nitrogen in solid solution. This contention is also supported by Domagala, McPherson, and Hanson<sup>(16)</sup> who find practically no variation in lattice parameter ( $4.567\overset{\circ}{\text{Å}}$  to  $4.569\overset{\circ}{\text{Å}}$ ) for zirconium nitride phases ranging from 10.5% to 13.5% nitrogen but find  $\alpha$  zirconium lines of increasing intensity in the nitride x-ray pattern as the nitrogen content drops. They suggest also that the  $ZrN$  phase may vary in composition on the metal-rich side as far as  $ZrN_{0.46}$  and make no effort to predict the nitrogen-rich boundary.

Hahn<sup>(17)</sup> has studied the vanadium-nitrogen system and found two nitrides,  $VN$  with the NaCl structure and  $VN_{0.37-0.43}$  with a hexagonal structure, both of which exist over a composition range. He gives the following data on the composition limits:

Upper Boundary		Lower Boundary	
$VN_{1.00}$	$a = 4.126\overset{\circ}{\text{Å}}$	$VN_{0.71}$	$a = 4.064\overset{\circ}{\text{Å}}$
$VN_{0.43}$ (10.5%N)	$a = 2.835\overset{\circ}{\text{Å}}$	$VN_{0.37}$ (9.3%N)	$a = 2.831\overset{\circ}{\text{Å}}$
	$c = 4.541\overset{\circ}{\text{Å}}$		$c = 4.533\overset{\circ}{\text{Å}}$

This agrees with Fountain and Chipman<sup>(13)</sup> who found two vanadium nitrides existing in solid iron and gave their nominal compositions as VN and V<sub>2</sub>N.

Schonberg has studied the systems niobium-nitrogen<sup>(18)</sup> and tantalum-nitrogen<sup>(19)</sup>. In the niobium-nitrogen system he finds four different nitride phases in addition to a metal phase containing dissolved nitrogen. He gives x-ray lattice parameter and crystal structure data on the nitrides and assigns them the following compositions:

NbN<sub>1.00</sub> (hexagonal), NbN<sub>~0.95</sub> (hexagonal-close packed), NbN<sub>~0.80 - ~0.90</sub> (WC type), NbN<sub>0.40 - 0.50</sub> or Nb<sub>2</sub>N (metal atoms hexagonally close packed with N interstitially dissolved). In the tantalum-nitrogen system he again finds four nitride phases in addition to a practically pure metal phase. He assigns the nitride phases the compositions TaN<sub>~0.05</sub>, TaN<sub>~0.40 - ~0.45</sub>, TaN<sub>0.80 - 0.90</sub>, and TaN.

Finally Taylor and Lenie<sup>(20)</sup> have investigated the properties of aluminum nitride. They state that the Al/N ratio in pure nitride has the stoichiometric composition AlN but that the material often contains some Al<sub>2</sub>O<sub>3</sub> or Al<sub>2</sub>OC. They state that AlN is hexagonal with  $a = 3.111 \text{ \AA}$  and  $c = 4.980 \text{ \AA}$ . This agrees with the data of Paretzkin<sup>(21)</sup> who gives the values  $a = 3.114 \text{ \AA}$  and  $c = 4.986 \text{ \AA}$ .



### III. OUTLINE OF THE PROBLEM

#### A. General

The problem may be simply stated in thermodynamic terms as the determination of the solubility product of various alloy nitrides in liquid iron. The two important variables to be dealt with are the composition of alloying element and nitrogen at which the nitride is formed and the temperature. A thorough investigation of these should permit the derivation of all the thermodynamic functions of the nitride systems.

#### B. Systems Chosen For Experimentation

In selecting suitable systems for experimental investigation a natural starting point is those systems which previous investigators have noted as forming a solid phase, possibly nitride, in the presence of nitrogen while in solution in liquid iron. In this category are aluminum, titanium, zirconium, columbium, and vanadium. Two other elements silicon and boron were known to form stable nitrides in the pure state, although there was no experimental evidence as to whether or not these nitrides were stable in the presence of liquid iron.

On examining this list it is seen to contain a majority of elements which markedly increase the solubility of nitrogen in liquid iron. Two others known to have this property are tantalum and chromium. However published data on the solubility of nitrogen in pure liquid chromium indicate no formation of a chromium-nitride phase. The nitride would then certainly be unstable in liquid iron-chromium alloys so this system was disregarded. These eight systems aluminum, silicon, titanium, zirconium,

boron, columbium, vanadium and tantalum form the experimental basis of the research.

### C. Experimental Methods

The relative merits and demerits of the two basic methods of investigating the thermodynamic equilibrium between a gas phase and a liquid metal phase, the Sieverts method and the quenching or sampling method, have been the subject of considerable discussion. The choice between the two is normally determined by the system to be studied. Some of the factors to be considered in this choice are discussed in a later section.

In this research both methods were employed in order to give a comparison of results in several systems. Primary emphasis was placed on the Sieverts method since by this method more variables could be tested in a single determination. However the fact that the equilibrium measurements were to be made in the presence of a solid nitride phase permitted the quenching method to be used employing a nitride crucible to contain the melt. This eliminated one of the main drawbacks to the Sieverts method, the necessity of holding the melt in an oxide crucible with the resultant possibility of oxygen contamination.

### D. Possible Methods of Correlating the Experimental Results

1. Determination of the nitride solubility limit by measuring the point of departure of the gas solubility from Sieverts' Law

The method of determining the solubility limit of an alloy nitride phase by equilibrating the system with various partial pressures of nitrogen and locating the dissolved nitrogen concentration at which

the solution departs from the Sieverts Law relation has been applied by Fountain and Chipman<sup>(13)</sup> to solid iron alloys and by Rao and Parlee<sup>(12)</sup> to liquid iron alloys. The method however necessarily contains assumptions, and failure to carefully note these assumptions when the method is applied to an experimental system can lead to errors. An analysis of the method according to the phase rule is helpful in pointing out these assumptions.

Let the following definitions be adopted.

U = the total number of independent variables necessary to specify a system in equilibrium under a given set of conditions with constant temperature and pressure throughout the system.

N = the number of chemical individuals in the system.

G = the number of independent distribution relations between concentrations of the same chemical individual distributed between different phases.

E = the number of additional independent relations among chemical individuals.

P = the number of phases in the system. A phase is defined as any homogenous portion of matter bounded by a physical surface, not necessarily continuous.

C = the number of components in the system, defined by  
 $C = N - E$ .

V = the degrees of variance of the system, the difference between the number of variables U and the total number of independent conditions relating them.

The phase rule may then be expressed in either of the following two forms:

$$V = U - G - E \quad (2)$$

$$V = C + 2 - P \quad (3)$$

Let this formulation of the phase rule be applied to the system of a melt of liquid iron at temperature T containing a dissolved alloying element

$j$  in equilibrium with nitrogen gas at pressure  $P_{N_2}$ . The notation  $\underline{j}$  and  $\underline{N}$  will be used to signify alloying element  $j$  and nitrogen in solution in liquid iron. The respective concentrations by weight of  $\underline{j}$  and  $\underline{N}$  will be signified by  $\%j$  and  $\%N$ . The solid nitride phase precipitated from solution by  $j$  and  $N$ , of unknown composition, will be designated  $j_x N$ .

Three different cases must be considered:

Case 1 - at  $\%j$  and  $\%N$  below the solubility limit of  $j_x N$ .

System: gas phase containing  $N_2$ ; liquid phase containing Fe,  $\underline{j}$ , and  $\underline{N}$ ;

$$N = 4, G = 0, P = 2, U = 4,$$

$E = 1$  - the Sieverts Law relation between  $P_{N_2}$  in the gas phase and  $\%N$  in the liquid phase which may be written  $\%N = C \sqrt{P_{N_2}}$

From Equation (2) or (3):

$$V = 4 - 0 - 1 = 3 \text{ or } V = (4-1) + 2 - 2 = 3$$

If  $T$  and the total  $\%j$  in the system are fixed by experimentally imposed conditions, in terms of the above defined quantities adding two more relations  $E$ , then  $V = 1$ . This means that for each value of  $P_{N_2}$  there is a discrete  $\%N$  in accordance with the experimentally observed fact that  $\%N = C \sqrt{P_{N_2}}$  which is called Sieverts' Law. This case is shown by line segment a in Figure 1 where the slope of the line segment is characteristic of the element  $j$  and the  $\%j$ .

Case 2 - at  $\%j$  and  $\%N$  slightly above the solubility limit of  $j_x N$  but close enough to the solubility limit that the following assumptions hold:

- a.  $j_x N$  has a fixed composition, i.e.  $x$  does not change during the course of the precipitation.

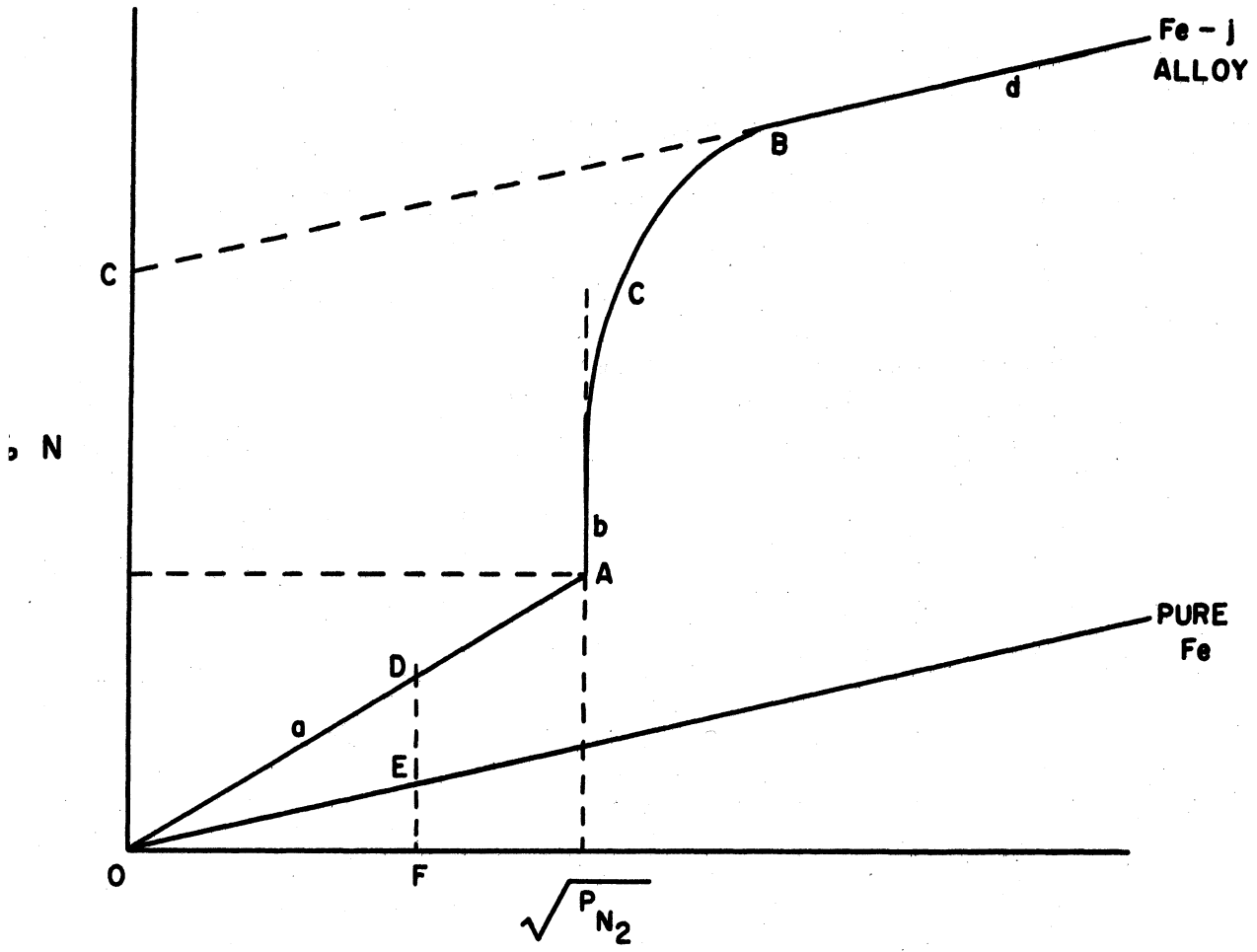


Figure 1. Absorption of Nitrogen by an Fe-j Melt.

- b. The weight of  $j$  in  $j_x N$  is negligible compared to the weight of  $j$  in the liquid phase.

System: gas phase containing  $N_2$ ; solid phase containing  $j_x N$ ; liquid phase containing Fe,  $j$ , and  $N$ ;

$$N = 5, G = 0, P = 3, U = 4$$

$$E = 2 - \%N = C \sqrt{P_{N_2}} \quad \text{and} \quad K = \%j \times \%N$$

$$V = 2$$

If  $T$  and total  $\%j$  are fixed,  $V = 0$ . This means that only one  $\%N$  and  $P_{N_2}$  are permitted. In terms of Figure 1 where the ordinate is the total  $\%N$  in the solid and liquid phases, not just the  $\%N$  in the liquid phase, the curve must follow a vertical or constant pressure line as in region b.

However before the precipitation of  $j_x N$  has proceeded very far either or both of the assumptions made in case 2 may break down resulting in an increase in  $V$ . If  $x$  varies as the precipitation of  $j_x N$  proceeds then one of the conditions  $E$  becomes invalid resulting in  $V = 1$ . Or if sufficient  $j_x N$  precipitates so that the weight of  $j$  used up becomes appreciable then the fixing of the total  $\%j$  does not fix  $\%j$ . Since total  $\%j$  is not one of the variables  $U$ , a condition  $E$  is again lost and  $V = 1$ . Thus for either or both of these reasons the absorption curve in Figure 1 may begin to deviate from vertical as the precipitation of  $j_x N$  proceeds. This is shown in region c.

Case 3 - at  $\%N$  far enough above the solubility limit of  $j_x N$  and with  $j_x N$  sufficiently insoluble that the concentration of  $j$  in the liquid phase is negligible.

System: gas phase containing  $N_2$ ; solid phase containing  $j_x N$ ; liquid phase containing Fe and  $\underline{N}$ ;

$$N = 4, G = 0, P = 3, U = 3$$

$$E = 1 - \%N = C \sqrt{P_{N_2}}$$

$$V = 2$$

If  $T$  and total  $\%j$  are fixed  $V = 1$ . Again there is a discrete  $\%N$  for each  $P_{N_2}$  and these are related by the Sieverts Law relation  $\%N = C \sqrt{P_{N_2}}$  as shown by the line segment  $d$  in Figure 1 where now the slope of  $d$  approaches the slope of the Sieverts Law line of nitrogen in pure liquid iron. By extrapolating the line segment  $d$  back to  $P_{N_2} = 0$  and finding its intercept  $C$  on the ordinate the weight of nitrogen contained in the phase  $j_x N$  can be found. From this and the initially fixed total  $\%j$  in the system the composition of  $j_x N$  (i.e. the value of  $x$ ) can be found. This however is only an average composition. It should be noted that it is quite possible for the value of  $x$  to change between point  $A$  and point  $B$ . It is also possible that the nitride might be a complex containing iron of the type  $(Fe, j)_x N$  in which case this method obviously cannot be used to calculate even its average composition.

The  $\%N$  at  $A$ , the  $\%j$  in the system, and the calculated composition of  $j_x N$  if it is the same as the composition at  $A$ , permit calculation of the weight percent solubility product  $K'$  where:

$$K' = (\%j)^x \cdot (\%N) \quad (4)$$

for the reaction:



The value of  $K'$  will vary systematically with  $\%j$  and  $\%N$ . In order

to calculate the solubility product  $K$  which is a true constant at constant temperature it is necessary to take into account the Fe-j-N interactions in liquid solution.

## 2. Wagner's method of interaction parameters

Wagner<sup>(22)</sup> has suggested representing the activity coefficient of a solute 1 in a solvent also containing solutes 2,3,4,... by the following equation:

$$\ln \gamma_1 = \ln \gamma_1^0 + \left( \frac{\partial \ln \gamma_1}{\partial X_1} \right) X_1 + \left( \frac{\partial \ln \gamma_1}{\partial X_2} \right) X_2 + \left( \frac{\partial \ln \gamma_1}{\partial X_3} \right) X_3 + \left( \frac{\partial \ln \gamma_1}{\partial X_4} \right) X_4 + \dots \quad (6)$$

where  $\gamma_i$  is the activity coefficient of component  $i$  based on Raoult's Law with the standard state pure  $i$ , the infinitely dilute solution,  $\gamma^0$  is the activity coefficient at infinite dilution, and  $X_i$  is the mole fraction of  $i$  in solution. He then defines the interaction parameter  $\epsilon_i^j$  by:

$$\epsilon_i^j = \frac{\partial \ln \gamma_i}{\partial X_j} \quad (7)$$

The corresponding equation for the activity coefficient based on Henry's Law with the activity equal to the weight per cent at infinite dilution is:

$$\log f_1 = \frac{\partial \log f_1}{\partial \%1} \cdot \%1 + \frac{\partial \log f_1}{\partial \%2} \cdot \%2 + \frac{\partial \log f_1}{\partial \%3} \cdot \%3 + \dots \quad (8)$$

and for the interaction parameter:

$$\epsilon_i^j = \frac{\partial \log f_i}{\partial \%j} \quad (9)$$

The solubility product of  $j_x N$  in liquid iron may be written:

$$K = \frac{(a_j)^x a_N}{a_{j_x N}} = (\%j)^x (f_j)^x (\%N) (f_N) \quad (10)$$



where  $a_{\underline{j}}$  and  $a_{\underline{N}}$  are the activities of  $\underline{j}$  and  $\underline{N}$  in liquid solution,  $a_{j_x N}$  is taken as one since  $j_x N$  is assumed pure, and the other quantities are as previously defined. Now using the representation of Equations (8) and (9) for  $f_{\underline{j}}$  and  $f_{\underline{N}}$  in Equation (10) and taking  $x = 1$  gives:

$$\log K = \log K' + e_{\underline{j}}^j(\% \underline{j}) + e_{\underline{j}}^N(\% \underline{N}) + e_{\underline{N}}^N(\% \underline{N}) + e_{\underline{N}}^j(\% \underline{j}) \quad (11)$$

where  $K'$  is given in Equation (4). If the reference state is taken as the infinitely dilute solution of nitrogen in pure liquid iron then  $f_{\underline{N}}$  is defined by:

$$\lim_{\% \underline{N} \rightarrow 0} (a_{\underline{N}} / \% \underline{N}) = f_{\underline{N}} = 1 \quad (12)$$

As a result of this reference state and the fact that nitrogen obeys Sieverts' Law in Fe-N solutions the activity coefficient of nitrogen in Fe-j-N solutions is given by:

$$f_{\underline{N}} = \left[ \frac{(\% \underline{N})_{\text{pure Fe}}}{(\% \underline{N})_{\text{alloy}}} \right]_{P_{N_2}, T} \quad (13)$$

In Figure 1  $f_{\underline{N}}$  is represented by the ratio EF/DF which is obviously independent of what  $P_{N_2}$  is chosen. As a result of the fact that nitrogen obeys Sieverts' Law in Fe-j-N solutions below the solubility limit of  $j_x N$  the interaction parameter  $e_{\underline{N}}^N$  in Equation (11) is zero.

The interaction parameter  $e_{\underline{N}}^j$  may be found from the slopes of the Sieverts Law lines of a series of plots like Figure 1 for various  $\% \underline{j}$ . The  $f_{\underline{N}}$  calculated by Equation (13) at some  $P_{N_2}$  is plotted on a log scale against  $\% \underline{j}$  and the slope of this curve is  $e_{\underline{N}}^j$ .  $e_{\underline{N}}^N$  may then be found from the Wagner reciprocity relation derived from the Gibbs-

Duhem Equation which says that in dilute solution:

$$\epsilon_i^j = \epsilon_j^i \quad (14)$$

and:

$$e_i^j = e_j^i \frac{M_i}{M_j} \quad (15)$$

where  $M_i$  and  $M_j$  are the molecular weights of  $i$  and  $j$ .

The interaction parameter  $e_j^j$  can not be found directly from the nitrogen absorption curves in the Fe-j-N system. It is a property of the binary system Fe-j and is a measure of how fast the activity of  $j$  departs from Henry's Law as the  $\%j$  increases in the Fe-j binary.

### 3. Approximation of $e_j^j$ from data on the Fe-j-N ternary

With sufficient data on the variation of  $K'$  with  $\%j$  it is possible to find an approximate value of  $e_j^j$  by a trial and error method. From Equation (11) it can be seen that the variation of  $K'$  with  $\%j$  and  $\%N$  depends on the signs and relative magnitudes of  $e_j^N$ ,  $e_N^j$ , and  $e_j^j$ . Since  $e_j^N$  and  $e_N^j$  are available from the nitrogen absorption curves it is possible to assume a value for  $e_j^j$  and use this along with several experimental values of  $\%j$  and  $\%N$  to calculate a series of  $K$  values from Equation (11). If these values of  $K$  still show a systematic variation with  $\%j$  or  $\%N$  then this must be due to error in the assumed value of  $e_j^j$ . The assumed value is corrected, the direction of the correction being determined by the direction of the variation in  $K$  with  $\%j$  and the sign of  $e_N^j$  and  $e_j^N$ , and the  $K$  values are recalculated. This is repeated until there is no longer an observable systematic variation of

K with  $\%j$ . The variation in K then remaining is assumed to be experimental and the value assumed for  $e_j^j$  the true one. Obviously a fair number of values of  $\%j$  and  $\%N$  are necessary to insure reasonable accuracy in  $e_j^j$ .

#### 4. Estimation of $j$ activity from the Fe-j binary

If the nitride  $j_xN$  is quite soluble it may require quite high  $\%j$  to precipitate it. Thus the solution may become so concentrated in  $j$  that  $e_j^j$  can no longer be considered even approximately constant. The same condition applies to a system in which the activity of  $j$  in the Fe-j binary departs greatly from Henry's Law at low  $j$  concentrations. In such a case it may be more accurate to approximate the activity of  $j$  in the Fe-j-N ternary solution by the activity of  $j$  in the Fe-j binary at the same  $j$  concentration. Of course care must be taken to express all the activities relative to the same standard state. The binary  $j$  activity may then be corrected for the effect of  $N$  on it by means of the term  $e_j^N(\%N)$ .

This effect is often negligible since in systems in which the  $j$  concentration in equilibrium with  $j_xN$  is high the  $N$  concentration is likely to be correspondingly low making the term  $e_j^N(\%N)$  small.

#### 5. Determination of the $N$ activity from the gas phase

It is also possible in the case of a very soluble nitride phase that the  $j$  concentration in equilibrium with it may be high enough that  $e_N^j$  may not be approximated as constant. This can introduce considerable error since  $e_N^j$  must be multiplied by  $\%j$  which is large. In this case a more exact method of estimating the  $N$  activity in the solution may be

employed since this is fixed by the  $P_{N_2}$  in the gas phase. According to Equation (13):

$$[a_N]_{P_{N_2}, T} = [\%N \times f_N]_{P_{N_2}, T} = [(\%N)_{\text{pure Fe}}]_{P_{N_2}, T} \quad (16)$$

So the activity of  $\underline{N}$  in equilibrium with a solid nitride phase is equal to the equilibrium  $\%N$  in pure liquid iron at the same equilibrium  $P_{N_2}$ . This method of course requires accurate determination of the equilibrium Sieverts Law line for nitrogen in pure liquid iron at temperature  $T$ .

6. Determination of  $K$  by the extrapolation of  $K'$  to zero  $\%j$

An alternative method to Equation (11) of finding  $K$  from  $K'$  is to plot values of  $\log K'$  versus  $\%j$  and extrapolate with a straight line to zero  $\%j$ . As  $\%j$  approaches zero the terms  $e_j^j(\%j)$  and  $e_N^j(\%j)$  also approach zero. Therefore again in this method of analysis the term  $e_j^N(\%N)$  must be neglected, after which Equation (11) yields:

$$\lim_{\%j \rightarrow 0} \log K = \log K' \quad (17)$$

In order to insure that the term  $e_j^N(\%N)$  is negligible the values of  $K'$  must be at large  $\%j$ . This requires a graphical extrapolation over a fairly wide range of  $\%j$ .

#### IV. EXPERIMENTAL METHODS AND PROCEDURES

##### A. Comparison of Sieverts Method and Quenching Method

There are basically only two experimental methods available for the study of gas-liquid metal phase equilibria because of the high equilibration temperatures normally required. In the Sieverts method the equilibration is made in a closed system with the measurement of the volume of gas absorbed by the liquid metal being made directly at the equilibration temperature. In the quenching or sampling method the equilibration is usually made in an open system and the liquid metal phase is then sampled or quenched in such a way that the gas solubility representative of the equilibration temperature is preserved during solidification and cooling of the metal to room temperature for subsequent analysis. Both methods contain inherent and unavoidable sources of error. The choice between them is normally determined by the particular gas and liquid alloy to be studied.

In this research both the Sieverts method and the quenching method were employed in order to gain a comparison of the effectiveness of the two different methods in the systems under consideration. The advantages and disadvantages of each method may be briefly summarized in tabular form.

TABLE II

ADVANTAGES AND DISADVANTAGES  
OF THE SIEVERTS METHOD

Advantages:

1. There is a positive measure of the approach of the system to equilibrium.
2. The gas solubility measurement is made directly under the equilibration conditions.
3. Several of the variables temperature, nitrogen pressure, and composition may be varied over fairly wide ranges during a single determination.
4. There is no necessity to place primary dependence for determination of liquid phase composition on chemical analyses.

Disadvantages:

1. The system must be held for an extended period at pressures below one atmosphere. This can cause vaporization of volatile components out of the melt.
2. The melt is held in an oxide crucible. This presents the possibility of melt-crucible reaction contaminating the melt, particularly with oxygen.

Quenching Method

Advantages:

1. The system remains always at a total pressure of one atmosphere, minimizing vaporization from the melt and permitting measurements to be made on a liquid alloy containing one or more volatile components.
2. The melt is held in a nitride crucible which reduces the possibility of oxygen contamination.

Disadvantages:

1. Since the gas solubility in the liquid phase usually changes with temperature the amount of gas dissolved may change during the quenching.

TABLE II  
(CONT'D)

2. There is the possibility of contaminating the melt by reaction with the quenching medium.
3. The partial pressure of the active gas can be controlled only by diluting it with an inert gas. This means that the accuracy of the nitrogen partial pressure depends on the accuracy of the metering system and introduces the possibility of error through thermal diffusion in the gas phase.
4. When the entire melt is quenched only a single set of values of the temperature, nitrogen pressure, and composition may be studied in a single determination.

The most important source of error in the Sieverts method is the possibility of metal vaporizing out of the melt while the system is being equilibrated at pressures below one atmosphere, causing metal powder to deposit on the cooler walls of the reaction bulb. This introduces three important errors. First it changes the hot volume of the reaction bulb during the course of the experiment. Second the experimental gas may react chemically with or become adsorbed on the fine metal powder causing an apparent increase in the measured solubility. Third and most important, vaporization changes the composition of the melt. A small change in melt composition can have a large effect on the solubility of the experimental gas, particularly if the volatile component being lost is present as a dilute solute. These effects are more pronounced in using the Sieverts method to measure the solubility limit of a nitride phase than in simply making a nitrogen determination under atmospheric pressure of nitrogen. This is due to the necessity of varying the nitrogen pressure over a wide range below atmospheric pressure and to the much longer equilibration times required by the presence of the nitride phase.

Another error which may be encountered with the Sieverts method is a reaction between melt and crucible. Since the crucible material is an oxide, in this study  $\text{Al}_2\text{O}_3$  or  $\text{ZrO}_2$ , this can introduce into the melt oxygen as well as Al, Zr, or some other element present in the crucible. These elements may all effect the apparent nitrogen solubility. The effect of oxygen is particularly serious since Pehlke and Elliott<sup>(1,23)</sup> have shown that small amounts of oxygen have a strong retarding effect on the kinetics of nitrogen solution as well as a decreasing effect on the solubility. If the oxygen content of the melt is too high it is possible for the approach to equilibrium to be so slow that the equilibrium nitrogen solubility is not reached in an experimentally reasonable time. The absorption of oxygen by the melt from the crucible can occur even if there is no chemical reaction since the crucible surface generally contains adsorbed oxygen which is impossible to remove even by long outgassing at a high temperature.

The most important source of error in the quenching method is the possibility that the gas content of the metal may change appreciably during quenching due to the change in equilibrium gas solubility with temperature. In particular the phase change from liquid to solid may have a large effect on the gas solubility. The avoidance of this error simply requires a rapid enough quench to maintain in metastable equilibrium the gas solubility representative of the equilibration temperature. The loss of gas by solid state diffusion after quenching is negligible in the case of nitrogen although it might become appreciable in the case of a more rapidly diffusing gas such as hydrogen.

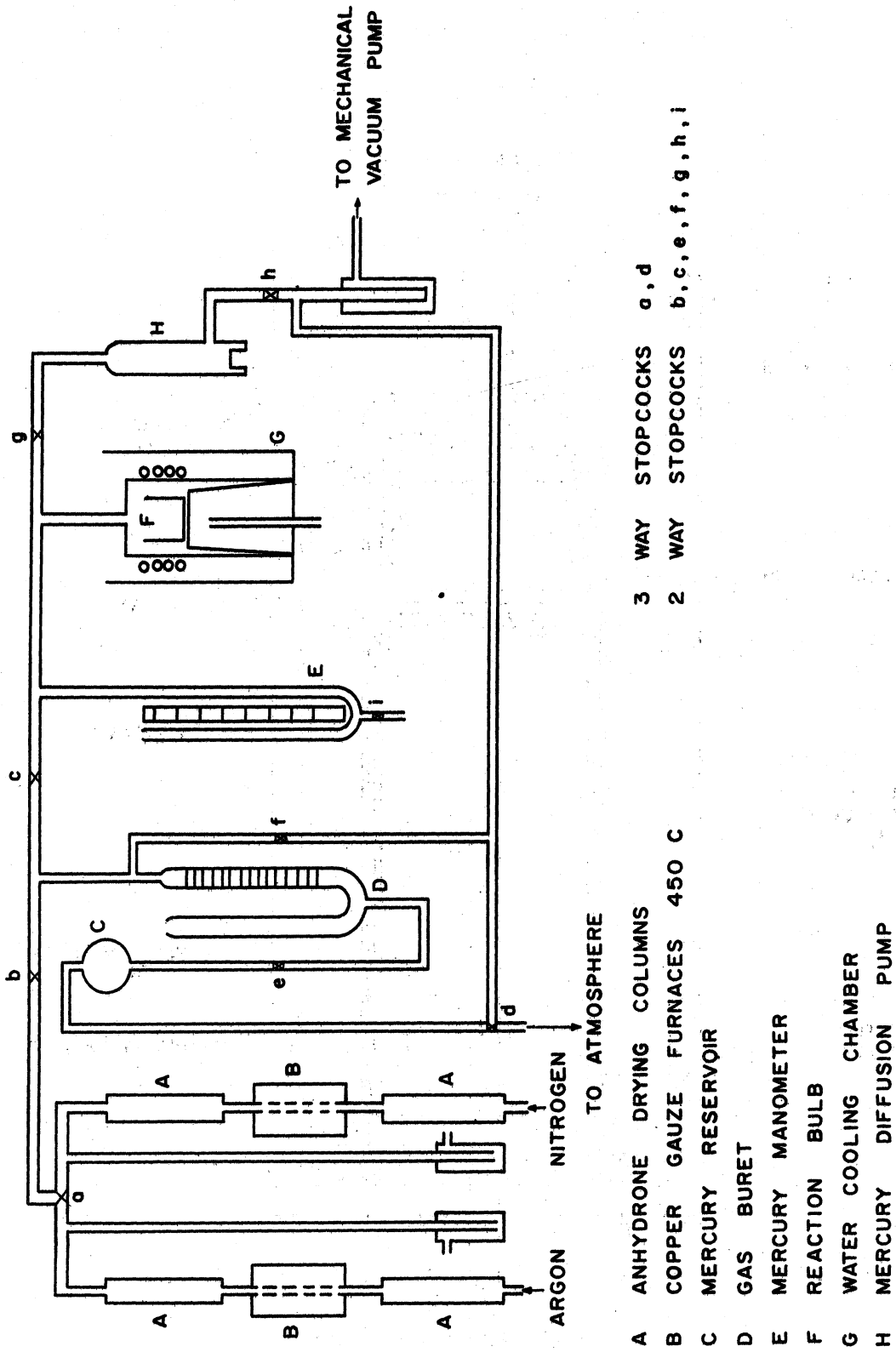


Since the composition of the metal phase cannot be determined directly with the quenching method as it can with the Sieverts method, reliable methods of chemical analysis are a necessity.

#### B. Experimental Procedure for the Sieverts Method

In the Sieverts method the equilibration is carried out in a closed system with a measured volume of purified nitrogen gas being admitted to the reaction chamber and the equilibrium pressure it produces being measured by a mercury manometer. A schematic diagram of the apparatus is shown in Figure 2. The reaction bulb is Vycor and is designed so as to minimize the free volume of the closed system in which the equilibration takes place. The heating is done by means of an induction coil driven by a high frequency generator which provides stirring of the liquid melt to aid the approach to equilibrium.

To make a determination weighed charges of vacuum melted iron (Ferrovac E) and alloying element of highest possible purity were placed in a crucible 1 1/4" in diameter and 1 1/2" deep which was surrounded by a larger crucible to act as a radiation shield. A summary of the analyses of the charge materials used is given in Appendix A. Inner and outer crucibles of recrystallized alumina were used for all systems except zirconium. The Fe-Zr alloys were found to react with alumina crucibles removing the zirconium from the melt and forming  $ZrO_2$ . Hence zirconia crucibles were found more suitable for this system. The inner crucible was covered with an alumina or zirconia lid and Alundum insulating discs were placed on the top and bottom as shown in Figure 3.



- A ANHYDRONE DRYING COLUMNS
  - B COPPER GAUZE FURNACES 450 C
  - C MERCURY RESERVOIR
  - D GAS BURET
  - E MERCURY MANOMETER
  - F REACTION BULB
  - G WATER COOLING CHAMBER
  - H MERCURY DIFFUSION PUMP
- 3 WAY STOPCOCKS a, d  
 2 WAY STOPCOCKS b, c, e, f, g, h, i

Figure 2. Schematic Diagram of Sieverts Apparatus.

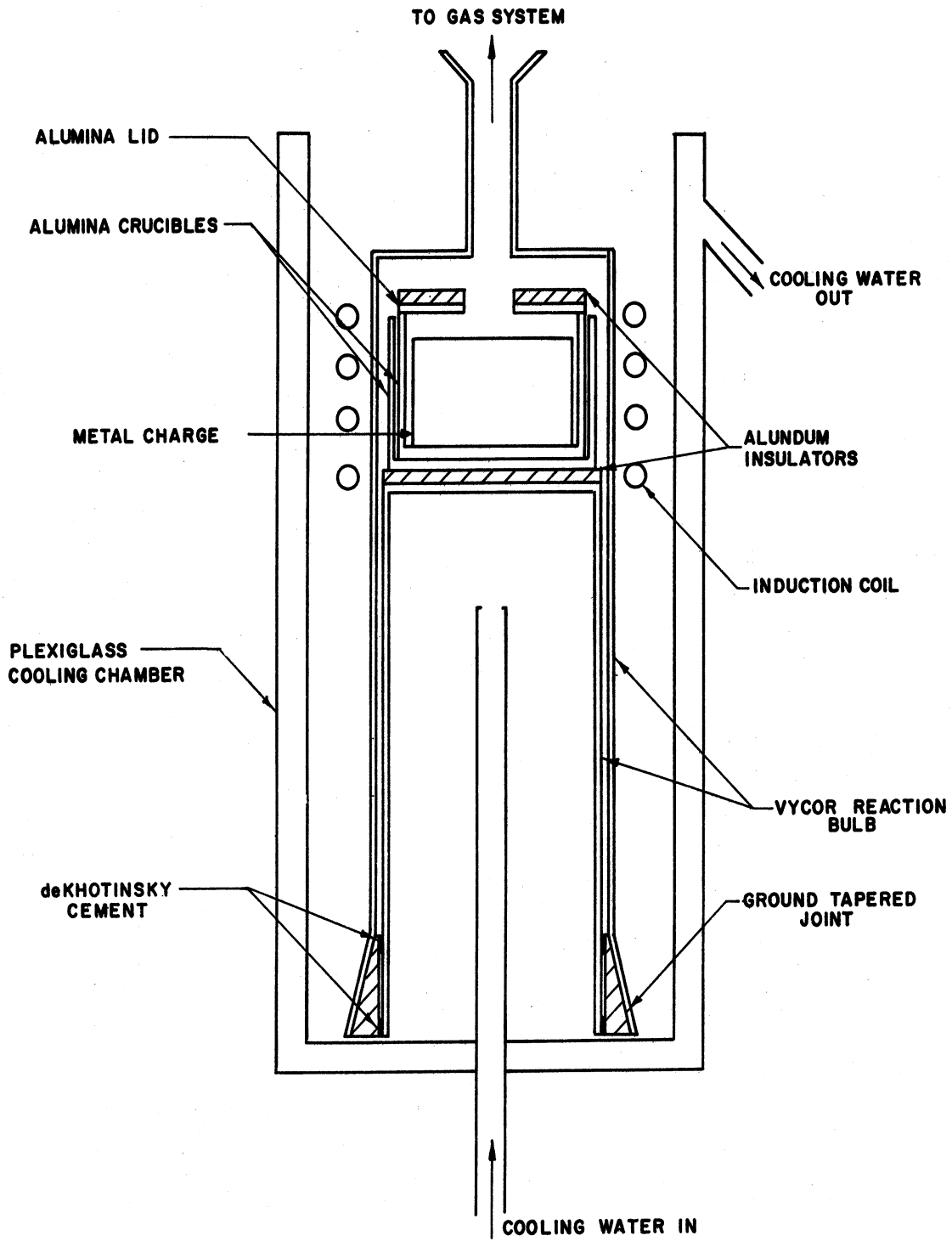


Figure 3. Sieverts Apparatus Reaction Chamber.

After the reaction bulb had been sealed, evacuated, and checked for leaks purified argon was admitted to a pressure of about half an atmosphere. Power was then turned on and the charge raised gradually to its melting point. If the alloy addition was in powder or sponge form the reaction bulb was held under hard vacuum until the charge reached about 1000°C at which temperature the charge was held for 15 to 30 minutes to remove adsorbed gases. Then the bulb was isolated from the vacuum system and pressurized to half an atmosphere with argon to prevent vaporization of metal when the charge was melted. The time for complete outgassing of the charge could be determined by periodically isolating the reaction bulb and checking for a spontaneous pressure rise in the system

The melt temperature was measured with a Leeds and Northrop disappearing filament type optical pyrometer sighted vertically downwardly on the center of the melt surface. The temperature scale was calibrated against the observed melting point of pure iron taken as 1536°C. The emissivity of all melts was assumed to be that of pure iron, taken as 0.43,<sup>24</sup> and was assumed not to change with temperature or composition. A detailed calculation of the relation between the true and observed temperature scales is given in Appendix B.

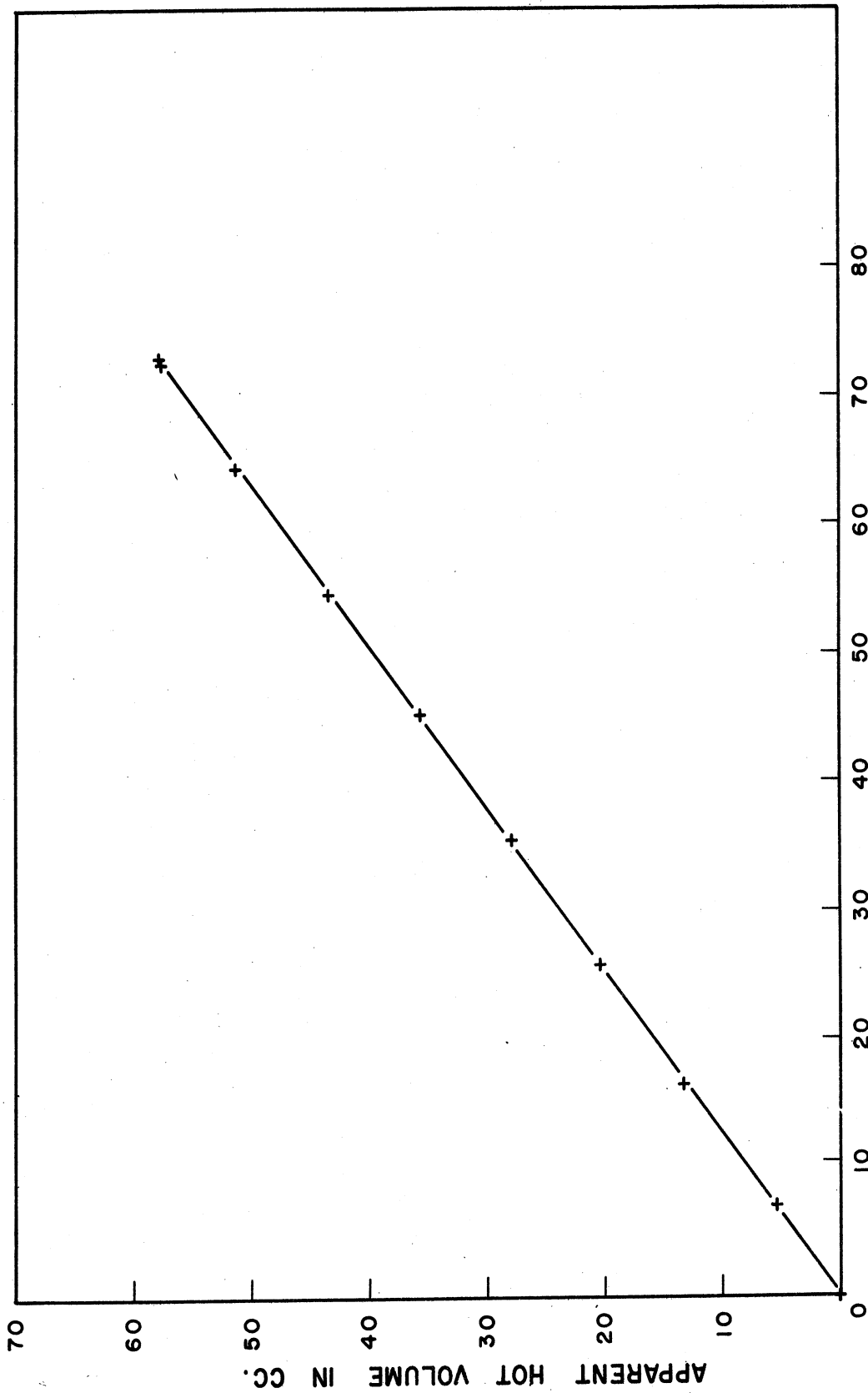
With several of the systems studied pure alloying element could not be added to the melt. Master alloys of 10 to 15 percent alloying element in iron were prepared by melting in the same apparatus under atmospheric pressure of argon. With aluminum this was necessary because the comparatively low melting point of aluminum causes it to be molten for some time before the iron melts. In a melt of 1 to 2 percent aluminum this could cause a sufficient loss of aluminum to make a significant change

in the melt composition. With titanium and zirconium the percentages required for nitride precipitation were so small that again a small loss would be significant even though these elements melt at higher temperatures than iron. With all other alloying elements the composition required was generally greater than 5% so these were added as the pure element. All master alloy compositions were aimed either at a binary eutectic composition or within the solid solubility range in order to minimize any segregation which might occur on solidification. Vertical cross section pieces of the ingot were used as additions since any segregation which did take place should be on a micro-scale and not a macro-scale.

After the charge had melted the reaction bulb was evacuated as rapidly as possible and then stopcock g was closed and a measured volume of purified argon was admitted to bring the bulb pressure up to one atmosphere. The volume was measured by drawing the argon into the closed leg of the gas buret and then balancing the two mercury legs with stopcocks b and c closed and reading the mercury height on the buret scale. Stopcock c was then opened, the argon was drawn into the reaction bulb, the mercury legs rebalanced, and the height again read on the buret scale. The difference between the two buret readings was the volume of gas drawn into the reaction chamber at atmospheric pressure and ambient temperature. The perfect gas law could then be used to calculate the volume at STP. Since argon is insoluble in liquid iron this gives the free volume of the reaction chamber at the equilibration temperature which is hereafter referred to as the hot volume.

The perfect gas law predicts that the apparent hot volume or the volume of gas measured atmospheric pressure and ambient temperature which is required to fill the hot volume at some pressure less than atmospheric varies linearly with the pressure at which it is measured. Actually there is a slight variation from linearity since the volume of the closed leg of the mercury manometer which is included in the hot volume varies with pressure. However this variation is small and the calibration curve shown in Figure 4 is substantially linear. The deviation at the high end of the pressure scale is caused by friction in the mercury legs of the manometer and solubility measurements very close to but slightly below atmospheric pressure were avoided through out the research because of this inaccuracy in the pressure reading. The variation of hot volume with equilibration temperature is also essentially linear. However the hot volume was determined individually at each equilibration temperature for each run before the start of the solubility measurements.

After suitable determinations of the hot volume the argon was pumped out of the reaction chamber as rapidly as possible to minimize the length of time that the melt would be exposed to a hard vacuum. Measured volumes of purified nitrogen were then admitted to the reaction chamber and the equilibrium pressure reached in the chamber was measured by the manometer. The difference between the apparent hot volume at that pressure and the volume of nitrogen admitted was the volume of nitrogen absorbed by the melt. In order to accurately determine the nitrogen absorption curve it was necessary to admit nitrogen in small increments and take a large number of data points.



**PRESSURE IN CM. OF MERCURY**

Figure 4. Relation Between Apparent Hot Volume of Reaction Bulb and Pressure at 1600°C.

The admission of nitrogen was continued until several equilibrations produced the same or nearly the same equilibrium pressure indicating that the vertical segment of the absorption curve (segment b in Figure 1) had been reached. Then the admission of nitrogen was stopped and the melt temperature raised 50°C. Since in all of the systems studied the solubility of the nitride increased with temperature, this temperature rise caused the nitride formed to redissolve. This was possible only if the nitrogen admission had been stopped in time to prevent too much nitride from precipitating. Then by admitting more nitrogen in sufficiently small increments several data points could be obtained below the new nitride solubility limit to establish the Sieverts Law line at the higher temperature. Nitrogen was then admitted in additional increments until another "pressure halt" was observed. This procedure was repeated until the limit of one atmosphere pressure imposed by the design of the reaction bulb was reached. For some systems the nitride solubility limit could be measured at as many as five different temperatures in a single determination. In the more insoluble systems determinations were made to establish the absorption curve at nitrogen concentrations well past the break point to attempt to determine the composition of the nitride phase.

In order to check the approach to equilibrium, measurements were made by both adding nitrogen to and withdrawing it from the same melt. It was found that below the nitride phase solubility limit both methods gave substantially the same Sieverts Law line. However above the solubility limit the two curves were different and the position of the break point depended greatly upon whether it was approached from the low nitrogen or high nitrogen side. The reversability of the equilibrium



with temperature however proved to be much more favorable. Melts in equilibrium with nitrogen pressures below the nitride solubility limit were cooled 50 or 100°C precipitating the nitride and sharply reducing the nitrogen pressure. On heating the melt up to its original temperature the nitrogen pressure returned to its original value.

C. Experimental Procedure for the Quenching Method

In the quenching method the equilibration is carried out in an open system with a stream of gas passing over the molten metal. A schematic diagram of the quenching apparatus is shown in Figure 5.

The system consists of a gas-tight vertical tube furnace with a pedestal of adjustable height to support the crucible and charge which is heated by an induction coil. A sliding seal in the bottom furnace closure permits the crucible to be lowered out of the heating coil and quenched by a blast of helium while maintaining the furnace atmosphere. The nitrogen pressure over the melt was controlled by mixing metered streams of purified nitrogen and argon gases. The method used to calibrate the flowmeters and compute the value of  $P_{N_2}$  is described in Appendix C. In this method as well as the Sieverts method the temperature was measured with an optical pyrometer and the calculation of the true and observed temperature scales is shown in Appendix B.

A charge of about 40 grams of pure iron was placed in a crucible made of the nitride whose solubility product was being determined, and this was surrounded by an alumina crucible as a radiation shield. In cases where the size of the nitride crucible left an annular space between the two crucibles this space was filled with alumina grain. No crucible lid

was used, the top of the melt being left uncovered to increase the quenching rate. After the system had been sealed and purged for 30 minutes and the nitrogen partial pressure set at the desired value the power was turned on and the iron charge melted and brought up to the equilibration temperature. It was desirable to do this as rapidly as possible since the temperature readings tended to become less accurate as time elapsed because fumes from the crucible and melt, which were carried on the moving gas stream, tended to cloud the optical port.

After a suitable equilibration period the power was turned off and the melt was lowered into the bottom of the furnace tube and quenched by a blast of helium. The helium flow was controlled by valve a. in Figure 5. Tank helium was used without further purification and the small amount of oxygen it contained occasionally caused a slight tarnishing of the top surface of the ingot. This did not appear to affect the results however, the oxidation probably taking place after the ingot had solidified. On quenching from 1600°C solidification took place too rapidly to follow visually, probably in less than a second. On quenching from 1700°C however the solidification took up to five seconds and could easily be followed visually. The ingot was then removed from the crucible and a vertical cross section cut from it and analyzed by wet chemical methods for both nitrogen and the alloying element. A summary of the analytical procedures used is given in Appendix D.

This method obviously was limited to the more insoluble nitrides from which crucibles could be fabricated sufficiently dense to contain liquid iron for a reasonable equilibration time. Three nitrides were

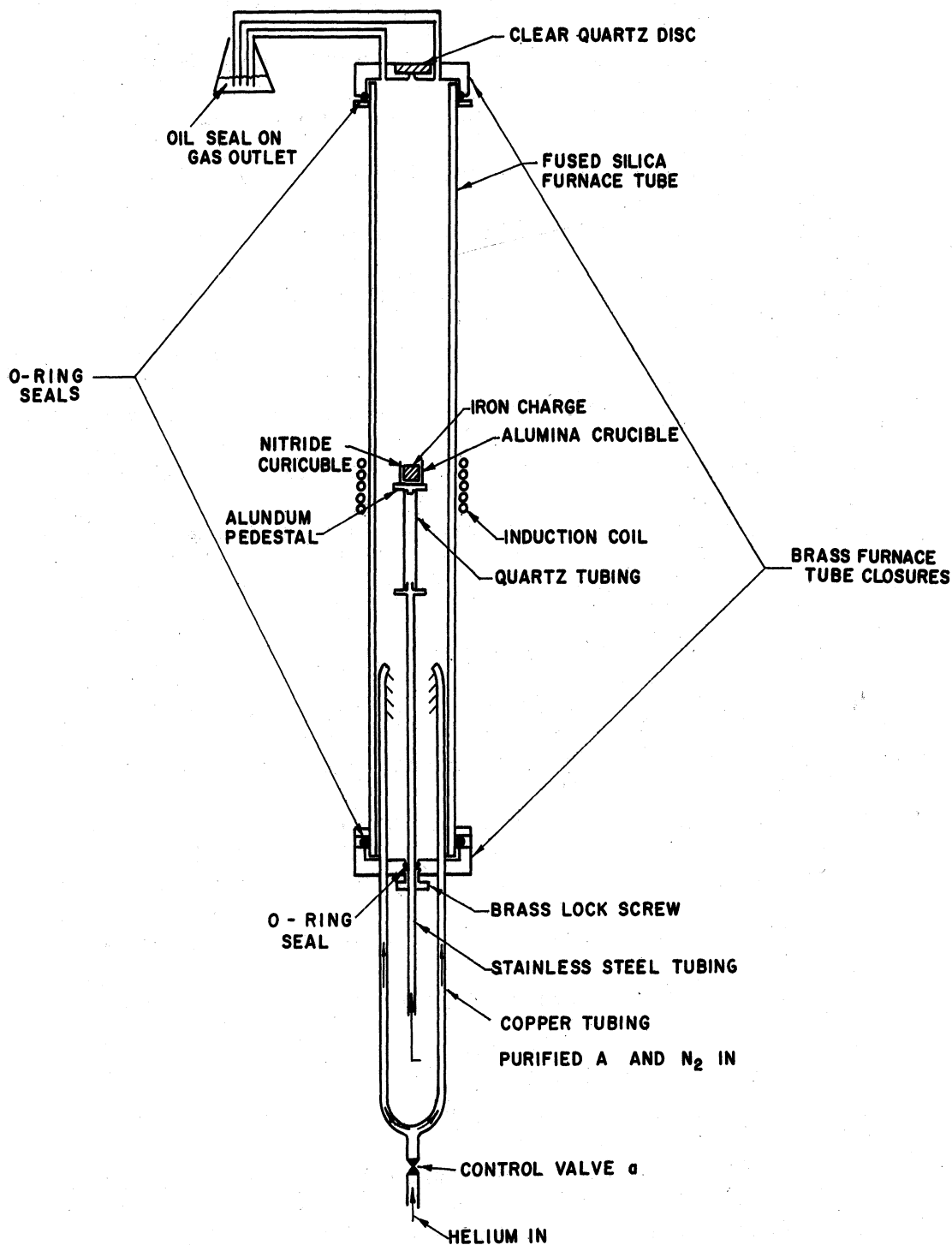


Figure 5. Schematic Diagram of Quenching Apparatus.

studied in this way, aluminum nitride, boron nitride, and titanium nitride. Three AlN crucibles fabricated by hot pressing were donated by the Carborundum Company of Latrobe, Pennsylvania. Details of the hot pressing method are given in Appendix E. The crucibles contained some material, apparently a binder or lubricant, which burned out at about 800°C causing considerable smoke in the furnace chamber. However this smoke was soon removed by the gas stream and no difficulty in temperature measurement was encountered for the remainder of the run.

BN crucibles were machined from commercially available bar stock. This stock contained about 2.5%  $B_2O_3$  which began to vaporize as soon as liquid iron formed in the crucible. This vapor quickly coated the optical pyrometer port making accurate temperature measurement impossible. However by rapidly raising the melt temperature to 1600°C the temperature could be stabilized with the pyrometer before the coating on the port got too heavy. The temperature could then be controlled reasonably accurately for the rest of the equilibration period by controlling the power input to the induction coil. Because of this temperature control problem however measurements could not be made with BN crucibles at temperatures above 1600°C. An attempt to burn out the  $B_2O_3$  by prolonged heating in air at 2500°F caused complete deterioration of the BN compact.

TiN crucibles were produced from commercially available TiN powder by a cold pressing and a sintering method developed by Sponseller<sup>(25)</sup> and described in detail in Appendix E. These crucibles contained no volatile material but proved slightly porous to liquid iron. It was necessary to cut the equilibration time somewhat to keep enough melt in the

crucible to give a sample at the end of the equilibration.

Before making any runs with nitride crucibles the effectiveness of the quenching method and the apparatus design were first evaluated by making a series of equilibrations of pure iron in alumina crucibles at various temperatures and partial pressures of nitrogen and comparing the results with data obtained by the Sieverts method.

#### D. Determination of the Nitride Phase Composition

Two direct experimental methods were tried to determine the compositions of the various nitride phases precipitated, x-ray lattice parameter measurements and wet chemical analyses. A method described by Beeghly<sup>(26)</sup> was found very effective in extracting the nitrides from the solidified ingots from the Sieverts method determinations. The alumina crucibles were broken away from the ingots. Then the top 1/8" was cut off with a metal lathe and the chips collected. These were placed in a 250 ml. round bottom flask which was fitted with an 18" long indented West Type reflux condenser. A solution of 3 ml. bromine and 13 ml. methyl acetate for each gram of chips was added to the flask, and the solution was heated with an electric hot plate until it boiled vigorously. The solution was allowed to reflux for four hours during which the iron matrix was completely dissolved. The residue of pure nitride was then filtered off, washed with methyl acetate to remove the bromine, and dried for six hours at 220°F. Care was taken to prevent the nitride from coming in contact with water since this could easily cause oxidation.

Both x-ray diffraction techniques and wet chemical analyses were used to attempt to identify the compositions of the nitride residues.

Debye - Scherrer powder patterns were made of the nitrides and the  $d$  spacings compared with ASTM standard patterns taken of synthetically prepared nitrides. In addition lattice parameter measurements were made on the residues and compared with available data on the systematic variation of lattice parameter with chemical composition in some of the systems. Wet chemical analyses of the residue for metal and nitrogen were made in one system but these were hampered by the small quantity of residue which could be extracted, even from an entire ingot. However x-ray patterns of extracted residues showed a complete absence of iron lines indicating that the extraction procedure when properly carried out was very effective in producing the pure nitride phase. A complete summary and discussion of the results of these analyses is given in a later section.

## V. RESULTS AND DISCUSSION

### A. Calculation of Results From the Sieverts Measurements

The weight percent of nitrogen absorbed by the melt at any nitrogen pressure was calculated from the difference between the volume of nitrogen introduced into the reaction chamber and the apparent hot volume at that pressure. This is expressed by the equation:

$$\begin{aligned}\%N &= (V-h) \times \frac{273}{T} \times \frac{P}{76.0} \times \sqrt{\frac{76.0}{P}} \times \frac{28}{22,400} \times \frac{100}{W} \\ &= (V-h) \frac{34.1}{TW} \sqrt{\frac{P}{76.0}}\end{aligned}\quad (18)$$

In Equation (18)  $V$  is the volume of nitrogen introduced into the reaction bulb in cubic centimeters which produces an equilibrium pressure  $p$ .  $P$  and  $T$  are atmospheric pressure and ambient temperature in centimeters of mercury and degrees Kelvin, the conditions which apply to the gas buret and hence to the measurement of the volume  $V$ .  $W$  is the weight of the metal charge in grams. The apparent hot volume  $h$  is the volume of gas measured under conditions  $P$  and  $T$  which is required to fill the free volume of the reaction chamber at the equilibration pressure  $p$ . It is calculated from the linear relation predicted by the perfect gas law:

$$h = \frac{Hp}{P}\quad (19)$$

where  $H$  is the hot volume at atmospheric pressure (i.e. with  $p = P$ ).

The factor  $\sqrt{\frac{76.0}{P}}$  enters Equation (18) in order to correct the  $\%N$  measured at pressure  $P$  to that which would be measured at a pressure of one standard atmosphere or 76.0 cm. of mercury. This correction

assumes that the absorption of nitrogen by the melt follows Sieverts' Law. Even where this is not true such as above the solubility limit of a nitride phase the error is small since the difference between P and one standard atmosphere is small. It is also apparent that since W the weight of the metal charge is used in calculating  $\%N$ , the weight of dissolved nitrogen has been neglected with respect to W. W lies generally between 100 and 140 grams while the weight of nitrogen dissolved is at most 0.5 grams and usually much less. Thus the error involved in this assumption is negligible.

B. Summary of the Nitrogen Absorption Curves Determined by the Sieverts Method

The nitrogen absorption curves for all compositions of the eight alloy systems studied are presented in Appendix F with all experimental points plotted to scale. As outlined in the experimental procedure each determination in the Sieverts Apparatus, which is represented by a single graph in Appendix F, was made at a constant alloy composition with absorption curves for this composition determined at from one to five different temperatures. All measured nitrogen absorption values were corrected for the residual nitrogen contained in the charge materials by adding to them the weight percent nitrogen contained in the iron melting stock as given by the supplier's lot analysis. These values were 0.0018%, 0.0001%, and 0.0002% for the three lots of Ferrovac E used in this study. The amount of nitrogen added to the melts by the residual nitrogen in the alloying elements was negligibly small.

It should be noted that not all absorption curves of the same determination can be considered equally accurate. Since the nitride was



precipitated and redissolved several times in most determinations there is the possibility that in some cases part of the nitride was slow to redissolve or did not redissolve at all. This could be due to adherence to the crucible walls or to the more sluggish kinetics attending the presence of a solid phase. It would effectively remove some nitrogen from the equilibrium and is reflected in a number of the absorption curves by the fact that the first point or two in the Sieverts Law region of a curve for a higher temperature lies above the Sieverts Law line. This means that most of the nitride eventually did redissolve at the higher temperature. However in a few of the curves such as those of the zirconium system the Sieverts Law lines at the higher temperatures do not pass through the origin but have a fairly large positive intercept on the ordinate at zero nitrogen pressure. This indicates that the nitride formed at the lowest temperature never completely redissolved and that only the absorption curve for the lowest temperature in each determination can be depended upon for any degree of accuracy. This condition was particularly bad for the zirconium system because the zirconia crucibles which had to be used to prevent crucible reaction with the Fe-Zr alloys had much more porous surfaces than the alumina crucibles used for the other systems. This caused the nitride to adhere much more readily to the zirconia crucible walls. In the case of the silicon system also, the higher temperature absorption curves are not considered as accurate because of the possibility of reaction between silicon and the  $\text{Al}_2\text{O}_3$  crucible. This effect presumably would become worse the longer the liquid metal charge was held in the crucible.

In most of the systems one absorption curve was run both in the direction of increasing nitrogen pressure and in the direction of decreasing nitrogen pressure. Decreasing nitrogen pressure was found to shift the part of the curve above the break point to lower pressures giving a lower nitride solubility limit than is found with increasing nitrogen pressures. This "hysteresis" effect is thought to be due to non-equilibrium conditions caused again by the sluggishness of the nitride in redissolving. The true nitride solubility limit is taken as the break point in the absorption curve determined with increasing nitrogen pressure.

The opposite effect, supersaturation with increasing nitrogen pressure, can also be observed in a number of the absorption curves. This causes several points on the Sieverts Law line to be measured at nitrogen pressures higher than the equilibrium pressure which exists after the first nitride formation. This effect is not apt to cause error in the determination of the nitride solubility limit however, since the vertical or constant pressure portion of the absorption curve can simply be extended downward until it intersects the Sieverts Law portion. The point of intersection then denotes the nitride solubility limit.

### C. Calculation and Summary of the Interaction Parameters $e_N^j$ and $e_j^N$

The interaction parameter  $e_N^j$  was defined in Equation (9). Equation (13) gives the activity coefficient  $f_N$  from which  $e_N^j$  is calculated. In order to apply Equation (13) to the experimental nitrogen solubility data it was necessary to select a reference pressure. A value of  $P_{N_2} = 20.25$  cm. (0.267 atm.) or  $\sqrt{P_{N_2}} = 4.50$  (cm.)<sup>1/2</sup> was selected since it

was low enough to be below the nitrogen pressure required for nitride precipitation in most of the experiments and high enough so that the differences in nitrogen solubility in the various alloys could be read accurately from the absorption curves. In the few cases where the pressure at which the nitride formed was below 20.25 cm. the Sieverts Law line was extrapolated up to this reference pressure. As was previously noted the choice of reference pressure theoretically makes no difference in  $f_{\underline{N}}$  as long as all alloys obey Sieverts' Law below the nitride solubility limit. However at very low nitrogen pressures the pressure measurement becomes more difficult causing the low pressure end of the absorption curve to be less accurate and resulting in less accuracy in  $f_{\underline{N}}$  if the reference pressure is chosen too low. Similarly if the reference pressure is chosen too high then in a large number of cases the Sieverts Law portion of the absorption curve must be extrapolated graphically far beyond the break point and again less accuracy in  $f_{\underline{N}}$  may result.

Using Equation (13) and the reference pressure  $P_{N_2} = 20.25$  cm.,  $f_{\underline{N}}$  was calculated for each absorption curve. For each temperature  $\log f_{\underline{N}}$  was then plotted against  $\%j$  and the average slope of this curve was taken as the value of  $e_{\underline{N}}^j$ . These plots are shown in Figure 6 through Figure 13. From these values of  $e_{\underline{N}}^j$ ,  $e_j^N$  was then calculated by Equation (15). The numerical values of  $e_{\underline{N}}^j$  and  $e_j^N$  are summarized in Table III and compared with the values of other experimenters. (1,3,12,27,28,29)

The value of  $e_{\underline{N}}^j$  is actually given by the limiting slope of the curve of  $\log f_{\underline{N}}$  versus  $\%j$  as  $\%j$  approaches zero. However in this study the  $\%j$  had to be high enough to cause nitride precipitation at less than one atmosphere nitrogen pressure so no data points could be

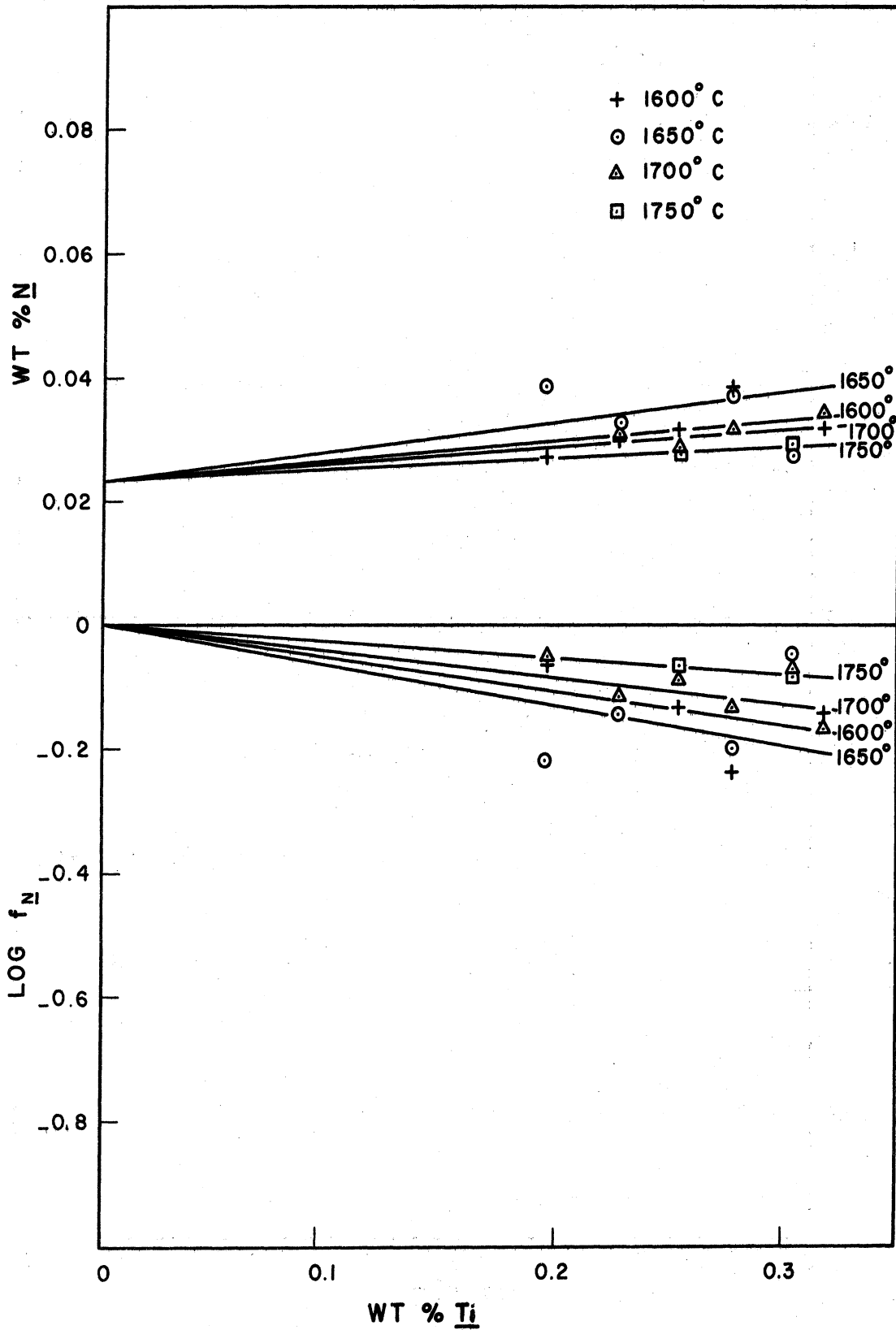


Figure 6. Effect of Titanium on the Solubility of Nitrogen.

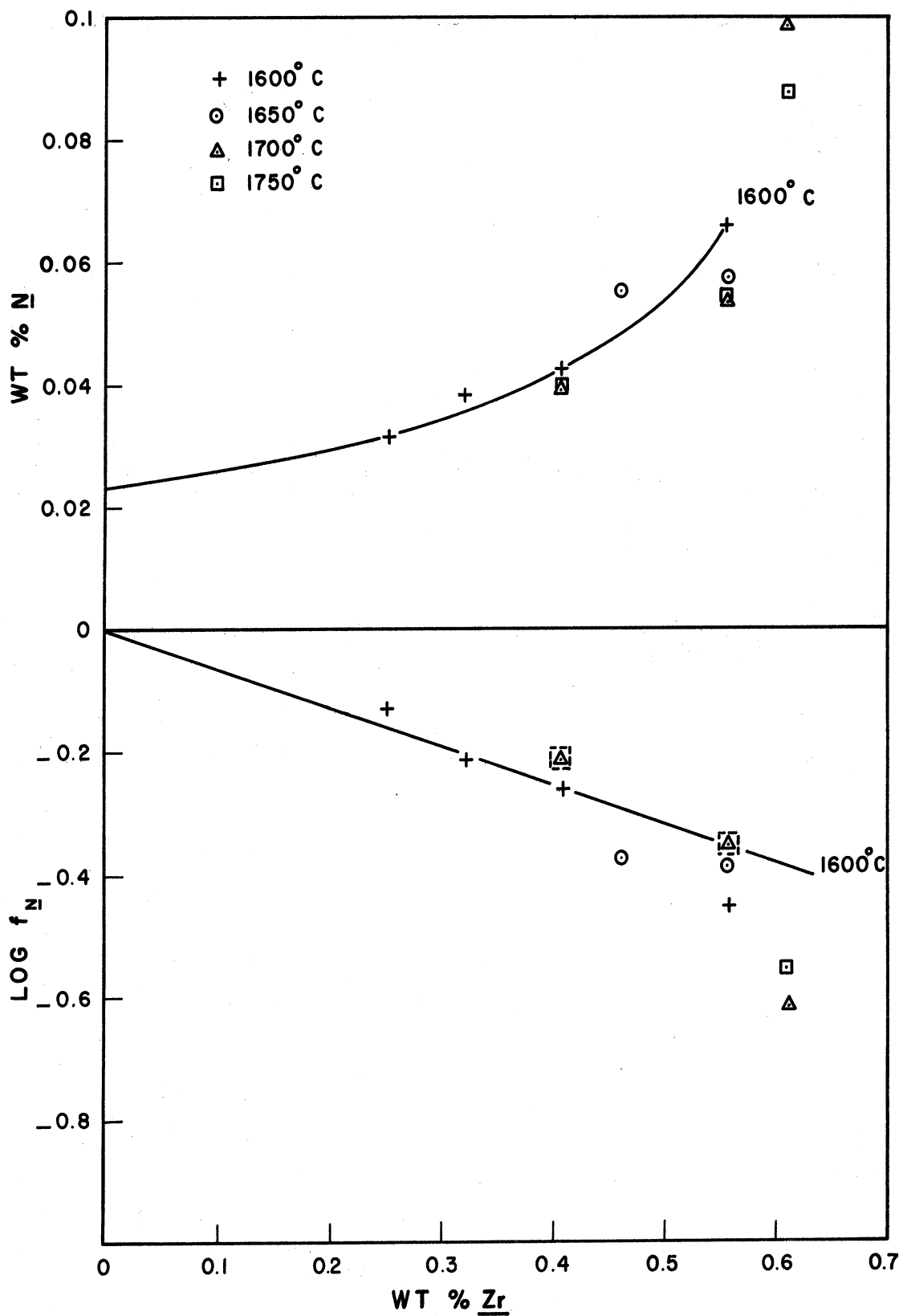


Figure 7. Effect of Zirconium on the Solubility of Nitrogen.

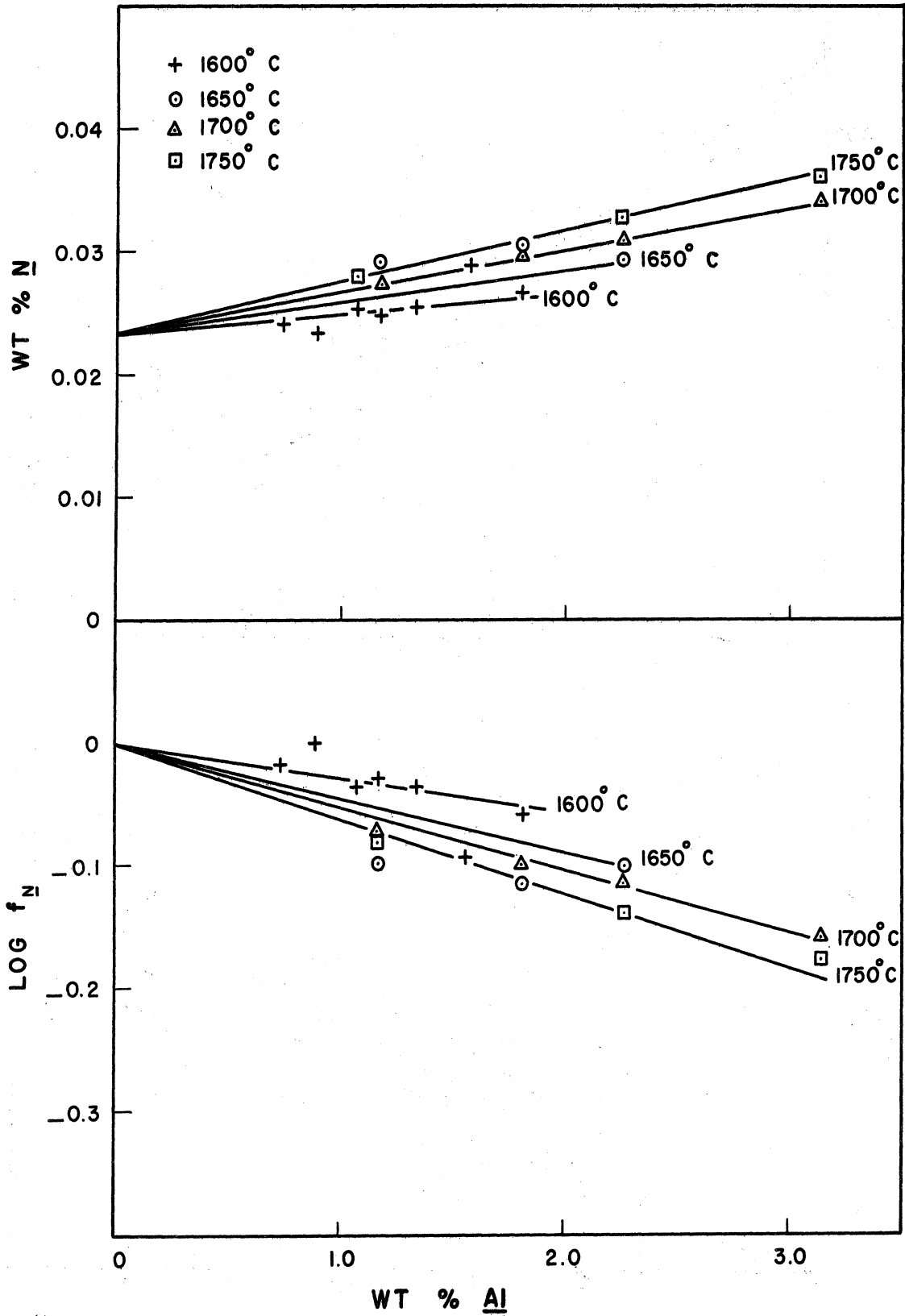


Figure 8. Effect of Aluminum on the Solubility of Nitrogen.

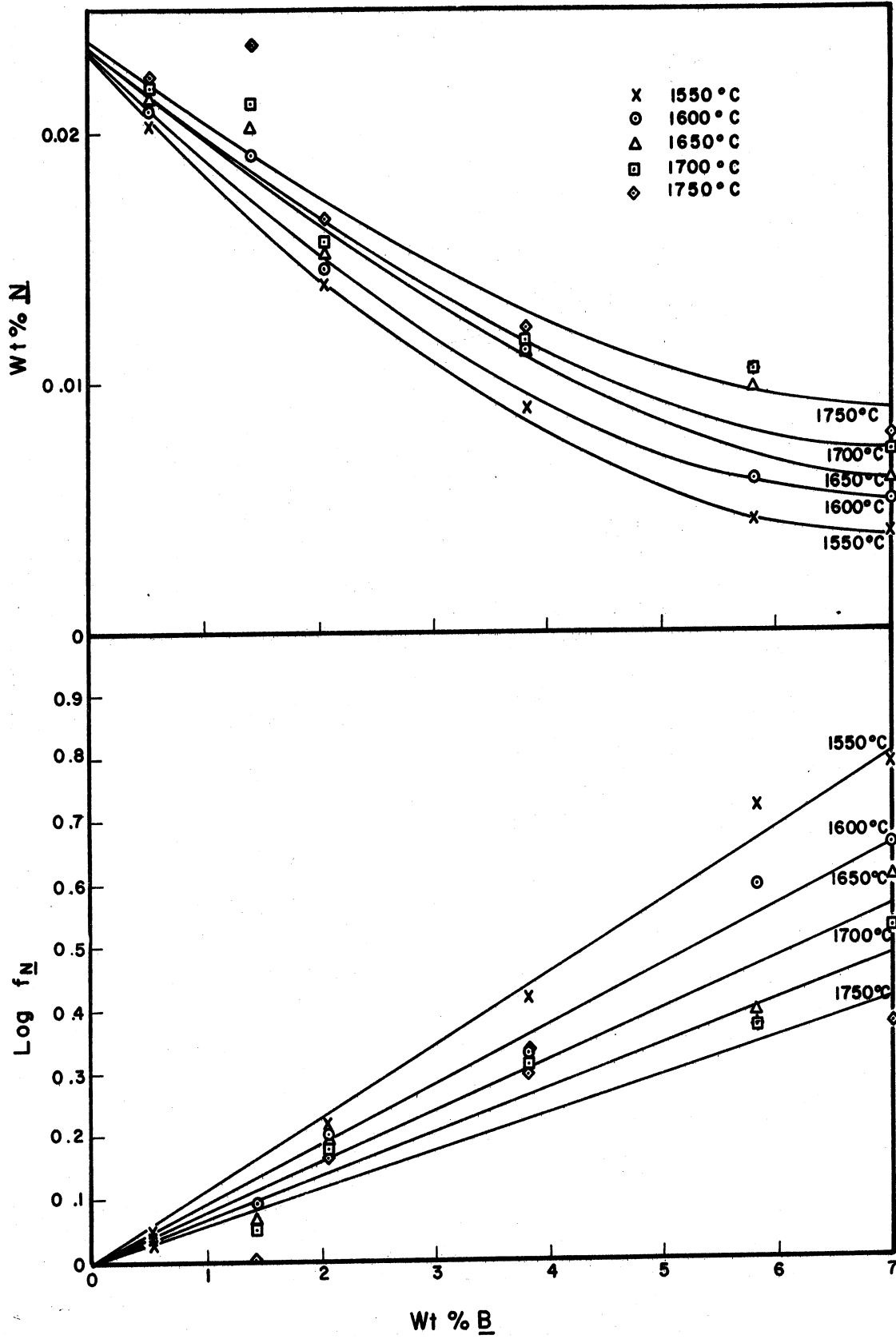


Figure 9. Effect of Boron on the Solubility of Nitrogen

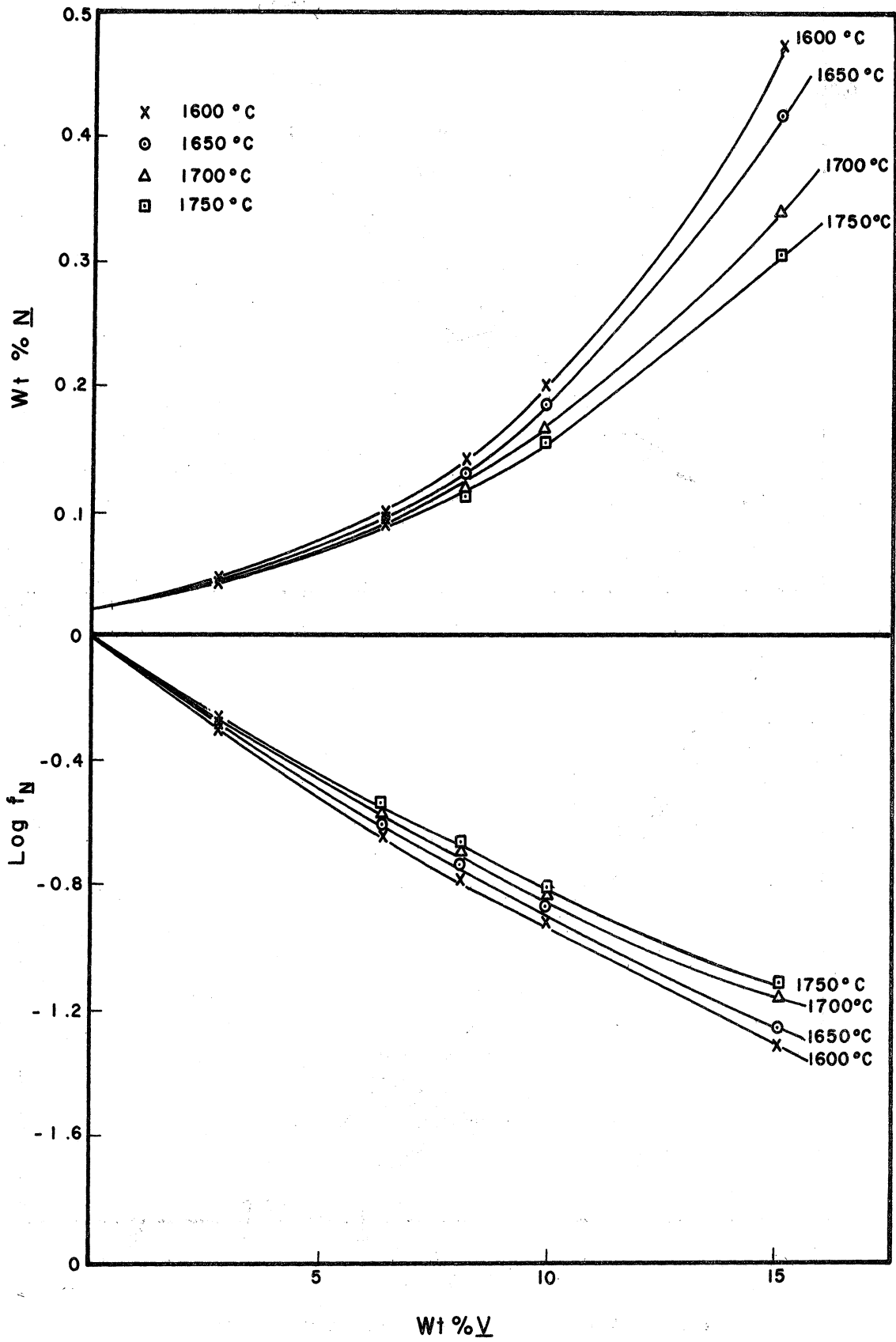


Figure 10. Effect of Vanadium on the Solubility of Nitrogen



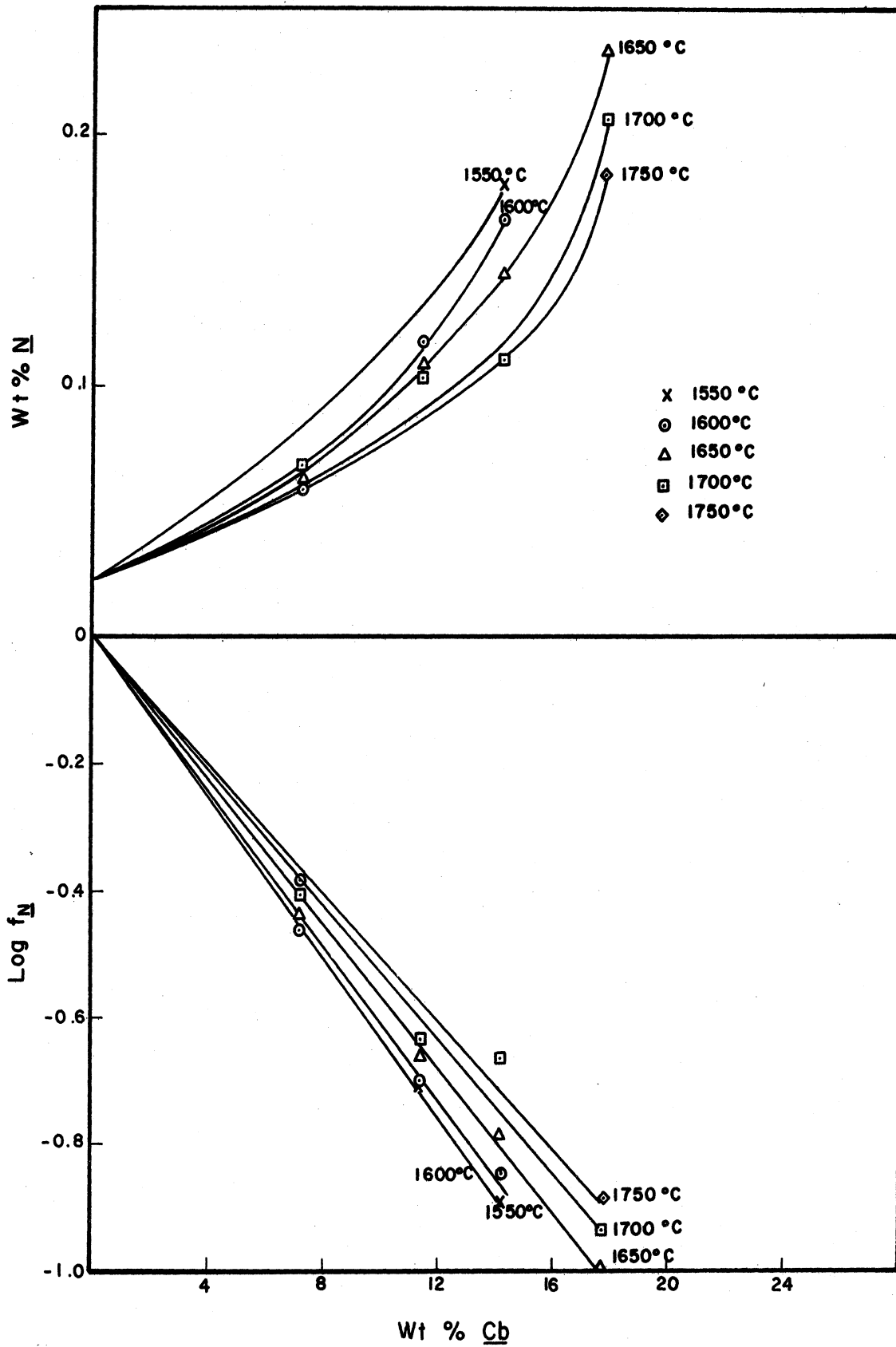


Figure 11. Effect of Columbium on the Solubility of Nitrogen

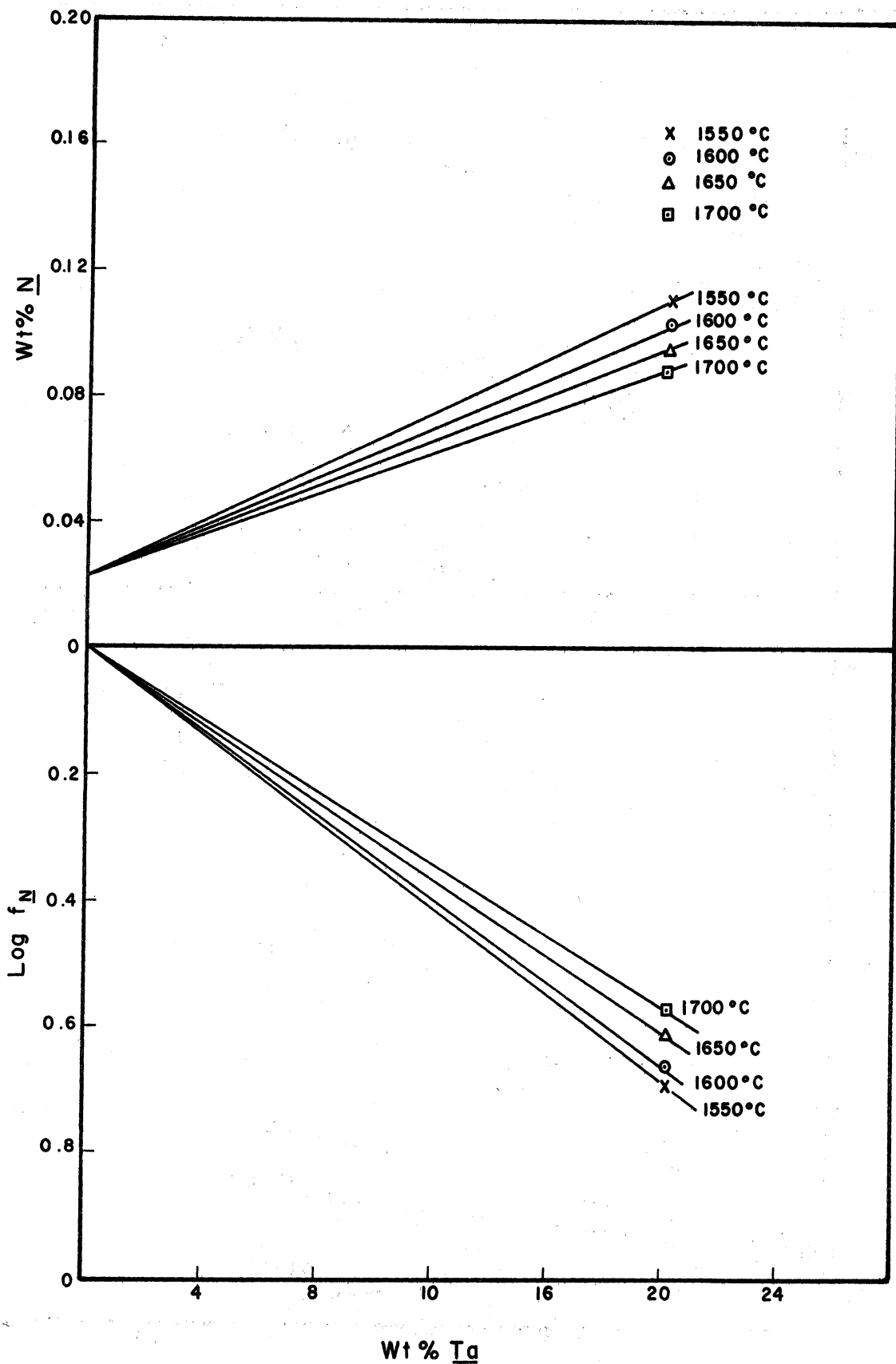


Figure 12. Effect of Tantalum on the Solubility of Nitrogen

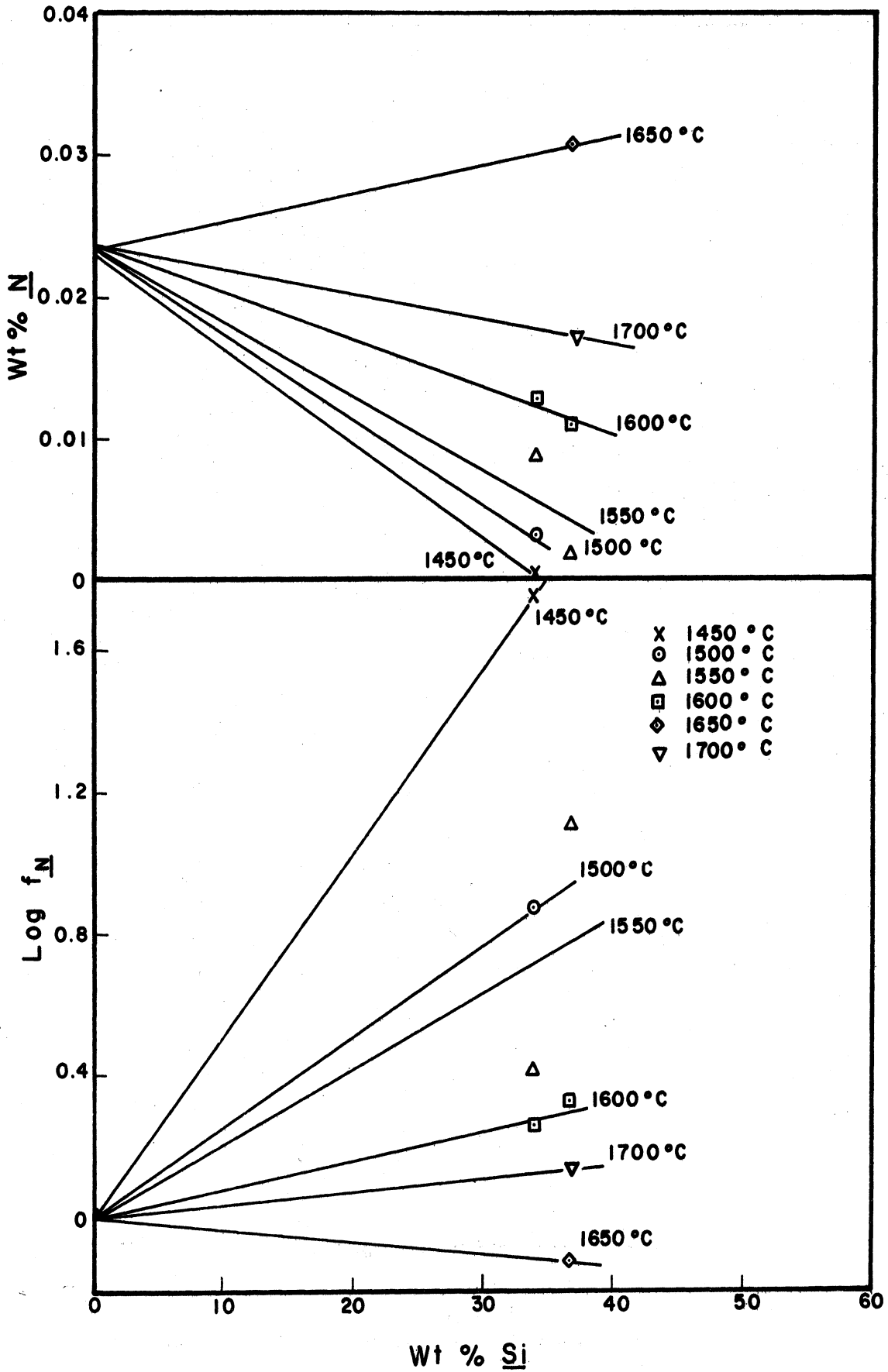


Figure 13. Effect of Silicon on the Solubility of Nitrogen

obtained for very low  $\%j$  except in the systems titanium and zirconium where the nitrides are very insoluble. This necessity for using an average slope causes the values of  $e_N^j$  to be slightly lower than those of other experimenters which were determined at very low  $\%j$  as evidenced by Table III. However with the exception of the silicon system in which the nitride is extremely soluble the agreement is quite good. This indicates that the values of  $e_N^j$  and  $e_j^N$  can be considered reasonably constant in some cases up to surprisingly high  $\%j$ .

Dealy and Pehlke<sup>(30)</sup> have suggested in view of the relation:

$$\frac{d\epsilon_i^j}{d(1/T)} = \frac{1}{R} \left( \frac{\partial^2 H}{\partial x_i \partial x_j} \right)_{x_i = x_j = 0} \quad (20)$$

which can be derived from the Van't Hoff equation, that  $\epsilon_i^j$  should be proportional to  $1/T$  over short temperature ranges in which the derivative of molar enthalpy with respect to mole fractions of the two dilute solutes can be considered independent of temperature. The same conclusion certainly applies to  $e_i^j$  since it is related to  $\epsilon_i^j$  by a constant:

$$e_i^j = \frac{M \text{ solvent}}{(2.303)(100) M_j} \epsilon_i^j \quad (21)$$

or in the case of this research in which the solvent is iron:

$$e_i^j = \frac{0.2425}{M_j} \epsilon_i^j \quad (22)$$

Therefore to test the consistency of the values of  $e_i^j$  given in Table III, the  $e_N^j$  for each system were plotted against  $1/T$ . These plots are shown in Figure 14 through Figure 17. It can be seen that for the systems aluminum vanadium, columbium, and tantalum the values of  $e_N^j$  fit very well a

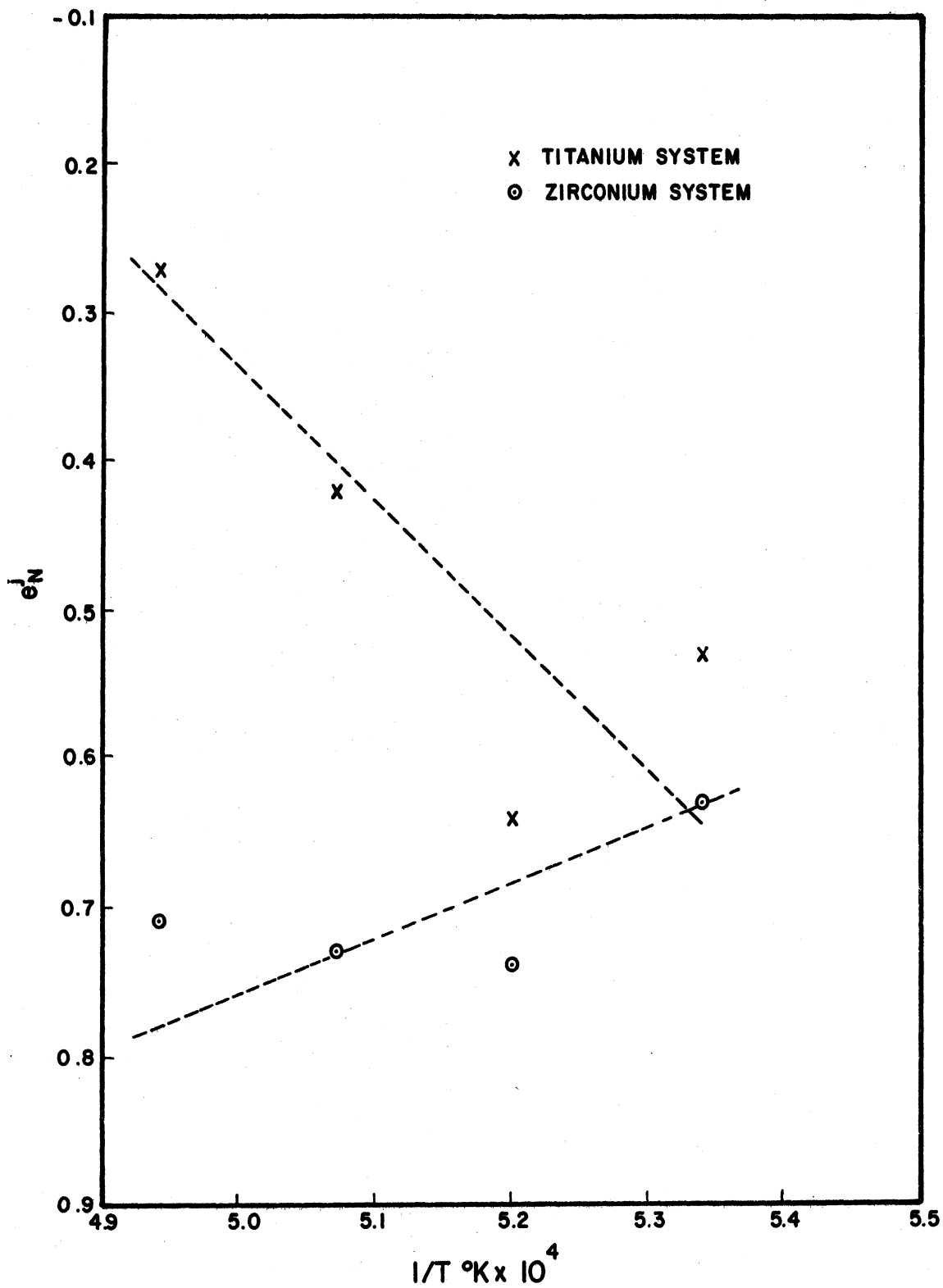


Figure 14. Variation of  $e_N^{\text{Ti}}$  and  $e_N^{\text{Zr}}$  with Reciprocal Temperature

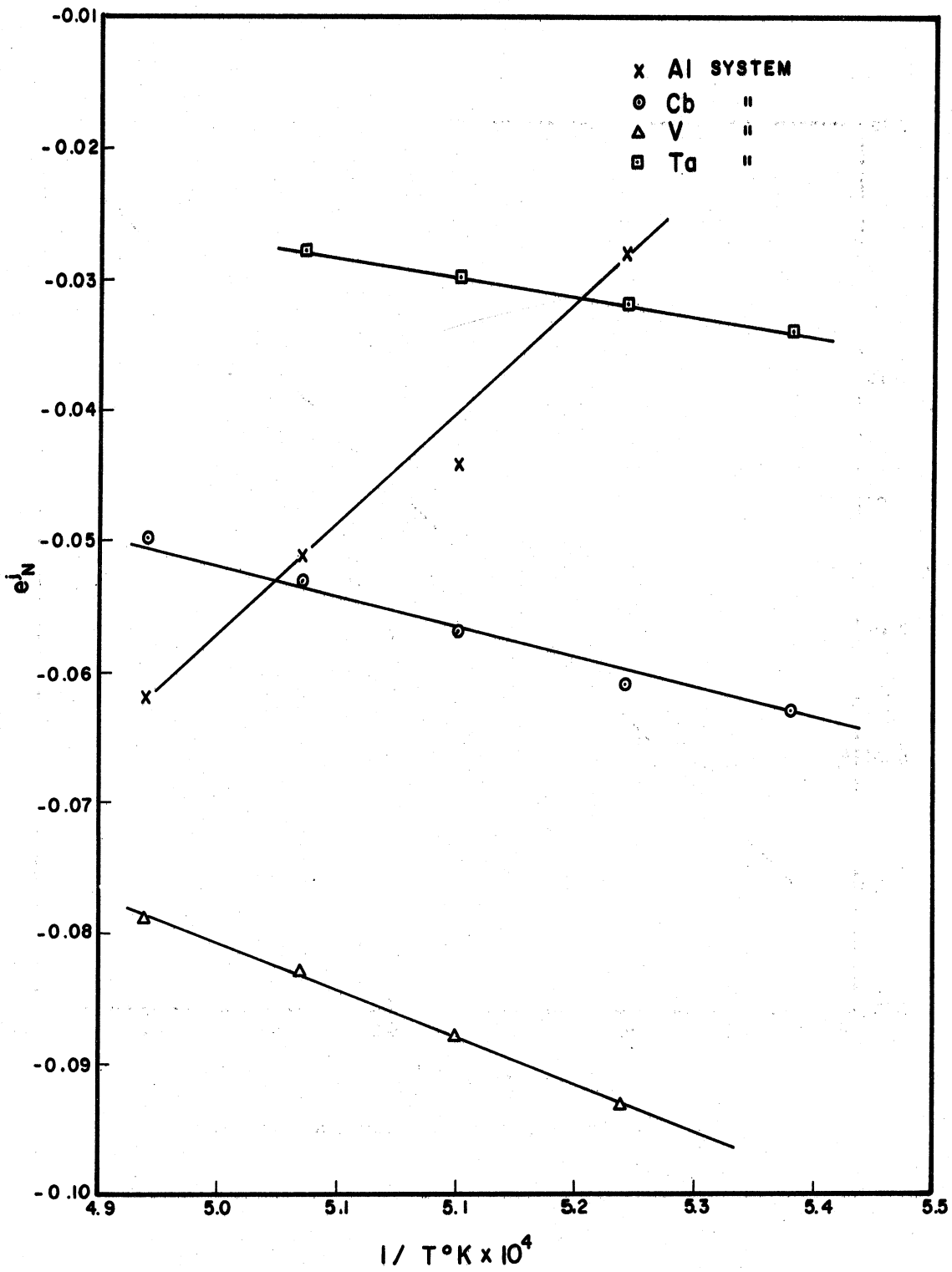


Figure 15. Variation of  $e_N^{Al}$ ,  $e_N^{Cb}$ ,  $e_N^V$ , and  $e_N^{Ta}$ , with Reciprocal Temperature

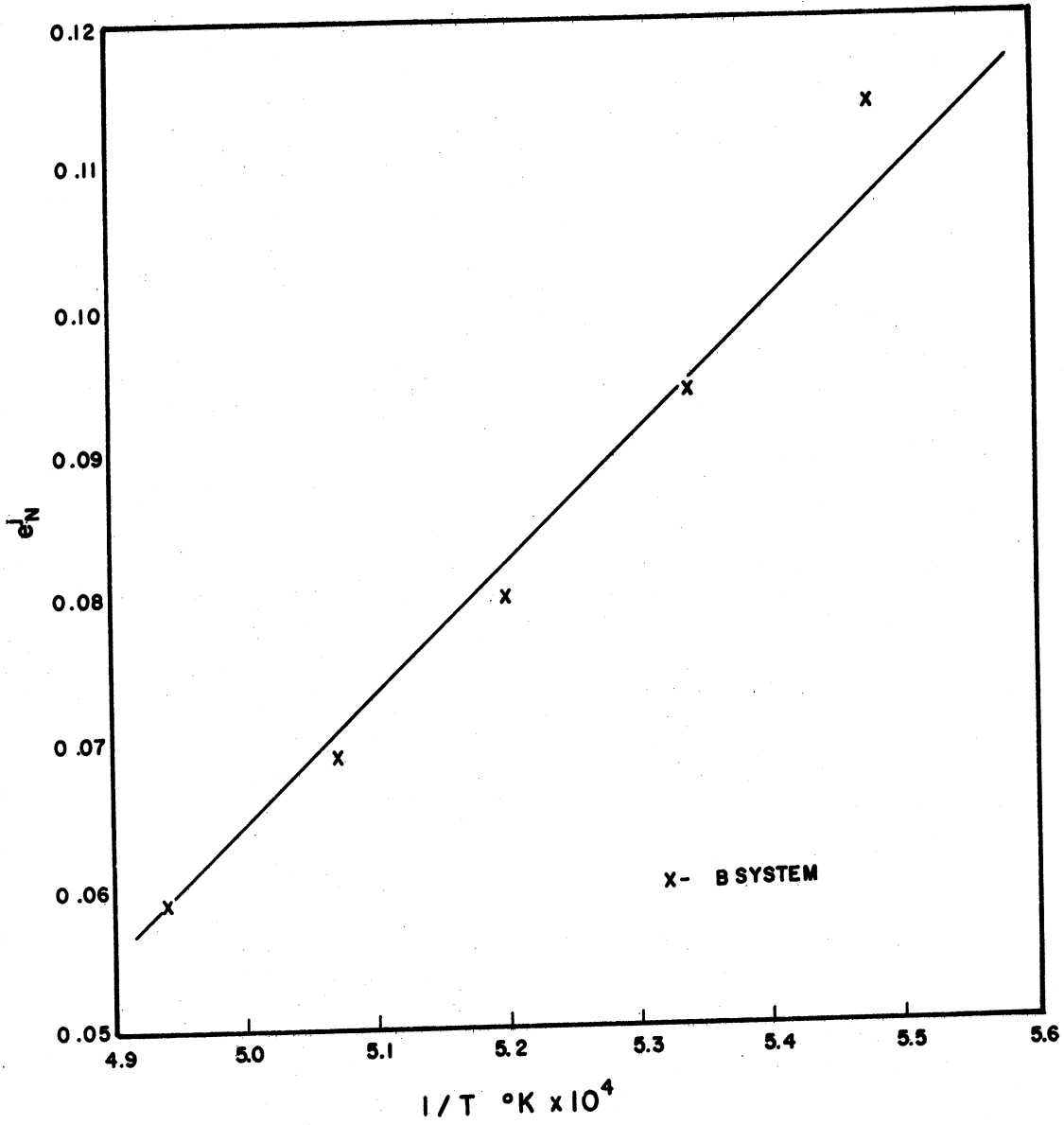


Figure 16. Variation of  $e_N^B$  with Reciprocal Temperature

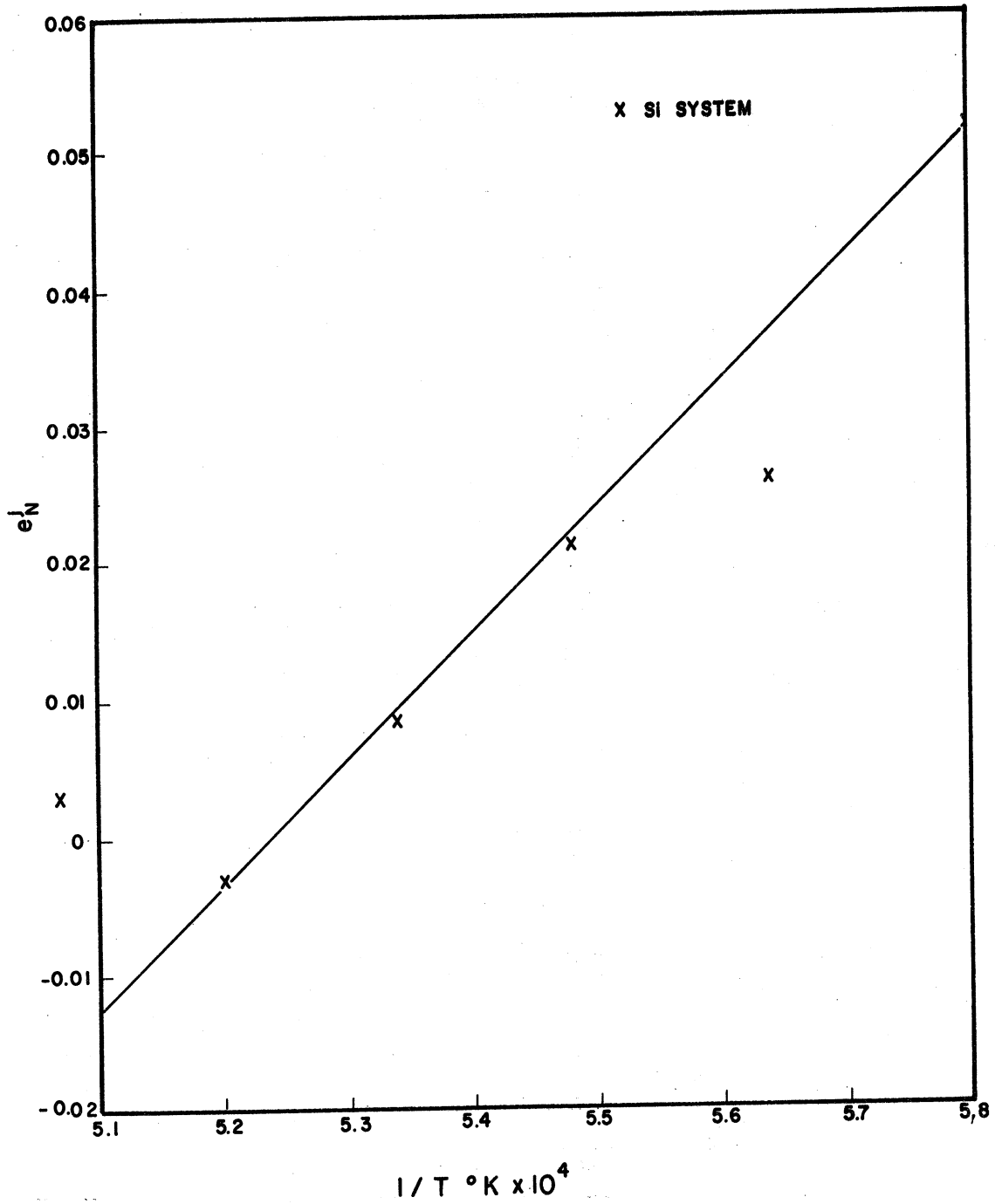


Figure 17. Variation of  $e_N^{Si}$  with Reciprocal Temperature



TABLE III  
SUMMARY OF MEASURED VALUES OF THE INTERACTION  
PARAMETERS  $e_N^j$  AND  $e_j^N$

Element j	Temp °C	$e_N^j$	$e_j^N = e_N^j \frac{M_j}{M_N}$	Values of other experimenters for $e_N^j$		
				Pehlke Elliott <sup>(1)</sup>	Maekawa Nakagawa <sup>(27,28)</sup>	Others
Ti (6 runs)	1600	-0.53	-1.82			
	1650	-0.64	-2.20		-0.64	-0.93
	1700	-0.42	-1.44		-0.63	Rao and Parlee <sup>(12)</sup>
	1750	-0.27	-0.93			
Zr (6 runs)	1600	-0.63	-4.09			
	1650	-0.74	-4.81			
	1700	-0.73	-4.75			
	1750	-0.71	-4.62			
Al (9 runs)	1600	-0.028	-0.054	0.0025	-0.04	-0.0103 <sup>(29)</sup>
	1650	-0.044	-0.085			Eklund <sup>(29)</sup>
	1700	-0.051	-0.098			
	1750	-0.062	-0.120			
B (6 runs)	1550	0.114	0.088			
	1600	0.094	0.073			
	1650	0.080	0.062			
	1700	0.069	0.053			
	1750	0.059	0.046			
V (5 runs)	1600	-0.093	-0.338	-0.10	-0.11	-0.105
	1650	-0.088	-0.320			Kashyap and Parlee <sup>(3)</sup>
	1700	-0.083	-0.302			
	1750	-0.079	-0.288			
Cb (4 runs)	1550	-0.063	-0.419			
	1600	-0.061	-0.404	-0.067		
	1650	-0.057	-0.387			
	1700	-0.053	-0.351			
	1750	-0.050	-0.331			
Ta (1 run)	1550	-0.034	-0.437			
	1600	-0.032	-0.413	-0.034		
	1650	-0.030	-0.390			
	1700	-0.028	-0.367			
Si (2 runs)	1450	0.052	0.104			
	1500	0.026	0.051			
	1550	0.021	0.043			
	1600	0.0084	0.017	0.047	0.048	
	1650	-0.0032	-0.0064			
1700	0.0038	0.0076				

a  $1/T$  dependence. For the boron system the fit is fairly good, while the titanium and zirconium systems show some scatter. For the zirconium system this can be explained by the difficulty experienced in redissolving the nitride as previously mentioned.

The  $e_N^j$  values for the silicon system show a reasonably good fit to the  $1/T$  dependence, but for the line as drawn in Figure 17  $e_N^{Si}$  becomes negative for temperatures of  $1650^\circ\text{C}$  and above. This would indicate that at these temperatures and silicon concentrations silicon increases the solubility of nitrogen in liquid iron. This conflicts with all other known data on the iron-nitrogen-silicon system which indicate that silicon decreases the nitrogen solubility in liquid iron. This discrepancy is probably caused by reaction between silicon and the  $\text{Al}_2\text{O}_3$  crucible and as a result the entire line of Figure 17 is somewhat questionable.

#### D. Calculation and Summary of the Interaction Parameters $e_j^j$

The interaction parameter  $e_j^j$  can be determined from information on the variation of the activity of  $j$  with composition in binary Fe- $j$  solutions. Wilder and Elliott<sup>(31)</sup> have used the electrolytic cell method to study the liquid Al-Ag system. From their data in combination with that of Chipman and Floridis<sup>(32)</sup> on the distribution of aluminum between liquid iron and silver layers a value of  $e_{Al}^{Al}$  can be calculated for the solvent liquid iron at  $1600^\circ\text{C}$ . The data show this value to be valid up to about 13% Al. Elle and Chipman<sup>(33)</sup> have studied oxygen activities in liquid Fe-Cb alloys using gas mixtures of  $\text{H}_2$  and  $\text{H}_2\text{O}$ . From their data and previously determined values of the free energy of formation of  $\text{CbO}_2$  a value of  $e_{Cb}^{Cb}$  can be calculated which however is expected to be

strictly valid only in very dilute solutions. Chipman et al<sup>(34)</sup> from measurements on the distribution of Si between liquid iron and liquid silver found a value for  $e_{Si}^{Si}$  in liquid iron which is valid to about 30% Si but becomes invalid with small amounts of additional silicon. Chipman<sup>(35)</sup> gives a value for  $e_{Ti}^{Ti}$  calculated from data on the equilibrium of titanium, oxygen, and TiO in liquid iron.

It was previously noted that the  $e_j^j$  interaction parameter could also be estimated from data on the Fe-j-N ternary system provided sufficient data were available to show a systematic variation of  $K'$  for jN with  $\%j$ . This method was used to estimate values of  $e_V^V$  and  $e_B^B$ . Finally for the zirconium and tantalum systems no known data on the liquid binaries are available and the ternary data were not of sufficient quantity or quality to show the necessary systematic variation of  $K'$  with  $\%j$ . In view of correlations between interaction parameter and atomic number such as the one found by Turkdogan and coworkers<sup>(36)</sup>  $e_j^j$  was estimated by comparing  $e_j^j$  for the unknown element with  $e_j^j$  for a known element in the same group in the periodic table.

A summary of the  $e_j^j$  and  $e_j^j$  values used and the sources from which they are derived is given in Table IV. These values are valid only at 1600°C. However because of complete lack of data on the variation of  $e_j^j$  with temperature it was necessary to apply the values in Table IV at all experimental temperatures which ranged from 1450°C to 1750°C.

In all of the systems studied  $e_j^j$  was positive and in four of the systems the effect of the j-j interactions was small or negligible compared to the j-N interactions. In the titanium and zirconium systems  $e_j^j$  is small while  $e_N^j$  is large and negative and  $\%j$  is also small.

TABLE IV

SUMMARY OF VALUES OF THE INTERACTION PARAMETER  $e_j^j$

Element $j$	$e_j^j$	Source	$e_j^j$
Ti	0.046	Chipman <sup>(35)</sup>	9.0
Zr	0.025	Estimated from $e_{Zr}^{Zr} = e_{Ti}^{Ti}$	9.0
Al	0.048	Wilder and Elliott <sup>(31)</sup>	5.3
B	0.038	Estimated from experimental data	1.7
V	0.043	Estimated from experimental data	9.0
Cb	0.0081	Elle and Chipman <sup>(33)</sup>	3.2
Ta	0.0014	Estimated from $e_{Ta}^{Ta} \approx 1/3 e_{Cb}^{Cb}$ since $e_{Cb}^{Cb} \approx 1/3 e_V^V$	1.0
Si	0.029	Chipman <u>et al</u> <sup>(34)</sup>	3.4

Therefore the term  $e_j^j (\%j)$  in Equation (11) makes a negligible contribution to  $K$ . In the columbium and tantalum systems  $e_j^j$  is very small while  $e_N^j$  is very large and negative so although  $\%j$  is large the term  $e_j^j (\%j)$  again makes a negligible contribution to  $K$ . In the aluminum system  $e_j^N$  and  $e_N^j$  are both small and negative while  $e_j^j$  is slightly larger and positive. This makes  $e_j^j$  important and causes the terms  $e_j^j (\%j)$ ,  $e_N^j (\%N)$ , and  $e_N^j (\%j)$  to nearly cancel each other making  $K$  nearly equal to  $K'$ . In the boron, vanadium, and silicon systems the term  $e_j^j$  is appreciable with respect to  $e_N^j$  while  $\%j$  is large, particularly in the case of vanadium and silicon.

In the boron, columbium, vanadium, tantalum, and silicon systems the  $\%j$  to precipitate nitride must be high, hence the assumption of a constant  $e_j^j$  is questionable. This is particularly true of silicon

since it was noted that Chipman et al<sup>(34)</sup> found rapid deviations from Henry's Law over a short composition range beginning at about 30% silicon, while the silicon content required to precipitate  $\text{Si}_3\text{N}_4$  from liquid iron solution under less than one atmosphere nitrogen pressure is about 35%. However since for the majority of these systems no activity data on the Fe-j binary is available it is necessary to assume that  $e_j^j$  can be approximated as constant out to the  $\%j$  required to precipitate the nitride.

E. Calculation of the Nitride Solubility Product by the Method of Interaction Parameters

Using Equation (11) and the interaction parameters listed in Tables III and IV a value of the nitride solubility product  $K$  was calculated for each of the absorption curves in Appendix F which shows a point of deviation from Sieverts' Law. The  $\%j$  and  $\%N$  associated with the break point of each absorption curve are summarized in Table V together with the values of  $K'$  and  $K$  calculated from them.

F. Calculation of the Nitride Solubility Product Using the Nitrogen Activity Determined by the Gas Phase

It was noted that in the systems boron, vanadium, columbium, and tantalum which have rather soluble nitrides  $e_N^j$  may not remain constant up to the  $\%j$  required to precipitate the nitride. Although the  $e_N^j$  measured in this study generally agree well with the values of other experimenters obtained in more dilute solutions, any error involved in assuming  $e_N^j$  constant can be at least partially eliminated by calculating the nitrogen activity in solution directly from the nitrogen activity in the gas phase which is fixed by the equilibrium nitrogen pressure. This

TABLE V

SUMMARY OF THE SOLUBILITY PRODUCTS K' AND K  
CALCULATED BY THE INTERACTION PARAMETER METHOD

Element j	Temp °C	% <u>j</u>	% <u>N</u>	K' = % <u>Ti</u> x % <u>N</u>	K	
Ti	1600	0.195	0.0193	0.00376	0.00289	
		0.228	0.0178	0.00408	0.00294	
		0.254	0.0145	0.00368	0.00262	
		0.277	0.0138	0.00382	0.00266	
		0.318	0.0100	0.00318	0.00214	
	1650	0.195	0.0390	0.00760	0.00479	
		0.228	0.0343	0.00782	0.00481	
		0.277	0.0348	0.00964	0.00565	
		0.304	0.0172	0.00523	0.00320	
	1700	0.228	0.0457	0.01042	0.00739	
		0.254	0.0403	0.01023	0.00722	
		0.277	0.0517	0.01432	0.00955	
		0.304	0.0287	0.00872	0.00613	
		0.318	0.0292	0.00929	0.00644	
	1750	0.304	0.0501	0.01522	0.01172	
	Zr	1600	0.253	0.0425	K' = % <u>Zr</u> x % <u>N</u> 0.01076	0.00506
			0.322	0.0432	0.01391	0.00591
			0.409	0.0225	0.00921	0.00419
			0.558	0.0185	0.01032	0.00396
		1650	0.462	0.0765	0.0353	0.00723
0.558			0.0453	0.0253	0.00607	
1700		0.612	0.0787	0.0482	0.00744	
1750		0.612	0.1120	0.0686	0.00790	
Al		1600	1.07	0.0458	K' = % <u>Al</u> x % <u>N</u> 0.0490	0.0512
			1.17	0.0381	0.0445	0.0477
			1.34	0.0318	0.0426	0.0450
			1.57	0.0298	0.0468	0.0500
	1.81		0.0211	0.0382	0.0414	
	1650	1.81	0.0394	0.0693	0.0697	
		2.26	0.0307	0.0694	0.0702	
	1700	2.26	0.0495	0.112	0.109	
		3.14	0.0312	0.098	0.095	
		3.85	0.0310	0.119	0.115	
	1750	3.14	0.0541	0.170	0.151	

TABLE V  
(CONT'D)

Element j	Temp °C	% <u>J</u>	% <u>N</u>	$K' = \%B \times \%N$	K	
B	1550	3.82	0.0104	0.0397	0.151	
		5.83	0.0028	0.0163	0.125	
		7.06	0.0018	0.0127	0.150	
	1600	5.83	0.0045	0.0262	0.154	
		7.06	0.0033	0.0233	0.199	
	1650	5.83	0.0123	0.0717	0.349	
		7.06	0.0050	0.0353	0.236	
	1700	7.06	0.0079	0.0557	0.324	
	1750	7.06	0.0163	0.115	0.557	
	V	1600	8.05	0.238	$K' = \%V \times \%N$ 1.92	0.634
			9.93	0.243	2.41	0.637
			15.04	0.280	4.21	0.593
1650		9.93	0.303	3.01	0.858	
		15.04	0.369	5.55	0.890	
1700		15.04	0.478	7.19	1.282	
1750		15.04	0.545	8.20	1.640	
Cb		1550	14.17	0.1625	$K' = \%Cb \times \%N$ 2.30	0.327
	11.41		0.209	2.38	0.486	
	1600	14.17	0.218	3.08	0.446	
		14.17	0.257	3.64	0.589	
	1750	17.71	0.232	4.38	0.484	
Ta	1700	14.17	0.257	3.64	0.589	
		17.71	0.232	4.38	0.484	
	1700	17.71	0.205	5.79	0.780	
		1550	20.2	0.141	$K' = \%Ta \times \%N$ 2.85	0.547
Si	1450	34.0	0.0006	$K' = (\%Si)^{3/4} \times \%N$ 0.0078	2.47	
	1500	34.0	0.0054	0.0702	2.85	
	1550	36.7	0.0021	0.0313	1.19	
	1600	34.0	0.0218	0.284	3.04	
		36.7	0.0117	0.174	2.14	
	1650	36.7	0.0360	0.536	2.58	
	1700	36.7	0.0252	0.376	3.27	

will not completely eliminate any error in  $K$  since the  $j$  activity required for the calculation of  $K$  depends upon  $e_j^N$  which in turn is calculated from the experimentally determined value of  $e_N^j$  by means of Equation (15). However  $e_j^N$  appears in Equation (11) multiplied by  $\%N$  which is small, while  $e_N^j$  appears multiplied by  $\%j$  which is large. Therefore the use of the nitrogen activity determined from the gas phase should definitely lessen any error in  $K$  which might be introduced by variation of  $e_N^j$  at higher  $\%j$ . The recalculation of  $K$  by this method for the systems boron, vanadium, columbium, and tantalum is shown in Table VI.

By comparing the  $K$  values in Table V and Table VI it can be seen that the use of the nitrogen activity determined by the gas phase causes the  $K$  values for the boron system to become much more nearly constant at a given temperature. This indicates that the experimentally determined values of  $e_N^B$  given in Table III may not be constant up to 7% B. For the boron system the values of  $K$  in Table VI are probably more accurate than those in Table V.

For the columbium and tantalum systems the  $K$  values in Table VI are very near the  $K$  values in Table V and the differences are considered to be within the limit of accuracy of the experimental method. This is further evidence that  $e_N^{Cb}$  and  $e_N^{Ta}$  can be considered constant up to the columbium and tantalum contents at which the experiments were run.

For the vanadium system the values of  $K$  in Table VI show much more scatter at a given temperature than the values of  $K$  in Table V. Moreover they show a systematic increase with increasing  $\%V$ . This is an indication that the value of  $e_V^V$  given in Table III which was estimated from the ternary Fe-V-N data is too high. In Table VII the  $K$  values



TABLE VI

SUMMARY OF THE SOLUBILITY PRODUCTS K' AND K CALCULATED  
USING THE NITROGEN ACTIVITY DETERMINED FROM THE  
GAS PHASE FOR THE SYSTEMS BORON,  
VANADIUM, COLUMBIUM, AND TANTALUM

Element j	Temp °C	%j	%N	K' = %B x %N	K	
B	1550	3.82	0.0104	0.0397	0.145	
		5.83	0.0028	0.0163	0.143	
		7.06	0.0018	0.0127	0.143	
	1600	5.83	0.0045	0.0262	0.175	
		7.06	0.0033	0.0233	0.197	
	1650	5.83	0.0123	0.0717	0.292	
		7.06	0.0050	0.0353	0.260	
	1700	7.06	0.0079	0.0557	0.346	
	1750	7.06	0.0163	0.115	0.498	
	V	1600	8.05	0.238	K' = %V x %N 1.92	0.581
			9.93	0.243	2.41	0.617
			15.04	0.280	4.21	0.736
1650		9.93	0.303	3.01	0.821	
		15.04	0.369	5.55	0.974	
1700		15.04	0.478	7.19	1.570	
1750		15.04	0.545	8.20	1.969	
Cb		1550	14.17	0.1625	K' = %Cb x %N 2.30	0.329
	11.41		0.209	2.38	0.486	
	1600	14.17	0.218	3.08	0.464	
		14.17	0.257	3.64	0.618	
	1650	17.71	0.232	4.38	0.498	
		17.71	0.205	5.79	0.716	
	1700	17.71	0.205	5.79	0.716	
		17.71	0.205	5.79	0.716	
Ta	1550	20.2	0.141	K' = %Ta x %N 2.85	0.550	

for the vanadium system from Table V have been reproduced in the column labeled  $K_1$  and the  $K$  values from Table VI reproduced in the column labeled  $K_2$ . The  $K$  were then recalculated using the activity of nitrogen determined from the gas phase and lower value of  $e_V^V = 0.028$  ( $\epsilon_V^V = 6.0$ ). These values are shown in Table VII in the column labeled  $K_3$ . It can be seen that they are much more nearly constant for a given temperature, and the value of  $e_V^V = 0.028$  is therefore expected to be nearer to the correct value.

TABLE VII

COMPARISON OF  $K$  VALUES FOR THE VANADIUM SYSTEM CALCULATED FOR DIFFERENT VALUES OF THE INTERACTION PARAMETER  $e_V^V$

Temp °C	%V	%N	$K' = \%V \times \%N$	$K_1$	$K_2$	$K_3$
1600	8.05	0.238	1.92	0.634	0.581	0.455
	9.93	0.243	2.41	0.637	0.617	0.454
	15.04	0.280	4.21	0.593	0.736	0.457
1650	9.93	0.303	3.01	0.858	0.821	0.590
	15.04	0.369	5.55	0.890	0.974	0.624
1700	15.04	0.478	7.19	1.282	1.570	0.954
1750	15.04	0.545	8.20	1.640	1.969	1.193

The fact that the  $K_1$  values are not as constant as the  $K_3$  values and in particular that the  $K_1$  value for 15.04% V is lower than the other two values for lower vanadium contents indicate that there is probably some change in the value of  $e_N^V$  with increasing vanadium contents. This is borne out by the work of Pehlke and Elliott<sup>(1)</sup> who found a value of  $e_N^V = -0.10$  to be good only out to about 5% V. Beyond that composition they found a slight change in slope of the curve of  $\log f_N$

versus  $\%V$ . However the change in slope was small so the error produced in  $K$  by assuming  $e_N^V$  constant should be correspondingly small.

G. Calculation of the Nitride Solubility Product Using the  $j$  Activity Estimated From Fe-j Binary Data

Because of the high solubility of  $Si_3N_4$  in liquid iron the silicon content required to precipitate  $Si_3N_4$  below one atmosphere of nitrogen pressure is in excess of 30%. It was previously noted that this is beyond the silicon concentration for which  $e_{Si}^{Si}$  may be approximated as constant. Consequently the use of the interaction parameter method to approximate the silicon activity in Fe-Si-N solutions may lead to serious error producing a low value for the silicon activity and therefore also a low value for the solubility product of  $Si_3N_4$ .

In order to avoid this error the  $K$  values for the silicon system were recalculated with the silicon activity estimated from the activity data of Chipman et al<sup>(34)</sup> which cover the entire composition range of the Fe-Si system. The nitrogen activity in solution was determined from the nitrogen activity in the gas phase.

The activity data of Chipman et al<sup>(34)</sup> for 1420°C are shown graphically in Figure 18 and numerical values are given in Table VIII. From these data silicon activities are calculated for the various experimental temperatures used in this study from the relation:

$$\frac{\partial \ln \gamma}{\partial (1/T)} = \frac{\bar{L}_{Si}}{R} \quad (23)$$

where  $\bar{L}_{Si}$  represents the relative partial molal enthalpy of silicon in binary Fe-Si solutions relative to pure silicon and defined by the

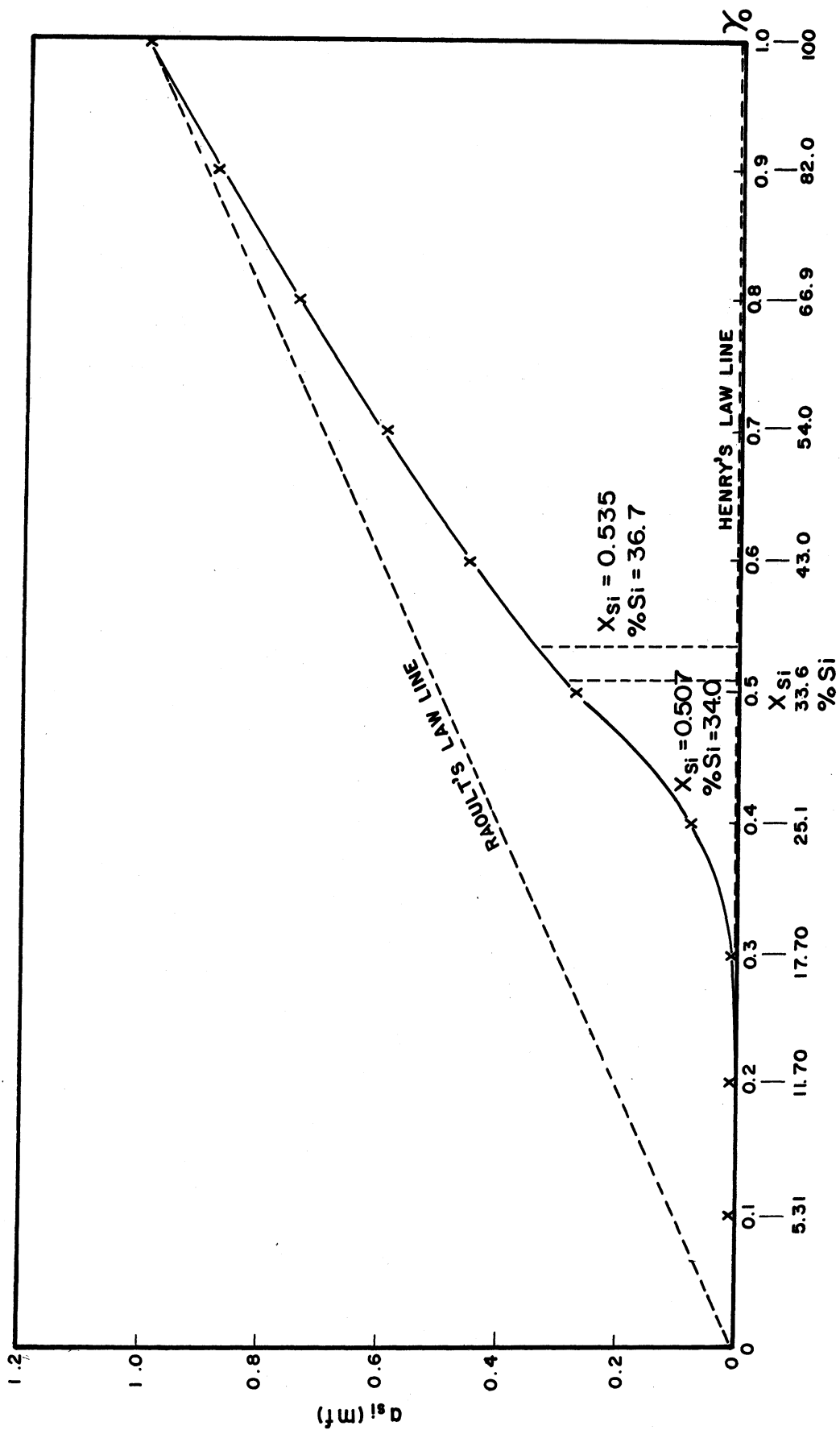


Figure 18. Activity of Silicon in Binary Fe-Si Solutions at 1420°C  
From Data by Chipman, Fulton, Gokcen, and Caskey(34)

equation:

$$\bar{L}_{Si} = \bar{H}_{Si} - H_{Si}^{\circ} \quad (24)$$

TABLE VIII

ACTIVITY OF SILICON IN Fe-Si SOLUTIONS AT 1420°C.  
FROM THE DATA OF CHIPMAN ET AL (34)

Si mole fr.	$-\bar{L}$ K cal.	$-\log \gamma_{Si}$	$\gamma_{Si}$	$a_{Si}$ (mf) = $X_{Si} \gamma_{Si}$
1.0	0.0	0.00	1.00	1.000
0.9	0.1	0.01	0.98	0.882
0.8	0.4	0.03	0.93	0.744
0.7	1.7	0.07	0.85	0.595
0.6	4.4	0.12	0.76	0.456
0.535 (36.7%)	7.2	0.19	0.64	0.343
0.507 (34.0%)	8.1	0.24	0.57	0.290
0.5	8.4	0.26	0.55	0.275
0.4	13.4	0.72	0.19	0.076
0.3	19.3	1.45	0.036	0.0108
0.2	24.1	2.09	0.0081	0.00162
0.1	27.8	2.34	0.0046	0.00046
0.0	28.5	2.50	0.0032	0.00000

$\bar{L}_{Si}$  is known from the work of Korber and Oelsen<sup>(37)</sup>. For lack of other information it is necessary to assume that  $\bar{L}_{Si}$  is constant with temperature and treat it as a function of composition only. The silicon activities given by Chipman et al<sup>(34)</sup> are expressed relative to Raoult's Law with the activity of silicon related to mole fraction and the standard state taken as pure liquid silicon. To use these silicon activities in conjunction with the experimental data they must be expressed relative to Henry's Law with the activity of silicon related to weight percent and the standard state taken as the infinitely dilute solution of silicon in pure liquid iron. This conversion is made by means of the equation:

$$\frac{a_{Si} \text{ (m.f. - Raoult's Law)}}{a_{Si} \text{ (\% - Henry's Law)}} = \frac{0.5585\gamma^{\circ}}{M_{Si}} \quad (25)$$

where  $\gamma^\circ$  is the slope of the  $a_{\text{Si}}$  versus mole fraction Si plot at infinite dilution. Implicit in Equation (25) are the assumptions that the mole fraction of silicon is proportional to the weight percent silicon up to the experimental silicon contents and that the weight of silicon is negligible with respect to the total weight of the solution. An exact calculation shows that these assumptions produce an error of 5% to 10% in the calculated silicon activity with respect to Henry's Law. This is a negligible correction compared to the uncertainty in the experimental data.

The silicon activities calculated for all experimental temperatures and compositions are shown in Table IX. The effect of the silicon-nitrogen interaction on the activity of silicon can be shown to be negligible because of the very small  $\%N$  in a solution containing over 30% Si.

The values of K for  $\text{Si}_3\text{N}_4$  calculated by this method from the break points of the nitrogen absorption curves are given in Table X. By comparing these K values with the K values given for the silicon system in Table V it can be seen that the values in Table X are larger as would be expected. However they still do not show the expected systematic variation with temperature. This is probably due to error in the experimental data rather than error in the methods of estimating the silicon and nitrogen activities.

#### H. Calculation and Summary of Enthalpy and Entropy of Decomposition of Nitrides in Liquid Iron

The variation of the nitride solubility product with temperature is given by the Van't Hoff Equation:

TABLE IX  
CALCULATED ACTIVITY OF SILICON IN Fe-Si SOLUTIONS OF 34.0% SILICON AT TEMPERATURES FROM  
1420° to 1700°C

Temp °C	$\gamma_{Si}$		$A_{Si}$ (mf -Raoult's Law)		$\frac{\gamma^{\circ}}{A_{Si} \text{ at } X_{Si} = 0.1}$		$A_{Si}$ (% - Henry's Law)	
	$X_{Si} = 0.1$	$X_{Si} = 0.507$	$X_{Si} = 0.535$	$X_{Si} = 0.1$	$X_{Si} = 0.507$	$X_{Si} = 0.535$	$X_{Si} = 0.507$	$X_{Si} = 0.535$
1420	0.0046	0.57	0.64	0.00046	0.290	0.343	0.0046	3180
1450	0.0054	0.60	0.68	0.00054	0.304	0.364	0.0054	2840
1500	0.0066	0.65	0.71	0.00066	0.330	0.380	0.0066	2500
1550	0.0083	0.69	0.76	0.00083	0.350	0.407	0.0083	2120
1600	0.0102	0.72	0.80	0.00102	0.365	0.428	0.0102	1802
1650	0.0123	0.78	0.83	0.00123	0.396	0.444	0.0123	1621
1700	0.0148	0.81	0.87	0.00148	0.411	0.465	0.0148	1398

$$\frac{d(\ln K)}{d(1/T)} = \frac{-\Delta H^\circ}{R} \quad (26)$$

TABLE X

CALCULATED ACTIVITY OF SILICON IN Fe-Si SOLUTIONS OF 34.0% and 36.7% SILICON AT TEMPERATURES FROM 1420°C to 1700°C

Temp °C	%Si	%N	$K' = (\%Si)^{3/4} \%N$	K
1450	34.0	0.0006	0.0078	13.10
1500	34.0	0.0054	0.0702	14.02
1550	36.7	0.0021	0.0313	9.45
1600	34.0	0.0218	0.284	10.99
	36.7	0.0117	0.174	7.91
1650	36.7	0.0360	0.536	7.66
1700	36.7	0.0252	0.376	8.74

If log K is plotted versus 1/T the slope of the curve gives  $\Delta H^\circ$  the standard enthalpy of decomposition of the nitride and the intercept at 1/T = 0 gives  $\Delta S^\circ$  the standard entropy of decomposition of the nitride in liquid iron, i.e. for the reaction as given by Equation (5). The usual procedure is to assume that  $\Delta H^\circ$  and  $\Delta S^\circ$  are constant over short temperature ranges and therefore to fit a straight line to the points on the Van't Hoff plot. These plots for the seven experimental systems in which the temperature variation of K has been studied are shown in Figure 19 through Figure 25. To obtain these plots the values of K from Tables V, VI, VII, and X for a given system were averaged at each temperature and plotted against the reciprocal temperature. The values of  $\Delta H^\circ$  and  $\Delta S^\circ$  were calculated from these plots by the integrated form of Equation (26):

$$\ln K = \frac{-\Delta H^\circ}{R} (1/T) + \frac{\Delta S^\circ}{R} \quad (27)$$



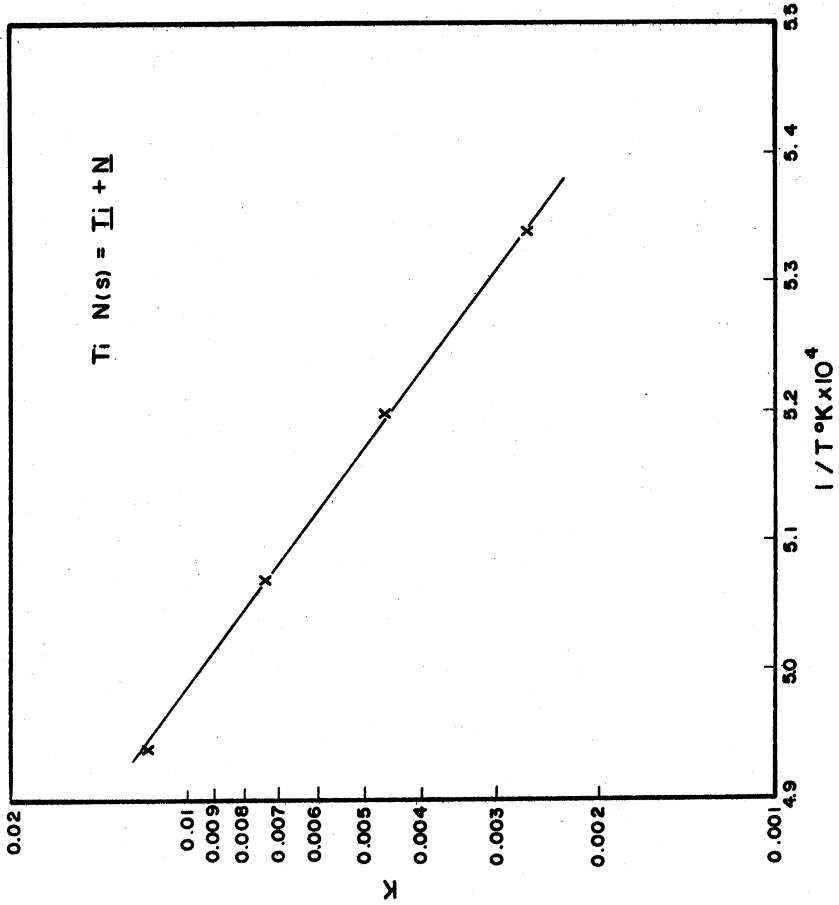


Figure 19. Variation of Equilibrium Constant with Temperature for the Reaction  $TiN(s) = Ti + N$

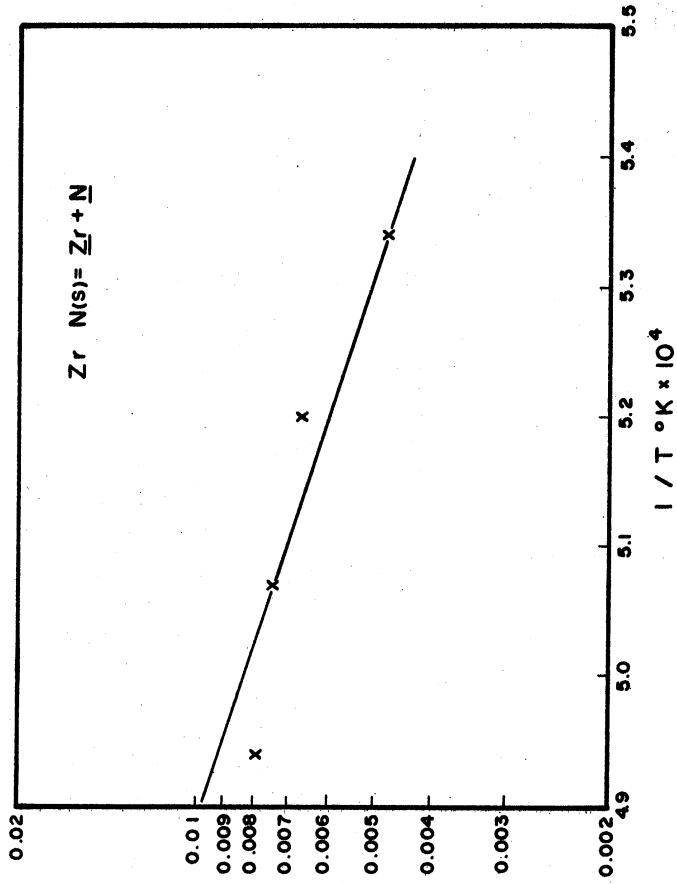


Figure 20. Variation of Equilibrium Constant with Temperature for the Reaction  $ZrN(s) = Zr + N$

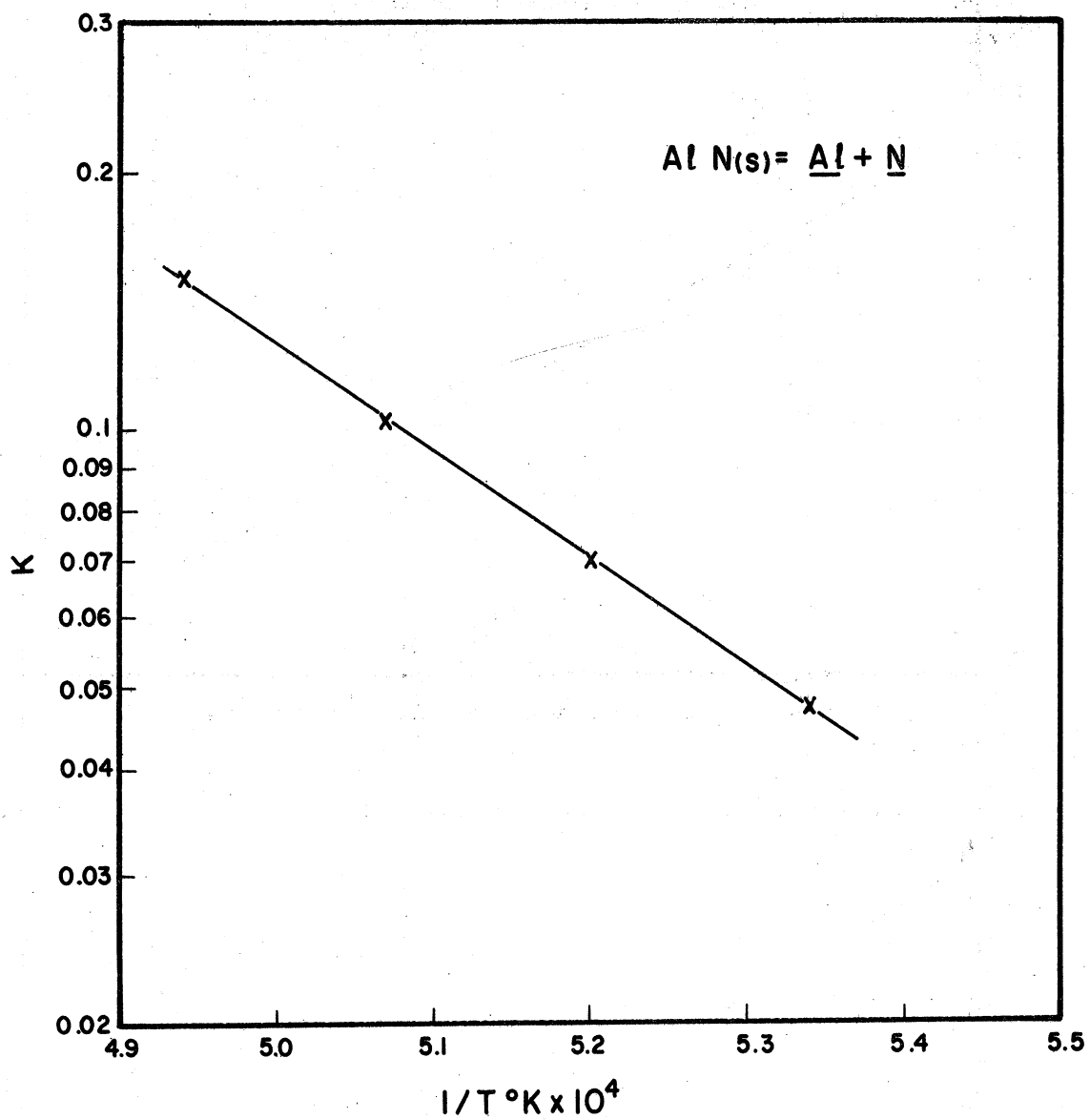


Figure 21. Variation of Equilibrium Constant with Temperature for the Reaction  $\text{AlN}_{(s)} = \underline{\text{Al}} + \underline{\text{N}}$

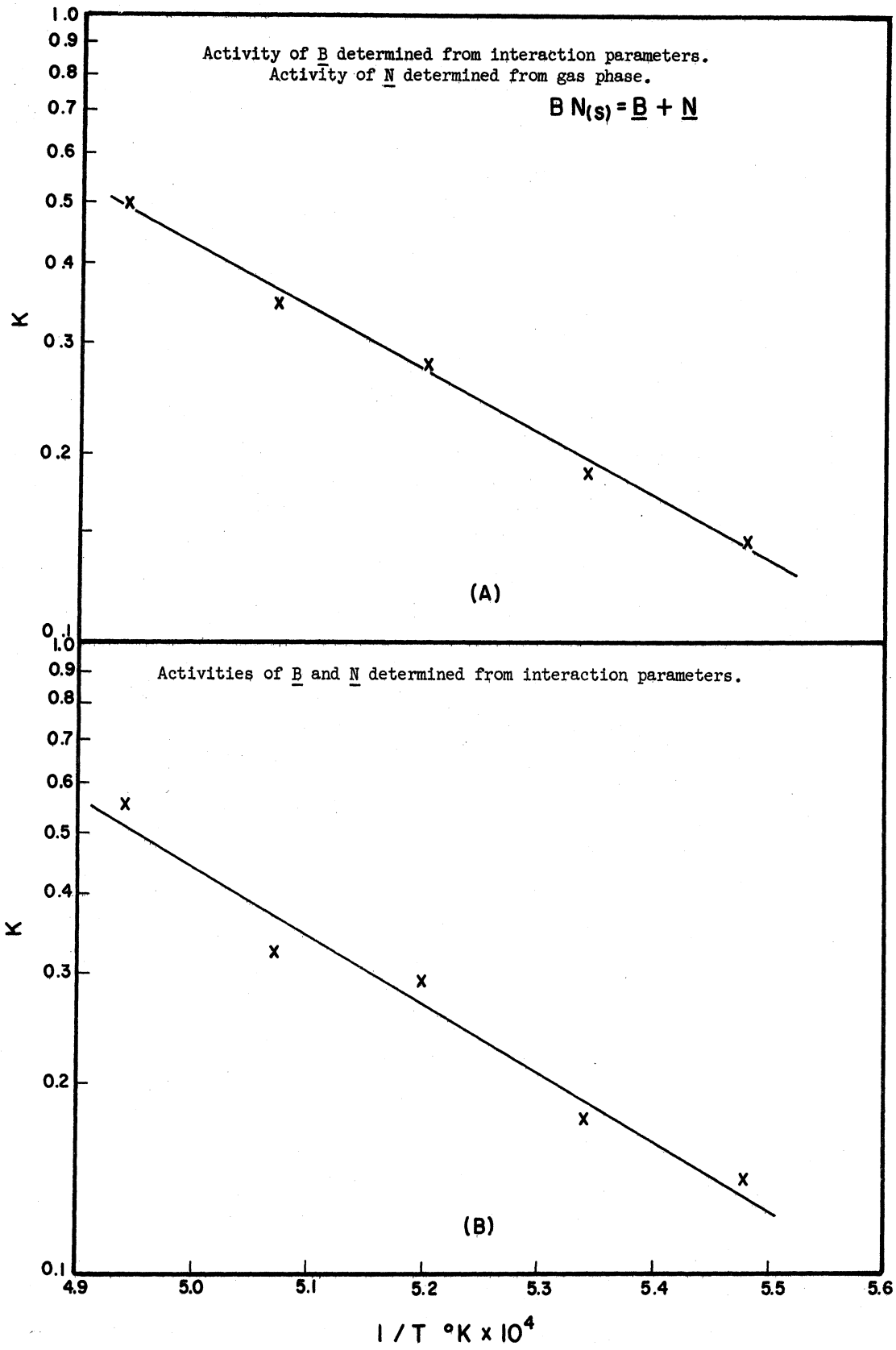


Figure 22. Variation of Equilibrium Constant with Temperature for the Reaction  $BN(s) = \underline{B} + \underline{N}$

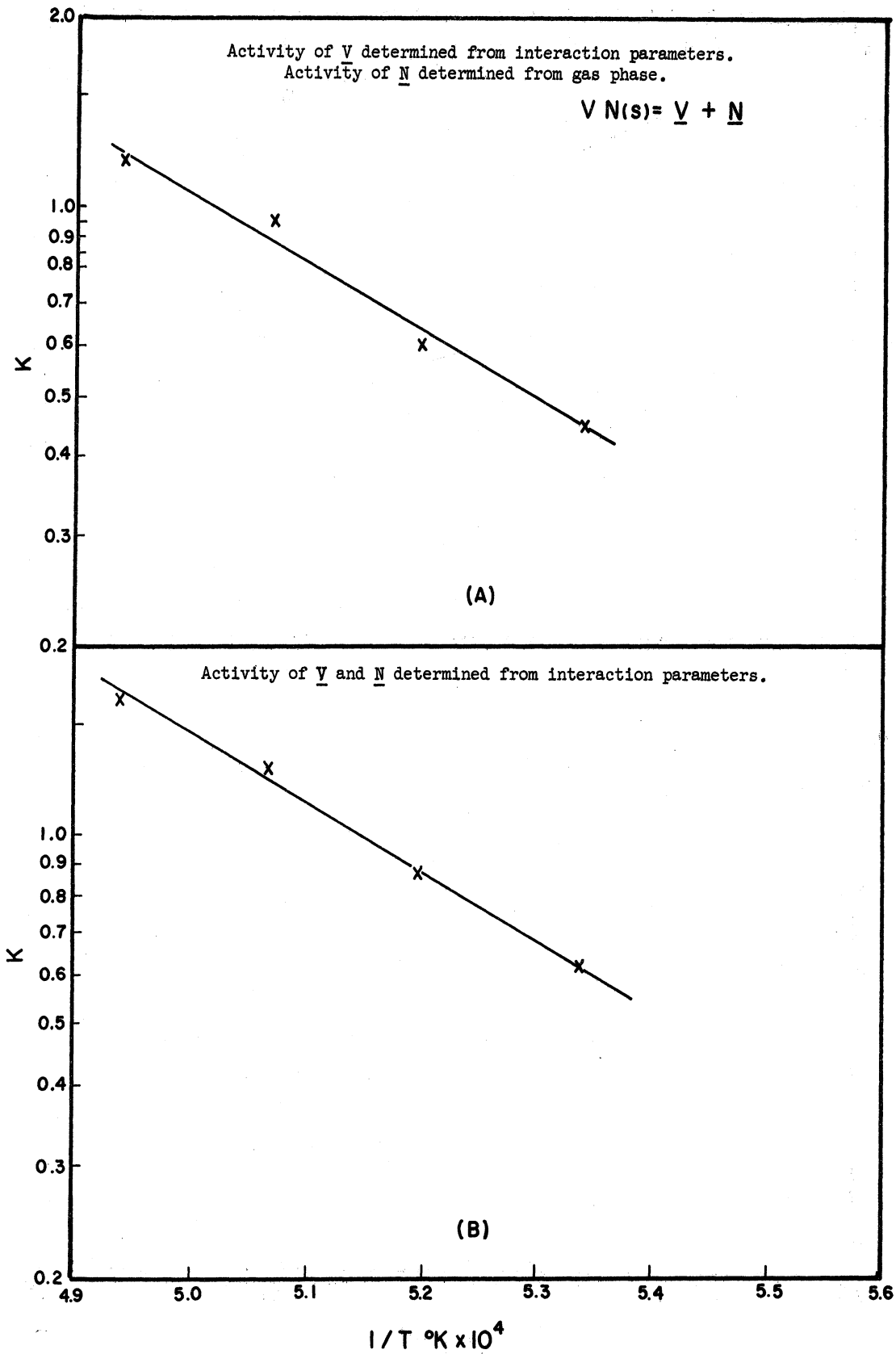


Figure 23. Variation of Equilibrium Constant with Temperature for the Reaction  $VN(s) = \underline{V} + \underline{N}$

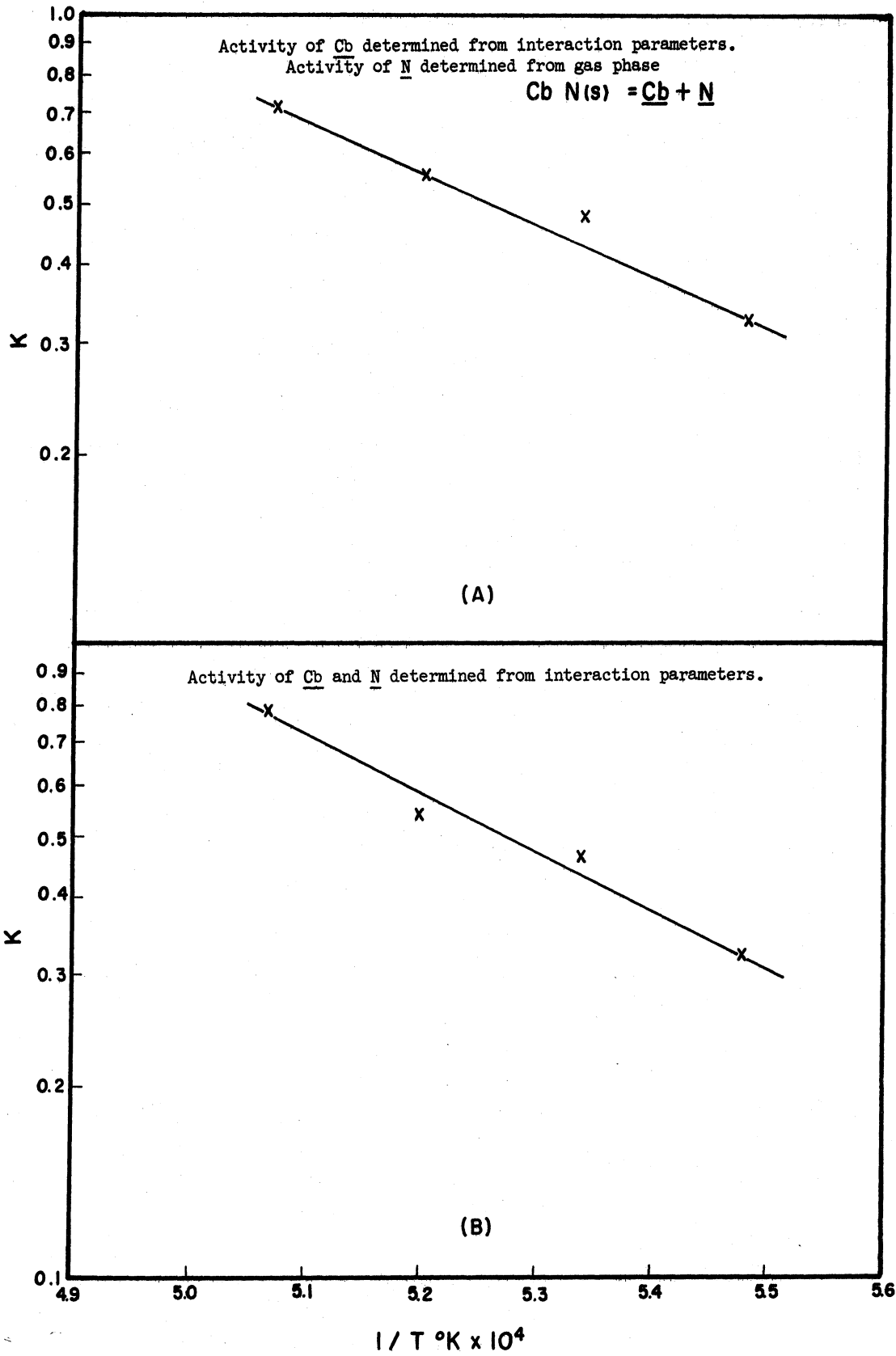


Figure 24. Variation of Equilibrium Constant with Temperature for the Reaction  $\text{CbN}_{(s)} = \underline{\text{Cb}} + \underline{\text{N}}$

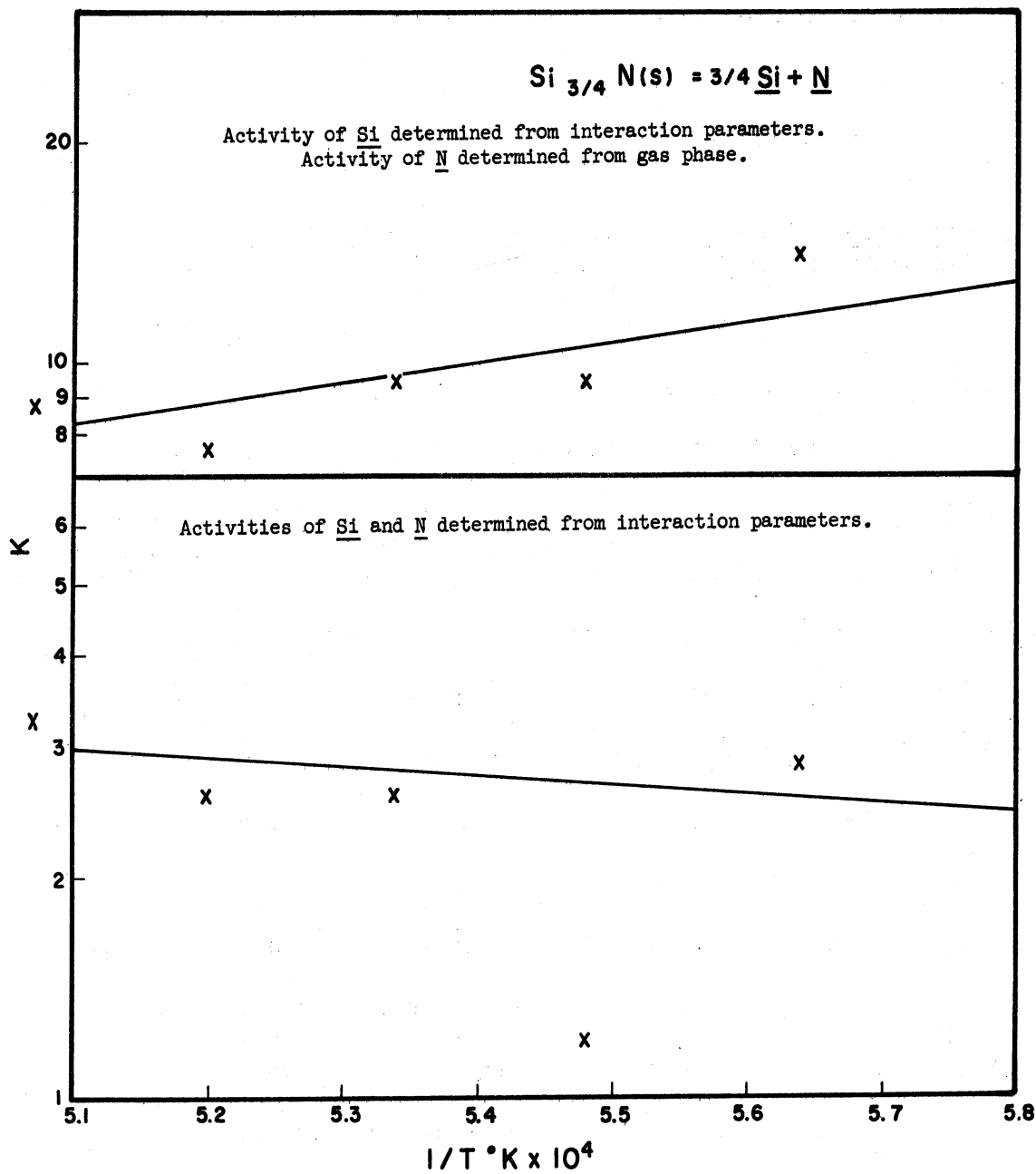


Figure 25. Variation of Equilibrium Constant with Temperature for the Reaction  $\text{Si}_{3/4} \text{N(s)} = 3/4 \underline{\text{Si}} + \underline{\text{N}}$

They are given in Table XI along with the assumed nitride compositions which were used to calculate  $K$ . Also given in Table XI are the values of  $\Delta F^\circ$  for the decomposition of the nitrides in liquid iron at  $1600^\circ\text{C}$  as calculated from the given values of  $\Delta H^\circ$  and  $\Delta S^\circ$  according to the relation:

$$\Delta F^\circ = \Delta H^\circ - T \Delta S^\circ \quad (28)$$

#### I. Discussion of Results of the Various Methods Used to Calculate the Nitride Solubility Products

Because of the possibility of variation in  $e_N^j$  and  $e_j^N$  at high solute concentrations it is felt that the values of  $\Delta H^\circ$ ,  $\Delta S^\circ$ , and  $\Delta F^\circ_{1600}$  for the more soluble nitride systems given in the second and third sections of Table XI are more accurate than the values for the same systems given in the first section. For the three more insoluble nitride systems titanium, zirconium, and aluminum the values of  $\Delta H^\circ$ ,  $\Delta S^\circ$ , and  $\Delta F^\circ_{1600}$  were calculated by the interaction parameter method only, since in these systems the solute concentrations are low enough that the interaction parameters should definitely remain constant over the required composition range.

By comparing Figure 22a with Figure 22b it can be seen that the use of the nitrogen activity determined by the gas phase for the boron system considerably reduced the data scatter in the Van't Hoff plot. The lower values of  $\Delta H^\circ$  and  $\Delta S^\circ$  they yield are consequently considered more accurate. With the vanadium system the  $K$  values calculated from the nitrogen activity determined by the gas phase (values in column  $K_3$  of Table VII) show about the same scatter in the Van't Hoff plot as the  $K$  values calculated by the method of interaction parameters. This is seen

TABLE XI

SUMMARY OF K VALUES FOR THE SILICON SYSTEM CALCULATED USING THE ACTIVITY OF SILICON ESTIMATED FROM Fe-Si BINARY DATA

Element j	Temp Range °C	$\Delta H^\circ$ Cal/Mole	$\Delta S^\circ$ Cal/Mole °K	$\Delta F^\circ$ 1600°C Cal/Mole	assumed nit-ride composition	Comments
Ti	1600-1750	75,200	28.34	22,100	TiN	Activities of $\bar{j}$ and $\bar{N}$ determined from interaction parameters
Zr	1600-1750	32,600	6.69	20,100	ZrN	
Al	1600-1750	63,700	27.91	11,400	AlN	
B	1550-1750	50,200	23.47	6,200	BN	
V	1600-1750	50,700	26.15	1,800	VN	
Cb	1550-1700	42,200	20.93	3,000	CbN	
Si	1450-1700	3,600	3.89	-3,300	Si <sub>3</sub> /4N	
B	1550-1750	45,900	21.25	6,100	BN	Activity of $\bar{j}$ determined from interaction parameters. Activity of $\bar{N}$ determined from gas phase
V	1600-1750	49,000	24.58	3,000	VN	
Cb	1550-1700	35,000	17.08	3,000	CbN	
Si	1450-1700	-10,500	-0.75	-11,900	Si <sub>3</sub> /4N	Activity of $\bar{j}$ estimated from Fe-j binary data. Activity of $\bar{N}$ determined from gas phase



from Figure 23a and Figure 23b. However as was previously noted the K values calculated from the nitrogen activity determined by the gas phase are much more constant at a given temperature and therefore the slightly lower  $\Delta H^\circ$  and  $\Delta S^\circ$  they yield are also considered more accurate. Figure 24a and Figure 24b which show K values calculated from the two different methods for the columbium system also show about the same scatter and as previously noted the comparison of the K values in Table V and Table VI show small differences within the limits of experimental error. Nevertheless the values of  $\Delta H^\circ$  determined from the two different sets of K values show an appreciable difference of about 7,000 calories/mole. This emphasizes the difficulty involved in trying to make an accurate determination of  $\Delta H^\circ$  from a Van't Hoff plot over a comparatively small temperature range. Although there is no experimental evidence of error introduced by variation in  $e_N^{Cb}$  and  $e_{Cb}^N$ , the lower values of  $\Delta H^\circ$  and  $\Delta S^\circ$  determined using the nitrogen activity determined by the gas phase are considered more accurate in the columbium system as well as in the boron and vanadium systems.

The  $\Delta H^\circ$  and  $\Delta S^\circ$  values in Table XI show that the results for two systems, zirconium and silicon, are inconsistent with the results of the other five systems. The problem with zirconium is that it is a very strong oxide former. Calculations made from data after Elliott and Gleiser<sup>(38)</sup> and Chipman<sup>(7)</sup> show that at 1600°C the  $\Delta F^\circ$  of decomposition of  $ZrO_2$  in liquid iron exceeds the  $\Delta F^\circ$  of  $ZrN$  by more than 60,000 cal./mole of  $Zr$  and exceeds the  $\Delta F^\circ$  of  $Al_2O_3$  by about 5,000 cal./mole of  $O$ . This indicates that  $ZrO_2$  is more stable than either  $Al_2O_3$  or  $ZrN$  in contact with liquid iron at this temperature. This

explains the previously noted reaction between Fe-Zr alloys and  $\text{Al}_2\text{O}_3$  crucibles which resulted in the formation of  $\text{ZrO}_2$  floating on top of the melt with an attendant drop in the zirconium content of the solution. Appendix F contains three nitrogen absorption curves for melts of iron plus up to 0.422% Zr made in  $\text{Al}_2\text{O}_3$  crucibles. These curves all show a Sieverts Law line almost identical with that for pure iron all the way to one atmosphere nitrogen pressure. This indicates that nearly all the zirconium was removed from solution by reaction with the  $\text{Al}_2\text{O}_3$  crucible because if even small amounts of zirconium had remained in solution the nitrogen solubility would have been appreciably increased. It is also quite possible that the reduction of the  $\text{Al}_2\text{O}_3$  crucible by zirconium caused appreciable quantities of aluminum to be dissolved into the melt. However the effect of aluminum on nitrogen solubility is small (i.e.  $e_N^{\text{Al}} \approx 0$ ) and its presence therefore would not be reflected in the slope of the Sieverts Law line.

The data on the zirconium system consequently were obtained using  $\text{ZrO}_2$  crucibles to contain the melt. However even these caused the formation of small amounts of floating solid on top of the melt under a hard vacuum. This solid is thought to be  $\text{ZrO}_2$  formed from oxygen adsorbed on the crucible walls and zirconium from the melt. Another possible source of oxygen is  $\text{Y}_2\text{O}_3$  which is contained in the  $\text{ZrO}_2$  crucible. The zirconium recovery in the melt therefore may have been somewhat lower than the calculated charge compositions causing the calculated values of  $K'$  and  $K$  to be slightly high and the values of  $e_N^{\text{Zr}}$  and  $e_{\text{Zr}}^{\text{N}}$  to be slightly low. It is noteworthy however that although the quantity of floating solid formed appeared to vary considerably from run to run the

values obtained for the nitrogen solubility and the nitride solubility limit are reasonably self consistent.

The initial data for the zirconium system were obtained with  $ZrO_2$  crucibles of  $3/4$ " inside diameter and 2" deep. However with these deep narrow crucibles very little stirring of the molten metal could be observed visually. Moreover on examination of the solidified ingots it appeared in several cases that the charge had never become a completely homogenous melt. Therefore several melts were made with  $ZrO_2$  crucibles of  $1\ 13/16$ " inside diameter  $1\ 7/16$ " deep. In these melts the amount of stirring observed was much greater and the solidified ingots all appeared definitely homogenous. However the results obtained were identical to those obtained on the smaller diameter  $ZrO_2$  crucibles.

It can be seen from Appendix F that in some of the nitrogen absorption curves for the zirconium system the deviation from the Sieverts Law line is in a horizontal instead of a vertical direction. The reason for this is that when sufficient  $ZrN$  precipitates to form a continuous film on top of the melt the gas phase is effectively insulated from the liquid phase. Equilibrium between the gas and liquid phases at higher nitrogen pressures can be achieved then only by diffusion of nitrogen through the solid film into the liquid phase where it can react with the zirconium in solution to precipitate more  $ZrN$ . This process is so slow that equilibrium is not achieved in an experimentally reasonable time. Consequently once the nitride film has formed the melt will absorb almost no more nitrogen and the only volume of gas required to further increase

the nitrogen pressure is that necessary to fill up the hot volume. Of course these absorption curves with a horizontal deviation cannot be considered to define the nitride solubility limit as accurately as the absorption curves with the normal vertical deviation, since the concentering effects of horizontal deviation due to nitride film formation and vertical deviation due to nitride precipitation may cause the experimental points to appear to follow a straight Sieverts Law line beyond the true nitride solubility limit. However the nitride solubility limits measured from these horizontal deviation absorption curves agree reasonably well with those absorption curves for the zirconium system which show the normal vertical deviations.

The effect of nitride film formation was evident for the other alloy systems as well as zirconium. It was reflected in the much longer times required to reach pressure equilibrium at nitrogen pressures above the nitride solubility limit. Below the nitride solubility limit the equilibrium pressure was reached in 5 to 10 minutes while above the nitride solubility limit 30 minutes was minimum and equilibration times of 60 to 90 minutes were not uncommon. However with all systems except zirconium the nitride films were apparently porous enough that the absorption curves showed normal vertical breaks if sufficiently long equilibration times were used.

The apparent inconsistency in  $\Delta H^\circ$  and  $\Delta S^\circ$  for the silicon system is attributed to the extreme solubility of  $\text{Si}_3\text{N}_4$  which makes estimation of the activities of Si and N less accurate and to the possible reaction of silicon with the  $\text{Al}_2\text{O}_3$  crucibles which may have produced erroneous values of  $K$  at the higher temperatures in each

determination. The experimental values of  $K'$  and  $K$  are felt to be correct within an order of magnitude, but little faith can be placed in the values of  $\Delta H^\circ$  and  $\Delta S^\circ$  calculated from them. These are thought to be considerably low. A calculation using the data of Pehlke and Elliott<sup>(1,39)</sup> and Chipman<sup>(7)</sup> indicates that the values should be  $\Delta H^\circ = 21,500$  cal./mole,  $\Delta S^\circ = 20.21$  cal./mole  $^\circ\text{K}$ , and  $\Delta F^\circ_{1600} = -16,300$  cal./mole. The fact that this value of  $\Delta F^\circ_{1600}$  corresponds reasonably to the value in the third section of Table XI is further evidence of an order of magnitude accuracy in the  $K$  values, at least for temperatures of  $1600^\circ\text{C}$  and below.

The values of  $\Delta F^\circ_{1600}$  given in Table XI are a measure of the relative stabilities of the various nitrides in contact with liquid iron at  $1600^\circ\text{C}$ . They show that the resistance of the nitrides listed in Table XI to liquid iron at  $1600^\circ\text{C}$  decreases from top to bottom of the table. Only TiN, ZrN, and possibly AlN can be considered as refractory materials which will be reasonably resistant to attack by liquid iron at this temperature. Table XI shows that BN, although it is used in contact with solid iron base alloys at elevated temperatures in a number of applications particularly in nuclear reactor components and is advertised as being resistant to attack from liquid metals such as silicon, aluminum, copper, zinc, and iron, is soluble to a fair degree in liquid iron. Table V suggests that if BN is equilibrated with liquid iron at  $1600^\circ\text{C}$  under atmospheric pressure of nitrogen gas the melt should dissolve 4 to 5 percent boron. If the partial pressure of nitrogen over the melt is less than one atmosphere the amount of boron dissolved by the melt will be

correspondingly higher. The solubility of BN in liquid iron is certainly great enough that if BN is used as a refractory to contain liquid iron the melt will become seriously contaminated with boron. Also if the mass of the melt is sufficiently large with respect to the mass of the refractory the melt may easily dissolve enough BN to corrode through the refractory and run out.

Determination of nitride solubility products from the experimental data by the method of extrapolation of  $\log K'$  to zero  $\%j$  proved to be generally less accurate than the other methods of calculation. For the titanium and zirconium systems the interaction parameters  $e_j^N$  are large and negative. This means that the assumption that the term  $e_j^N(\%N)$  is negligible over any appreciable range of  $\%j$  is not valid. The plot of  $K'$  versus  $\%j$  for the aluminum and boron systems is shown in Figure 26 and for the columbium and vanadium systems in Figure 27. The values of  $K$  given in Figure 26 show reasonable agreement with the  $K$  values for the aluminum and boron systems given in Table V. The  $K$  values given in Figure 27 are slightly higher than the values given in Table V for columbium and in the last column of Table VII for vanadium. This is probably due to the fact that the interaction parameters  $e_V^N$  and  $e_{Cb}^N$  are also large and negative.

#### J. Summary of the Nitride Solubility Products Measured by the Quenching Method

The experimental results obtained by the quenching method are summarized in Table XII. The first section of the table gives the results of the calibration runs made with pure iron using  $Al_2O_3$  crucibles and compares them with results for the solubility of nitrogen in pure liquid

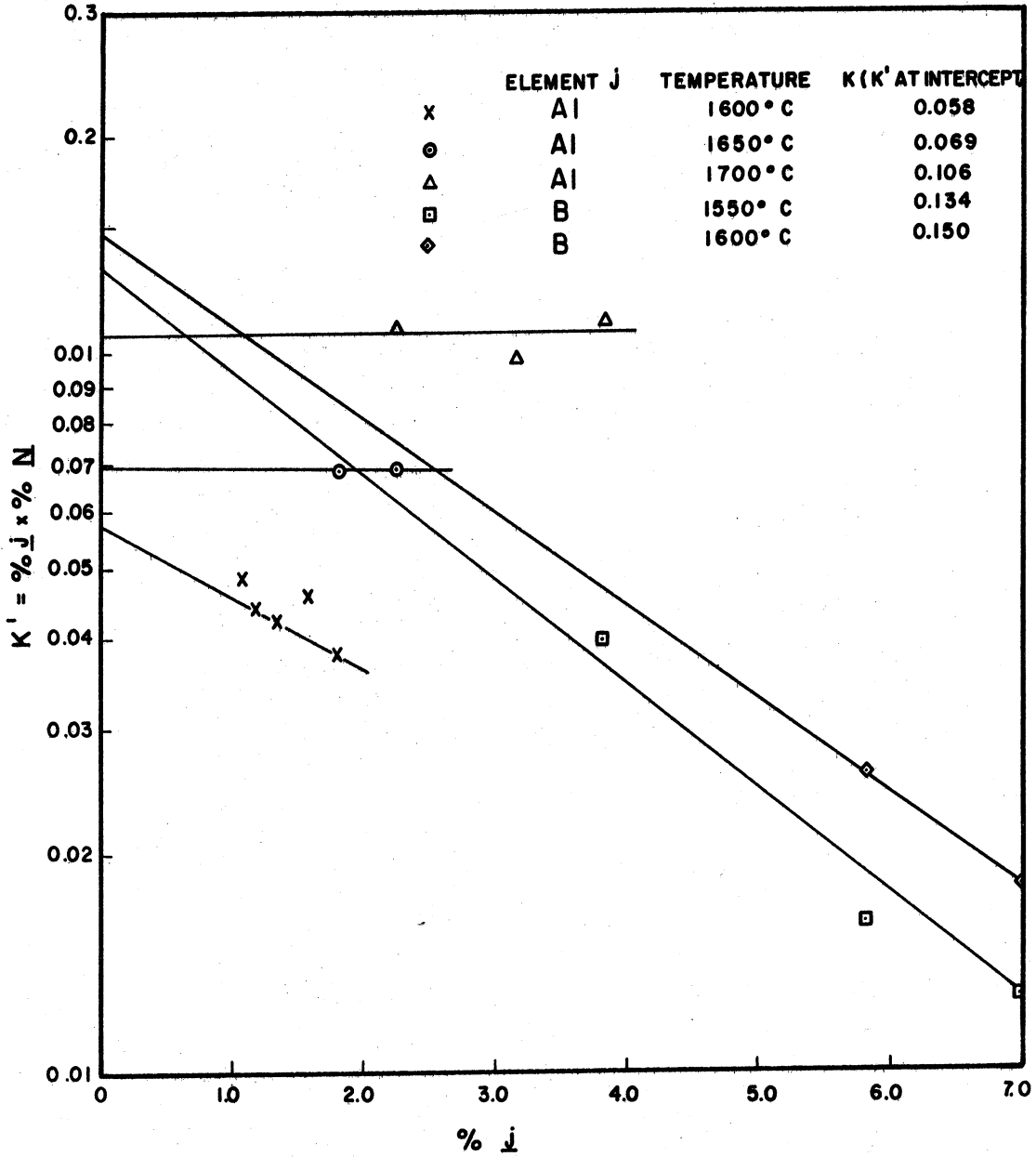


Figure 26. Extrapolation of K' to Zero %j in the Aluminum and Boron Systems

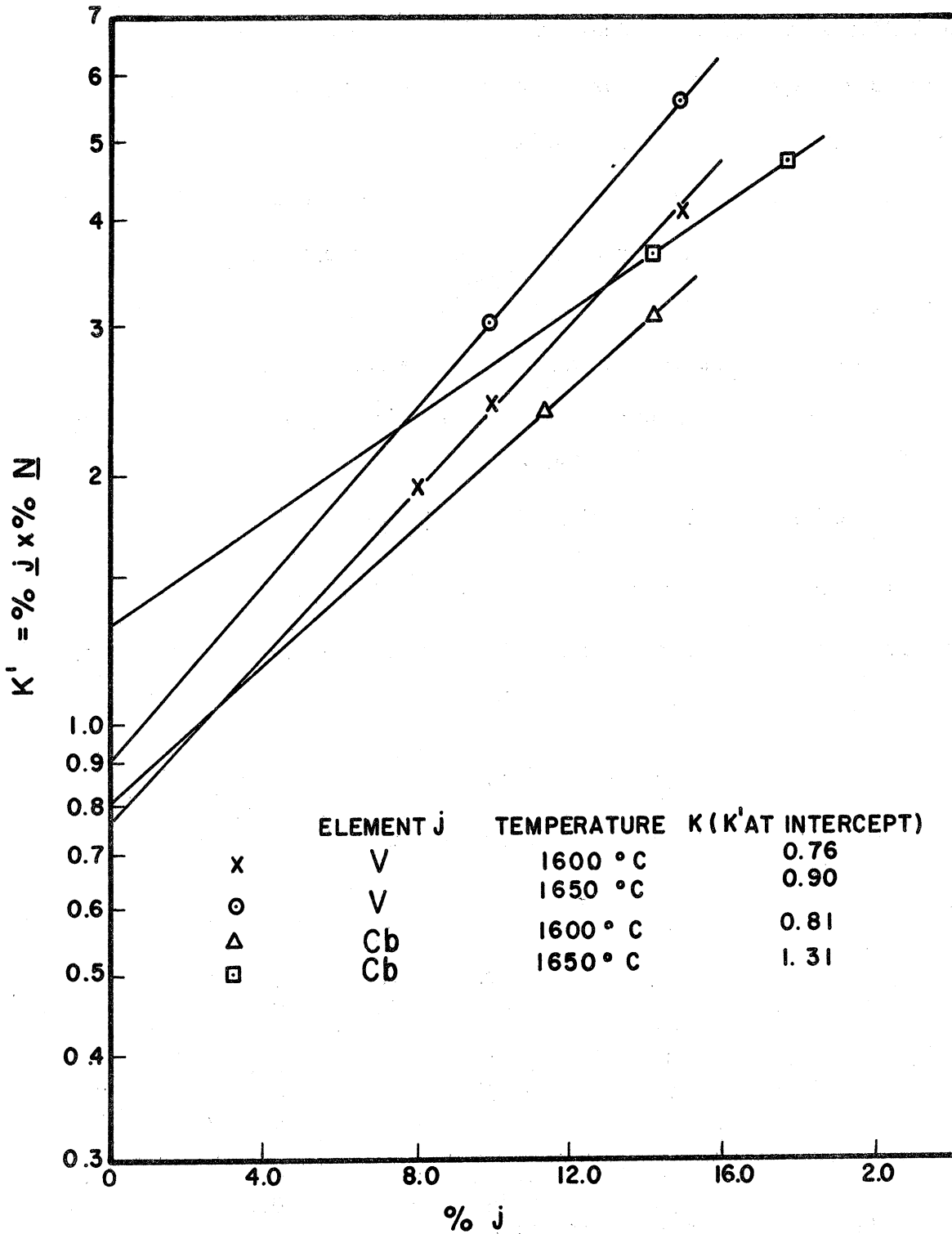


Figure 27. Extrapolation of K' to Zero %j in the Vanadium and Columbian Systems



iron measured by the Sieverts method.

The first three runs were made at 1600°C for various equilibration times under atmospheric pressure of nitrogen gas. The nitrogen solubilities determined by Kjeldahl analysis were corrected to one standard atmosphere of nitrogen pressure by multiplying them by  $\sqrt{\frac{P}{76.0}}$ . P is the atmospheric pressure existing during the equilibration which was read from a mercury barometer. In order to determine if the liquid seal at the gas stream outlet caused the build-up of a pressure appreciably above atmospheric in the furnace chamber one outlet line was connected to a manometer and the maximum gas flow to be used was passed through the system. The manometer showed no measurable pressure build-up indicating

TABLE XII

SUMMARY OF RESULTS OBTAINED BY THE QUENCHING METHOD

Element j	Temp °C	Time (min)	P <sub>N<sub>2</sub></sub> (atm)	%N	Sieverts <sup>(1)</sup> %N Method	K'
NONE	1600	15	1.000	0.0452	0.0451	
	1600	30	1.000	0.0456		
	1600	60	1.000	0.0456		
	1600	30	0.762	0.0399	0.0393	
	1600	30	0.332	0.0288	0.0262	
	1700	30	1.000	0.0442	0.0460	
	Ti	1600	30	0.332	$\frac{\%j}{0.36}$	$\frac{\%N}{0.0149}$
1700		15	0.331	0.38	0.0056	0.00213
1700		15	0.977	1.20	0.0094	0.01128
1700*+		5	0.979	0.11	0.0391	0.00430
Al	1600	30	0.331	1.44	0.0381	0.0549
	1600*	30	0.972	1.15	0.0547	0.0629
	1650*+	2-5	0.971	0.50	0.0329	0.0164
B	1600	30	0.978	3.49	0.0060	0.0210
	1600	30	0.764	2.51	0.0053	0.0133

\*quench not completely satisfactory

+equilibration ended prematurely by equipment failure

that it was less than one millimeter of mercury and therefore could be considered negligible. The excellent agreement among the first three runs at 1600°C and one standard atmosphere nitrogen pressure and the Sieverts method value for the same conditions indicated that equilibrium between liquid and gas phases in the quenching apparatus was reached within 15 minutes. This however is in the absence of a solid nitride phase. Because the presence of the nitride phase slowed the attainment of equilibrium in the Sieverts measurements an aim equilibration time of 30 minutes was selected for the equilibrations using nitride crucibles.

The next two pure iron runs were made to test the effectiveness of the gas metering system in controlling the nitrogen partial pressure in the quenching apparatus. The results obtained are plotted and compared with the Sieverts method data in Figure 28. While the agreement at one atmosphere and 0.76 atmosphere nitrogen pressure is excellent, the quenching method solubility value at 0.33 atmosphere is slightly higher than the Sieverts method solubility value at the same pressure. This might be the effect of thermal diffusion which would tend to cause enrichment of the lighter of two gases in a mixture at the hotter portions of the furnace chamber. This would have the effect of enriching the atmosphere immediately above the melt surface in nitrogen and depleting it in argon, which would account for the higher nitrogen solubility value. However the difference between the quenching method solubility and the Sieverts method solubility is small and may only reflect a small error in the nitrogen analysis.

The final run on pure iron was made at 1700°C to test the effectiveness of the quenching system with this extra 100°C of superheat.

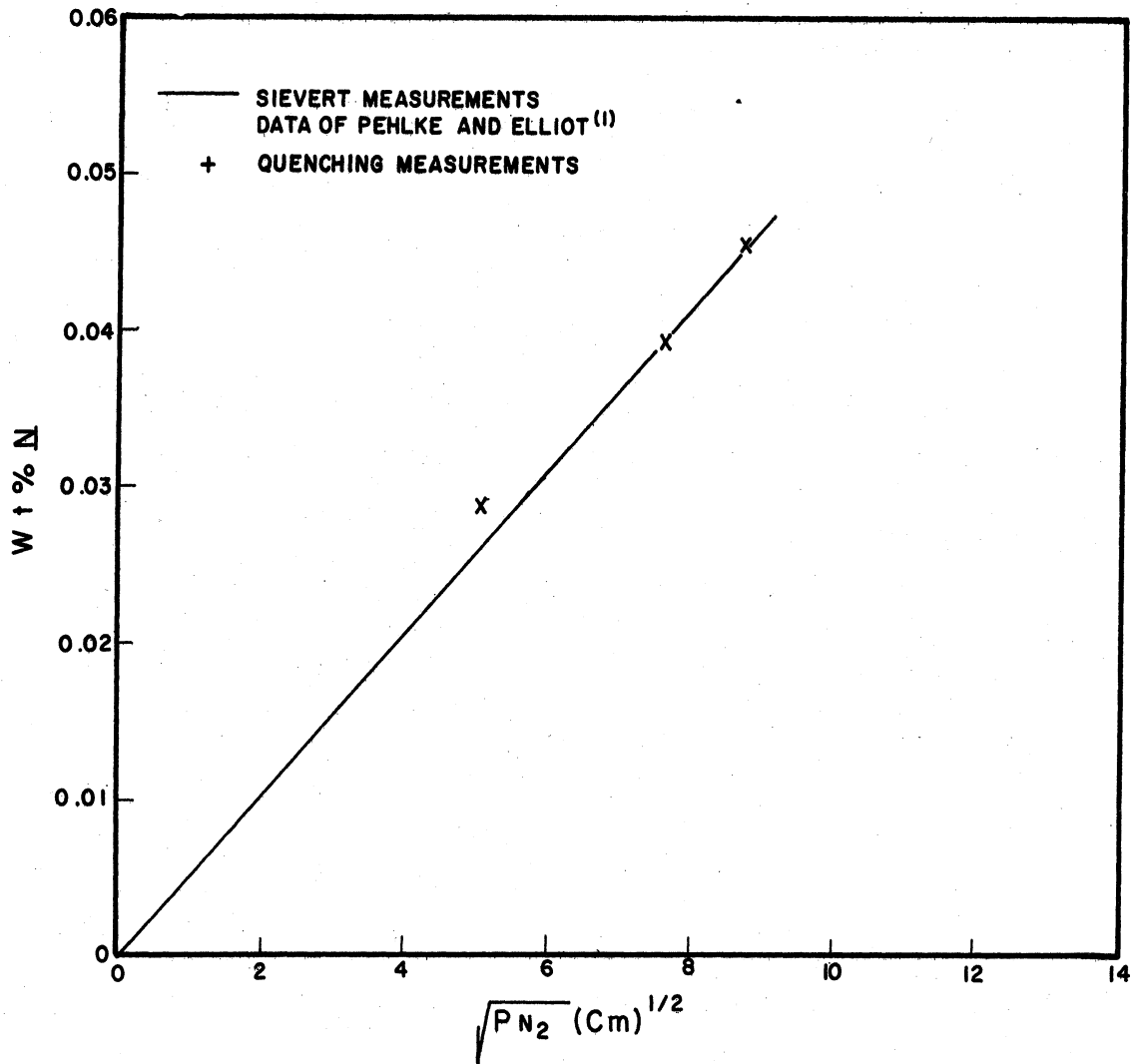


Figure 28. Solubility of Nitrogen in Pure Liquid Iron at 1600°C

The nitrogen solubility value obtained was lower than the solubility measured at 1600°C while the Sieverts method data indicates that the nitrogen solubility should increase slightly with increasing temperature. This indicates that on quenching from 1700°C a small but finite amount of nitrogen is lost from solution.

In order to determine if an appreciable temperature gradient existed across the diameter of the melt, optical pyrometer readings were taken both at the center and at the outer edge of the melt. These readings showed the melt edge to be approximately 10°C cooler than the melt center. This difference is nearly within the limits of the pyrometer accuracy and in any case is very small. This indicates that the temperature of the melt is substantially uniform and that most of the temperature drop between melt and surroundings is therefore through the crucible walls. These readings would appear to indicate that there is also little or no temperature gradient across a melt in the Sieverts apparatus where direct pyrometer readings cannot be taken since all except the center of the melt surface is covered by a crucible lid.

From the results of the pure iron calibration runs it was concluded that the design and operation of the quenching apparatus were basically sound. Equilibrium between melt and gas phase was reached within 15 minutes. The control over the nitrogen partial pressure and melt temperature were sufficiently precise. The quench was sufficiently fast to permit negligible amounts of nitrogen to escape from solution on quenching from 1600°C and very small amounts of nitrogen to escape from solution on quenching from 1700°C.

Four runs were made using titanium nitride crucibles and the results of these are summarized in the second section Table XII. It was previously noted that the TiN crucibles proved slightly porous to liquid iron and for this reason the aim equilibration time for all runs at 1700°C was cut to 15 minutes instead of the usual 30 minutes. The fourth run was terminated after 5 minutes by burning out of the induction coil, but the analyses are not very different from those obtained in the other three runs so equilibrium must have been approached even in this short time. Over heating of the induction coil had to be carefully guarded against with this system because the electrical and thermal properties of TiN caused the crucibles themselves to heat up to a temperature very near to that of the melt.

The agreement between the  $K'$  values for TiN in Table XII and those in Table V is only fair. Moreover the nitrogen and titanium analyses and the values of  $K'$  are not completely consistent among themselves. For example the second and fourth runs show a lower  $K'$  at 1700°C than the first run shows at 1600°C although it is certain from the Sieverts data that the solubility of TiN in liquid iron increases with increasing temperature. Although the third run shows a  $K'$  value which compares well with the  $K'$  values for TiN at 1700°C in Table V it is difficult to understand the high titanium analysis. In addition the nitrogen analyses are generally lower than the corresponding nitrogen values in Table V. This may be accounted for by the fact that difficulty was experienced with this system only in completely dissolving the samples for the Kjeldahl analyses. A small amount of black appearing residue invariably remained undissolved after the sample had been digested. This may

have been all or partly a nitrogen bearing compound and thus led to low nitrogen analyses.

The results of the three runs made with AlN crucibles are summarized in the third section of Table XII. The values of  $K'$  for  $1600^{\circ}\text{C}$  show good agreement with the values of  $K'$  at  $1600^{\circ}\text{C}$  for the aluminum system given in Table V. The Table XII values are slightly higher than the Table V values. This may be explained by the fact that with the quenching method the equilibrium is being approached with an excess of nitride present while in the Sieverts method the equilibrium is being approached with the nitride initially absent. The initial presence of the nitride in the quenching method may have the effect of increasing the tendency toward supersaturation in the solution. The aluminum and nitrogen analyses show self consistency, the  $\%N$  decreasing as the  $\%Al$  increases. The value of  $K'$  increases with decreasing  $\%Al$  which is the same trend shown by Table V and Figure 26. The run at  $1650^{\circ}\text{C}$  which was cut short by a burned out induction coil obviously did not stay at temperature long enough to reach equilibrium. This accounts for the low values of  $\%Al$ ,  $\%N$ , and  $K'$ . Even in this case however it is significant that the value of  $K'$  agrees within an order of magnitude with the  $K'$  values for the aluminum system at  $1650^{\circ}\text{C}$  given in Table V.

The fourth section of Table XII summarized the results of two runs made with BN crucibles. The values of  $\%B$ ,  $\%N$ , and  $K'$  agree quite well with the values for the boron system at  $1600^{\circ}\text{C}$  given in Table V. The  $\%B$  for the second run appears to be slightly low and this is thought to be an inaccuracy in the analysis.

K. Summary of Methods Used to Determine the Nitride Phase Compositions

Attempts were made to determine the compositions of the nitride phases formed both directly by x-ray and wet chemical analyses and indirectly by means of the previously described phase rule analysis and from the variation of the solubility product with temperature.

Only three of the alloy systems, titanium, zirconium, and aluminum, have nitrides sufficiently insoluble that the assumption of negligible  $\%j$  in solution which is inherent in Case 3 of the phase rule analysis might be expected to hold. Of these three, zirconium must be eliminated because of the extreme non-equilibrium conditions which were shown to exist at nitrogen pressures well above the nitride solubility limit. For the titanium and aluminum systems the majority of the nitrogen absorption curves are not suitable for calculation of the nitride phase composition since they were terminated slightly above the break points in order to redetermine the nitride solubility limit at a higher temperature. However two absorption curves in each of the two systems extended to sufficiently high nitrogen pressures to make a calculation of the nitride phase composition possible by the phase rule method. The graphical analysis of these absorption curves and the details of calculation of the nitride phase compositions are shown in Appendix G.

The results give nitride compositions of  $Ti_{2.2}N$  and  $Ti_{2.4}N$  for the titanium system and  $Al_{3.9}N$  and  $Al_{4.5}N$  for the aluminum system. Only for one absorption curve, the 0.228% Ti curve, can a line with the slope of the Sieverts Law line for pure iron be drawn through the data points at high nitrogen pressures with reasonable accuracy. The nitride

compositions calculated in Appendix G are all thought to be too high in metal. This is due to the difficulty in completely saturating the liquid and solid phases with nitrogen at a given nitrogen pressure once an initial nitride film has formed on the melt. Apparently even after times of 60 to 90 minutes complete equilibrium does not exist at nitrogen pressures well above the nitride solubility limit.

Since the variation of the nitride solubility products with temperature was known it was thought possible to at least infer limits on the nitride compositions by calculating values of  $K$  for various nitride compositions, i.e. various values of  $x$  in Equations (5) and (10), and determining which compositions gave the best fit to a linear relation between  $\log K$  and  $1/T$ . For at least three of the systems previous work had shown the possibility of the nitride existing with a metal rich stoichiometry. These systems are titanium,<sup>(12),(14)</sup> vanadium,<sup>(13),(17)</sup> and columbium.<sup>(18)</sup> Figure 29 shows the Van't Hoff plot of the Sieverts method data for the titanium system for assumed nitride compositions of  $TiN$ ,  $Ti_{1.7}N$  the composition calculated by Rao and Parlee<sup>(12)</sup>, and  $Ti_{2.4}N$  given as the upper composition limit by Ehrlich<sup>(14)</sup>. It can be seen that the composition for which the data points show the best fit to a straight line is  $TiN$ . The fit for  $Ti_{1.7}N$  is only slightly worse but the fit for  $Ti_{2.4}N$  is definitely worse. With both of the latter two nitride compositions the data points show some positive curvature. This indicates that the composition of the titanium nitride precipitated from liquid iron is no higher in metal than  $Ti_{1.7}N$  and probably not that rich in metal. It is definitely not as metal rich as the compositions  $Ti_{2.2}N$  and  $Ti_{2.4}N$  calculated from the phase rule analysis.



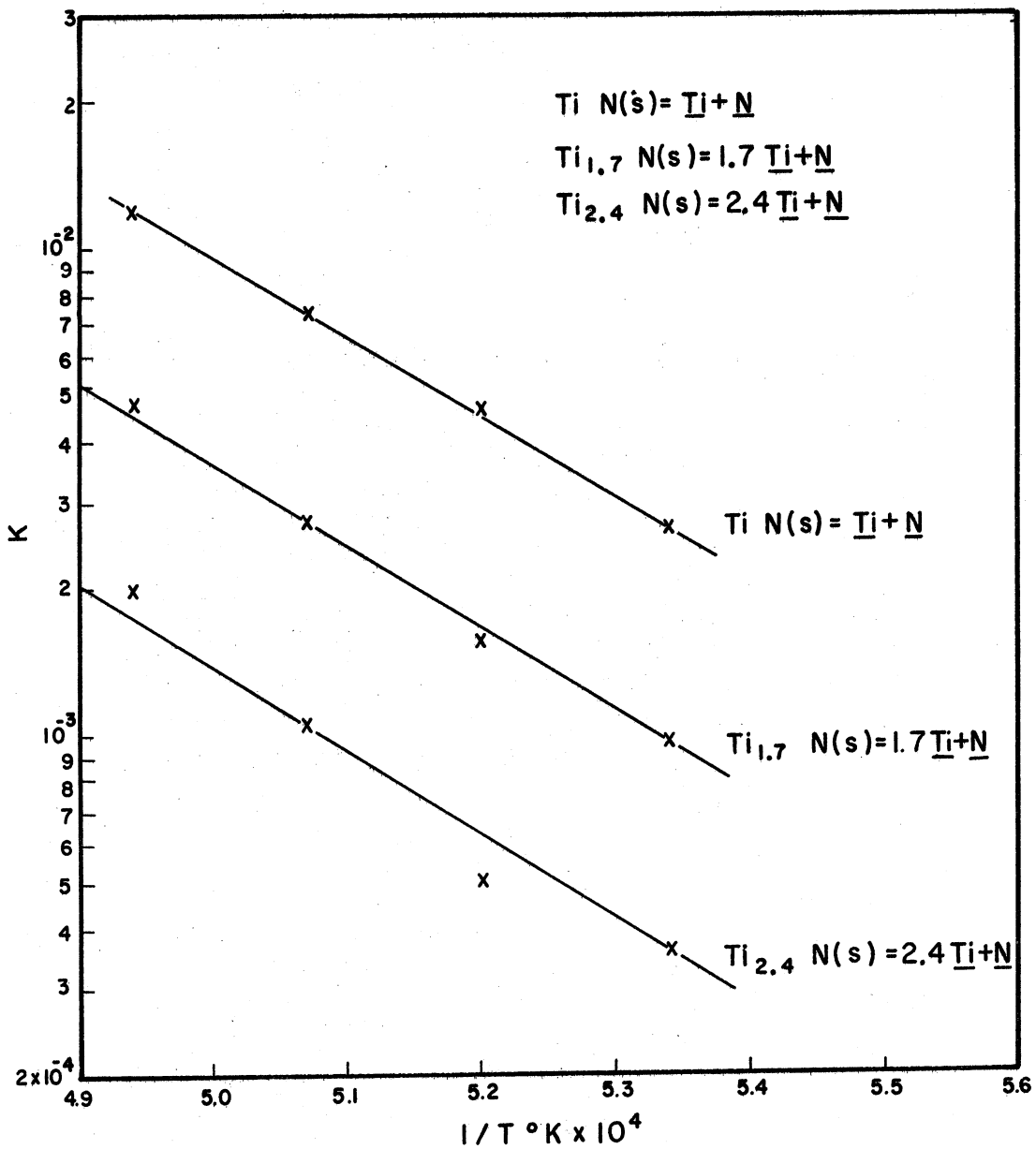


Figure 29. Variation of Equilibrium Constant with Temperature for the Reactions  $TiN(s) = \underline{Ti} + \underline{N}$ ,  $Ti_{1.7} N(s) = 1.7 \underline{Ti} + \underline{N}$ , and  $Ti_{2.4} N(s) = 2.4 \underline{Ti} + \underline{N}$

Figures 30 and 31 show Van't Hoff plots for the nitrides  $V_{2.5}N$  the composition given by Hahn<sup>(17)</sup>, and  $Cb_2N$  the most metal rich columbium nitride found by Schonberg<sup>(18)</sup>. Figure 29 shows greater data scatter than either Figure 23a or Figure 23b and evidence of possible negative curvature. Figure 30 shows slightly greater scatter than Figure 24a and Figure 24b and possible positive curvature. The indications are that the compositions of vanadium nitride and columbium nitride precipitated from liquid iron are not as metal rich as  $V_{2.5}N$  and  $Cb_2N$ , although compositions in the ranges  $V_{1.0-2.0}N$  and  $Cb_{1.0-1.5}N$  are quite possible.

Both wet chemical and x-ray analyses were attempted on samples of nitrides extracted from the solidified ingots of the Sieverts method determinations. Wet chemical analyses of the extracted nitrides were successfully used only with the aluminum system. They were hampered by the small quantities of nitride which could be extracted from an ingot and by the fact that the nitride residue was invariably slightly contaminated with  $Al_2O_3$  from the crucibles. In addition the inaccuracy inherent in wet chemical analyses is reflected by a comparatively large variation in the metal/nitrogen ratio of the nitride. The results obtained with the aluminum system are shown in Table XIII. Details of the analytical procedures used and their estimated accuracies are covered in Appendix D.

TABLE XIII

RESULTS OF WET CHEMICAL ANALYSIS OF  
EXTRACTED ALN RESIDUE

Total Al (wt. %)	Nitrogen (wt. %)	Calculated Nitride Composition
59.80	24.80	$Al_{1.25}N$
59.45	26.00	$Al_{1.18}N$

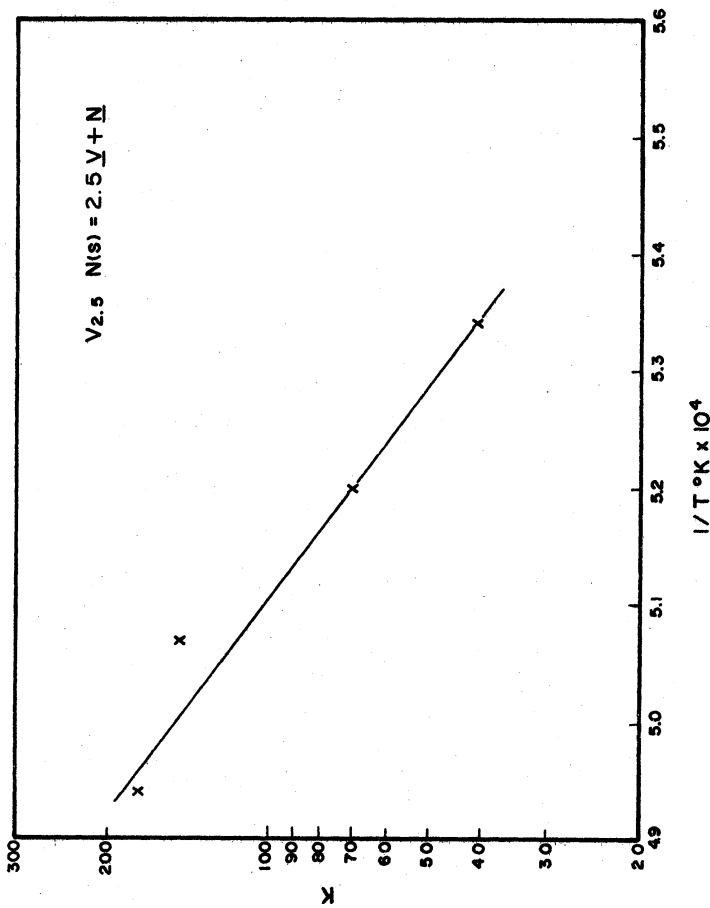


Figure 30. Variation of Equilibrium Constant with Temperature for the Reaction  $V_{2.5} N(s) = 2.5 V + N$

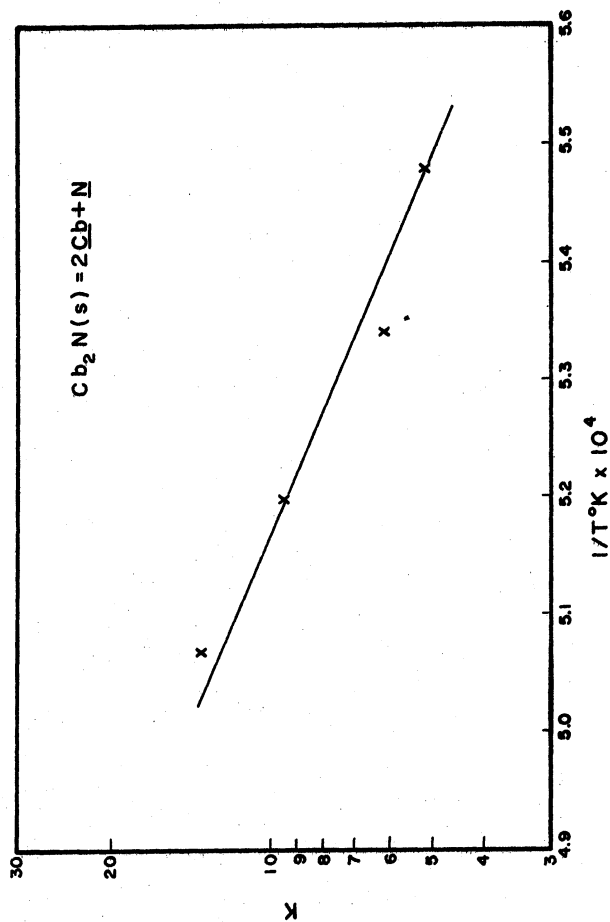


Figure 31. Variation of Equilibrium Constant with Temperature for the Reaction  $Cb_2 N(s) = 2 Cb + N$

The most generally successful method of identifying the nitride formed and determining its stoichiometry was by x-ray analysis of the extracted nitrides. Powder patterns were made using the Debye-Scherrer technique and the lattice parameters were determined by calculating  $a_0$  for small values of  $\sin^2 \theta$  and extrapolating to  $0^\circ$ . Since the amount of material required for this technique is very small (100 mg. or less) sufficient nitride could be extracted in all systems except zirconium. The details of the x-ray procedure and a summary of the results of the patterns run on each system are given in Appendix H.

Lattice parameter measurements on extracted titanium nitride gave a lattice constant of  $4.242 \text{ \AA}$ . This is in excellent agreement with Ehrlich's<sup>(14)</sup> value of  $4.23 \text{ \AA}$  which he claims corresponds to a composition of TiN. Lattice parameter measurements on two samples of extracted vanadium nitride gave lattice constants of  $4.062 \text{ \AA}$  and  $4.068 \text{ \AA}$ . According to Hahn<sup>(17)</sup> this lattice parameter corresponds to a composition of  $\text{VN}_{0.71}$  (or  $\text{V}_{1.4}\text{N}$ ) which is about the composition limit on the low nitrogen side for the nitride of nominal composition VN. These results are quite consistent with the composition limits indicated for these systems by the temperature variation of the solubility products.

The results of the efforts made to determine the nitride compositions precipitated from liquid iron solution cannot be considered conclusive. However they indicate that although there may be some composition variation on the metal rich side from the compositions assumed in Table XI it is small. The value of  $x$  in Equations (5) and (10) is thought to be less than 1.5 for all of the nitride systems. There is no composition for any system which is sufficiently indicated to justify

basing calculation of the thermodynamic quantities  $K$ ,  $\Delta H^\circ$ ,  $\Delta S^\circ$ , and  $\Delta F^\circ$  on any nitride compositions other than those in Table XI.

There is also the possibility that some of the nitrides may be complexes with iron. Powder patterns run on unextracted samples show intense alpha iron lines and weaker  $jN$  lines with no evidence of any  $FeN$  lines. This indicates that no complex of the type  $jN \cdot FeN$  is formed but does not rule out a complex of the type  $(Fe, j)N$  in which Fe atoms replace some of the  $j$  atoms in the  $jN$  structure. If this occurs it would show up in the powder pattern as a shift in the  $\theta$  values which could not be distinguished from the same shift produced by a varying  $j/N$  ratio. Its effect on the x-ray measurements would be to cause an error in the calculated lattice constant values. Its effect on the thermodynamic quantities would be to cause the values of  $K$  to be slightly low since the activity of  $jN$  in Equation (10) would not be unity as assumed but would be less than unity.

## VI. DISCUSSION OF ERRORS

### A. Sieverts Method

Humbert and Elliott<sup>(2)</sup> have discussed the major sources of error in a Sieverts apparatus substantially identical to the one used in this study and have attempted to estimate the error produced by each source on nitrogen solubility measurements in liquid Fe-Cr-Ni alloys. For some sources the error estimation can be made only in a qualitative way. Pehlke<sup>(11)</sup> in his analysis of the same apparatus being used to make nitrogen solubility measurements on a number of different binary liquid iron alloys has considered several additional factors. Some of the factors these investigations considered which are likewise important in this study are enumerated below.

#### a. Uncertainty in temperature

Humbert and Elliott<sup>(2)</sup> estimate an uncertainty in temperature measurement of  $\pm 10^{\circ}\text{C}$ . Pehlke<sup>(11)</sup> calculates an error of about  $7^{\circ}\text{C}$  in the calibration of the temperature scale and estimates an additional error of  $5^{\circ}\text{C}$  in temperature control throughout the run for a total uncertainty of  $\pm 12^{\circ}\text{C}$ . He also estimates that the error introduced by assuming constant emissivity of all melts over the necessary ranges of temperature and composition is less than the total uncertainty of  $\pm 12^{\circ}\text{C}$ . Both investigators agree that a temperature error of this magnitude leads to a maximum error in nitrogen solubility measurement of 1 to 1.5% for alloys of 10% solute or less. The temperature uncertainty in this study is probably of this same order of magnitude. For the very soluble nitride systems such as silicon, tantalum, columbium, and vanadium the uncertainty may be

slightly greater because of the high (15%-35%) alloy contents required to precipitate the nitride.

b. Uncertainty in gas volume

Errors in the measurement of gas volumes resulted from uncertainty in the gas buret reading and variation in the temperature of the gas buret. The uncertainty in the reading was  $\pm 0.1$  cubic centimeters. The variation in buret temperature was  $\pm 1^\circ\text{K}$  throughout the course of a six to ten hour run. The buret temperature variation was rather large because the gas buret was not surrounded with a water cooling jacket but varied with the room temperature. The maximum error in volume measurement occurs when a full buret of gas is used and is given by  $100 \times 1/273 + 0.1 \times 2 = 0.57$  cc because two buret readings are required for one volume measurement. The hot volume was essentially constant at about 50 cc so the error in its measurement was  $50 \times 1/273 + 0.1 \times 2 = 0.38$  cc. The total maximum error possible in the measurement of a volume of nitrogen absorbed is then  $0.57 + 0.38 = 0.95$  cc. A melt of pure iron at  $1600^\circ\text{C}$  weighing about 115 grams requires about 100 cc of nitrogen gas to saturate the melt and fill the hot volume. This represents a maximum error in volume measurement of 1%. Thus for all measurements made at pressures and compositions for which at least 100 cc of nitrogen was admitted to the reaction bulb the volume measurement error was probably less than 1%.

However because the majority of the measurements in this study had to be made at reduced pressure and therefore with small volumes of nitrogen admitted to the reaction bulb, the relative error was in some cases greater than this. In the systems titanium, zirconium, aluminum, vanadium, columbium, tantalum, and silicon all break points in the nitrogen

absorption curves occurred after nitrogen volumes of at least 20 cc had been admitted to the reaction bulb. This gives a maximum error of 0.65 cc and a maximum relative error of 3.2% at the nitride solubility limit. In the boron system several of the nitride solubility limits occur with nitrogen volumes as low as 5 cc in the reaction bulb. For this system the maximum error is 0.47 cc and the maximum relative error 10% at the nitride solubility.

c. Uncertainty in pressure

The solubility of nitrogen in an alloy may be expressed as a function of pressure through Sieverts' Law.

$$\%N = C \sqrt{P_{N_2}} \quad (29)$$

Differentiating this gives:

$$d(\%N) = \frac{C d P_{N_2}}{2 \sqrt{P_{N_2}}} \quad (30)$$

The relative error in percent is then:

$$\frac{d(\%N)}{(\%N)} = \frac{C dP_{N_2}}{2 \sqrt{P_{N_2}} (\%N)} \times 100 \quad (31)$$

where C has a value of 0.045%/(atm)<sup>1/2</sup> or 0.00872%/(cm)<sup>1/2</sup>. This obviously is most serious at low nitrogen pressures for alloys with low solubilities.

For this error also the least favorable case is the boron system. The pressure could be measured to ±0.2 cm of mercury for all systems. However for the boron system  $\sqrt{P_{N_2}}$  goes as low as 2.0 (cm)<sup>1/2</sup> with  $\%N$  equal to 0.002. This is a maximum relative error of about 45% at



the nitride solubility limit. For the silicon system the most unfavorable case is  $\sqrt{P_{N_2}} = 5.0 \text{ (cm)}^{1/2}$ ,  $\%N = 0.002$ , for a relative error of 8.7%. With the aluminum system the most unfavorable case is  $\sqrt{P_{N_2}} = 4.6 \text{ (cm)}^{1/2}$ ,  $\%N = 0.03$ , for a relative error of 0.6%. Thus it can be seen that for alloy systems with fairly soluble nitrides in which the element  $j$  does not decrease the solubility of nitrogen in the melt, the relative pressure measurement error at the nitride solubility limit rapidly becomes negligible. This applies to the systems aluminum, vanadium, columbium and tantalum. For the titanium and zirconium systems in which the nitride is quite insoluble but the element  $j$  has a strong increasing effect on the nitrogen solubility the most unfavorable case is  $\sqrt{P_{N_2}} = 1.5$ ,  $\%N = 0.01$ , for a maximum relative error of 5.8%.

It can be seen that in making gas solubility measurements at reduced pressures the pressure and volume measurement errors become much more important than they are with measurements at atmospheric pressure where the melt absorbs generally larger volumes of nitrogen. The total error in the measured nitrogen solubility at the nitride solubility limit varies widely from system to system, and within a given system depends on the alloy content at which the nitride forms.

#### d. Possible systematic errors

In addition there is the problem of vaporization of metal from the melt. This is an error which is inherent in the Sieverts method and for which no quantitative estimate can be made. None of the alloying elements used in this study has an extremely high vapor pressure in comparison to iron, such as manganese and chromium for which previous researchers have shown the vaporization error to be appreciable. On the other hand the

method used to measure the nitride solubility product required that the melt remain under pressures less than one atmosphere for the entire duration of the run, usually between six and ten hours. Although effort was made to adjust the  $j$  composition of the melt so that the nitride would be precipitated at as high a nitrogen pressure as possible, the requirement of reprecipitating the nitride at several higher temperatures made it necessary to make a number of runs at high  $j$  contents and therefore forced pressures of 0.1 to 0.5 atmospheres for times in excess of one hour. The appearance of a deposit in the reaction bulb particularly near the end of a run was seldom entirely avoided but the deposit was usually small.

In this connection it should be mentioned that a run was made on a melt of 0.741% aluminum without a cover being used on the crucible. This resulted in an extremely heavy deposit in the reaction bulb. Nevertheless the measured solubility for this run was quite consistent with the other data for the aluminum system.

#### B. Quenching Method

Two important systematic errors which may enter the quenching method are the changing of the solute contents on quenching of the melt and uncertainty in the equilibrium nitrogen pressure adjacent to the melt due to thermal diffusion in the gas phase. The calibration runs made on pure iron in the quenching apparatus indicate that these errors were avoided by proper design of the apparatus. The method of measuring the melt temperature was substantially the same as in the Sieverts apparatus, and the uncertainty in the measured values is therefore expected to be the same.

Concerning the error involved in the wet chemical analyses, the error in the metal analyses is estimated at  $\pm 0.02$  weight percent by Cochrane Laboratories Inc. which performed the analyses. The error in the nitrogen analyses is estimated at  $\pm 0.0005$  weight percent for the pure iron and iron-aluminum systems, and  $\pm 0.001$  weight percent for the iron-boron alloys. The error increases as the nitrogen content decreases because the volume of ammonia given off in the Kjeldahl distillation becomes smaller, and the relative importance of residual nitrogen in the reagent solutions increases. The nitrogen analyses for the iron-titanium system apparently contain some systematic error due to interference of titanium so no error can be estimated for them.

## VII. CONCLUSIONS

1. The solubility products of the nitrides of eight strong nitride formers in liquid iron have been measured at temperatures in the vicinity of 1600°C using both the Sieverts method and the quenching method. The results may best be summarized by the following equations giving the standard free energy of precipitation of the nitride from liquid iron solution:

$$\text{for TiN } \Delta F^\circ = 75,200 - 28.34T$$

$$\text{for ZrN } \Delta F^\circ = 32,600 - 6.69T$$

$$\text{for AlN } \Delta F^\circ = 63,700 - 27.91T$$

$$\text{for BN } \Delta F^\circ = 45,900 - 21.25T$$

$$\text{for VN } \Delta F^\circ = 49,000 - 24.58T$$

$$\text{for CbN } \Delta F^\circ = 35,000 - 17.08T$$

$$\text{for TaN } \Delta F^\circ_{1550^\circ\text{C}} = 2,240$$

$$\text{for } 1/4 \text{ Si}_3\text{N}_4 \text{ (Si}_{3/4}\text{N)} \Delta F^\circ = -10,500 + 0.75T$$

2. Only three of these eight systems form nitrides sufficiently stable to merit consideration for possible use as refractories in contact with liquid iron. These three in order of their stability are TiN, ZrN, and AlN. All the other nitrides listed in (1) above would allow serious contamination of a liquid iron melt if used as a refractory in contact with it under conditions approaching thermodynamic equilibrium.
3. The compositions of the nitrides precipitated from liquid iron solution approximate those given under (1). For the nitrides TiN, ZrN, CbN, and VN there is evidence that the composition may vary slightly toward the metal rich side. However in no case does the metal/nitrogen atom ratio appear to be larger than 1.5.

4. The nitrogen-metal interaction parameter in liquid iron was determined for boron and zirconium, two elements not previously studied. These results may be expressed by the following equations at 1600°C:

$$\log f_{\underline{N}} = -0.63(\%Zr)$$

$$\log f_{\underline{N}} = 0.11(\%B)$$

Zirconium increases the solubility of nitrogen in liquid iron while boron decreases it.

5. The nitrogen-metal interaction parameters for any one system showed a linear relation with reciprocal temperature as predicted from basic thermodynamic relations.
6. The Wagner method of interaction parameters gives a satisfactory representation of the activities of metal and nitrogen in solution in iron at concentrations up to the nitride solubility limit for all of the metal-nitride systems listed in (1) with the exception of the  $Si_3N_4$  system.

## VIII. APPENDICES

### APPENDIX A

#### CHARGE MATERIAL ANALYSES

Nine different metals, iron plus the eight alloying elements aluminum, boron, columbium, silicon, tantalum, titanium, vanadium, and zirconium were used in this study. These materials were of the highest purity obtainable. The suppliers of these metals and the suppliers' analyses are summarized in the following tables.

TABLE A-I

SUPPLIER'S ANALYSIS OF IRON MELTING STOCK  
Trade name Ferrovac E, supplied by Crucible Steel  
Company of America of Syracuse, New York in bar form.

<u>Element</u>	<u>Weight Percent</u>		
	Lot No. 1	Lot No. 2	Lot No. 3
C	0.004	0.004	0.008
Mn	0.001	0.001	0.001
P	0.002	0.005	0.004
S	0.009	0.007	0.007
Si	0.006	0.006	<0.006
Ni	0.033	0.035	0.015
Cr	0.01	0.01	<0.002
V	0.004	0.004	<0.004
Mo	0.01	0.01	0.001
Cu	0.01	0.005	<0.001
Co	0.01	0.007	0.005
N	0.0018	0.0001	0.0002
O	0.0075	0.0065	0.0022
H	0.00007	0.00003	0.00002

TABLE A-II

SUPPLIER'S ANALYSIS OF ALUMINUM MELTING STOCK  
Supplied by Aluminum Company of America  
Research Laboratories in ingot form.

<u>Element</u>	<u>Weight Percent</u>
Al	99.99+
Cu	0.001
Mn	0.002
Si	0.003
Fe	0.001

TABLE A-III

SUPPLIER'S ANALYSIS OF BORON MELTING STOCK  
Supplied by Cooper Metallurgical Associates of  
Cleveland, Ohio in the form of -325 mesh powder.

<u>Element</u>	<u>Weight Percent</u>
C	0.10
Fe	0.15
O	0.02

TABLE A-IV

SUPPLIER'S ANALYSIS OF COLUMBIUM MELTING STOCK  
Supplied by Fansteel Metallurgical Corporation of  
Chicago, Illinois in the form of 0.157" diameter rod.

<u>Element</u>	<u>Weight Percent</u>
O	0.018
C	0.015
N	0.015
Ta	0.09
Zr	0.020
Fe	0.015
Ti	0.010
Si	<0.01
W	<0.01
Ni	<0.007

TABLE A-V

SUPPLIER'S ANALYSIS OF SILICON MELTING STOCK  
Supplied by Union Carbide Metals Company of Niagara Falls,  
New York in the form of 60 to 150 mesh powder.

<u>Element</u>	<u>Weight Percent</u>
Si	99.85
Fe	0.018

TABLE A-VI

SUPPLIER'S ANALYSIS OF TANTALUM MELTING STOCK  
Supplied by Fansteel Metallurgical Corporation of Chicago,  
Illinois in the form of 0.157" diameter rod.

<u>Element</u>	<u>Weight Percent</u>
O	0.007
C	0.005
N	0.002
Cb	0.055
W	0.010
Fe	0.010
Mo	0.005
Si	<0.01

TABLE A-VII

SUPPLIER'S ANALYSIS OF TITANIUM MELTING STOCK  
Supplied by E. I. duPont  
in sponge form.

<u>Element</u>	<u>Weight Percent</u>
N	0.020
C	0.025
Mg	0.080
Cl	0.120
H	0.005
H <sub>2</sub> O	0.020
Mn	0.050
Fe	0.060
Si	0.040



TABLE A-VIII

SUPPLIER'S ANALYSIS OF VANADIUM MELTING STOCK  
Supplied by Union Carbide Metals Company of Niagara Falls,  
New York in the form of -1/4" diameter shot.

<u>Element</u>	<u>Weight Percent</u>
C	0.024
O	0.055
H	0.0018
N	0.039

TABLE A-IX

SUPPLIER'S ANALYSIS OF ZIRCONIUM MELTING STOCK  
Supplied by Mallory Sharon  
Metals Company in sponge form.

<u>Element</u>	<u>Weight Percent</u>
Fe	0.0309
C	0.0247
Si	0.006
Mn	<0.002
O	0.1162

## APPENDIX B

### TEMPERATURE CALIBRATION

The method used to determine the relation between the true melt temperature and the observed optical pyrometer readings for both the Sieverts apparatus and the quenching apparatus was the one proposed by Dastur and Gokcen<sup>(24)</sup> applied to the Sieverts apparatus by Pehlke and Elliott<sup>(1)</sup> and Humbert and Elliott<sup>(2)</sup>. The relation between true and observed temperatures is given by the Wien-Planck Equation:

$$\ln(E\alpha) = \frac{C_2}{\mu} (1/T_t - 1/T_a) \quad (B-1)$$

where:

E = melt emissivity

$\alpha$  = melt transmissivity

$C_2$  = Planck constant; 14,330 micron-degrees

$\mu$  = wave length of light used; 0.65 microns

$T_t$  = true temperature in °K

$T_a$  = observed temperature in °K

Assuming that E and  $\alpha$  change negligibly over the ranges of melt temperature and composition in this study Equation (B-1) may be rewritten:

$$\frac{1}{T_t} - \frac{1}{T_a} = K \quad (B-2)$$

The value of the constant K in Equation (B-2) may then be evaluated by measuring  $T_a$  for pure liquid iron in the apparatus and taking  $T_t$  as 1536°C. This value of K is then used to calculate the desired  $T_a$  for any other experimental  $T_t$ . The temperature scale set up by this method

for the Sieverts apparatus is shown in Table B-I and the temperature scale set up for the quenching apparatus is shown in Table B-II.

TABLE B-I

COMPARISON BETWEEN TRUE AND OBSERVED TEMPERATURE SCALES FOR THE SIEVERTS APPARATUS

<u>T<sub>t</sub> °C</u>	<u>T<sub>a</sub> °C</u>	
1450	1267	
1500	1307	
1536	1335	K = - 0.69 10 <sup>-4</sup>
1550	1347	
1600	1387	
1650	1427	
1700	1467	
1750	1507	

TABLE B-II

COMPARISON BETWEEN TRUE AND OBSERVED TEMPERATURE SCALES FOR THE QUENCHING APPARATUS

<u>T<sub>t</sub> °C</u>	<u>T<sub>a</sub> °C</u>	
1536	1350	K = - 0.63 10 <sup>-4</sup>
1600	1405	
1650	1445	
1700	1486	

Assuming Dastur and Gokcen's <sup>(24)</sup> value of 0.43 for the emissivity of pure liquid iron at 1536°C, Equation (B-1) gives a value of 0.51 for the transmissivity of the Sieverts apparatus and a value of 0.58 for the transmissivity of the quenching apparatus.

## APPENDIX C

### FLOWMETER CALIBRATION

The flowmeters used to measure the flow rates of argon and nitrogen gases into the quenching apparatus in order to control the partial pressure of nitrogen in the atmosphere were Fischer and Porter Flowrators with a maximum rated capacity of  $0.23 \text{ ft.}^3/\text{min.}$  of air measured at 14.7 p.s.i. and  $70^\circ\text{F}$ . Darken and Gurry<sup>(40)</sup> found that for CO-CO<sub>2</sub> mixtures the error in the gas composition due to thermal diffusion could be held to less than 0.25% by maintaining a linear flow rate in the furnace tube of at least 0.6 cm/sec. For a 2 1/4" i.d. furnace tube this is a minimum volume flow rate of  $1.96 \text{ ft.}^3/\text{hr.}$

The flowmeters were calibrated by inserting a 50 ml buret into the line between the flowmeter and the gas inlet to the furnace. A small amount of soap solution was then injected into the gas stream forming bubbles in the buret and the time necessary for a bubble to travel the length of the 50 ml scale on the buret was measured. Thus a direct measurement of the volume flow rate of the gas could be obtained for any given reading of the flowmeter. A series of 10 time measurements was made at each calibration point and these were averaged to determine the volume flow rate. The meters were calibrated for readings of 10%, 15%, 20%, and 25%. It was impossible to obtain accurate calibration readings at higher flow rates since the rate of travel of the bubbles in the buret was too fast to allow accurate time measurements. However these four calibration points permitted a variation of nitrogen partial pressure from about 1/3 atmosphere to one atmosphere which was quite sufficient for this

study. In order to determine if this method of calibration would give a sufficiently precise control over the nitrogen partial pressure the calibration of the nitrogen flowmeter was repeated on a second occasion. The correspondence of the two sets of calibration data is excellent as shown by Table C-I below.

TABLE C-I

FLOWMETER CALIBRATION DATA FOR THE QUENCHING APPARATUS

N <sub>2</sub> Flowmeter Setting	Time for 50cc Travel (sec.)		Vol. Flow Rate (ft. <sup>3</sup> /hr.)	
	1st Cal.	2nd Cal.	1st. Cal.	2nd Cal.
10%	3.44	3.43	1.84	1.85
15%	2.30	2.28	2.76	2.78
20%	1.69	1.69	3.74	3.74
25%	1.32	1.35	4.81	4.80

A Flowmeter Setting	Time for 50 cc Travel (sec.)	Vol. Flow Rate (ft <sup>3</sup> /hr)
10%	4.80	1.32
15%	3.06	2.08
20%	2.23	2.84
25%	1.76	3.60

Table C-II shows the ratio of nitrogen pressure to total pressure for all possible combinations of flowmeter settings as calculated from the calibration data in Table C-I. To determine the nitrogen partial pressure corrected to one atmosphere total pressure for an equilibration in the quenching apparatus, the  $P_{N_2}/P_{total}$  value corresponding to the flowmeter settings used was multiplied by  $P/76.0$  where  $P$  was the atmospheric pressure existing at the time of the equilibration as measured by a barometer. In all equilibrations a combination of flowmeter settings was chosen such that the volume flow rate of gas was at least 3.74 ft.<sup>3</sup>/hr.

CALCULATED NITROGEN PRESSURE FOR VARIOUS  
COMBINATIONS OF FLOWMETER SETTINGS

Flowmeter Settings		$V_{N_2}/V_{total} = P_{N_2}/P_{total}$
$N_2$	A	
10	25	0.339
10	20	0.393
10	15	0.471
10	10	0.582
15	10	0.676
20	10	0.737
25	10	0.783
20	--	1.000

## APPENDIX D

### METHODS OF CHEMICAL ANALYSIS

The wet chemical analyses of the extracted residue and the analyses of the quenched ingots for the experiments involving titanium, aluminum, and boron were performed by Cochrane Laboratories, Inc. of Milwaukee, Wisconsin. The following short outlines of procedures were supplied by Cochrane Laboratories.

The titanium contents of the quenched ingots were determined colorimetrically after a cupferon separation to eliminate possible interfering elements. The aluminum contents were determined gravimetrically as the phosphate after a bicarbonate separation. The results were rechecked and verified by a hydroxyquinoline separation. The boron contents were determined by distillation as methyl borate and titration as standard alkali. These analyses are presented in Table XII on page 90.

In the analysis of the extracted AlN powder samples the aluminum was determined by quinolate precipitation after fusing the sample with carbonate to render all of it acid soluble. This procedure may have caused a slightly high Al/N ratio since it would also cause to be included in the analyzed aluminum content any aluminum present as  $\text{Al}_2\text{O}_3$ . X-ray analysis of the extracted AlN powder showed traces of  $\text{Al}_2\text{O}_3$  present as an impurity. The nitrogen content was determined by a modification of the Allen method. The accuracy of the analyses was hampered by the fact that only about 0.15 grams of nitride could be extracted, providing a rather small sample for these analytical procedures. The accuracy of the nitrogen analyses is estimated as  $\pm 0.5$  weight percent and the accuracy of the aluminum analyses as  $\pm 1$  weight percent. These analytical results are presented in Table XIII on page 99.

The analyses of the quenched ingots for dissolved nitrogen were performed by the author using the Kjeldahl method<sup>(41,42)</sup>. This method was chosen in preference to the vacuum fusion method for two reasons. First, the vacuum fusion method is inherently less accurate for nitrogen analysis because nitrogen is determined by the difference between the total volume of gas drawn out of the fused sample and the measured volumes of hydrogen and oxygen in it. Second, the vacuum fusion method tends to give low results if stable nitrides are present since it is difficult to decompose them.

The following is an outline of the Kjeldahl procedure used. The analytical sample was in the form of chips. This was found necessary to insure complete digestion. The digestion was accomplished in a solution of  $H_3PO_4$  and  $H_2SO_4$ . NaOH solution was then added and the dissolved nitrogen distilled off as  $NH_3$ . The  $NH_3$  was collected in a solution of  $H_3BO_3$  and then titrated against a standard solution of 0.1N HCl using a mixture of methyl red and methylene blue indicators. The HCl solution had previously been standardized against  $Na_2CO_3$  using methyl orange indicator<sup>(43)</sup>. Double distilled water was used in all reagent solutions to minimize errors due to residual nitrogen. The analytical results are presented in Table XII on page



## APPENDIX E

### METHODS OF FABRICATION OF NITRIDE CRUCIBLES

#### 1. Preparation of AlN Crucibles

The method used by the Carborundum Company to prepare the AlN crucibles which were used in this study is outlined by Taylor and Lenie<sup>(20)</sup>. Fine aluminum powder obtained from Alcoa was mixed with 1% by weight of sodium fluoride and heated in purified nitrogen. The crucible material used to contain the powder is not specified. The sodium fluoride is added because it catalyzes the nitriding at low temperatures. The temperature of the powder was raised rapidly to 650°C and then increased slowly over a period of 40 hours to a maximum of 1800°C. The product obtained was a porous sintered agglomerate. This was ball milled dry in a stainless steel ball mill with stainless steel balls. The product was a light gray powder with an average particle size of about five microns. Chemical analysis of the powder showed 96.0% AlN, 2.1% Al<sub>2</sub>O<sub>3</sub>, and 1.9% other elements including 0.2% C, 0.4% Si, and 0.1% Fe. The crucibles which were of about 1/2" inside diameter, 1/4" wall thickness, and 1 3/4" deep were formed by hot pressing the milled AlN powder in graphite dies. A pressing temperature of 2000°C and a pressing pressure of about 5000 p.s.i. were used. Compacts with a bulk density of 3.20 grams/cc or about 98% of the theoretical density for AlN were produced. The crucibles proved completely impervious to liquid iron after equilibration times of 30 minutes.

#### 2. Preparation of TiN Crucibles

The method used to prepare the TiN crucibles which were used in this study was developed by Sponseller<sup>(25)</sup>. The starting material was

-100 mesh TiN powder to which was added 24% by weight of TiH powder. Both materials were supplied by Metal Hydrides Inc. of Beverly, Mass. The powders were blended by ball milling for one hour using stainless steel balls and a glass jar as a container. A weight of paraffin equal to 2 1/2% of the dry powder weight was dissolved in xylene and added to the powder. A sufficient excess of xylene was added to make the powder about the consistency of thick cream. The slurry was then dried to 105% of the dry powder weight. It was found necessary to maintain close control over the weight of xylene and paraffin in the powder in order to produce sound crucibles of sufficient green strength. The powder must be stored in an air tight container and loaded into the pressing die as rapidly as possible in order to prevent excessive evaporation of xylene.

The pressing of the powder was done at room temperature in a hardened tool steel die ( $R_c$  50-55). The inner surfaces of the crucible were formed by a steel mandrel. A removable sleeve permitted this mandrel and the ram which formed the crucible walls to be loaded independently in two separate steps in the pressing operation. The die, rams, and mandrel were lubricated with a solution of stearic acid dissolved in methyl ether before the powder was loaded into the die. Pressures of 11,000 p.s.i. on the mandrel and 16,000 p.s.i. on the sleeve were used. The green compact was removed from the die by pressing it out the top of the die cavity.

The green crucibles were dewaxed by heating in air to 350°F for 1 hour, 425°F for 2 hours, and 500°F for 2 hours. They were then sintered in vacuum using an induction furnace with a molybdenum susceptor. The temperature was raised slowly to about 1500°F and held until the TiH had been completely decomposed. When a hard vacuum could be held on the

system indicating that all the hydrogen had been removed, the temperature was raised to 2950°F and held for one hour, then raised to 3350°F and held for one hour. After cooling the sintered crucibles were reheated in a gas fired kiln to 2300°F and held under purified nitrogen gas for 48 hours. This step was necessary to tie up as TiN the excess titanium which had been formed in the compacts by the decomposition of the TiH.

The sintered crucibles were about 5/8" inside diameter, 3/16" wall thickness, and 1 1/2" deep. They proved satisfactory although slightly porous to liquid iron. During a 30 minute equilibration at 1700°C about one half of a 40 gram melt of liquid iron would be lost by seepage through the crucible walls.

## APPENDIX F

### NITROGEN ABSORPTION CURVES

Figures F-1 through F-42 summarize the nitrogen absorption curves obtained by the Sieverts method. Each figure represents a single run in the Sieverts apparatus.

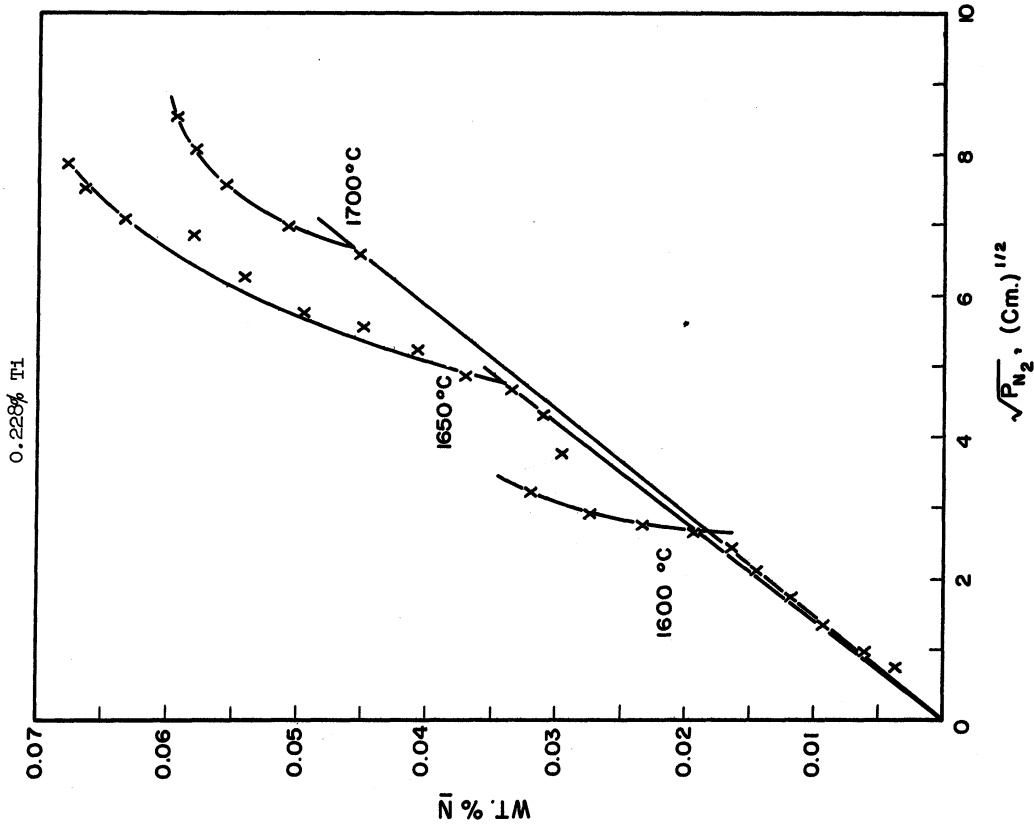


Figure F-2. Nitrogen Absorption Curves for the Aluminum System.

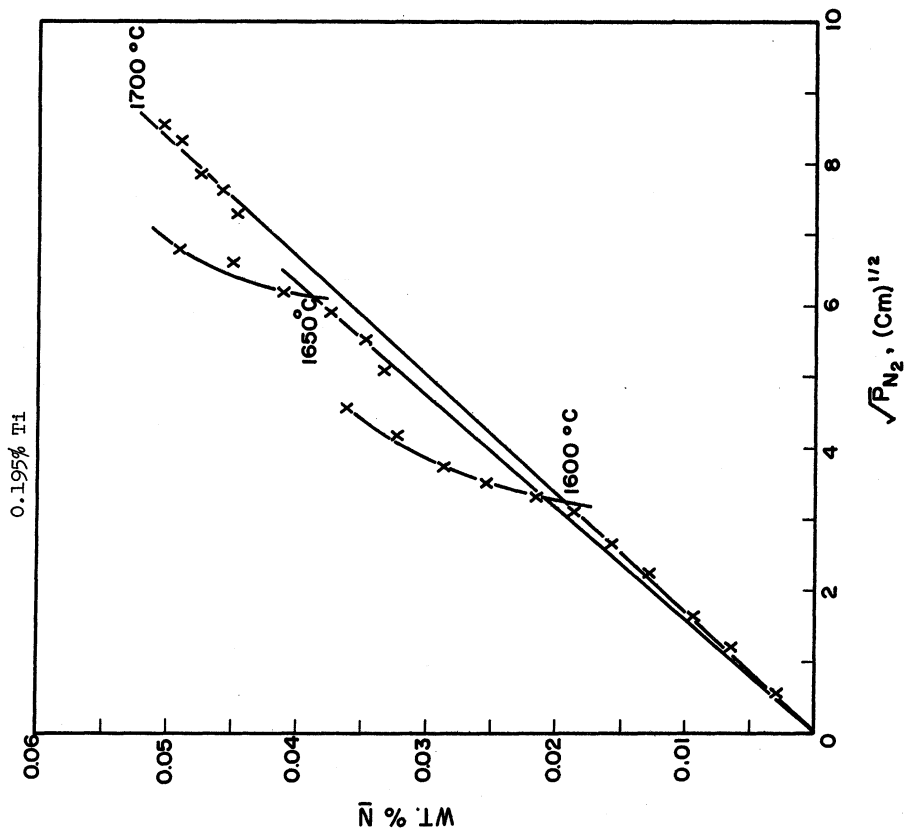


Figure F-1. Nitrogen Absorption Curves for the Titanium System.

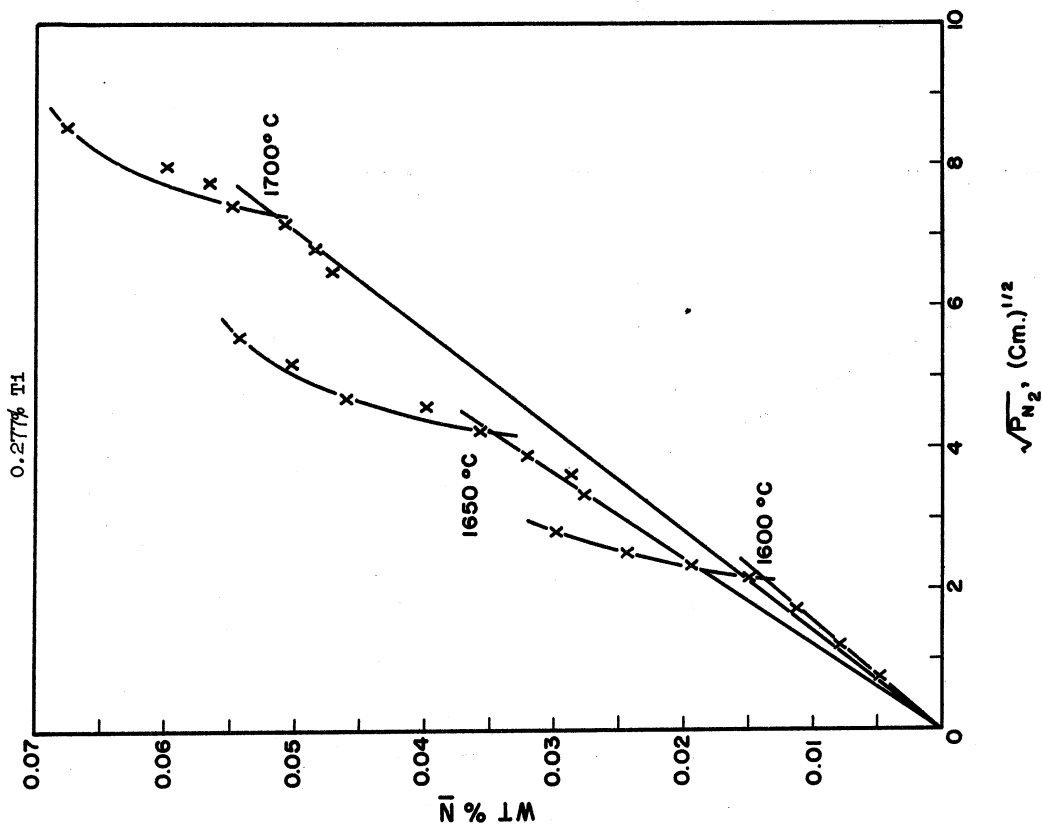


Figure F-4. Nitrogen Absorption Curves for the Titanium System.

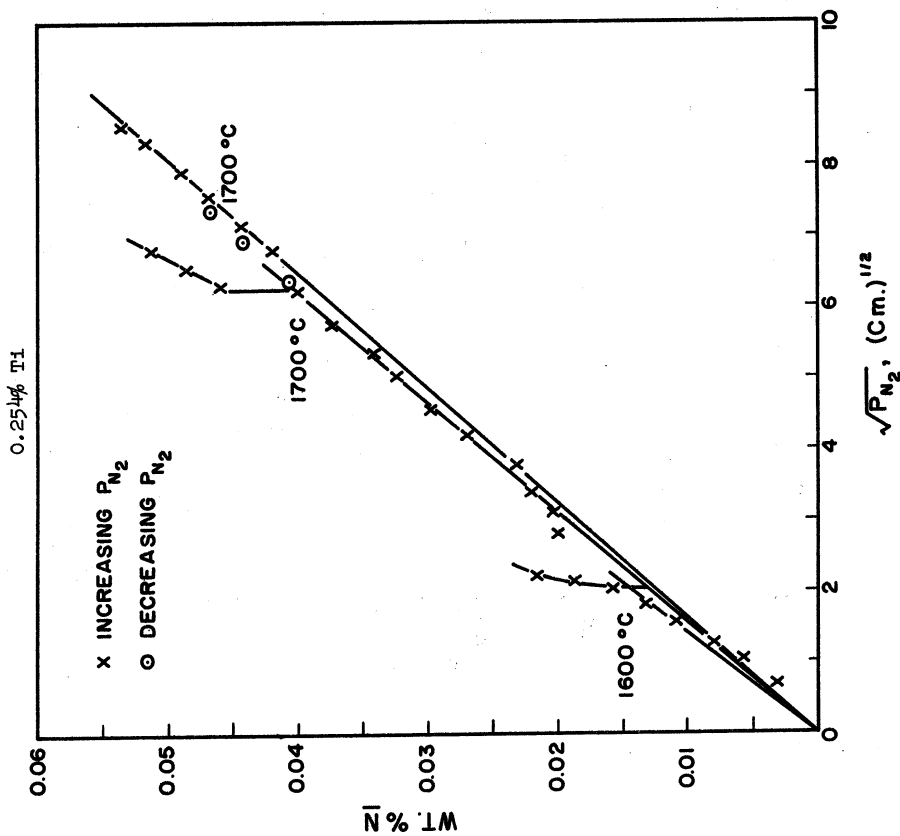


Figure F-3. Nitrogen Absorption Curves for the Titanium System.

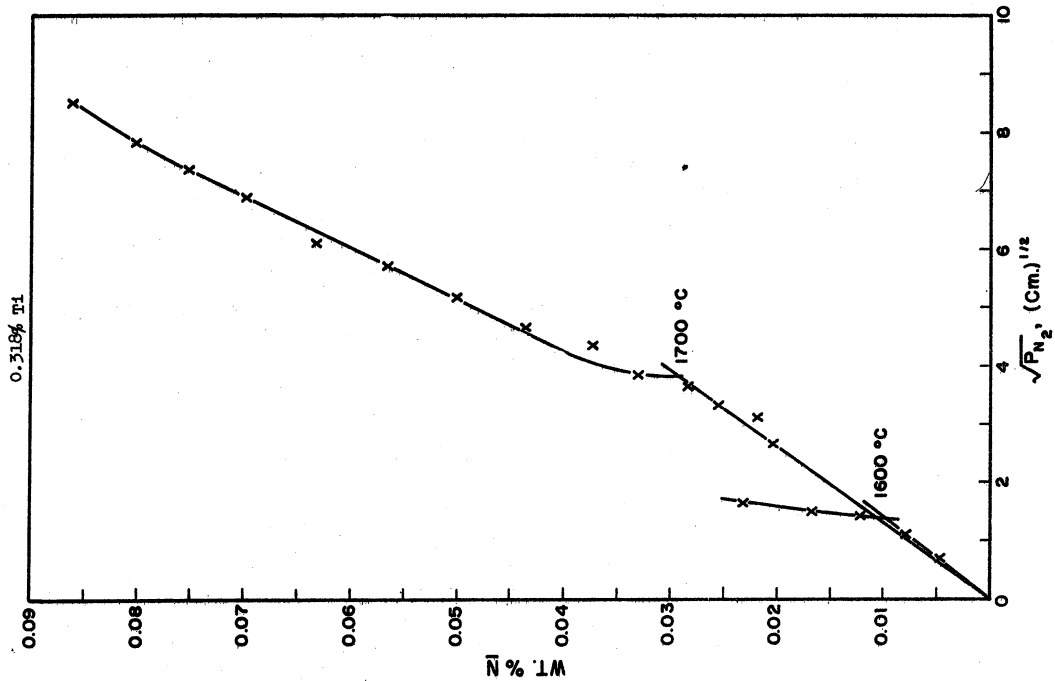


Figure F-6. Nitrogen Absorption Curves for the Titanium System.

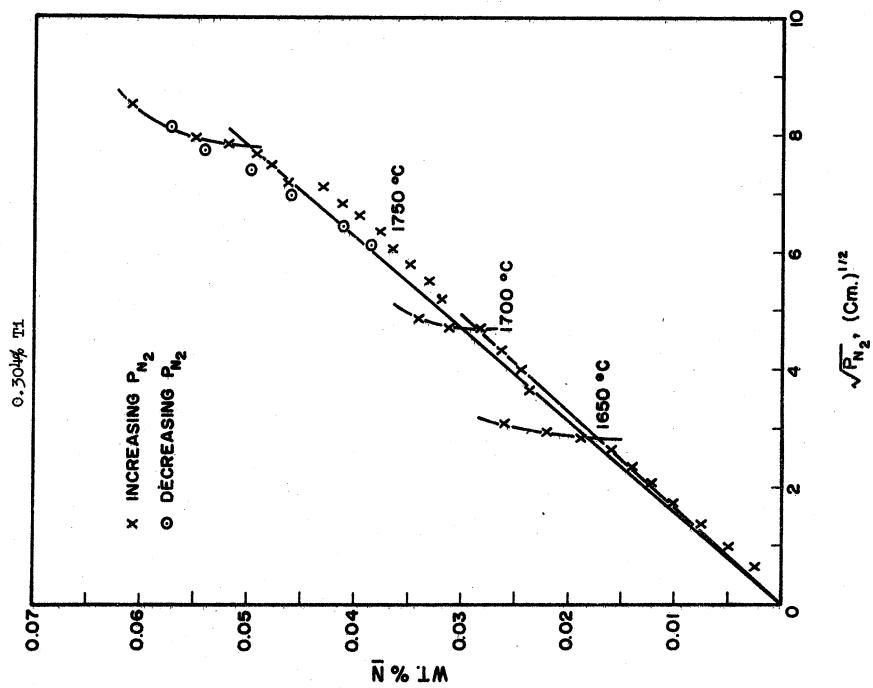


Figure F-5. Nitrogen Absorption Curves for the Titanium System.

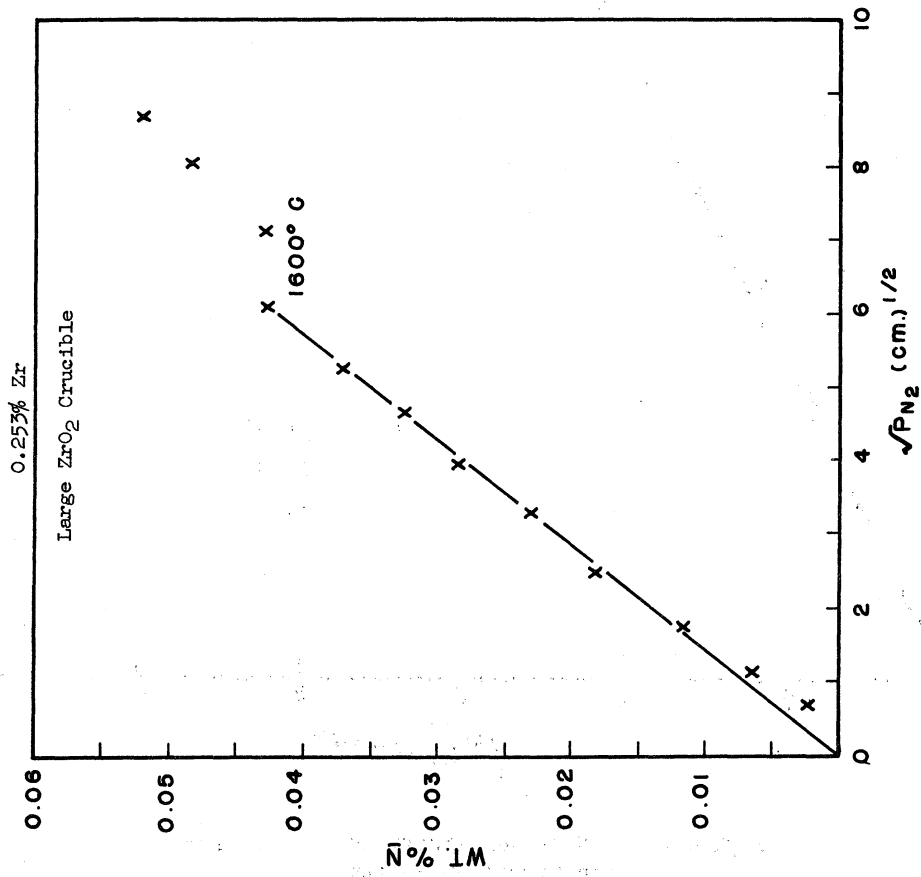


Figure F-7. Nitrogen Absorption Curves for the Zirconium System.

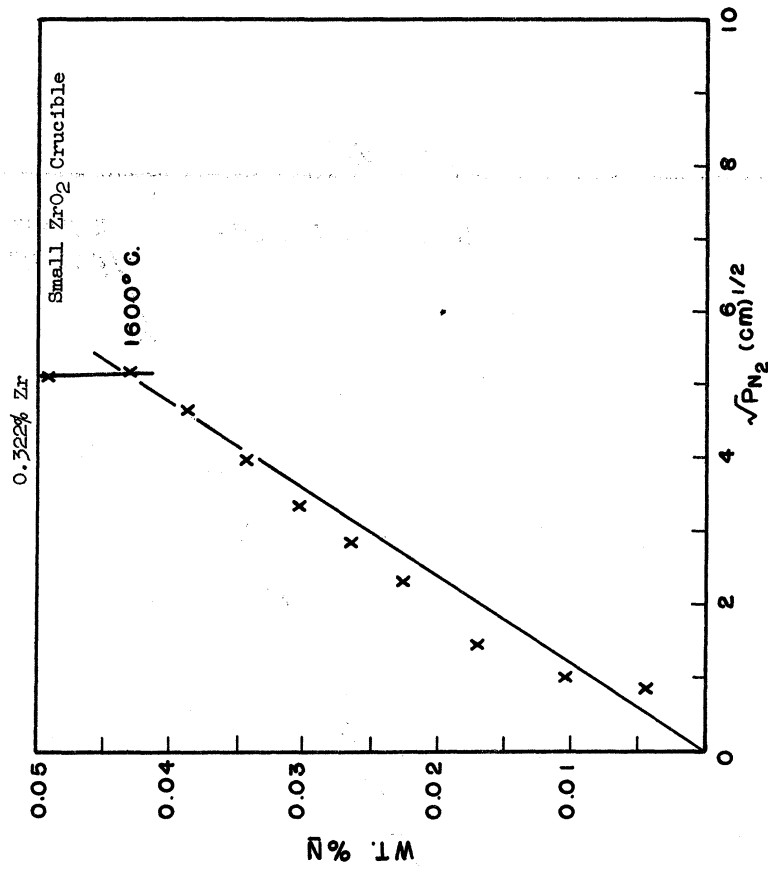


Figure F-8. Nitrogen Absorption Curves for the Zirconium System.



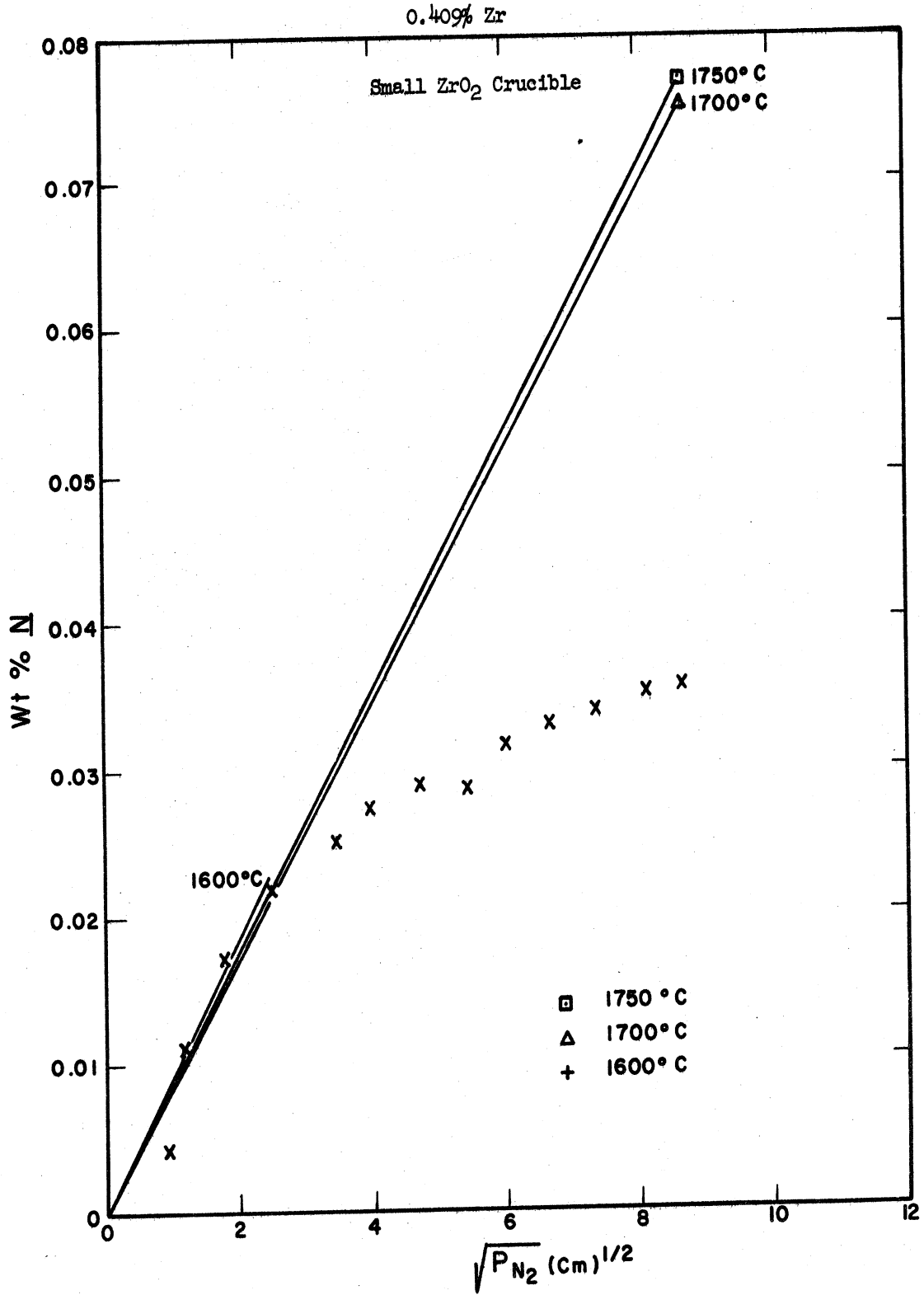


Figure F-9. Nitrogen Absorption Curves for the Zirconium System.

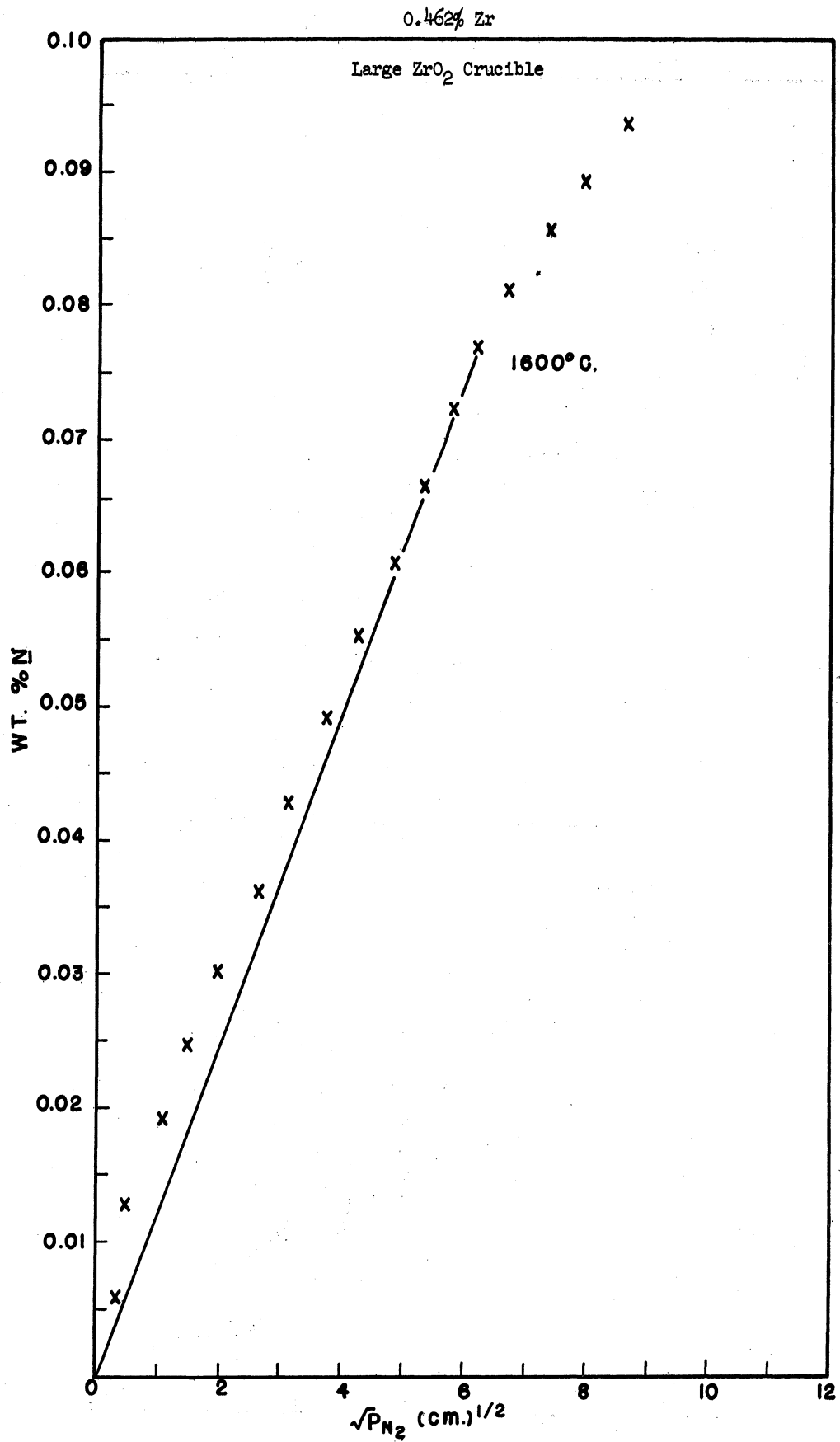


Figure F-10. Nitrogen Absorption Curves for the Zirconium System

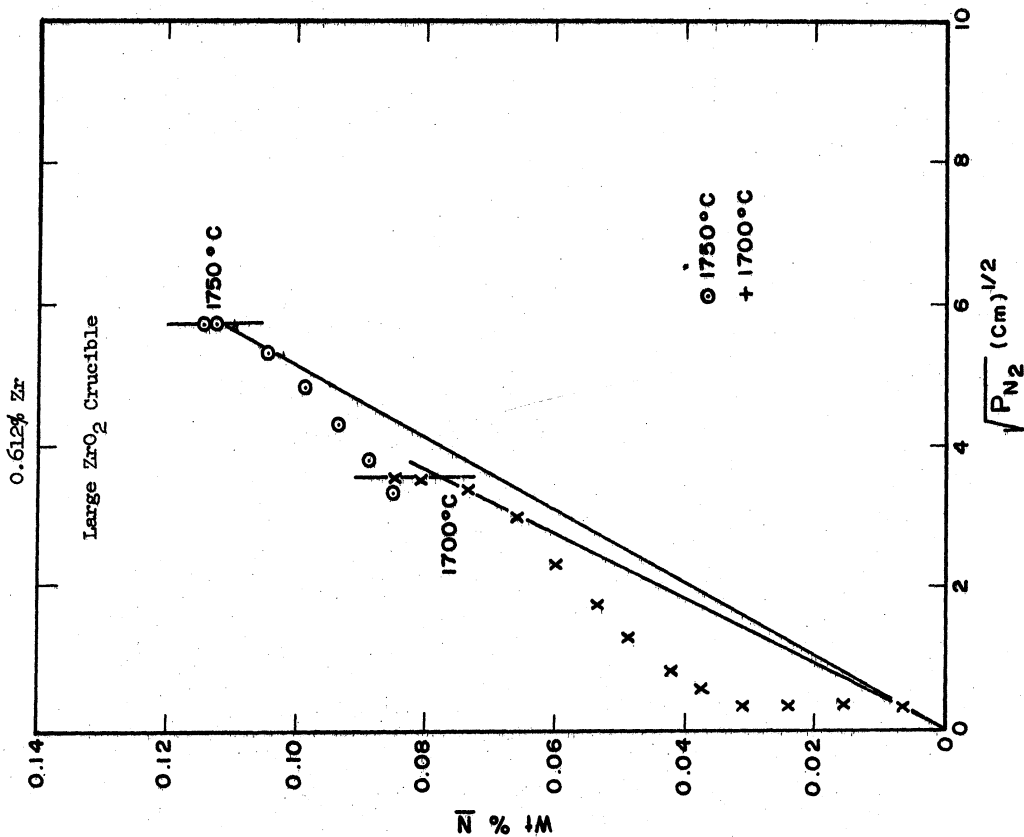


Figure F-12. Nitrogen Absorption Curves for the Zirconium System.

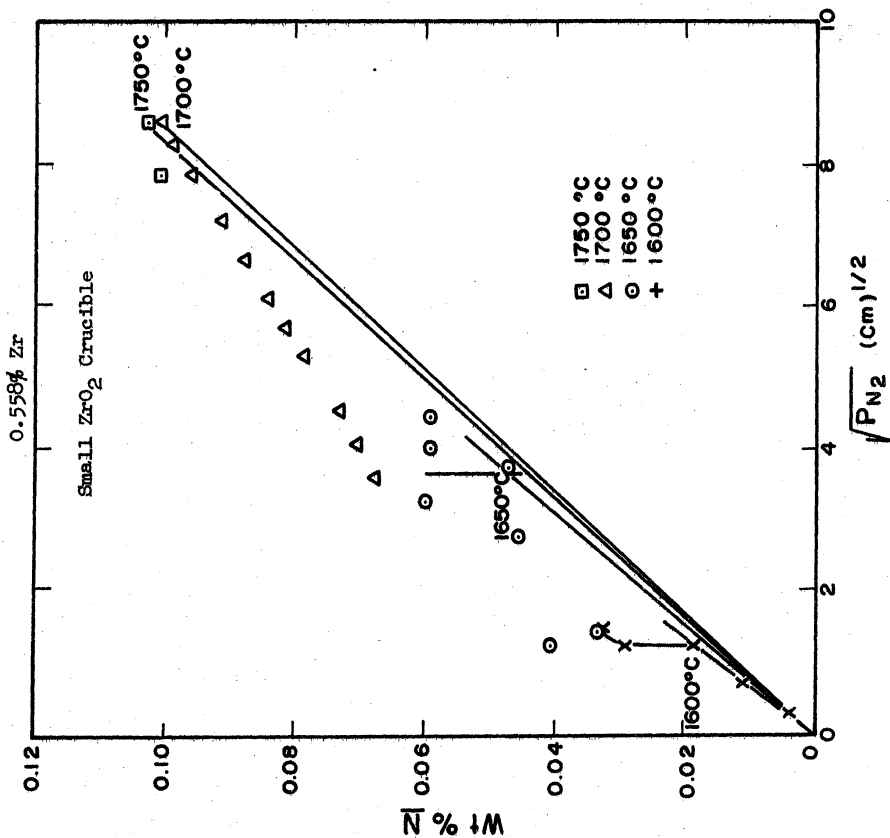


Figure F-11. Nitrogen Absorption Curves for the Zirconium System.

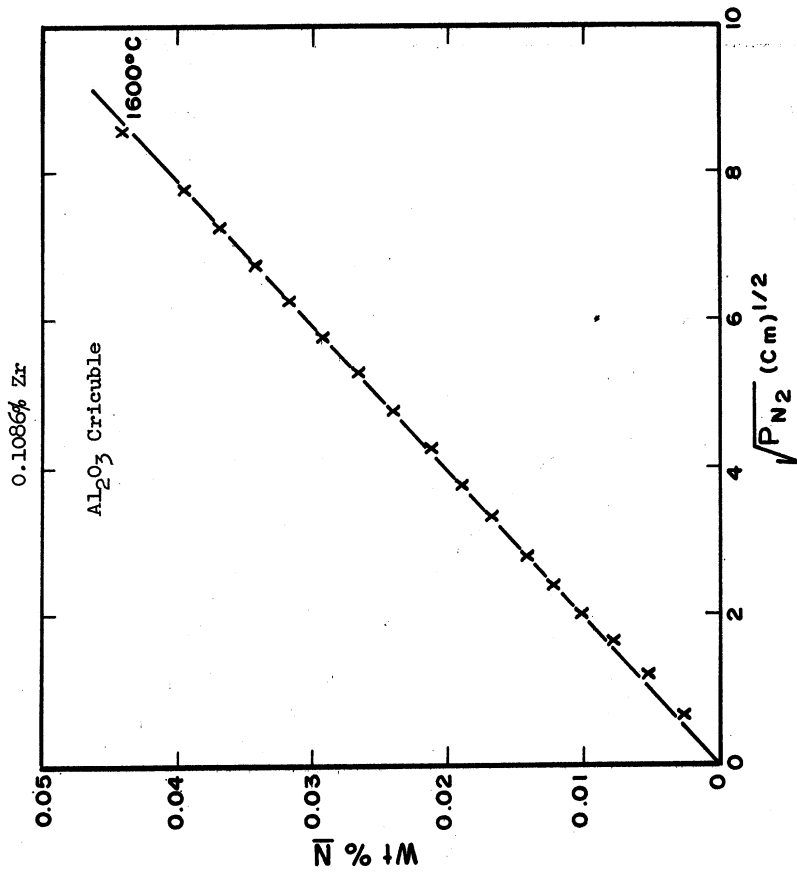


Figure F-14. Nitrogen Absorption Curves for the Zirconium System.

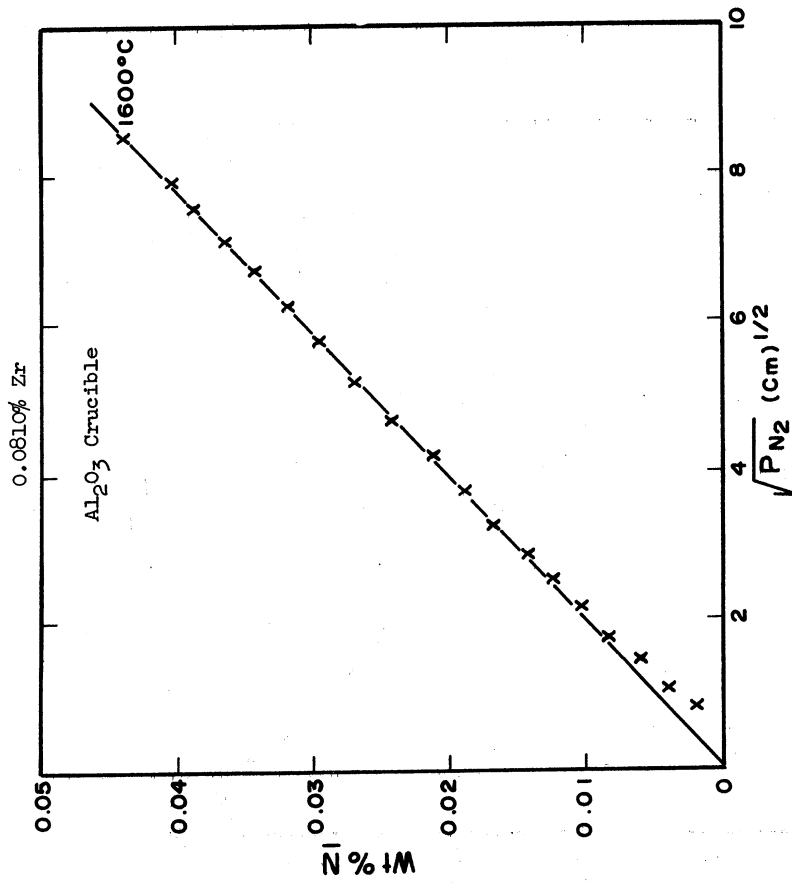


Figure F-15. Nitrogen Absorption Curves for the Zirconium System.

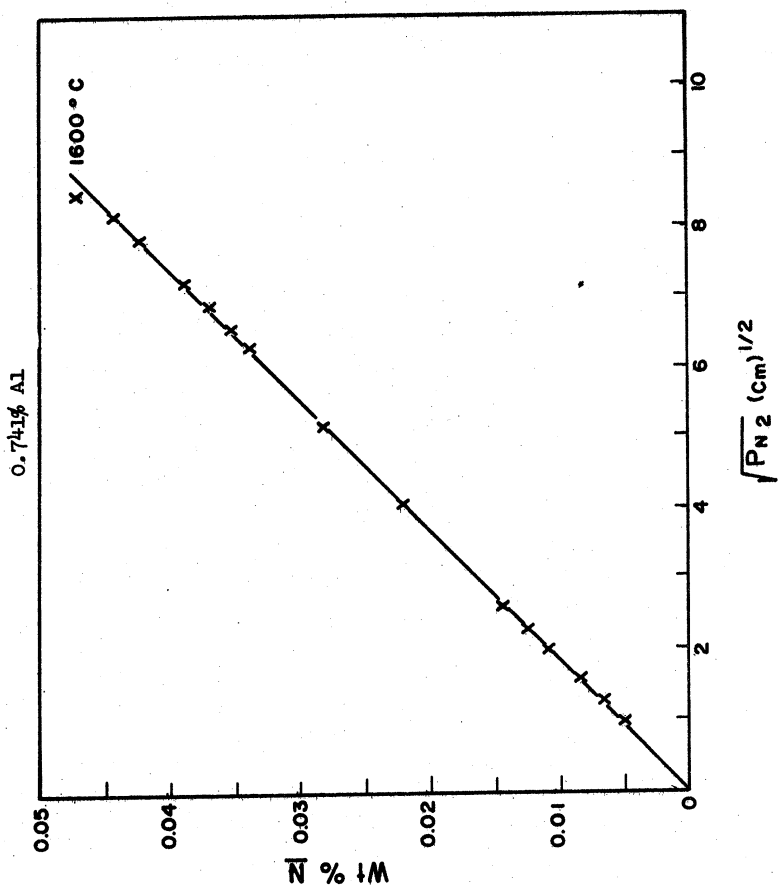


Figure F-16. Nitrogen Absorption Curves for the Aluminum System

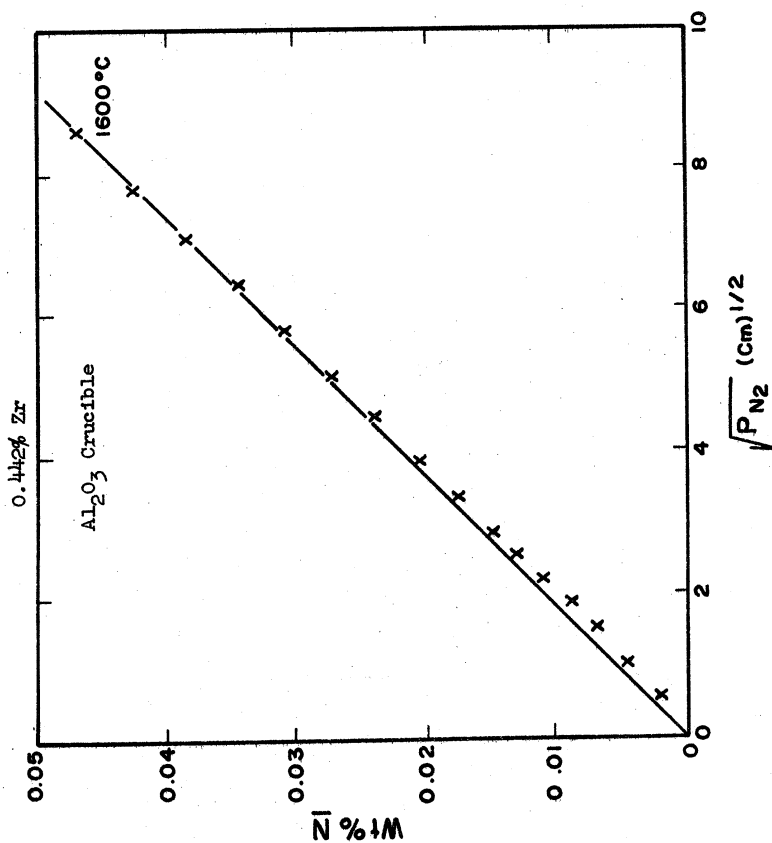


Figure F-15. Nitrogen Absorption Curves for the Zirconium System.

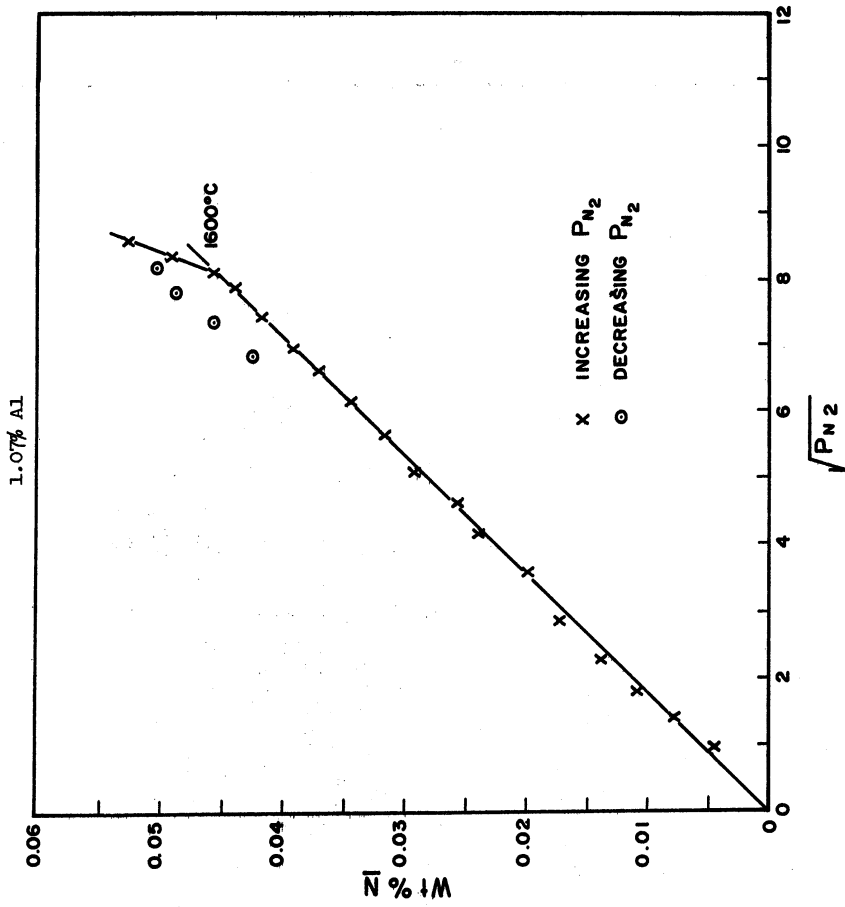


Figure F-18. Nitrogen Absorption Curves for the Aluminum System.

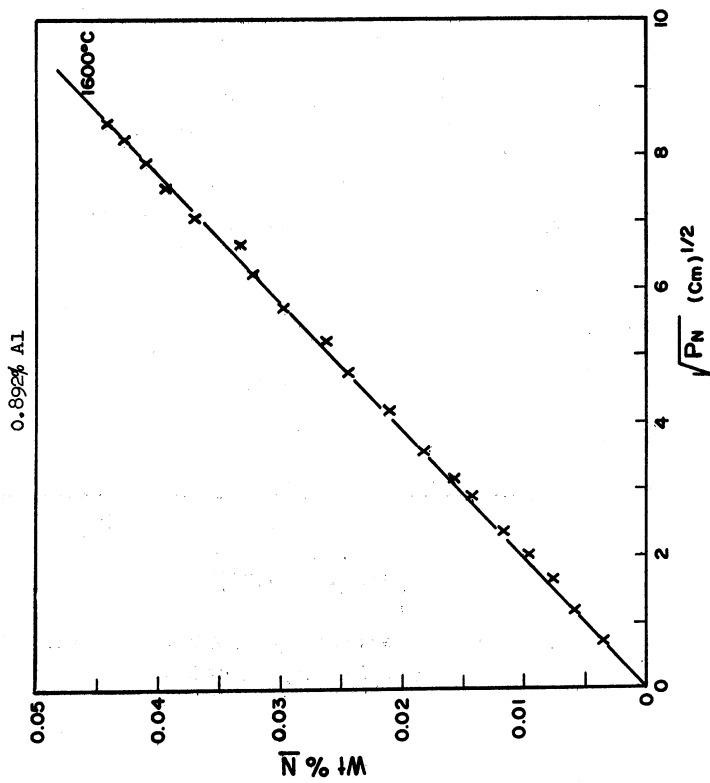


Figure F-17. Nitrogen Absorption Curves for the Aluminum System

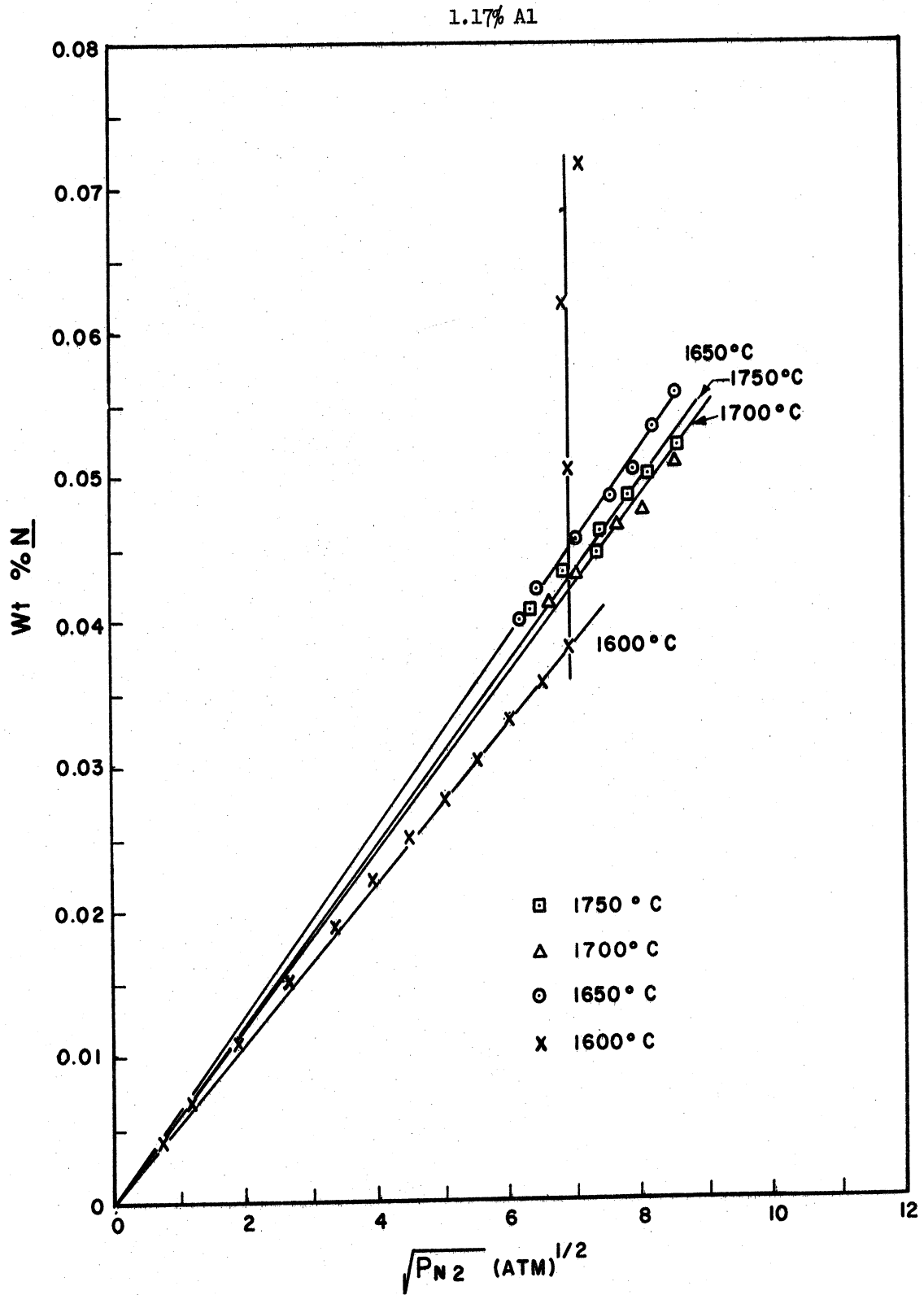


Figure F-19. Nitrogen Absorption Curves for the Aluminum System

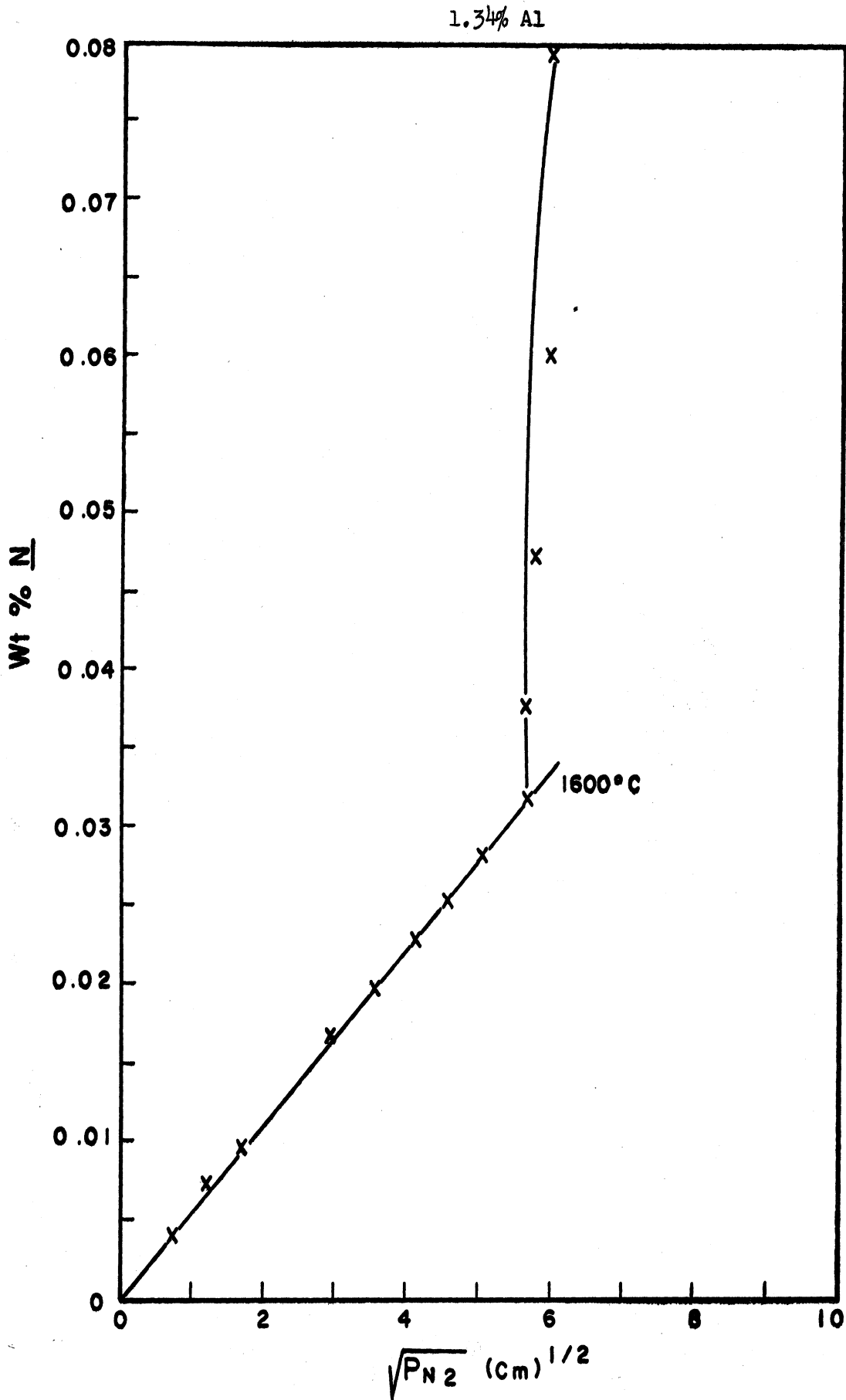


Figure F-20. Nitrogen Absorption Curves for the Aluminum System.



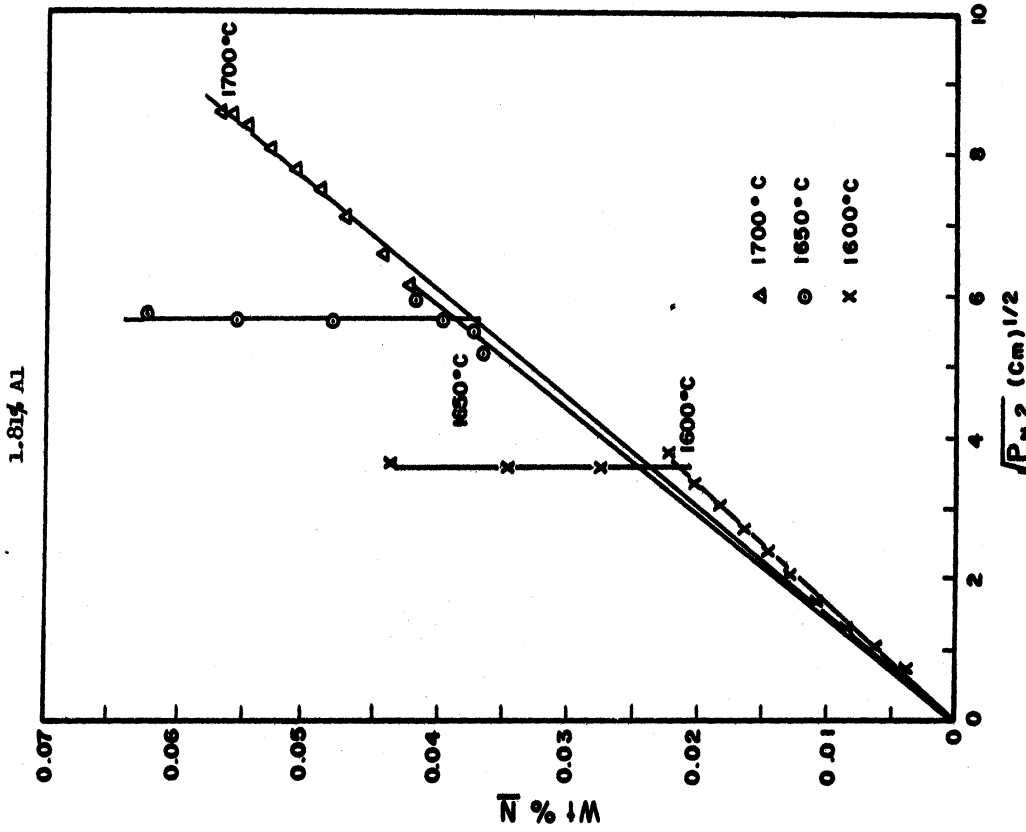


Figure F-22. Nitrogen Absorption Curves for the Aluminum System.

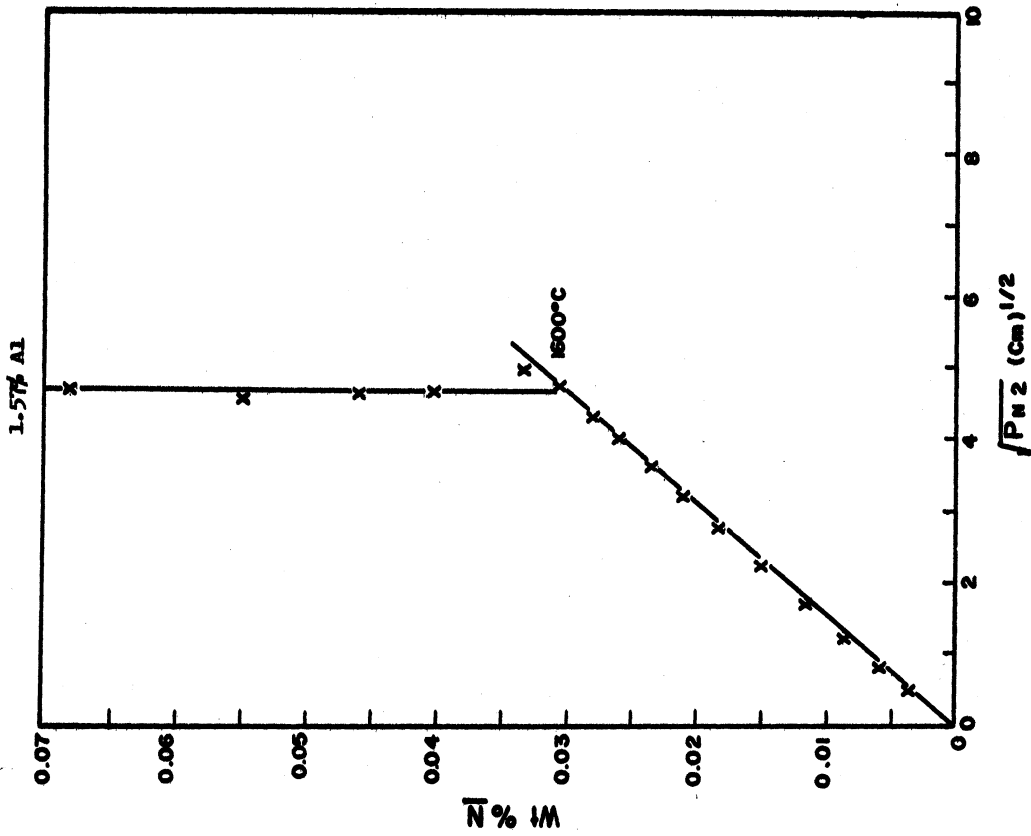


Figure F-21. Nitrogen Absorption Curves for the Aluminum System.

2.26% Al

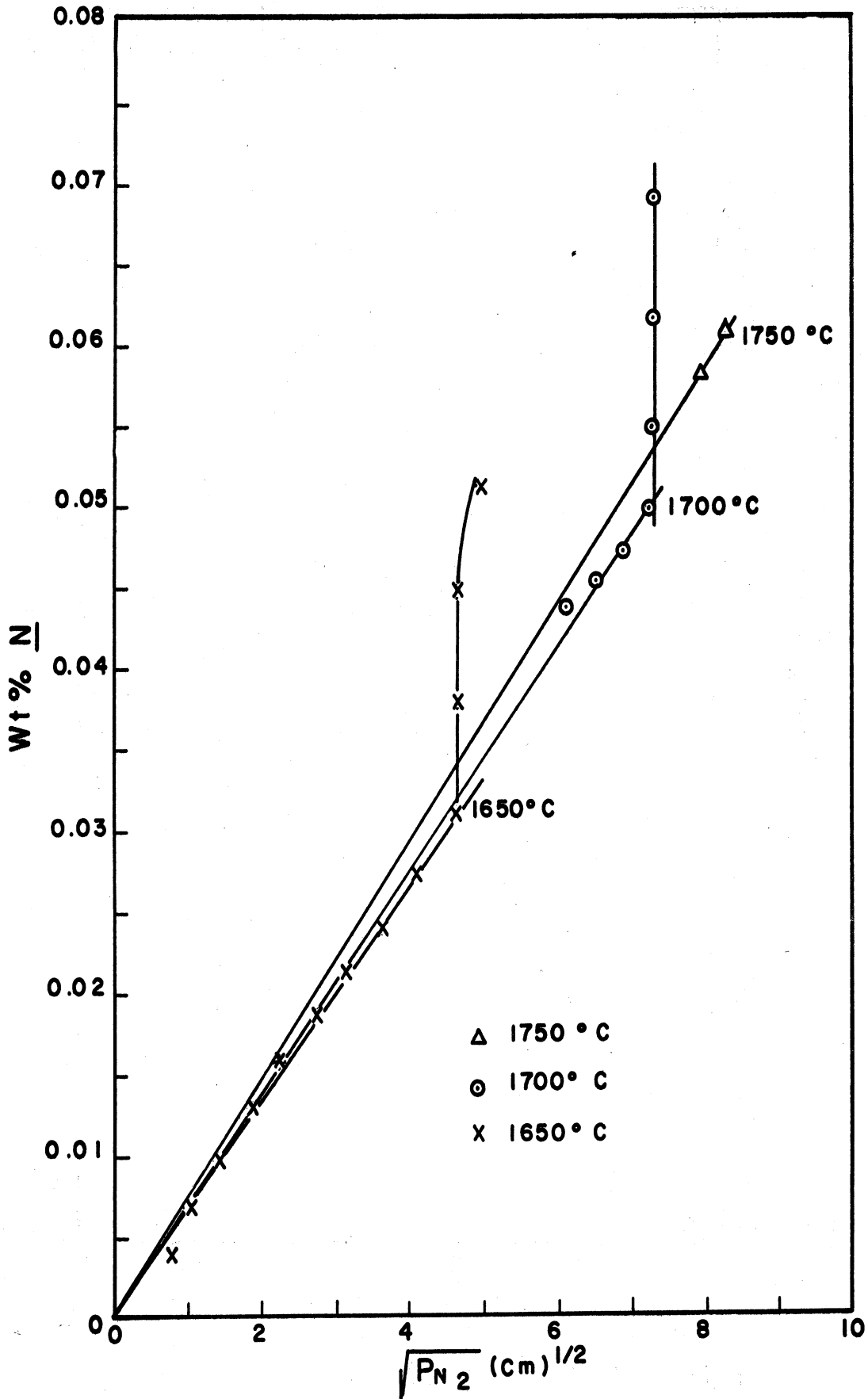


Figure F-23. Nitrogen Absorption Curves for the Aluminum System.

3.14% Al

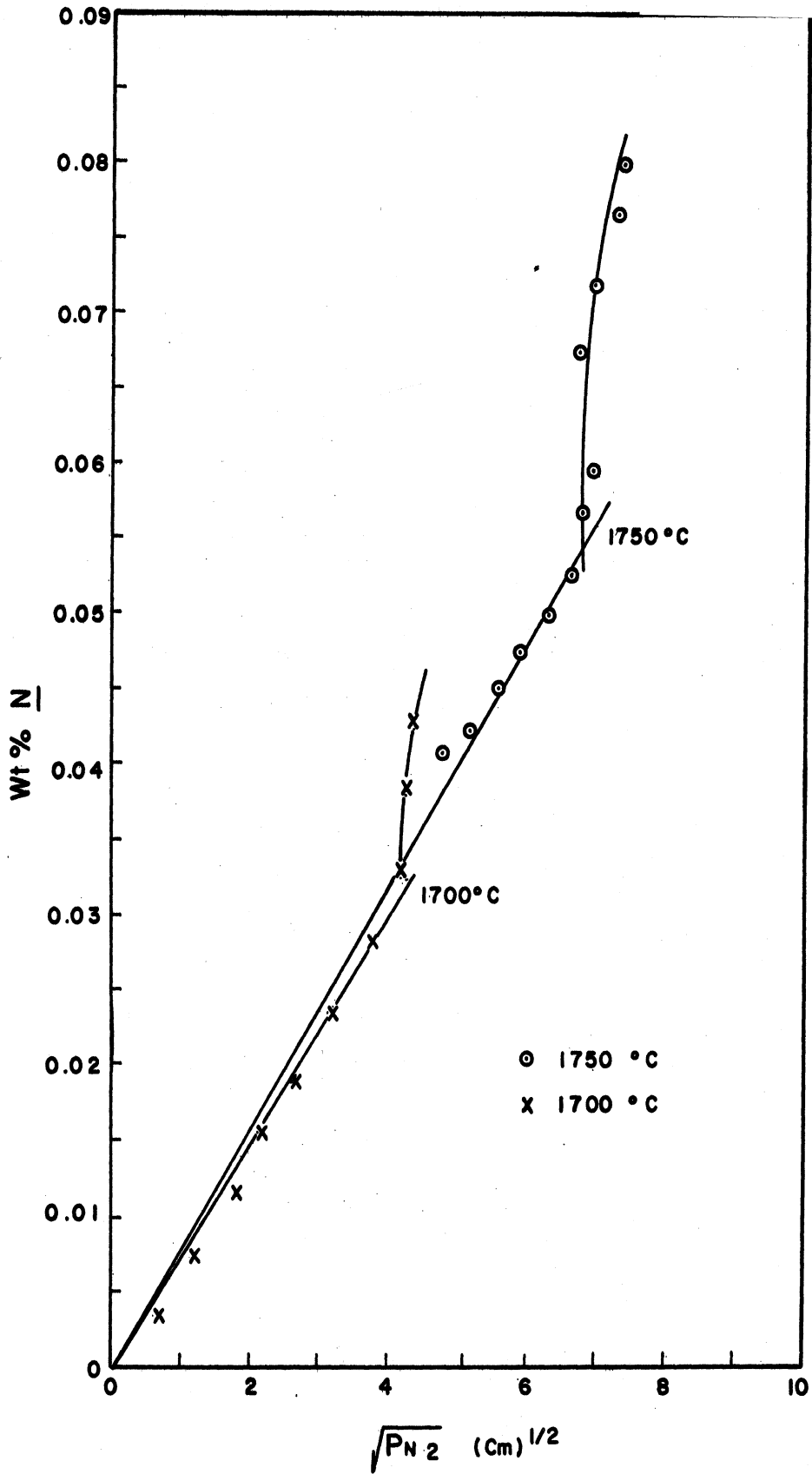


Figure F-24. Nitrogen Absorption Curves for the Aluminum System.

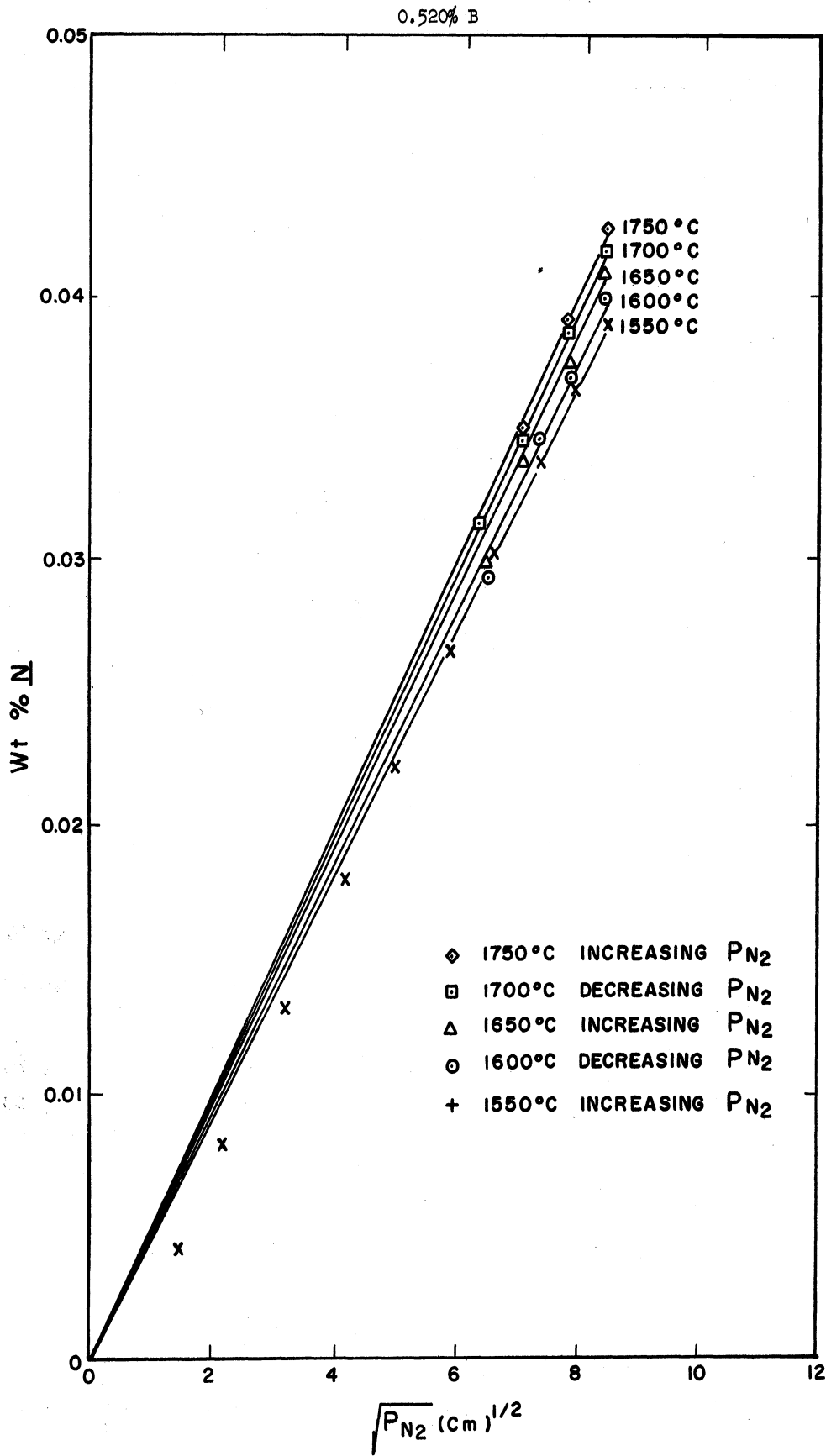


Figure F-25. Nitrogen Absorption Curves for the Boron System.

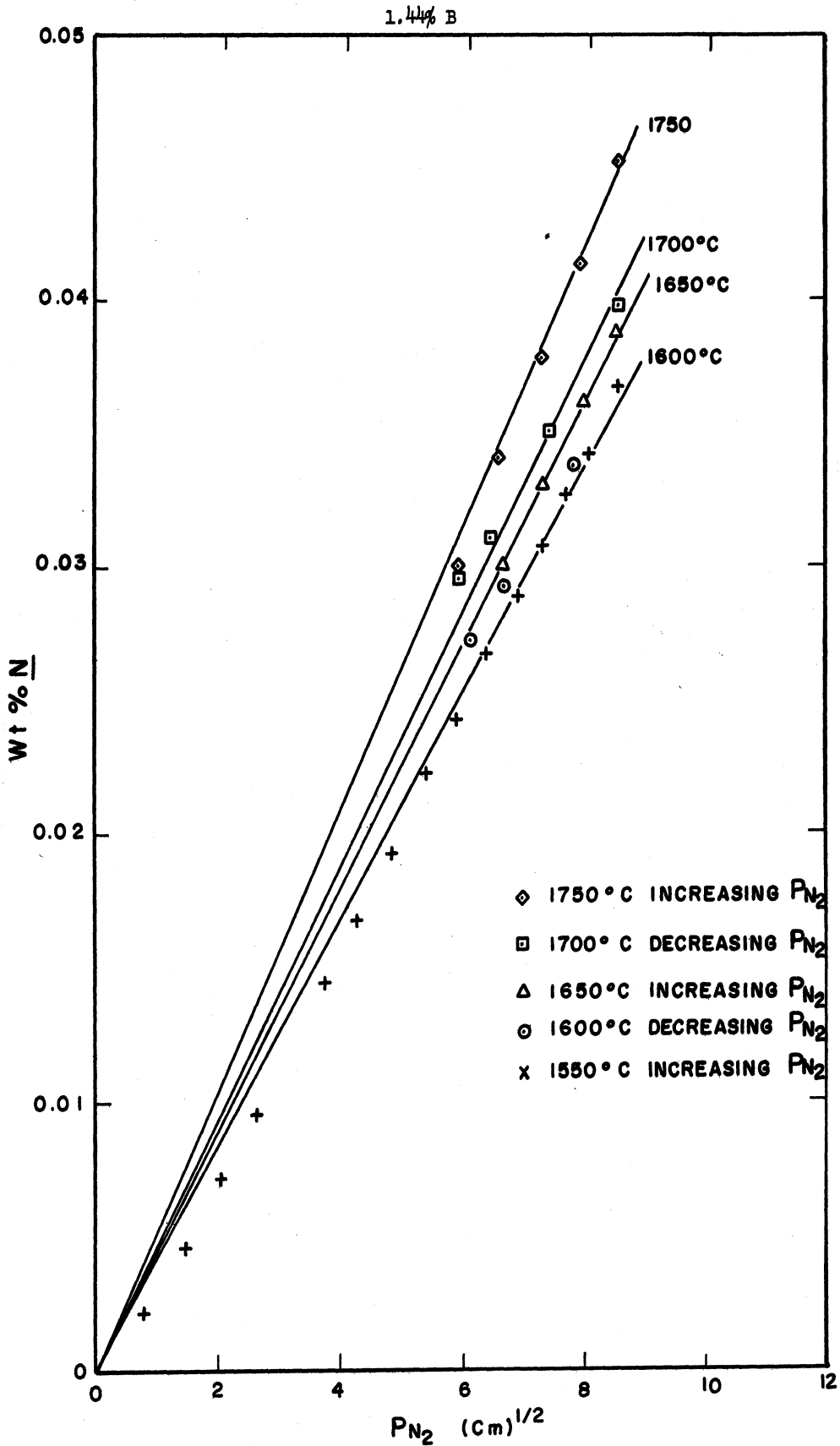


Figure F-26. Nitrogen Absorption Curves for the Boron System

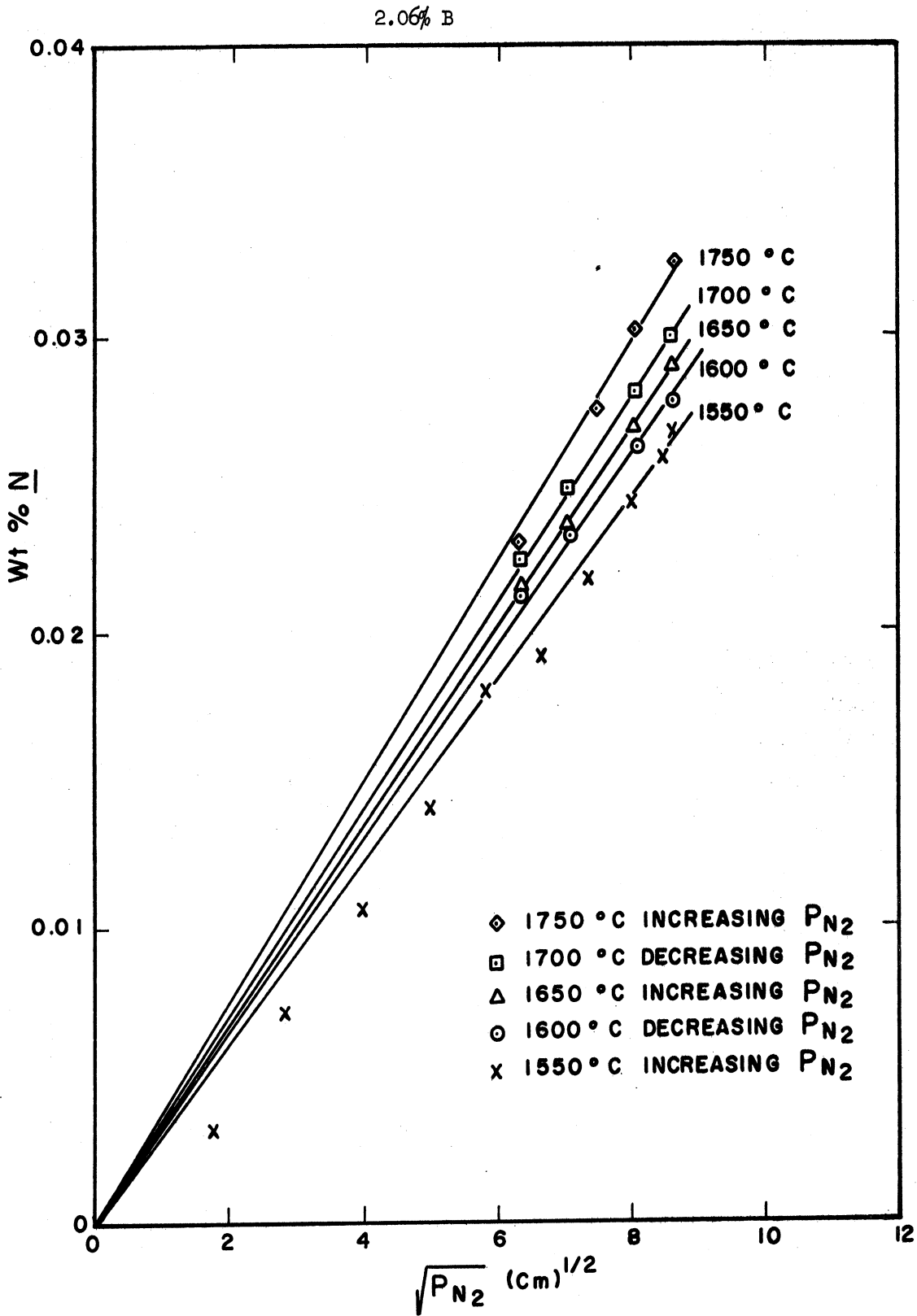


Figure F-27. Nitrogen Absorption Curves for the Boron System.

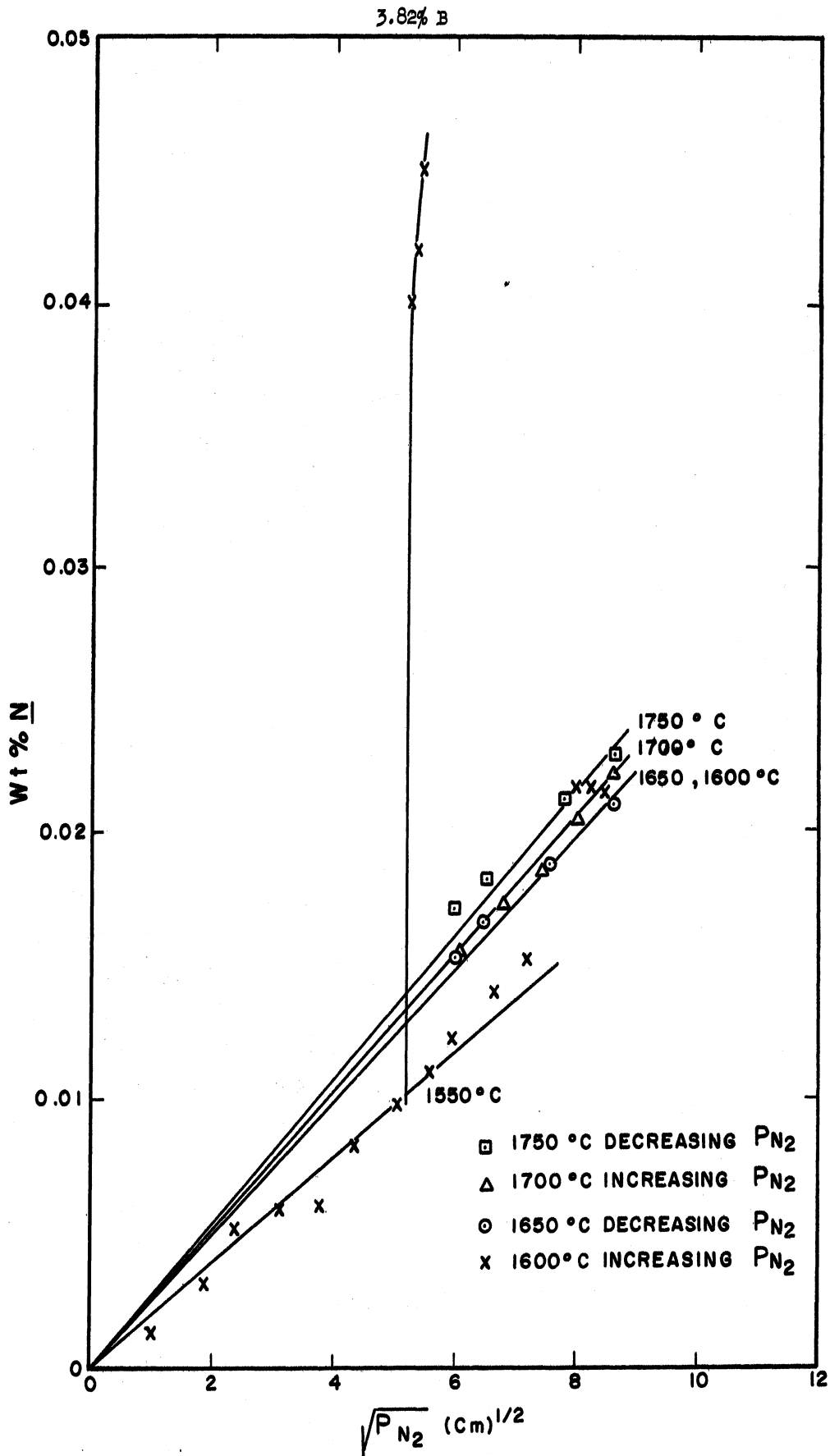


Figure F-28. Nitrogen Absorption Curves for the Boron System.

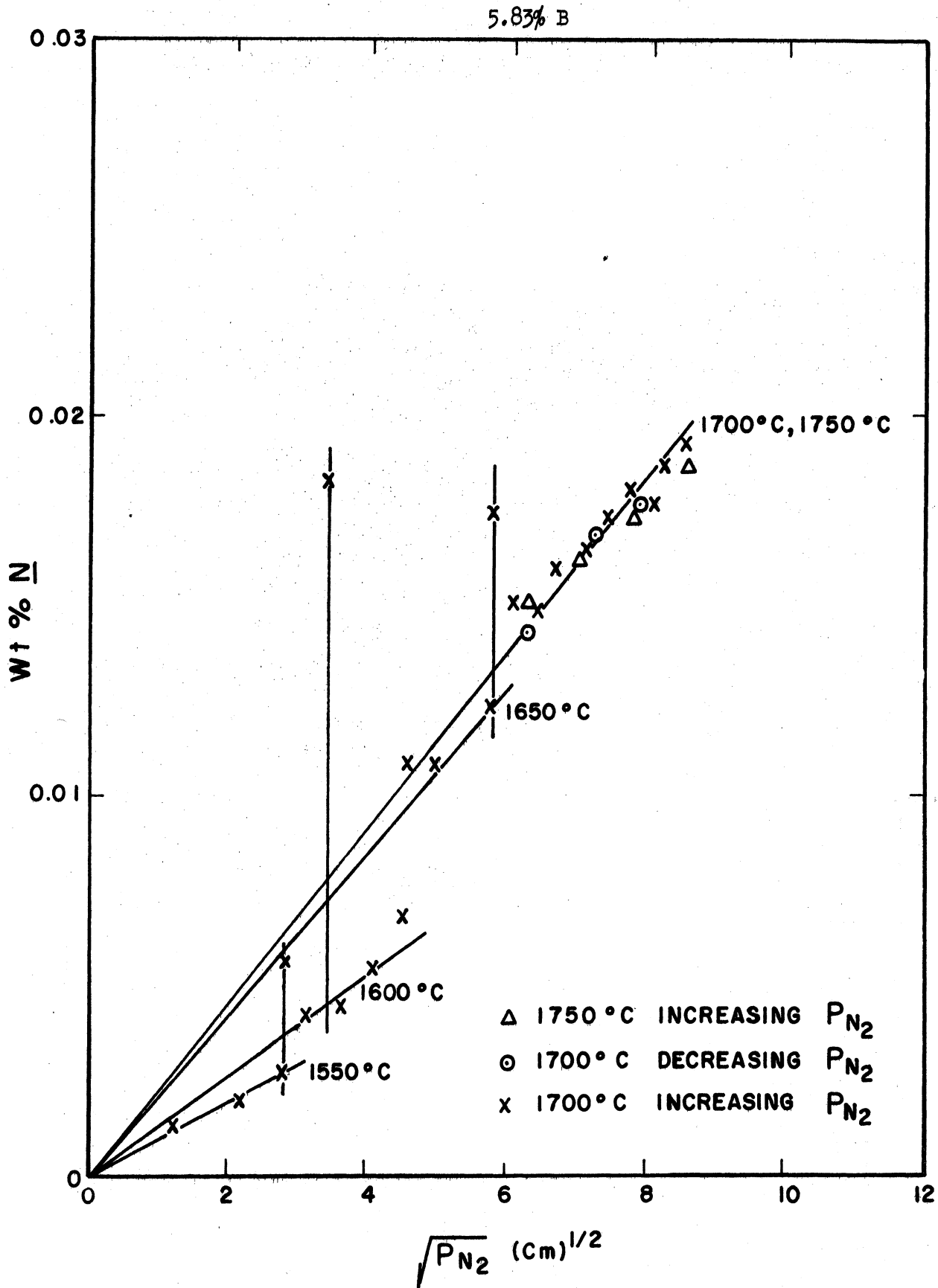


Figure F-29. Nitrogen Absorption Curves for the Boron System.



7.06% B

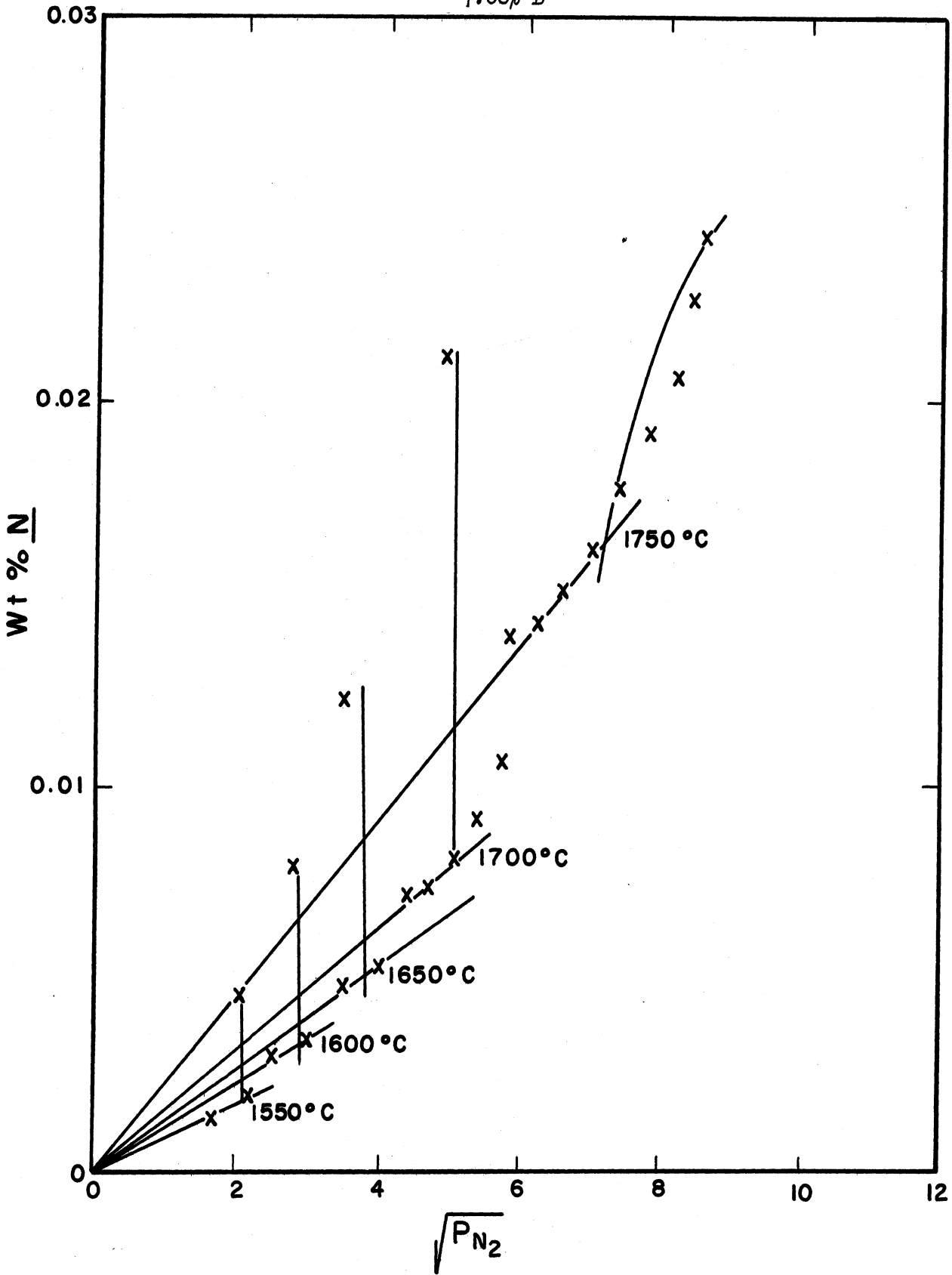


Figure F-30. Nitrogen Absorption Curves for the Boron System

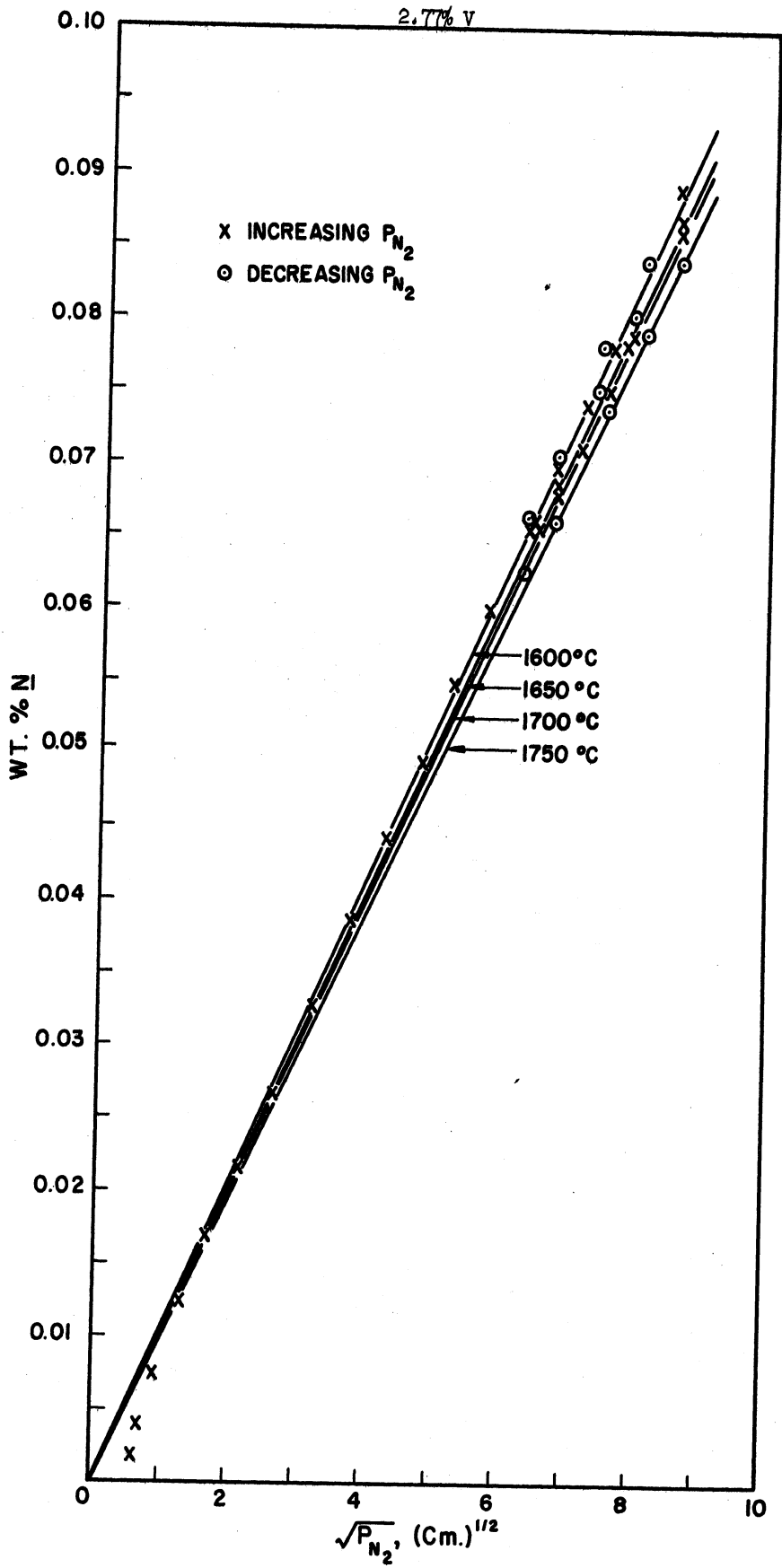


Figure F-31. Nitrogen Absorption Curves for the Vanadium System.

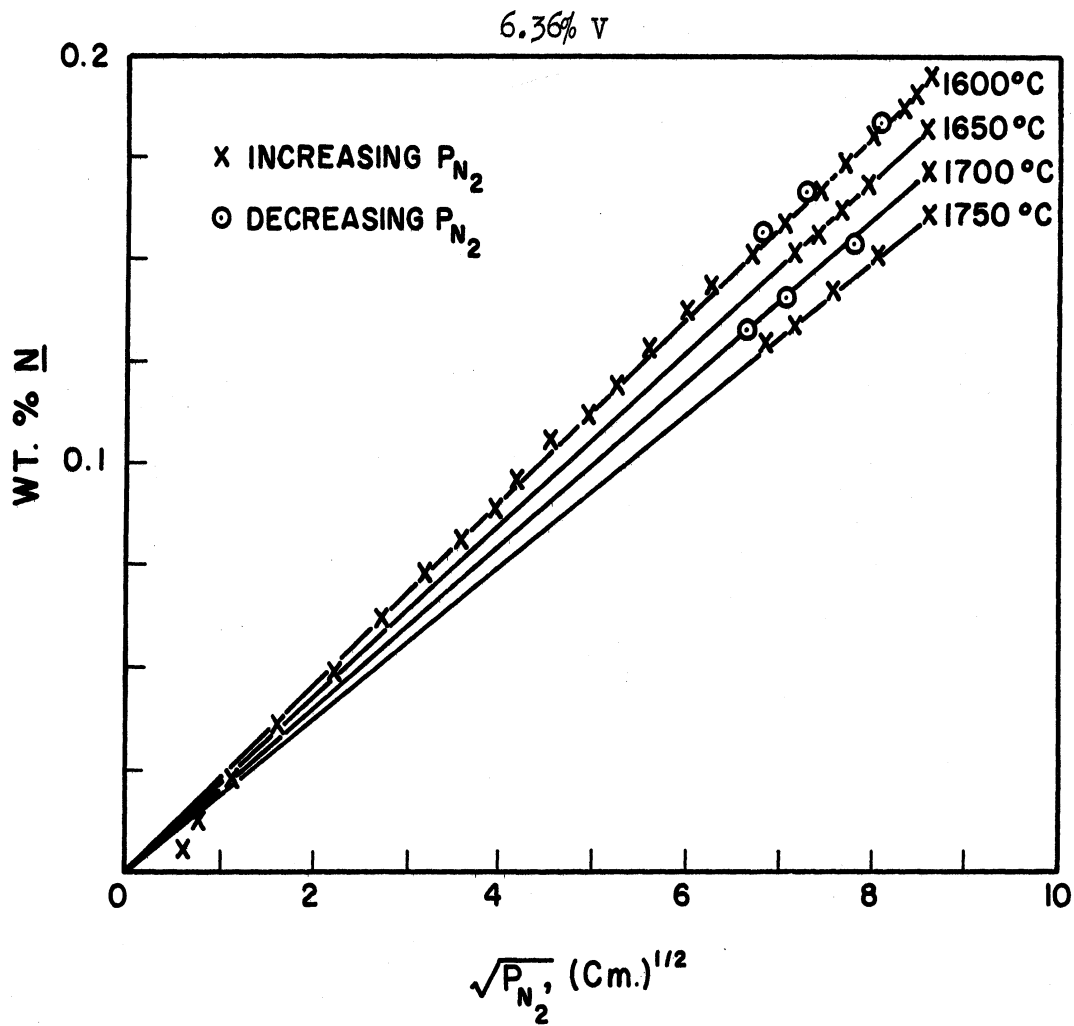


Figure F-32. Nitrogen Absorption Curves for the Vanadium System.

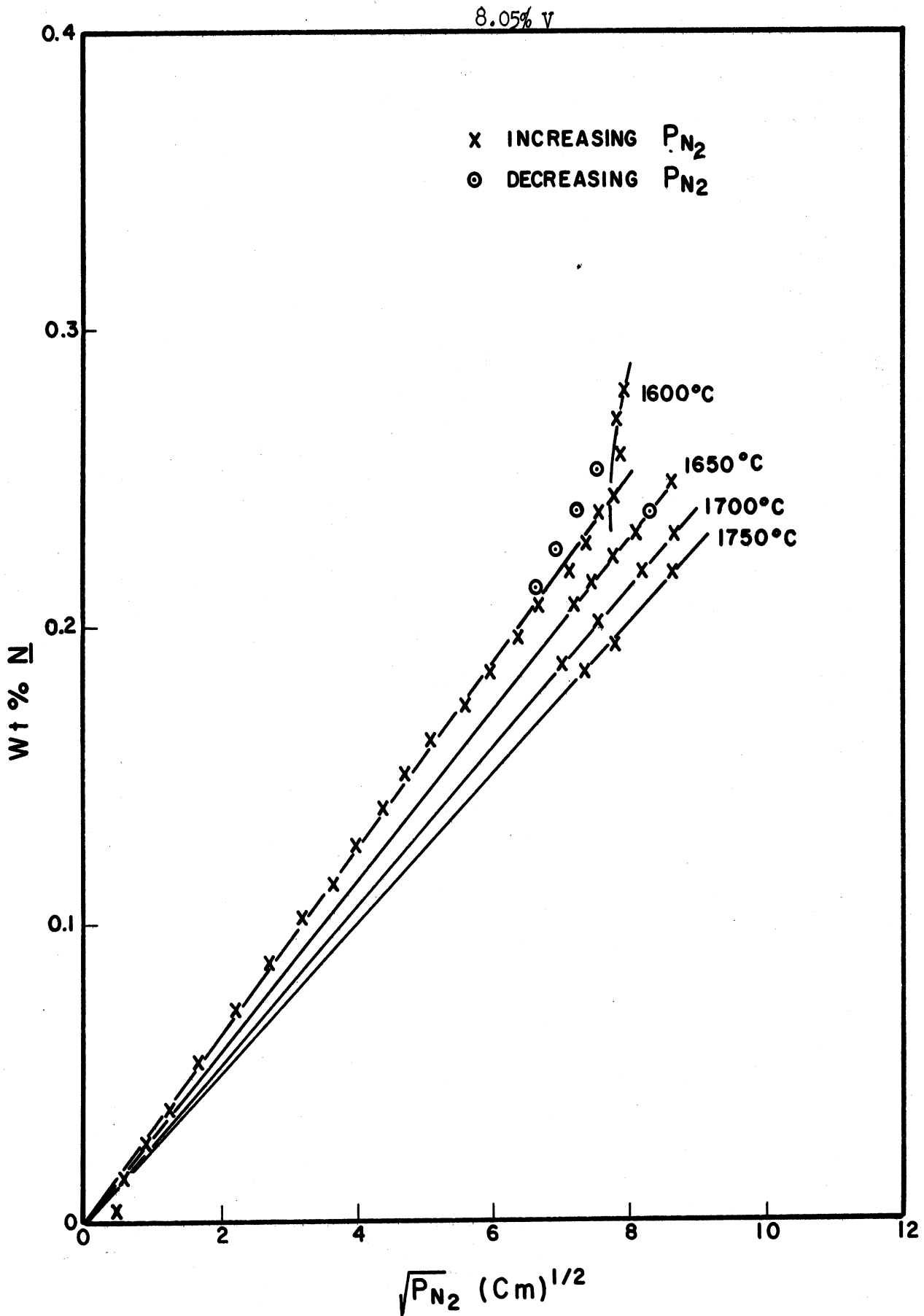


Figure F-33. Nitrogen Absorption Curves for the Vanadium System.

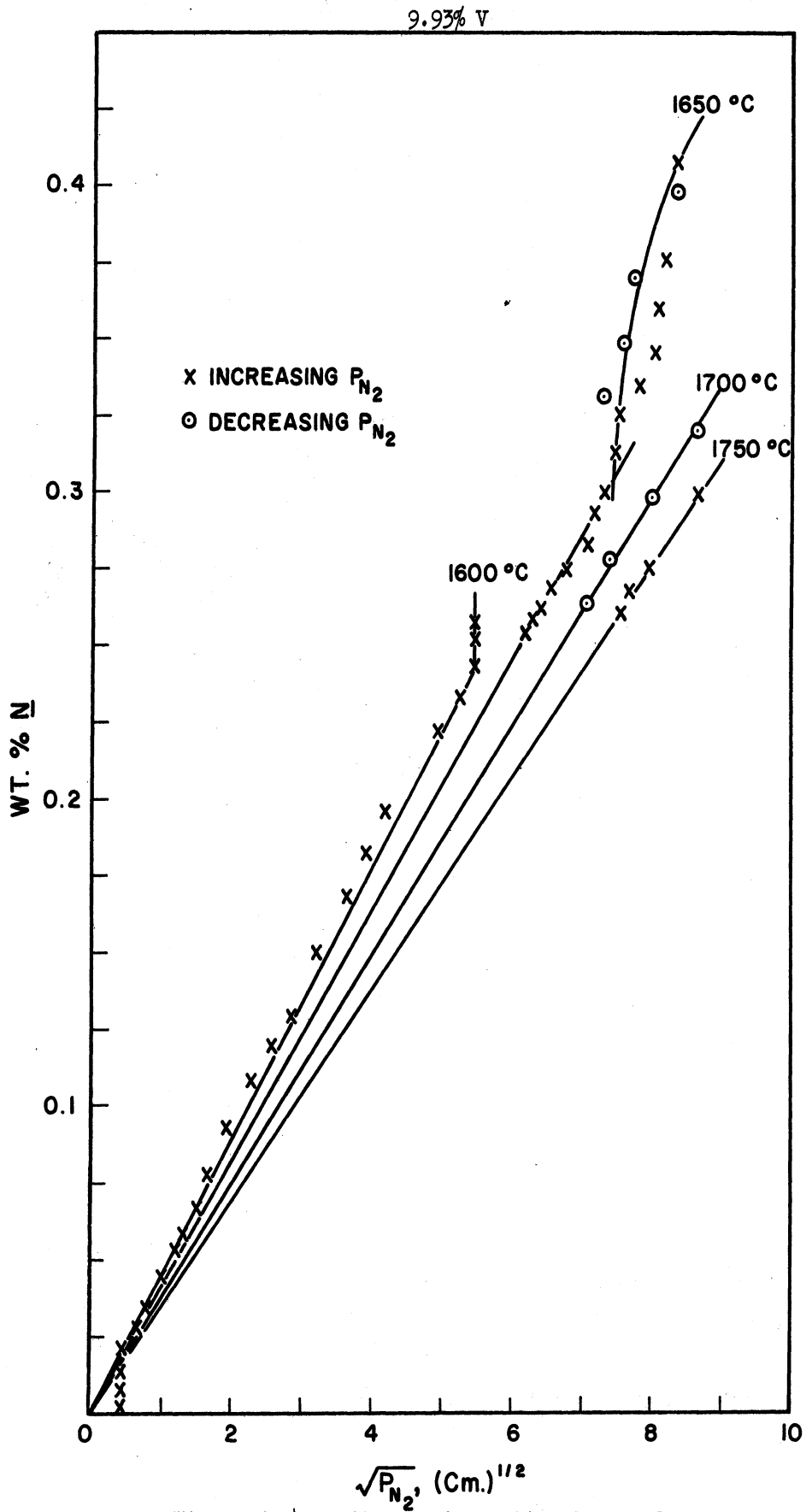


Figure F-34. Nitrogen Absorption Curves for the Vanadium System.

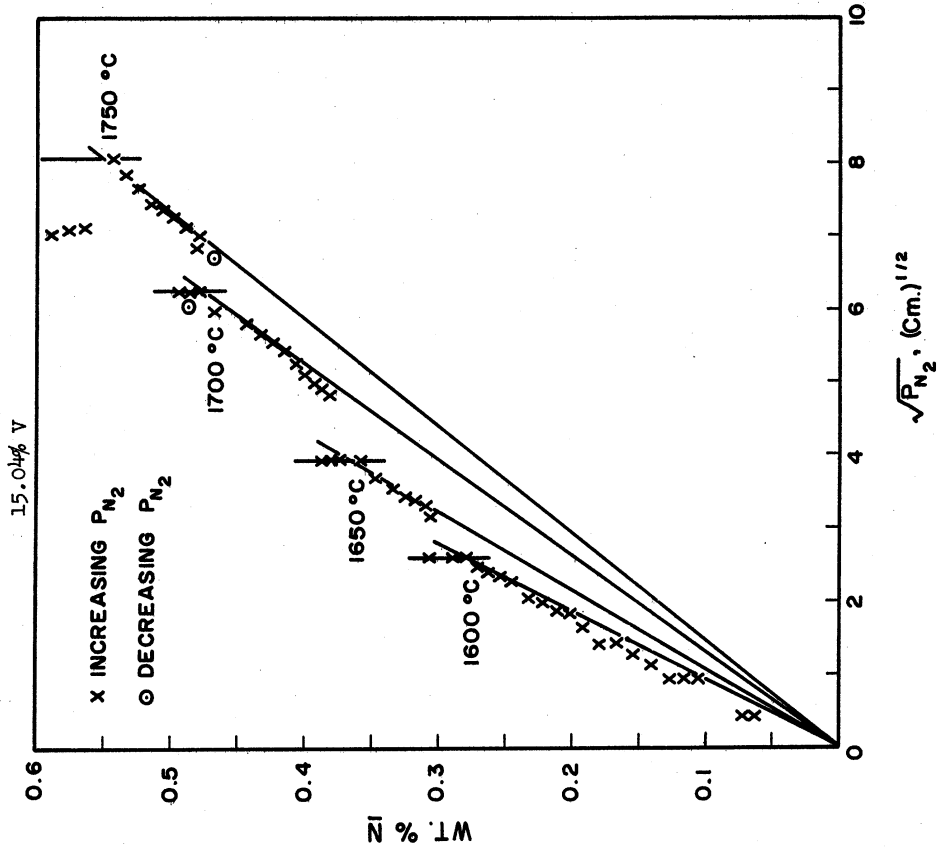


Figure F-35. Nitrogen Absorption Curves for the Vanadium System.

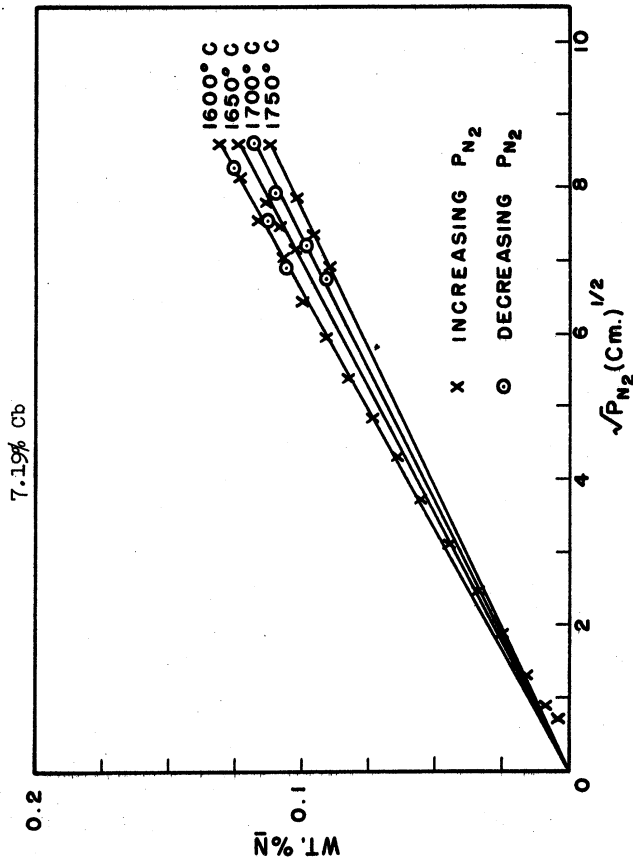


Figure F-36. Nitrogen Absorption Curves for the Columbium System.

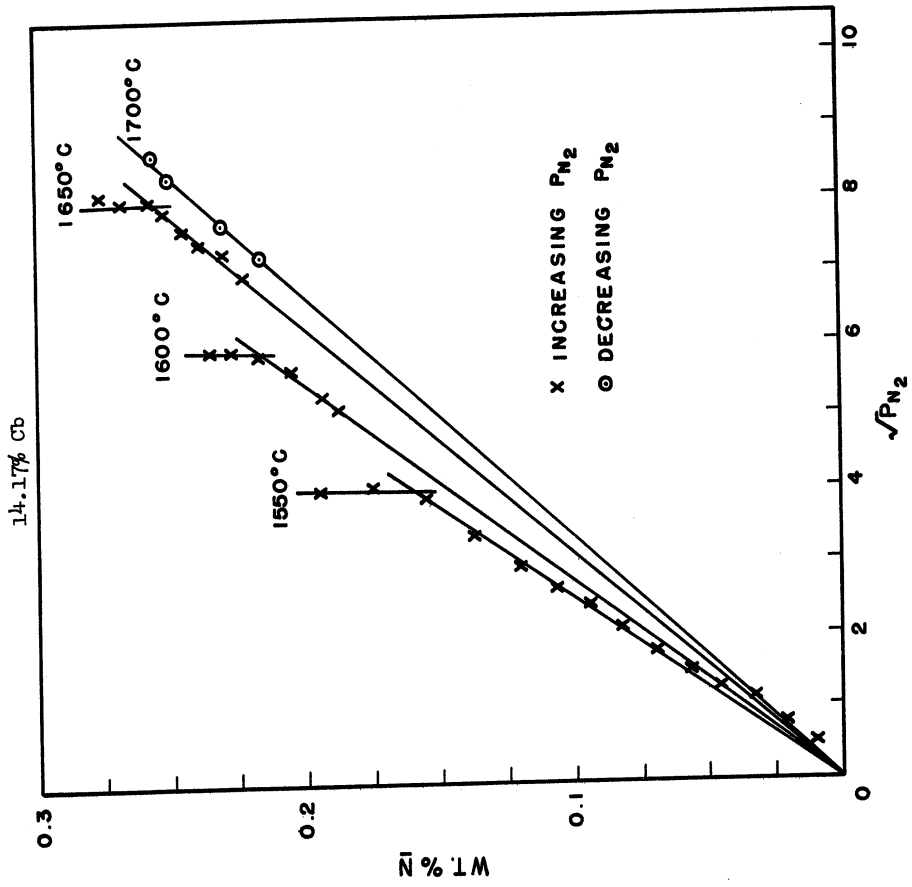


Figure F-38. Nitrogen Absorption Curves for the Columbium System.

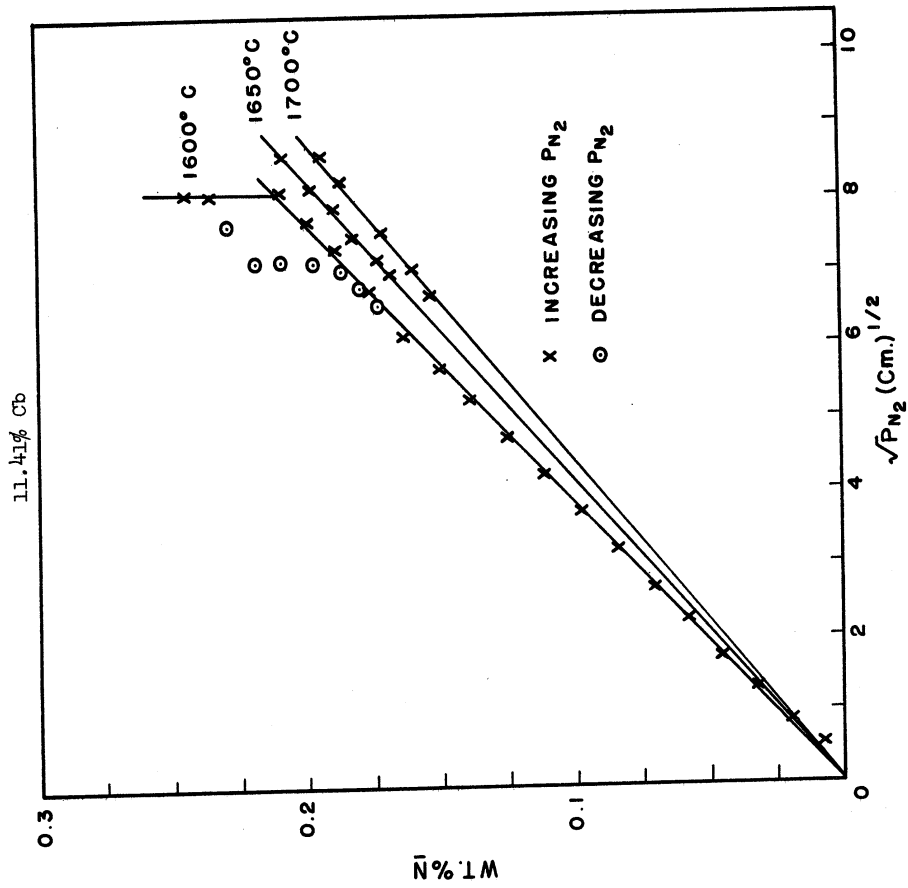


Figure F-37. Nitrogen Absorption Curves for the Columbium System.

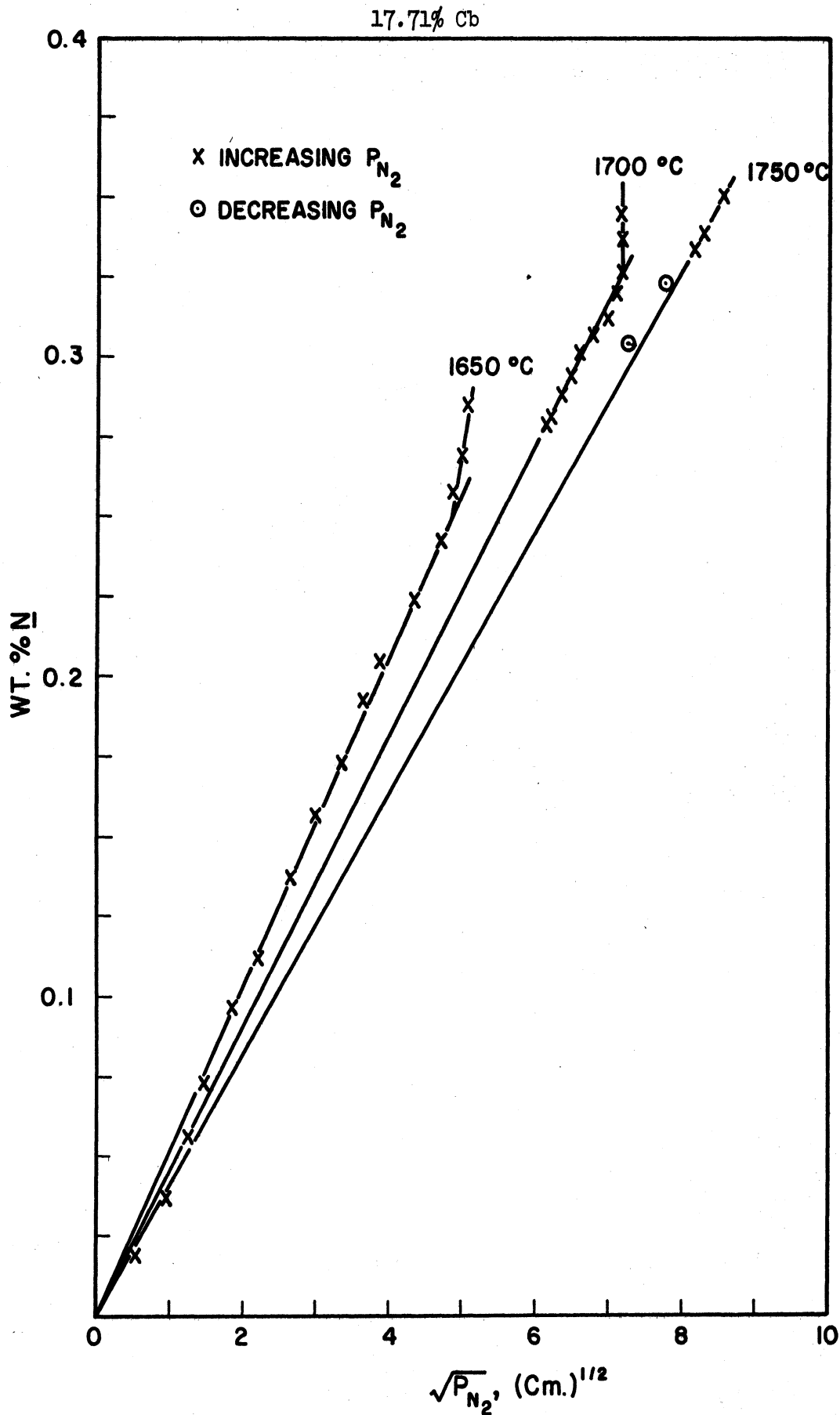


Figure F-39. Nitrogen Absorption Curves for the Columbian System



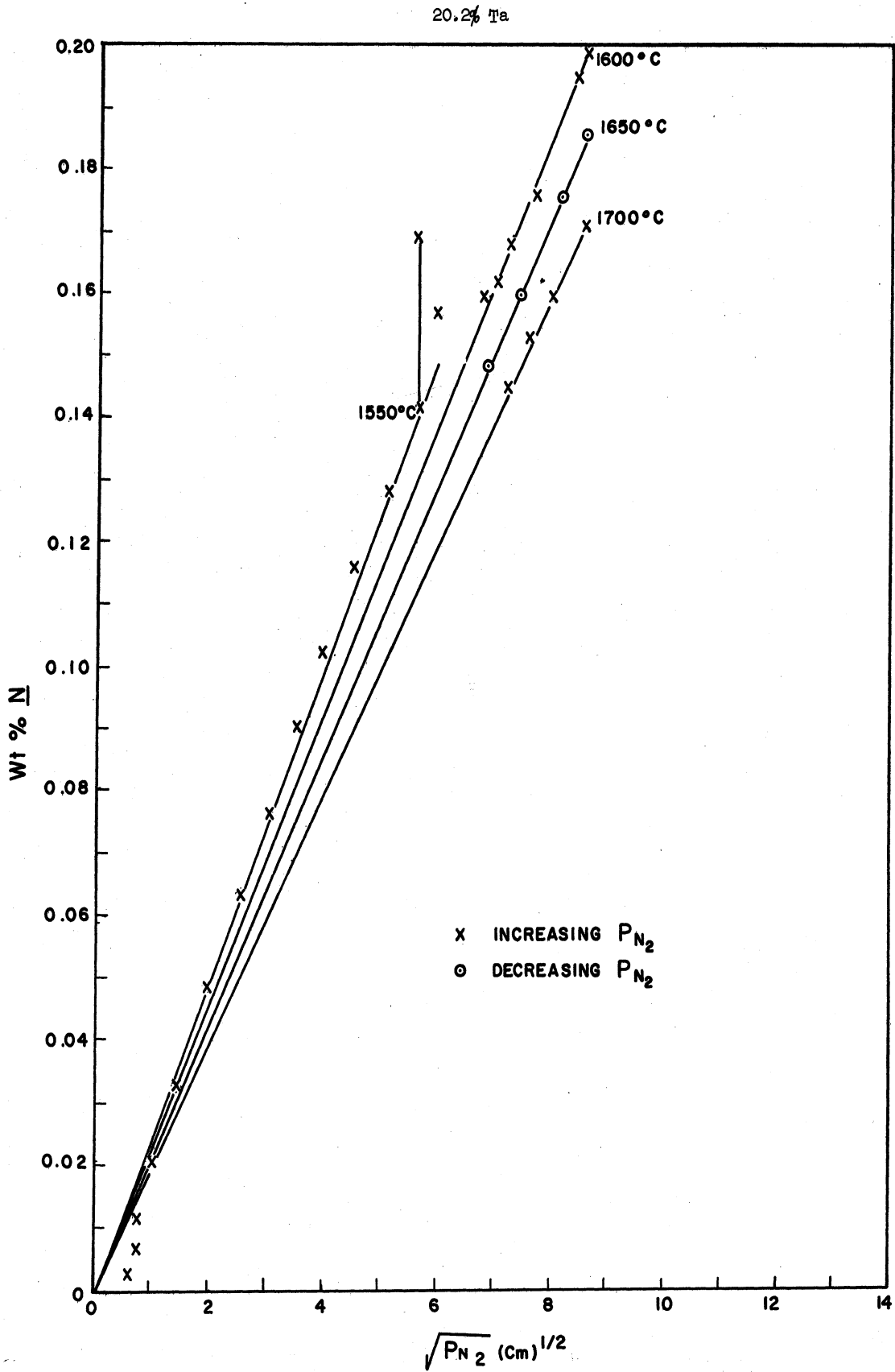


Figure F-40. Nitrogen Absorption Curve for the Tantalum System.

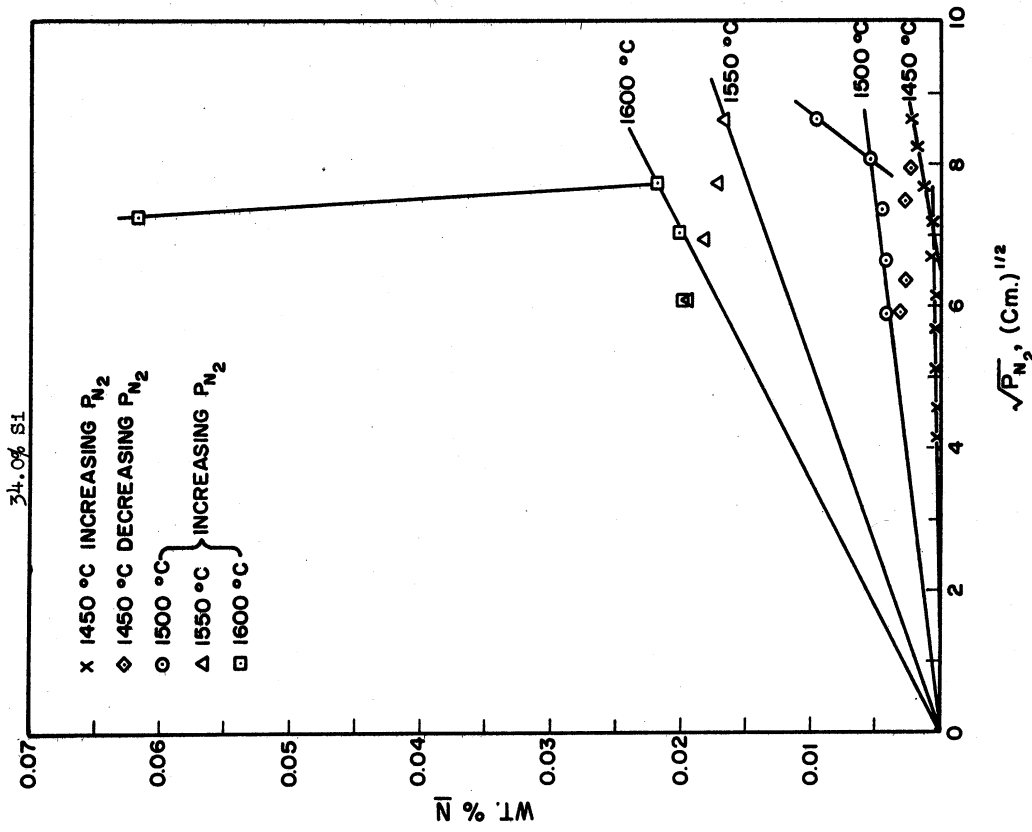


Figure F-41. Nitrogen Absorption Curves for the Silicon System.

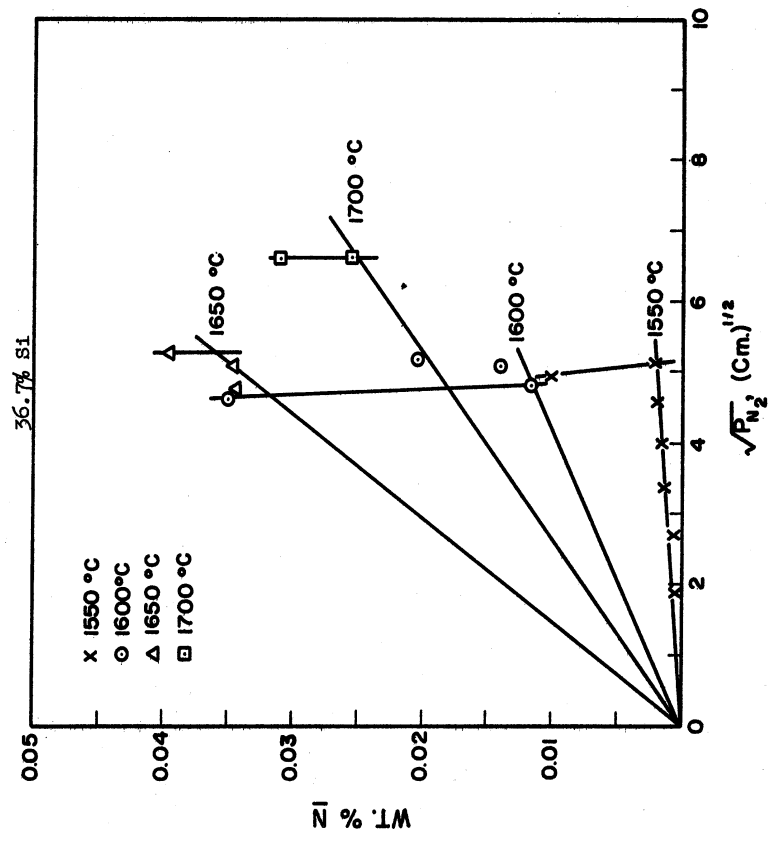


Figure F-42. Nitrogen Absorption Curves for the Silicon System.

APPENDIX G

CALCULATION OF NITRIDE COMPOSITIONS BY PHASE RULE ANALYSIS

A graphical phase rule analysis of the 0.228% Ti, 0.318% Ti, 1.34% Al, and 1.57% Al nitrogen absorption curves is shown in Figures G-1, G-2, G-3, and G-4. The calculation of the nitride phase composition for each curve is summarized in Table G-I below.

TABLE G-I

NITRIDE COMPOSITIONS CALCULATED FROM THE PHASE RULE ANALYSIS			
Temp. °C	Wt. % <u>j</u>	wt. % <u>N</u>	Calculated Nitride Composition
1650	0.228% Ti	0.0277	Ti <sub>2.4</sub> N
1700	0.318% Ti	0.0425	Ti <sub>2.2</sub> N
1600	1.34% Al	0.153	Al <sub>4.5</sub> N
1600	1.57% Al	0.212	Al <sub>3.9</sub> N

As previously noted the compositions given in Table G-I are considered incorrect, being too rich in metal. This error is due to the difficulty in reaching the equilibrium nitrogen pressure at pressures well above the break point in the absorption curve. In view of this difficulty, the validity of any method of calculating the nitride composition which employs the region of the absorption curve above the break point is considered extremely doubtful.

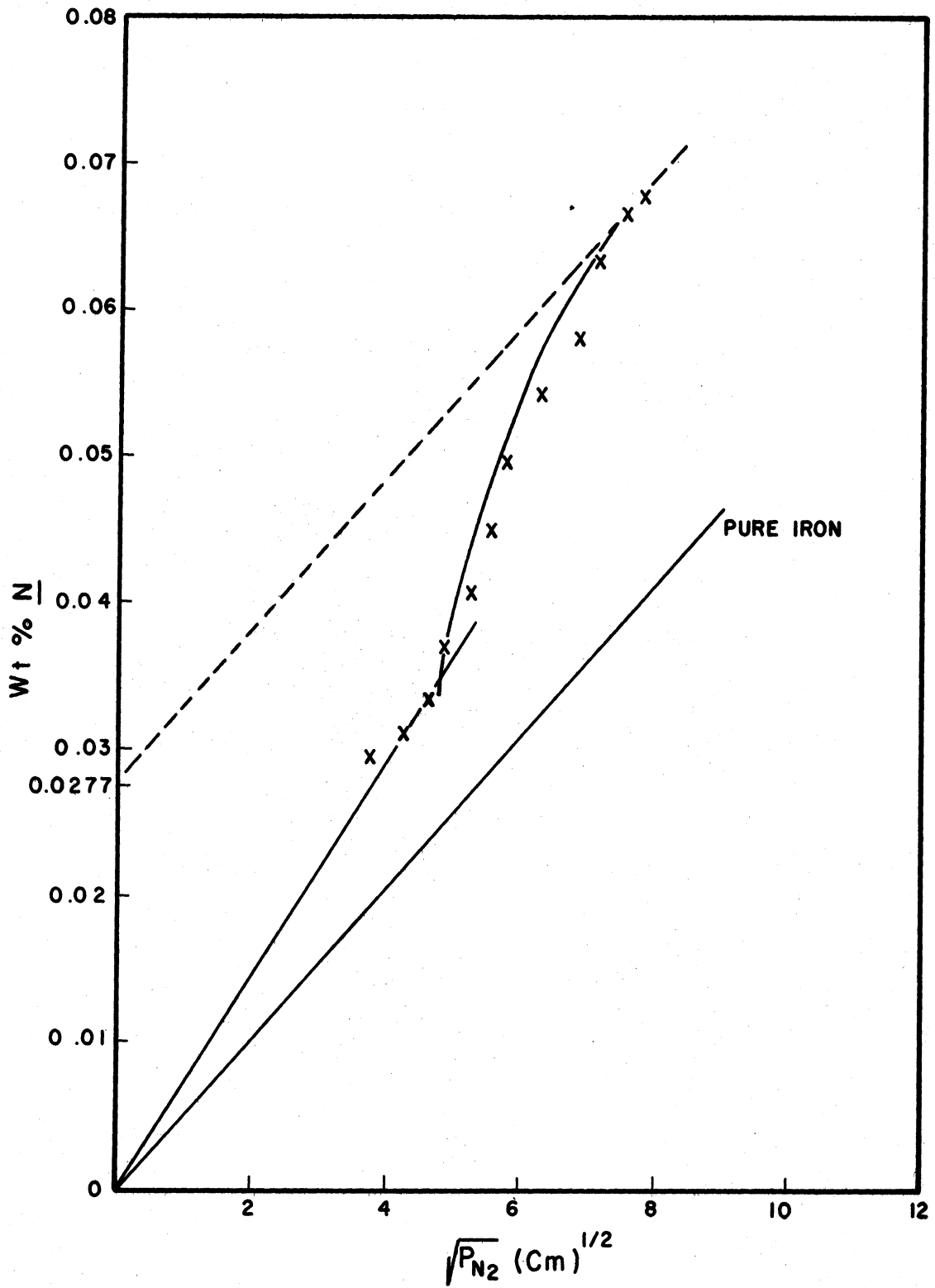


Figure G-1. Phase Rule Analysis of the 0.228% Titanium Nitrogen Absorption Curve.

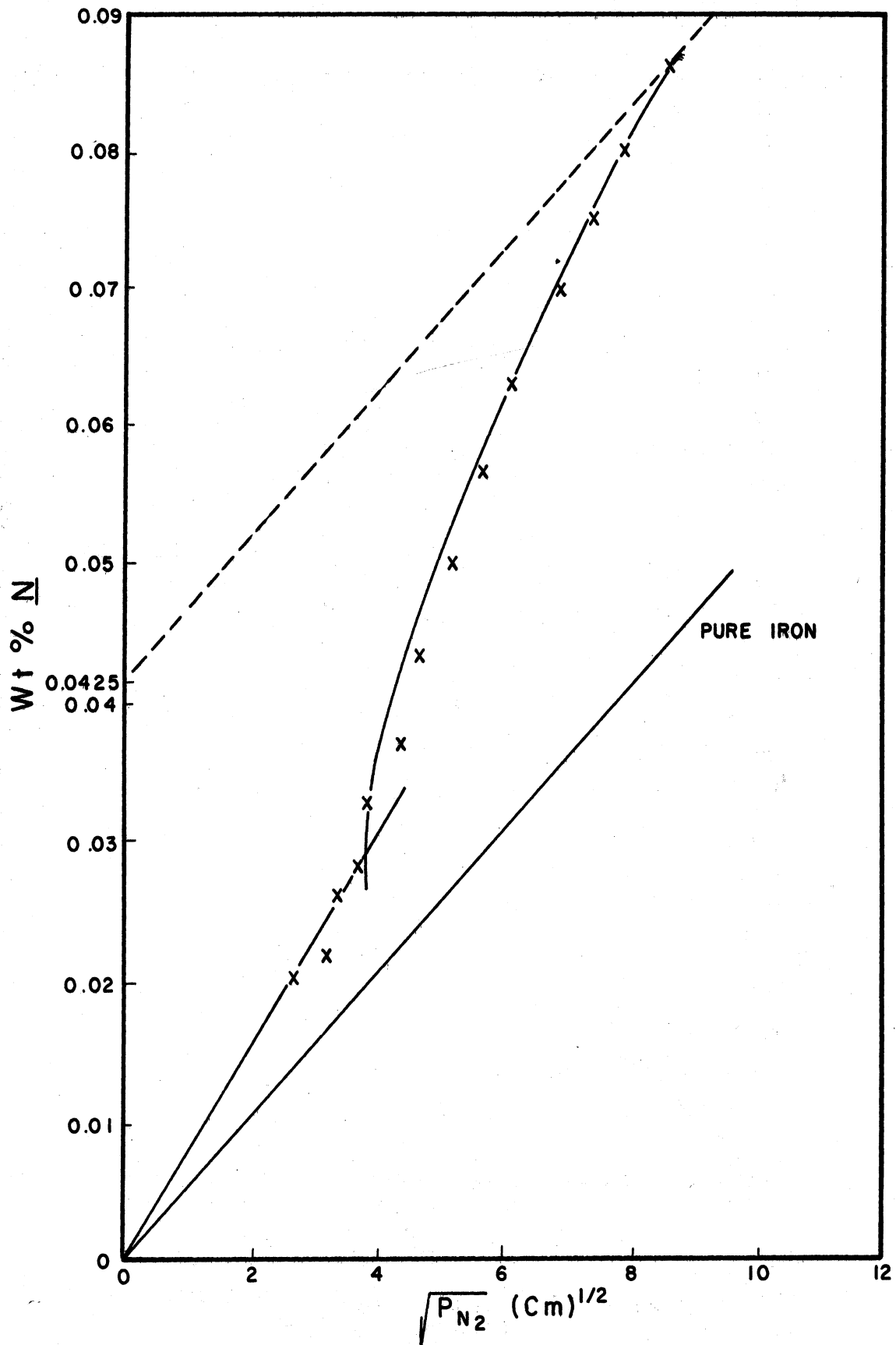


Figure G-2. Phase Rule Analysis of the 0.318% Titanium Nitrogen Absorption Curve.

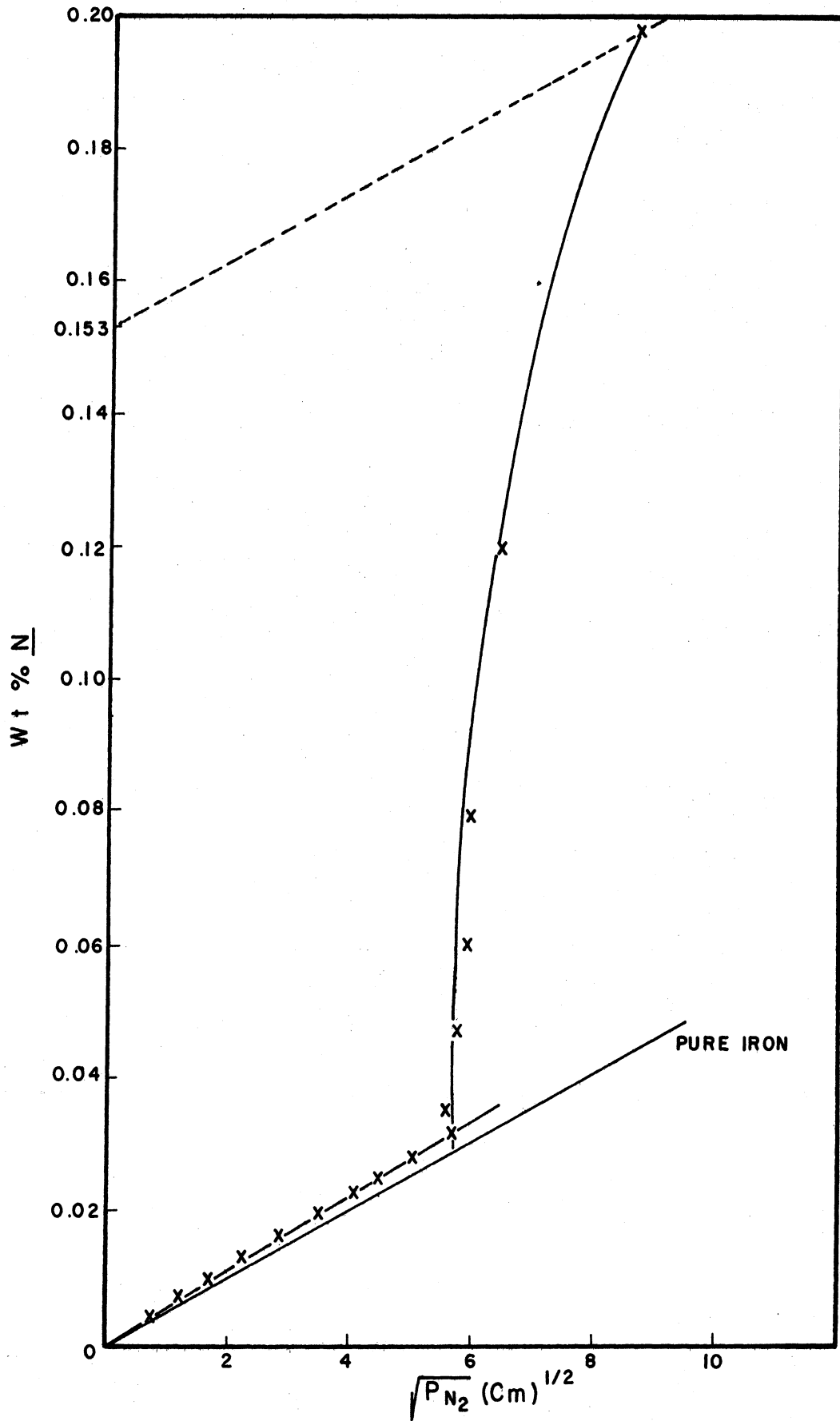


Figure G-3. Phase Rule Analysis of the 1.34% Aluminum Nitrogen Absorption Curve.

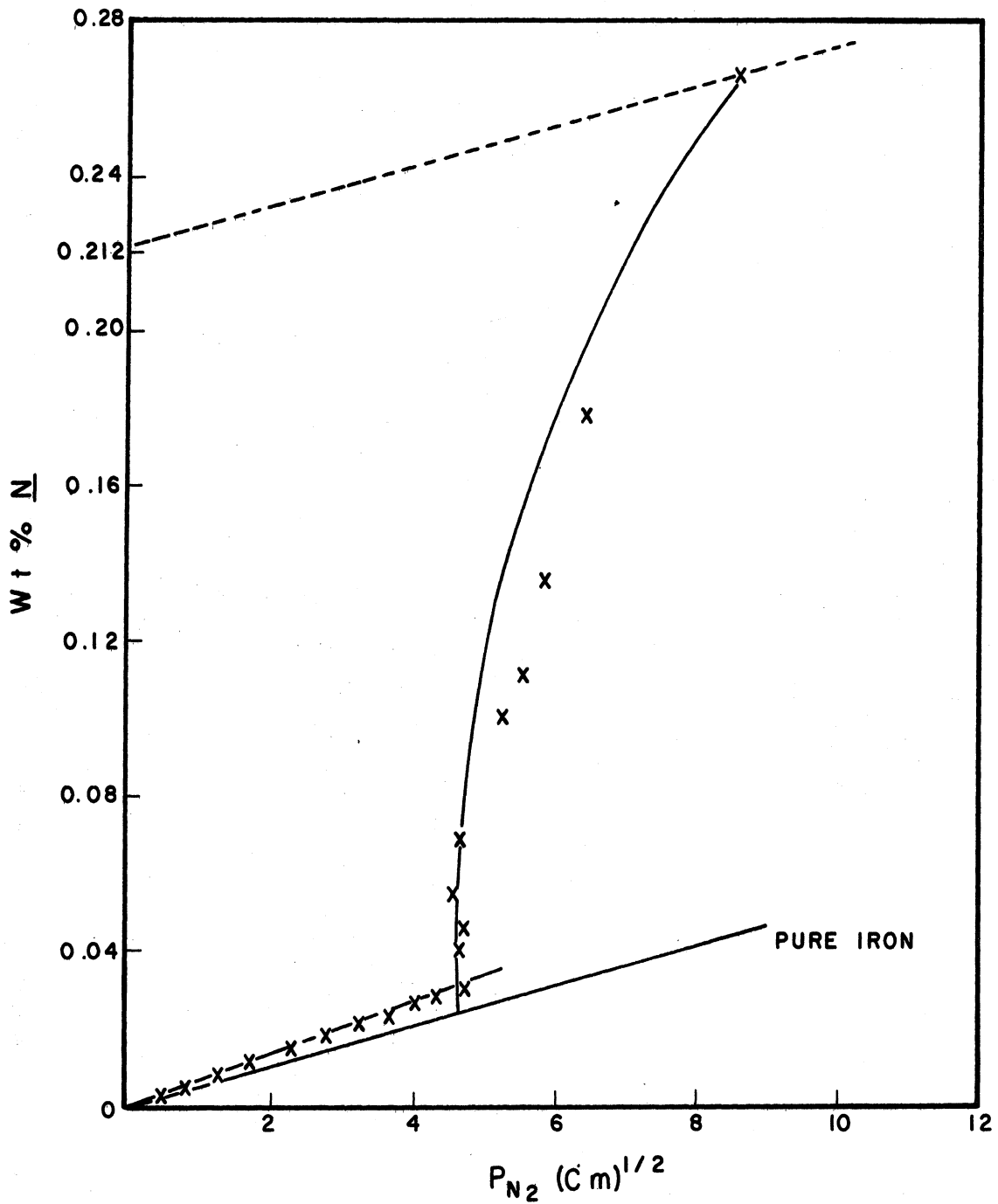


Figure G-4. Phase Rule Analysis of the 1.57% Aluminum Nitrogen Absorption Curve.

APPENDIX H

X-RAY DATA

The following tables give the results of Debye-Scherrer powder patterns run on samples chipped from solidified ingots removed from the Sieverts apparatus for which the nitrogen absorption curves indicated that a nitride had precipitated. The notation "extracted" indicates that the iron matrix was dissolved by the method of Beeghly<sup>(26)</sup> prior to running the powder pattern.

TABLE H-I

X-RAY DATA FOR TITANIUM NITRIDE SAMPLES FROM  
THE SIEVERTS APPARATUS

0.318% Ti, extracted Fe radiation, Mn filter		0.195% Ti, extracted Fe radiation, Mn filter	
<u>d observed</u>	<u>substance</u>	<u>d observed</u>	<u>substance</u>
2.563	Al <sub>2</sub> O <sub>3</sub>	2.442	TiN
2.439	TiN	2.128	TiN
2.372	Al <sub>2</sub> O <sub>3</sub>	1.505	TiN
2.120	TiN		
2.083	Al <sub>2</sub> O <sub>3</sub>		
1.599	Al <sub>2</sub> O <sub>3</sub>		
1.499	TiN		
1.405	Al <sub>2</sub> O <sub>3</sub>		
1.376	Al <sub>2</sub> O <sub>3</sub>		
1.278	TiN		
1.239	TiN		
1.215	Al <sub>2</sub> O <sub>3</sub>		
1.190	Al <sub>2</sub> O <sub>3</sub>		
1.147	Al <sub>2</sub> O <sub>3</sub>		
1.061	TiN		
1.035	Al <sub>2</sub> O <sub>3</sub>		
1.001	Al <sub>2</sub> O <sub>3</sub>		



TABLE H-II

X-RAY DATA FOR ALUMINUM NITRIDE SAMPLES FROM THE SIEVERTS APPARATUS

3.85% Al, extracted  
Fe radiation, Mn filter

1.07% Al, extracted  
Fe radiation, Mn filter

<u>d observed</u>	<u>substance</u>
3.44	Al <sub>2</sub> O <sub>3</sub>
2.679	AlN
2.532	Al <sub>2</sub> O <sub>3</sub>
2.468	AlN
2.353	AlN
2.109	Al <sub>2</sub> O <sub>3</sub>
1.822	AlN
1.729	Al <sub>2</sub> O <sub>3</sub>
1.412	AlN
1.401	Al <sub>2</sub> O <sub>3</sub>
1.371	Al <sub>2</sub> O <sub>3</sub>
1.344	AlN
1.317	AlN
1.298	AlN
1.245	Al <sub>2</sub> O <sub>3</sub>
1.182	AlN
1.078	Al <sub>2</sub> O <sub>3</sub>
1.046	AlN
1.044	Al <sub>2</sub> O <sub>3</sub>
1.019	AlN
1.016	AlN
0.999	AlN
0.996	AlN

<u>d observed</u>	<u>substance</u>
2.704	AlN
2.476	AlN
2.347	AlN
2.082	Al <sub>2</sub> O <sub>3</sub>
1.819	AlN
1.594	Al <sub>2</sub> O <sub>3</sub>
1.547	AlN
1.408	AlN
1.369	Al <sub>2</sub> O <sub>3</sub>
1.044	AlN
1.018	AlN
0.996	AlN

1.17% Al, unextracted  
Co radiation, Ni filter

<u>d observed</u>	<u>substance</u>
2.680	AlN
2.445	Al <sub>2</sub> O <sub>3</sub>
2.026	Fe
1.872	Al <sub>2</sub> O <sub>3</sub>
1.567	AlN
1.434	Fe
1.321	AlN
1.173	AlN
1.112	Al <sub>2</sub> O <sub>3</sub>
1.082	Al <sub>2</sub> O <sub>3</sub>
1.048	AlN
1.015	Fe
0.907	Fe

TABLE H-III

X-RAY DATA FOR BORON NITRIDE SAMPLES FROM THE SIEVERTS APPARATUS

7.06% B, extracted  
Fe radiation, Mn filter

3.82% B, unextracted  
Fe radiation, Mn filter

<u>d observed</u>	<u>substance</u>
3.66	?
3.33	BN
2.68	?
2.49	?
2.19	BN
2.112	B <sub>2</sub> O <sub>3</sub>

<u>d observed</u>	<u>substance</u>
3.32	BN
2.16	BN
2.112	B <sub>2</sub> O <sub>3</sub>
2.021	Fe
1.812	BN
1.662	BN

TABLE H-III  
(CONT'D)

7.06% B, extracted  
Fe radiation, Mn filter

<u>d observed</u>	<u>substance</u>
2.112	B <sub>2</sub> O <sub>3</sub>
1.999	?
1.678	BN
1.228	BN
1.146	BN

3.82% B, unextracted  
Fe radiation, Mn filter

<u>d observed</u>	<u>substance</u>
1.662	BN
1.428	Fe
1.252	BN
1.171	BN

The unidentified lines in the pattern of the 7.06% B sample in Table H-III were of an intensity approximately equal to the intensities of the BN lines. This sample apparently contains some impurity which cannot be identified.

TABLE H-IV

X-RAY DATA FOR COLUMBIUM NITRIDE SAMPLES FROM  
THE SIEVERTS APPARATUS

17.71% Cb, extracted  
Cu radiation, Ni filter

<u>d observed</u>	<u>substance</u>
2.523	CbN <sub>0.75</sub>
2.193	CbN <sub>0.75</sub>
2.152	CbN <sub>0.75</sub>
1.542	CbN <sub>0.75</sub>
1.321	CbN <sub>0.75</sub>
1.302	CbN <sub>0.75</sub>
1.256	CbN <sub>0.75</sub>
1.094	CbN <sub>0.75</sub>
0.997	CbN <sub>0.75</sub>
0.979	CbN <sub>0.75</sub>
0.894	CbN <sub>0.75</sub>
0.845	CbN <sub>0.75</sub>

14.17% Cb, extracted  
Fe radiation, Mn filter

<u>d observed</u>	<u>substance</u>
2.785	CbN (hexagonal)
2.531	CbN (cubic)
2.500	CbN <sub>0.75</sub>
2.313	CbN (cubic)
2.201	CbN (cubic)
2.174	CbN <sub>0.75</sub>
1.538	CbN <sub>0.75</sub>
1.321	CbN (cubic)
1.314	CbN <sub>0.75</sub>
1.261	CbN (hexagonal)
1.006	CbN (cubic)
0.999	CbN <sub>0.75</sub>
0.979	CbN <sub>0.75</sub>

TABLE H-IV  
(CONT'D)

11.41% Cb, extracted  
Co radiation, Fe filter

<u>d observed</u>	<u>substance</u>
2.513	CbN <sub>0.75</sub>
2.177	CbN <sub>0.75</sub>
1.546	CbN <sub>0.75</sub>
1.322	CbN <sub>0.75</sub>
1.308	CbN <sub>0.75</sub>
1.259	CbN <sub>0.75</sub>
1.007	CbN <sub>0.75</sub>
0.999	CbN <sub>0.75</sub>
0.981	CbN <sub>0.75</sub>
0.971	CbN <sub>0.75</sub>

Some of the observed d values for the three samples given in Table H-IV differ slightly from the d values given by Brauer and Jander<sup>(44)</sup> for the composition CbN<sub>0.75</sub>. This is an indication that all three samples do not have the exact composition CbN<sub>0.75</sub>. However because of the excellent correspondence of the pattern of the d values in all three samples their compositions must be very close to CbN<sub>0.75</sub>.

TABLE H-V

X-RAY DATA FOR VANADIUM NITRIDE SAMPLES FROM  
THE SIEVERTS APPARATUS

15.04% V, extracted  
Cu radiation, Ni filter

9.93% V, extracted  
Cu radiation, Ni filter

<u>d observed</u>	<u>substance</u>	<u>d observed</u>	<u>substance</u>
2.345	VN <sub>0.7</sub>	2.354	VN <sub>0.7</sub>
2.302	VN <sub>0.7</sub>	2.032	VN <sub>0.7</sub>
1.437	VN <sub>0.7</sub>	1.437	VN <sub>0.7</sub>
1.223	VN <sub>0.7</sub>	1.232	VN <sub>0.7</sub>
1.173	VN <sub>0.7</sub>	0.936	VN <sub>0.7</sub>
1.015	VN <sub>0.7</sub>	0.911	VN <sub>0.7</sub>
0.933	VN <sub>0.7</sub>	0.831	VN <sub>0.7</sub>
0.908	VN <sub>0.7</sub>		
0.831	VN <sub>0.7</sub>		

The  $d$  values in Table H-V show a considerable shift from the  $d$  values recorded by Becker and Ebert<sup>(45)</sup> for which they give the composition VN, although the patterns both indexed to give a face centered cubic structure. The small  $\theta$  lines were used to calculate lattice parameter values. The 15.04% V sample gave a value of  $a_0 = 4.062 \text{ \AA}$  while the 9.93% V sample gave a value of  $a_0 = 4.068 \text{ \AA}$ . The work of Hahn<sup>(17)</sup> indicates that these lattice parameters correspond to a composition of about  $\text{VN}_{0.71}$ . This is the composition limit on the low nitrogen side of the nitride VN which has the NaCl structure.

Table H-VI summarizes the results of powder patterns run on the materials from which the nitride crucibles used in the quenching runs were fabricated. The AlN from the hot pressed crucibles supplied by Carborundum Company and the BN bar stock obtained from the same source show excellent agreement with the A.S.T.M. standard patterns for AlN and BN. However the pattern of the TiN powder used to fabricate TiN crucibles shows several extra lines of weak intensity indicating the possible presence of some unidentifiable impurity.

TABLE H-VI

X-RAY DATA ON RAW MATERIALS USED TO FABRICATE  
NITRIDE CRUCIBLES FOR THE QUENCHING METHOD

TiN powder		AlN hot pressed crucible	
Fe radiation, Mn filter		Fe radiation, Mn filter	
<u><math>d</math> observed</u>	<u>substance</u>	<u><math>d</math> observed</u>	<u>substance</u>
2.698	?	2.70	AlN
2.449	TiN	2.493	AlN
2.343	?	2.369	AlN
2.123	TiN	1.831	AlN
1.652	?	1.559	AlN
1.499	TiN	1.417	AlN
1.279	TiN	1.322	AlN
1.224	TiN	1.046	AlN
1.061	TiN	0.999	AlN

TABLE H-VI  
(CONT 'T)

BN bar stock  
Cr radiation

<u>d observed</u>	<u>substance</u>
3.341	BN
2.171	BN
2.058	BN
1.661	BN
1.322	BN
1.252	BN
1.173	BN

## APPENDIX I

### CALCULATION OF ACTIVITY COEFFICIENTS IN LIQUID IRON

As an additional check on the consistency of the nitrogen absorption curves values of  $\gamma_j$ , the slope of  $a_j$  vs  $X_j$ , were calculated for the systems titanium, zirconium, aluminum, and boron.  $\gamma_j$  also represents the activity coefficient of  $j$  relative to pure  $j$ . It can be calculated at various dilute  $j$  concentrations from free energy data on the reaction:



and the nitrogen pressure at which the nitride forms in equilibrium with a melt of known  $j$  content. Free energy data on reaction (I-1) are given by Elliott and Gleiser<sup>(38)</sup> and values of nitrogen pressure corresponding to a given  $j$  content can be read from the break points of the nitrogen absorption curves in Appendix F.

The equilibrium constant for Equation (I-1) can be written according to the following equation:

$$\Delta F^\circ = -RT \ln K = -RT \ln \frac{a_{jN}}{a_j \times (P_{N_2})^{1/2}} = \frac{1}{(\gamma_j N_j) \times (P_{N_2})^{1/2}} \quad (I-2)$$

From Equation (I-2) a value of  $\gamma_j$  corresponding to each finite  $N_j$  was calculated at 1600°C. These are shown in Table I-I. In order to calculate the value of  $\gamma_j$  at infinite dilution, designated  $\gamma_j^\circ$ , free energy data on the reactions (I-1) and:



$$jN (s) = \underline{j} + \underline{N} \quad (I-5)$$

were combined to give the free energy of the reaction:

$$j(1 \text{ or } s) = \underline{j} \quad (I-6)$$

Free energy data of Pehlke and Elliott<sup>(1)</sup> for Equation (I-4) were used and free energy data for Equation (I-5) came from Table XI of this study.

The equilibrium constant for Equation (I-6) can now be written:

$$\Delta F^\circ = -RT \ln \frac{M_j}{0.5585\gamma_j^\circ} \quad (I-7)$$

and  $\gamma_j^\circ$  can be calculated from (I-7). These values are also presented in Table I-I.

The values of  $\gamma_{Al}$  in Table I-I are lower than those of Wilder and Elliott<sup>(31)</sup> or Chipman and Floridis<sup>(32)</sup>. The values of  $\gamma_{Zr}$  are considerably lower than the estimate of Chipman<sup>(7)</sup> and the values of  $\gamma_{Ti}$  are higher than Chipman's<sup>(35)</sup> estimate for this system. The differences in  $\gamma$  values are too large to be explained by the estimated uncertainty in the  $\Delta F^\circ$  values for reaction (I-1). The  $\gamma$  values in Table I-I for the titanium and zirconium systems show some scatter in that they do not progressively increase with increasing  $j$  content. The large difference between  $\gamma_B^\circ$  and the other two  $\gamma$  values for the boron system indicates that these solutions are sufficiently concentrated in boron to show large departures from Henry's Law. In addition the  $\gamma$  values in Table I-I are not strictly for the binary systems Fe-j but for the ternary Fe-j-N. However the effect of nitrogen can be shown to be negligible by writing the equation:

$$\ln \gamma_j = \ln \gamma_j^\circ + \epsilon_j^j X_j + \epsilon_j^N X_N \quad (I-8)$$

and noting that the term  $\epsilon_j^N X_N$  is small for the titanium, zirconium, aluminum, and boron systems.

TABLE I-I  
CALCULATED VALUES OF  $\gamma_j$  FOR THE TITANIUM, ZIRCONIUM,  
ALUMINUM, AND BORON SYSTEMS

element j	% j	$(P_{N_2})^{1/2} \text{ (cm)}^{1/2}$	$\gamma_j$
Ti	0		0.047
	0.195	3.22	0.038
	0.228	2.65	0.042
	0.254	2.03	0.049
	0.277	2.10	0.043
	0.318	1.40	0.056
Zr	0		0.0076
	0.253	6.10	0.0043
	0.322	5.10	0.0041
	0.409	2.40	0.0068
	0.558	1.25	0.0095
Al	0		0.019
	1.07	8.10	0.021
	1.17	6.95	0.022
	1.34	5.60	0.024
	1.57	4.65	0.025
	1.81	3.58	0.028
B	0		0.021
	5.83	3.38	0.399
	7.06	2.80	0.398



APPENDIX J

FREE ENERGY OF FORMATION OF ALN FROM THE PURE COMPONENTS

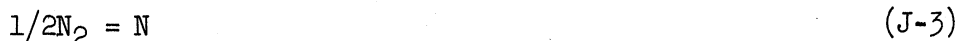
Of the four most stable nitride systems considered in Appendix I there is only one, aluminum, for which the nitride composition and the activity of the metal in iron solution are sufficiently well known to permit accurate calculation of the standard free energy of formation of the nitride from its pure components. For the reaction:



the free energy from Table XI of this study may be written:

$$\Delta F^\circ = 63,700 - 27.91T \quad (\text{J-2})$$

For the reaction:



Pehlke and Elliott<sup>(1)</sup> give the free energy as:

$$\Delta F^\circ = 860 + 5.71T \quad (\text{J-4})$$

The free energy for the reaction:



is given by the equation:

$$\Delta F^\circ = 4.575T \log \frac{0.5585 \gamma^\circ}{M_{\text{Al}}} \quad (\text{J-6})$$

where  $\gamma^\circ$  is the slope of the curve of aluminum activity versus aluminum mole fraction in liquid iron. However since  $\gamma^\circ$  is known only at 1600°C, it is necessary to know the heat of solution of aluminum in liquid iron, i.e. the  $\Delta H^\circ$  for Equation (J-5). If the dilute solution of aluminum in liquid iron is assumed to be regular, then the  $\Delta H^\circ$  for Equation (J-5) is given by:

$$\Delta H^\circ = 4.575T \log \gamma^\circ \quad (\text{J-7})$$

By combining Equations (J-6) and (J-7) the  $\Delta S^\circ$  for reaction (J-5) may be found:

$$\Delta S^\circ = - \frac{\Delta F^\circ - \Delta H^\circ}{T} = 4.575 \log \frac{0.5585}{M_{Al}} \quad (\text{J-8})$$

The results of Wilder and Elliott<sup>(31)</sup> give a value of  $\gamma^\circ = 0.063$  at 1600°C. Using this value and Equations (J-7) and (J-8) the free energy of reaction (J-5) may be written:

$$\Delta F^\circ = -10,280 - 7.70T \quad (\text{J-9})$$

By combining reactions (J-1), (J-3), and (J-5) the reaction:



results. The free energy of this reaction which is the standard free energy of formation of AlN from its pure components can be calculated from Equations (J-2), (J-4), and (J-9) as:

$$\Delta F^\circ = -73,100 + 25.29T \quad (\text{J-11})$$

The free energy values given by Equation (J-11) in the temperature range over which the experimental values for reaction (J-1) were measured are summarized in Table J-I.

TABLE J-I

FREE ENERGY OF FORMATION OF AlN FROM THE PURE COMPONENTS	
<u>Temperature °C</u>	<u>Δ F°</u>
1600	-24,600
1650	-23,300
1700	-22,000
1750	-20,700

## IX BIBLIOGRAPHY

1. Pehlke, R. D. and Elliott, J. F. "Solubility of Nitrogen in Liquid Iron Alloys. I. Thermodynamics," Trans. A.I.M.E., 218, 1088 (1960).
2. Humbert, J. and Elliott, J. F. "Solubility of Nitrogen in Liquid Iron-Chromium-Nickel Alloys," Trans. A.I.M.E., 218, 1076 (1960).
3. Kashyap, V. and Parlee, N. "Solubility of Nitrogen in Liquid Iron and Iron Alloys," Trans. Met. Soc. A.I.M.E., 212, 86 (1958).
4. Kootz, T. "Contribution to the Investigation of Nitrogen Absorption by Pure Molten Iron and by the Alloys Iron-Carbon, Iron-Phosphorus, and Iron-Chromium," Arch. Eisenhüttenw., 15, 77 (1941).
5. Brick, R. M. and Creevy, J.A. "Solubility of Nitrogen in Liquid Fe-Cr and Fe-V Alloys," Metals Tech. A.I.M.E., (Tech. Pub. No. 1165), April 10, 1940.
6. Schenk, H., Froberg, M., and Graf, H. "Investigation of the Influence of the Equilibria of Nitrogen with Liquid Iron Solutions by the Addition of Further Elements (II)," Arch. Eisenhüttenw., 30, 533 (1959).
7. Basic Open Hearth Steelmaking, Revised Edition, A.I.M.E., New York, 685 (1951).
8. Pearson, J. and Ende, U. "Thermodynamics of Metal Nitrides and of Nitrogen in Iron and Steel," J. Iron and Steel Inst., 175, 52 (1953).
9. Kelley, K. K. U.S. Bureau of Mines Bulletin No. 407 (1937).
10. Maekawa, S., Nakagawa, Y., and Yanagawa, Y. "Effect of Titanium, Aluminum, and Oxygen on the Solubility of Nitrogen in Liquid Iron," Tetsu to Hagane, 46, 241 (1960), Brucher Translation No. 4839.
11. Pehlke, R. D., Sc. D. Thesis, M.I.T. (1960).
12. Rao, M. M. and Parlee, N. "La solubilité de l'azote dans les alliages liquides fer-vanadium et fer-titane et l'équilibre dans la réaction  $x\text{Ti} + \text{N} = \text{Ti}_x\text{N}(\delta)$ ," Rev. Met., 58, 52 (1961).
13. Fountain, R. W. and Chipman, J. "Solubility and Precipitation of Vanadium Nitride in Alpha and Gamma Iron," Trans. A.I.M.E., 212, 737 (1958).
14. Ehrlich, P. "Concerning the Binary Systems Ti-N, Ti-C, Ti-B, Ti-Be," Z. Anorg. Chem., 259, 1 (1949).
15. Chiotti, P. "Experimental Bodies of High Melting Nitrides, Carbides, and  $\text{UO}_2$ ," J. Amer. Ceramic Soc., 35, 123 (1952).

16. Domagala, R. F., McPherson, D. J., and Hanson, M. "System Zirconium-Nitrogen," Journal of Metals, 8, 98 (1956).
17. Hahn, H. "Concerning the System Vanadium-Nitrogen," Z. Anorg. Chem., 258, 58 (1949).
18. Schonberg, N. "Some Features of the Nb-N and Nb-N-O Systems," Acta Chemica Scandinavica, 8, 208 (1954).
19. Schonberg, N. "An X-ray Study of the Tantalum-Nitrogen System," Acta Chemica Scandinavica, 8, 199 (1954).
20. Taylor, K. M., and Lenie, C., "Some Properties of Aluminum Nitride," J. Electrochem. Soc., 107, No. 4, 308 (1960).
21. Paretzkin, Polytechnic Institute of Brooklyn, A.S.T.M. X-ray Powder Data File No. 8-262.
22. Wagner, C., Thermodynamics of Alloys, Addison-Wesley Press, Inc., Reading, Mass., 51 (1952).
23. Pehlke, R. D., and Elliott, J. F., "Solubility of Nitrogen in Liquid Iron Alloys. II. Kinetics," To be published.
24. Dastur, M. N., and Gokcen, N. A., "Optical Temperature Scale and Emissivity of Liquid Iron," Trans. A.I.M.E., 185, 665 (1949).
25. Sponseller, D. L., Ph.D. Thesis, University of Michigan (1962).
26. Beeghly, H. F., "Determination of Aluminum Nitride Nitrogen in Steel," Analytical Chemistry, 21, 1513 (1949).
27. Maekawa, S., and Nakagawa, Y., "Solubility of Nitrogen in Liquid Iron and Iron Alloys," Tetsu to Hagane, (J. Iron and Steel Inst., Japan) 45, 255 (1959).
28. Nakagawa, Y., Private Communication, 1959 (letter to R. D. Pehlke).
29. Eklund, L., "Solubility of Nitrogen in Steel," Jernkontorets Annaler, 123, 545 (1939).
30. Dealy, J. M., and Pehlke, R. D., "Interaction Parameters in Dilute Molten Alloys," To be published.
31. Wilder, T. C., and Elliott, J. F., "Thermodynamic Properties of the Aluminum-Silver System," J. Electrochem. Soc., 107, 628 (1960).
32. Chipman, J., and Floridis, T., "Activity of Aluminum in Liquid Ag-Al, Fe-Al, Fe-Al-C, and Fe-Al-C-Si Alloys," Acta Metallurgica, 3, 456 (1955).

33. Elle, M., and Chipman, J., "The Columbiun-Oxygen Equilibrium in Liquid Iron," Trans. A.I.M.E., 221, 701 (1961).
34. Chipman, J., Fulton, J. C., Gokcen, N. A., and Caskey, G. R., "Activity of Silicon in Liquid Fe-Si and Fe-C-Si Alloys," Acta Metallurgica, 2, 439 (1954).
35. Chipman, J., "The Deoxidation Equilibrium of Titanium in Liquid Steel," Trans. A.I.M.E., 218, 767 (1960).
36. Turkdogan, E. T., Hancock, R. A., Herlitz, S. I., and Denton, J., "Thermodynamics of Carbon Dissolved in Iron Alloys; Part V: Solubility of Graphite in Iron-Manganese, Iron-Cobalt, and Iron-Nickel Melts," J. Iron and Steel Inst., 183, 69 (1956).
37. Korber and Oelsen, Mitt. Kaiser Wilhelm Institute Eisenforsch., 18, 365 (1936).
38. Elliott, J. F., and Gleiser, M., Thermochemistry For Steelmaking Vol. I, Addison-Wesley Press, Inc., Reading, Mass. (1960).
39. Pehlke, R. D. and Elliott, J. F., "High Temperature Thermodynamics of the Silicon, Nitrogen, Silicon-Nitride System," Trans. A.I.M.E., 215, 781 (1959).
40. Darken, L. S., and Gurry, R. W., "The System Iron-Oxygen. I. The Wustite Field and Related Equilibria," J. Amer. Ceramic Soc., 67, 1398 (1945).
41. A.S.T.M. Methods for Chemical Analysis of Metals, American Society for Testing Materials, Philadelphia, Pa., 157 (1960).
42. Steyermark and Blakiston, Quantitative Organic Microanalysis, Philadelphia, Pa. (1951).
43. Vogel, A. I., Quantitative Inorganic Microanalysis, Longmans Green and Co. (1939).
44. Brauer, G., and Jander, J., "The Nitrides of Niobium," Z. Anorg. Chem., 270, 177 (1952).
45. Becker, K., and Ebert, F., "The Crystal Structure of Some Binary Carbides and Nitrides," Zeit. Fur Physik, 31, 269 (1925).